Transcriptional program of osteoblast differentiation

Coordinated activation of Notch, Wnt, and TGF-β signaling pathways in MC3T3 cell line

Inauguraldissertation

zur
Erlangung der Würde eines Doktors der Philosophie
vorgelegt der
Philosophisch-Naturwissenschaftlichen Fakultät
der Universität Basel

von

Nataša Zamurović

aus Serbien und Montenegro

Basel, 2005

Genehmigt von der Philosophisch-Naturwissenschaftlichen Fakultät

auf Antrag von

Prof. Dr. Michael N. Hall

Dr. Mira Šuša Spring

PD Dr. Patrick Matthias

Basel, den 16.11.2004

Prof. Dr. H. J. Wirz

Acknowledgement

The work presented here has been carried out in the Bone Metabolism Department of the Musculoskeletal Disease Area, Novartis Institutes for BioMedical Research, in Basel, Switzerland, while the courses of the Ph.D. programme took part at the University of Basel, Switzerland. Everybody here, my group in Novartis, people at the University, and Basel itself, as charming as it is, made me feel like at home. This was not only a great scientific experience, but a great school of life as well, and a few people were a big part of it. As this part of my work is now coming to an end, I would like to mention them.

Above all, I would like to thank to my Ph. D. supervisor, Dr. Mira Šuša Spring. She enabled me to come and work in her group, first as a trainee, and then as a Ph.D. student, and without her initiative this project would not exist. Dr. Šuša was the best supervisor that anyone could wish for, giving me a lot of freedom and independence in my work, but always there with good advices, ready to share her big scientific knowledge, and invariably supportive. Hvala Vam mnogo!

Colleagues from my group were always a great support and fun to work with during these four years: Dr. David Cappellen, who introduced me the gene expression analysis and who was always ready to help, with good scientific advice or just a friendly chat. Daisy Rohner and Ngoc-Hong Luong-Nguyen, who lead me through first steps of cellular biology and from whom I learned a lot about state-of-art experimental work. Reinhard Moschitz, a trainee in our lab, who was teaching me how to be a supervisor.

All the colleagues from the Bone Metabolism department and from other groups in Novartis that we were collaborating with were invariably friendly and

supportive. I would just like to say thanks to Isabelle Delhon, Sabine Gutzwiller and Johann Wirsching for a numerous good advices and friendship.

At the end, a big Thanks to people who are making my life, in Basel and in Belgrade.

To Kaca and Bane, for being the best friends anyone could want. To all my Basel friends, for lots of positive energy!

To mum, dad and Ljubica.

To Seb, just for being mine.

TABLE OF CONTENTS

1 Summary

In order to examine the early events in osteoblast differentiation, three different model systems for osteoblast differentiation were compared: mouse pre-osteoblastic cell line MC3T3; mouse myoblastic cell line C2C12 and primary mouse calvarial osteoblasts. Quantitative RT-PCR conditions were set for analysis of 8 markers of the osteoblast differentiation process: alkaline phosphatase, Msx2, Cbfa1, parathyroide hormone receptor, osteocalcin, osteopontin, osteonectin and collagen I α1. Expression of these genes was analyzed in all three systems upon treatment with osteogenic supplement, at days 1 and 3, by comparison with a non-stimulated time-matched control. In addition, classical cytochemical tests for following the osteoblast differentiation process, ALP and mineralization staining, were used. MC3T3 cells were shown to be the best model for examining osteoblast differentiation on the cytochemical, as well as on the transcriptional level, with most marker genes upregulated. Then, Affymetrix GeneCHIP analysis was used to probe the changes induced by differentiation stimuli in MC3T3 cells. These cells were stimulated for 1 and 3 days with an osteogenic stimulus containing BMP-2. Total RNA was extracted and analyzed with Affymetrix GeneChip oligonucleotide arrays. A regulated expression of 394 known genes and 295 ESTs was detected. The sensitivity and reliability of detection by microarrays was shown by confirming the expression pattern for 20 genes by radioactive quantitative RT-PCR. Extensive functional classification of regulated genes was performed. The most interesting finding was concomitant activation of TGF-β, Wnt and Notch signaling pathways, confirmed by strong up-regulation of their target genes by PCR. The TGF-β pathway is activated by stimulated production of the growth factor itself, while the exact mechanism of Wnt and Notch activation remains elusive. We showed BMP-2 stimulated expression of *Hey1*, a direct Notch target gene, in mouse MC3T3 and C2C12 cells, in human mesenchymal cells and in mouse calvaria. Small interfering RNA-mediated inhibition of *Hey1* induction led to an increase in osteoblast matrix mineralization, suggesting that Hey1 is a negative regulator of osteoblast maturation. This negative regulation is apparently achieved via interaction with Runx2, as Hey1 completely abrogated Runx2 transcriptional activity. These findings identify the Notch-Hey1 pathway as a negative regulator of osteoblast differentiation / maturation, which is a completely

novel aspect of osteogenesis and could point to possible new targets for bone anabolic agents.

2 Introduction

2.1 Skeletal system

Bone is a specialized connective tissue that makes, together with cartilage, the skeletal system. In humans, skeletal system consists of 206 bones (Figure 1).

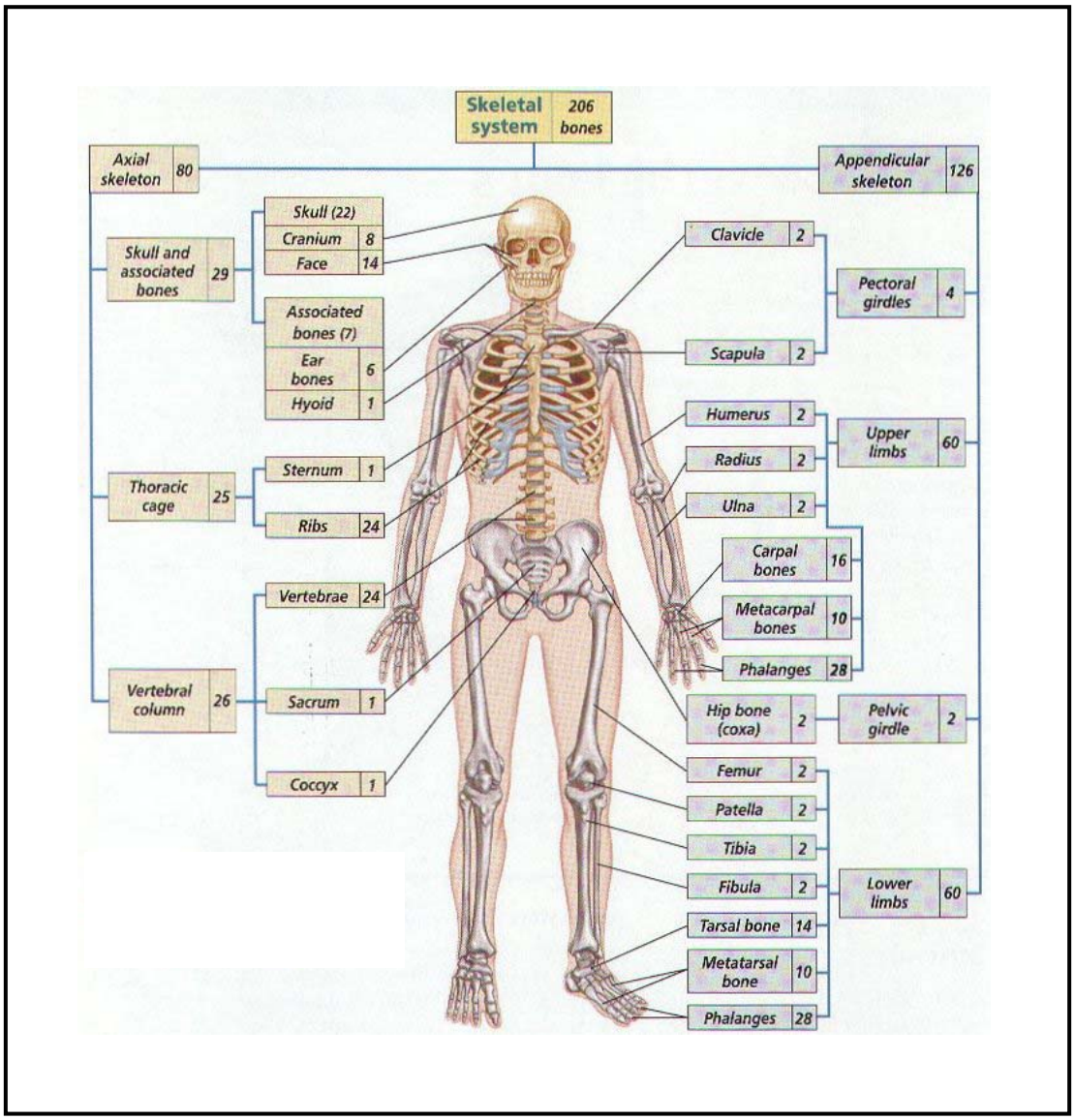

Figure 1: Organisation of human skeleton. Taken from a web site www.sirinet.net/~jgjohnso/ skeletonorg.html

Skeletal system serves three functions:

1. Mechanical, as a support and a site of muscle attachment for locomotion;
2. Protective, for vital organs and bone marrow; and
3. Metabolic, as a reserve of ions, especially calcium and phosphate, for the maintenance of their homeostasis in serum.

2.1.1 Macroscopic organisation of bone

Anatomically, two types of bones can be distinguished in the skeleton: flat bones (skull bones, scapula, mandible, and ileum) and long bones (tibia, femur, humerus etc.). A typical long bone (Figure 2) consists of the two wider extremities - the epiphyses, a cylindrical tube in the middle- the diaphysis, and a developmental zone between them - the metaphysis. The external part of the bone is formed by a thick and dense layer of calcified tissue, the cortex (compact bone), which encloses the medullar cavity in the diaphysis,. Towards the metaphysis and epiphysis the cortex becomes progressively thinner, and the internal space is filled with a network of thin, calcified trabeculae; this is the cancellous bone, also named spongy or trabecular bone. The spaces enclosed by the trabeculae are in continuity with the medullar cavity. This space is filled with haematopoietic bone marrow (red marrow) or with adipocyte tissue (yellow marrow).

There are two bone surfaces at which the bone is in contact with the soft tissues: an external surface (the periosteal surface), and an internal surface (the endosteal surface). These surfaces are lined with osteogenic cells organised in layers, the periosteum and the endosteum (Figure 2).

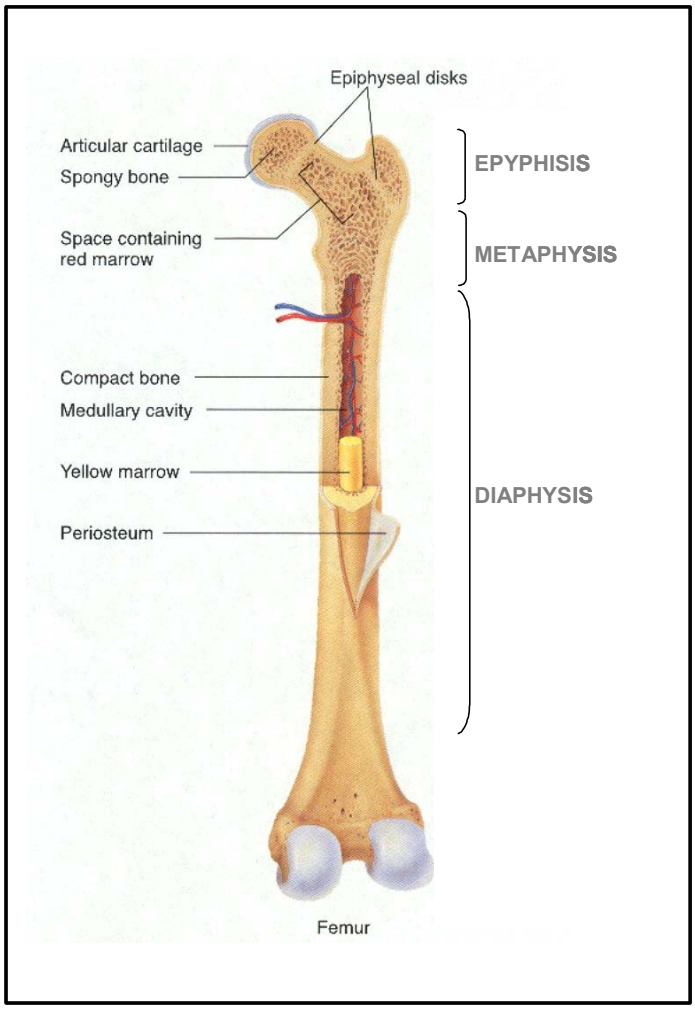

Figure 2: Schematic view of a long bone structure. Modified from a web site www.sirinet.net/~jgjohnso/ skeletonorg.html

During development, flat bones are formed by the process of *intramembranous* ossification, in which mesenchymal cells form a condensation within a highly vascularised area of the embryonic connective tissue by proliferating and differentiate directly into bone forming cells. Long bones are formed mainly by a process of *endochondral* ossification, in which mesenchymal cells differentiate into chondroblasts and a cartilage model of a future bone is formed first, to be replaced later by a bone tissue.

2.1.2 Bone tissue

Bone is a specialized connective tissue that consists of cells and mineralized extracellular matrix.

Organic component of the matrix called osteoid is mainly formed by collagen I fibers (90% of total proteins), usually oriented in a preferential direction and of ground substance. Inorganic component of the matrix consists of spindle- or plate-shaped crystals of hydroxyapatite [$3Ca_3(PO4)_2(OH)_2$], which are found on the collagen fibers, within them, and in the ground substance. The ground substance is primarily composed of noncollagenous matrix glycoproteins (osteocalcin, osteopontin, osteonectin, bone sialoprotein, thrombospondin etc.) and proteoglycans. The highly anionic complexes of ground substance have a high ion-binding capacity and are thought to play an important part in the calcification process and the fixation of hydroxyapatite crystals to collagen fibers. Bone matrix binds numerous cytokines and growth factors, that have important function in growth, differentiation and remodelling of the skeleton. They are released during the process of bone resorption.

The preferential orientation of the collagen fibers alternates in adult bone from layer to layer, giving bone a typical lamellar structure. This fiber organization allows the highest density of collagen per unit volume of tissue. The lamellae can be parallel to each other, if deposited along a flat surface (trabecular bone and periosteum), or concentric, if deposited on a surface surrounding a channel centred on a blood vessel and nerve fibers (Harvesian system). A second system of canals, called Volkmann's canals, penetrates the bone more or less perpendicular to its surface. These canals establish connections with the inner and outer surfaces of the bone. Vessels in Volkmann's canals communicate with vessels in the Haversian canals (Figure 3). However, when bone is being formed very rapidly, like during development or fracture healing, there is no preferential organisation of collagen fibers, which are then rather randomly oriented. This type of bone is called woven bone, as opposed to lamellar bone.

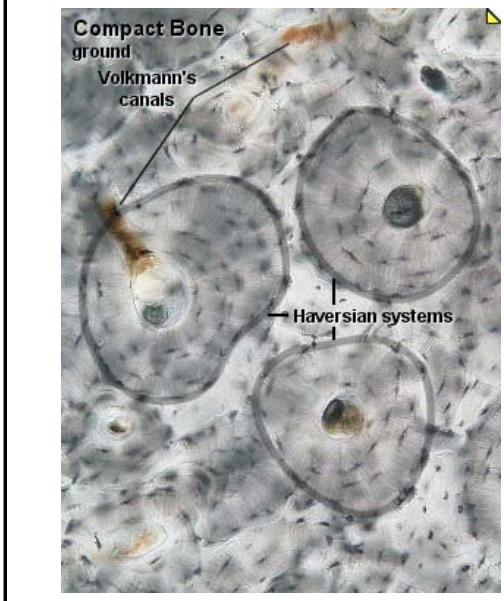

Figure 3: Harvesian and Volkmann's canals. Cross-section of a long bone. Taken from a website http://www.orthoteers.co.uk/Nrujp~ij33lm/Orthbone1.htm

Cells of the bone tissue are of osteoblastic lineage, comprising bone forming cells, and of osteoclastic lineage, comprising bone resorbing cells.

Mature osteoblasts are cuboidal cells responsible for the production of the matrix constituents (collagen and ground substance) and its subsequent mineralization. Osteoblasts originate form local mesenchymal stem cells (bone marrow stromal cells) that have the potential to differentiate into fat cells, fibroblasts, chondrocytes, muscle cells or osteoblasts. Osteoblasts deposit osteoid on the pre-existing mineralized matrix only. During this process, a proportion of osteoblasts become trapped in lacunae within the matrix of bone as osteocytes, connected by a system of canaliculi. Osteocytes probably function as mechanosensors, regulating the response of bone to the mechanical stimuli[1]. Other proportion of osteoblasts becomes bone lining cells, flat cells lining the surface of bone.

Osteoclasts are large, motile, multinucleated cells located on bone surfaces. They are formed by the fusion of mononuclear cells derived from haematopoetic stem cells of the macrophage/monocyte lineage in the bone marrow. Marrow stromal cells or their osteoblast progeny are necessary for osteoclast differentiation from macrophage precursor: they express two molecules that are essential and sufficient

to promote osteoclastogenesis: macrophage colony-stimulating factor (M-CSF) and receptor for activation of nuclear factor kappa B (NF-κB) (RANK) ligand (RANKL). (Figure 4). M-CSF binds to its receptor c-Fms, on early osteoclast precursor, providing signals required for their survival and proliferation[2]. RANKL is transmembane ligand on the stromal cells surface that binds to its receptor RANK on the surface of osteoclast precursor and drives osteoclast differentiation (Lacey *et al*., 1998). Stromal cells also express osteoprotegerin (OPG), a soluble "decoy" receptor that competes with RANK for RANKL[3].

The differentiated osteoclast polarizes on the bone surface, a process which involves matrix-derived signals transmitted by the cell attachment receptor αvβ3 integrin. After attaching to the bone, osteoclast forms so called "ruffled membrane", surrounded by the ring zone of tight attachment to the bone, "sealing" zone. Osteoclastic bone resorption initially involves mineral dissolution, followed by a degradation of the organic phase. Bone demineralization involves acidification of the isolated extracellular microenvironment, mediated by a H^+-ATPase in the cell's ruffled membrane that pumps H^+ ions into the resorption pit. Cl^- ion pass through a ruffled membrane-residing anion channel into the resorptive microenvironment. Intracellular pH is maintained by HCO_3-/Cl^- exchange at the cell's antiresorptive surface. The acidic milieu dissolves the mineral phase of bone and provides an optimal environment for organic matrix degradation, mainly by the lysosomal protease cathepsin K (reviewed in Teitelbaum SL, 2000[4] - Figure 4).

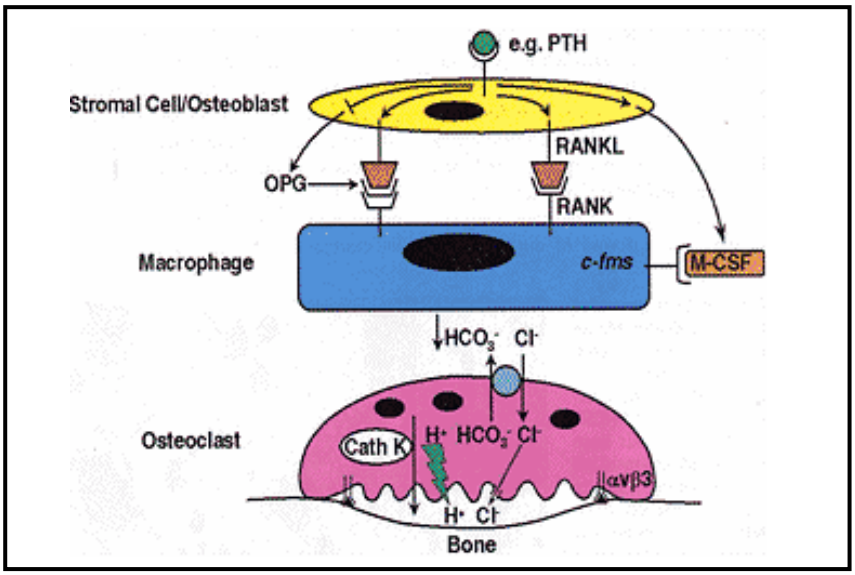

Figure 4: Mechanisms of osteoclastogenesis and osteoclastic bone resorption. Teitelbaum, 2000[4].

2.1.3 Bone remodeling and osteoporosis

Bone remodeling

Bone formation and resorption do not occur along the bone surface at random; they are either part of process of bone development and growth (modeling) or part of turnover mechanism by which old bone is replaced by new bone (remodeling). In the normal adult skeleton (after the period of development and growth), bone formation occurs for the most part only where bone resorption has previously occurred (remodeling). The sequence of events at the remodeling site is shown at Figure 5. In the initial phase of remodeling process, osteoclasts are recruited on the bone remodeling location, and they perform bone resorption. During the intermediate phase between resorption and formation (the reversal phase), macrophage-like, uncharacterized mononuclear cells are observed at the site of the remodeling, and a cement line is formed, which marks the limit of resorption in that remodeling cycle and acts to cement together the old and the new bone. In a bone formation phase, osteoblast synthesize organic matrix components (osteoid) first, that eventually becomes mineralized. The complete remodeling cycle at each microscopic site takes about 3-6 months, with resorption process lasting about 3 weeks and bone formation several months.

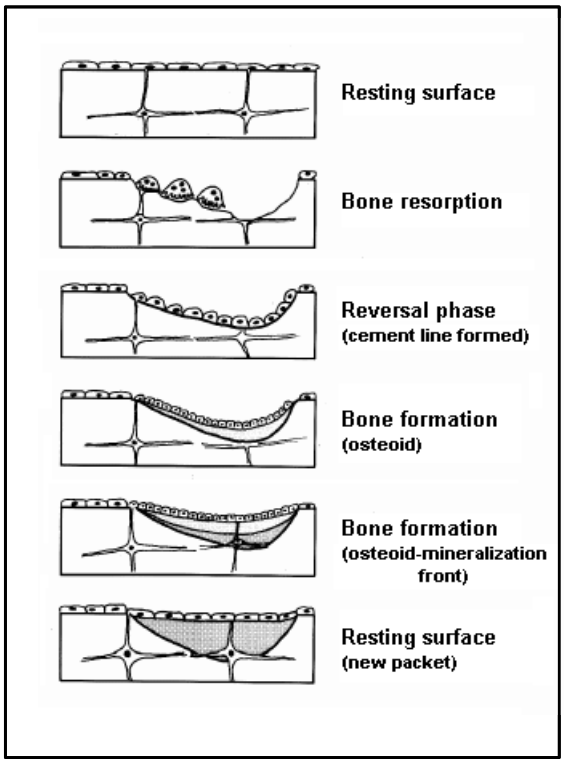

Figure 5: Bone remodeling cycle. Taken from http://www.orthoteers.co.uk/Nrujp~ij33lm/Orthbone1.htm#BONEFUNCTION

Unbalanced bone remodeling: osteoporosis

In young healthy individuals, bone resorption and bone formation are balanced processes. This balance is described as *coupling* of bone resorption and formation. Uncoupling of bone resorption from bone formation leads to skeletal disorders. The most common one is osteoporosis, where net bone resorption is greater that bone formation. The accepted full definition of osteoporosis is: a metabolic bone disease characterized by low bone mass and microarchitectural deterioration of bone tissue, leading to enhanced bone fragility and a consequent increase in fracture risk. (*Consensus Development Conference V 1993*). For every 10% of bone that is lost, the risk of fracture doubles[5]. In 1994, a World Health Organisation (WHO) study group have defined diagnostic categories for osteoporosis (Table 1).

Category	Definition by bone density
Normal	A value of Bone Mineral Density (BMD) that is not more than 1 SD below the young adult mean value
Osteopenia	A value for BMD that lies between 1 and 2.5 SD below the young adult mean value
Osteoporosis	A value for BMD that is more than 2.5 SD below the young adult mean value
Severe osteoporosis (established)	A value for BMD more than 2.5 SD below the young adult mean value in the presence of one or more fragility fractures

Table 1: Diagnostic categories for osteoporosis based on WHO criteria. Cooper *et al.*, 2003[6]

Epidemiological risk factors for development of osteoporosis are numerous (Table 2), but the most common cause of osteoporosis is estrogen deficiency in postmenopausal women. Estrogen deficiency is associated with elevated bone resorption caused by a rise of osteoclast number, which is driven by increase in the cytokines that regulate osteoclast generation. Effect of estrogen deficiency on the bone architecture in the rat is shown on Figure 6. Around 20% of all postmenopausal women in western countries would meet WHO criteria for osteoporosis, and around 1.3 milion fractures in the United States each year are attributable to the disorder[6].

Osteoporotic fractures, hip fractures in particular, result in significantly higher morbidity and mortality, and the costs of treatments are high.

Age, or Age-Related
Each decade associated with 1.4-1.8 fold increased risk
Genetic
Ethicity: Caucasians and Oriental > blacks and Polynesians
Gender: Female > male
Family history
Enviromental
Nutrition: calcium deficiency
Physical activity and mechanical loading
Medication, e.g. corticosteroids
Smoking
Alcohol
Falls (trauma)
Endogenous Hormones and Chronic Diseases
Estrogen deficiency
Androgen deficiency
Chronic diseases, e.g. gastrecomy, cirrhosis, hyperthyroidism, hypercortisolism
Physical Characteristics of Bone
Density (mass)
Size and geometry
Microarchitecture
Composition

Table 2: Risk factors for osteoporosis. Wasnich, 1997[7]

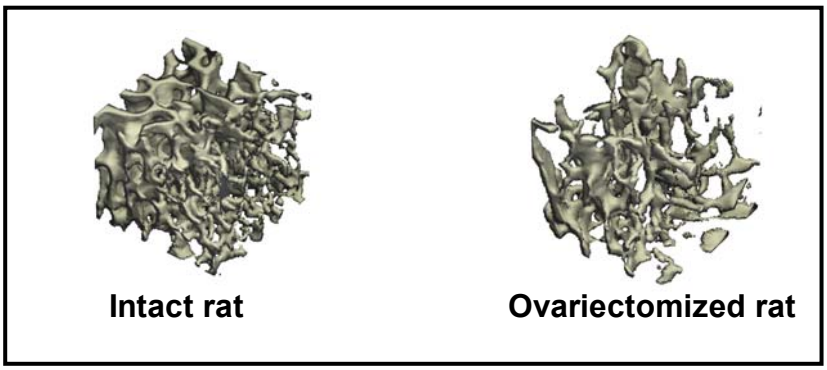

Figure 6: Effect of ovariectomy on the bone architecture of vertebrae. Missbach *et al.*, 1999[8]

Treatment of osteoporosis

Treatment of osteoporosis is a big research field nowadays. Most drugs available on market up to now are inhibitors of bone resorption. They act either via reducing osteoclast number (such as bisphosphonates and estrogen) or osteoclast activity

(cathepsin K inhibitors). However, in osteoporosis, bone loss may by far exceed the amount that can be restored by the inhibitors of resorption. Therefore, drugs that would act via promoting bone formation would be a tool for a highly desirable therapy. So far, injectable parathyroid hormone fragment (PTH) is the only known agent currently available for pharmacological stimulation of bone formation[9]. PTH therapy has quite a few limitations: different effects on different bones (concern about the quality of cortical bone), non-responder patient population, patient populations that should not receive it, limited duration of bone gain after the treatment, and treatment costs[10]. The research in a field of bone formation and control of osteoblast function is therefore very active, aiming for discovery of new and better anabolic agents.

2.2 Osteoblast lineage

The osteoblastic lineage cells that mediate the bone formation are comprising the following phenotypes: *mesenchymal stem cells (MSC)* that give rise to osteoprogenitor cells as well as the cells of other lineages; *osteoprogenitor cells* that contribute to maintaining the osteoblast population and bone mass; *pre-osteoblasts*, cells that started differentiation process but not yet synthesising bone matrix; *osteoblasts* that synthesise the bone matrix on bone forming surfaces; *osteocytes*, organised throughout the mineralized bone matrix that support bone structure; and the *lining cells* that protect the bone surface.

2.2.1 Mesenchymal stem cells

Postnatal bone marrow stroma contains cells that have both significant proliferative capacity and the capacity to form osteoblasts, chondroblasts, adipocytes, myoblasts and fibroblasts under appropriate conditions[11]. These are mesenchyme-derived stem cells, most commonly referred to as mesenchymal stem cells (MSCs) or stromal cells and are distinguished from the haematopoietic stem cell lineage present in bone marrow. Commitment of MSCs to tissue-specific cell types is orchestrated by transcriptional regulators that serve as “master switches” (Figure 7). Potency of these factors is reflected by their ability to induce cellular transdifferentiation of one phenotype to another through forced expression of a transcriptional regulator. For example, by expressing either adipocyte-specific transcription factor peroxisome proliferation-activated receptor γ2 (PPARγ2) in pre-osteoblasts or osteoblast-specific

transcription factor Runx2 in pre-adipocytes, respectively, the respective cell phenotype can be changed[12,13].

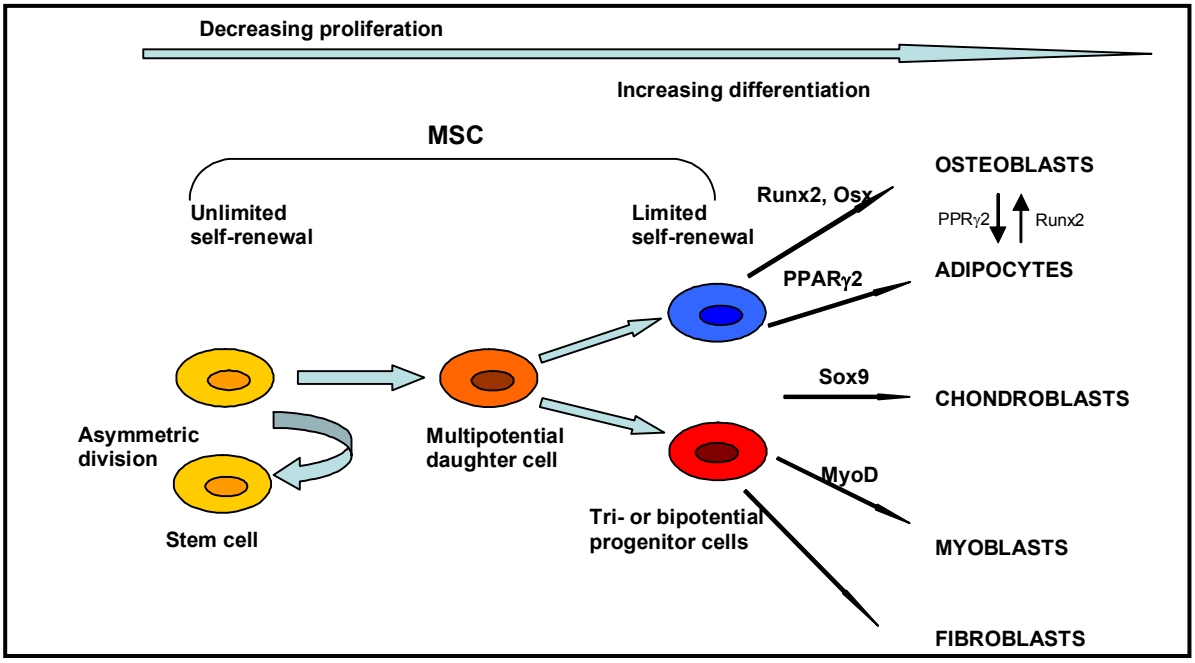

Figure 7: Stem cells commitment to mesenchymal phenotypes. Population of stem cells is dividing asymmetrically, each cell giving rise to one stem cell and one multipotential daughter cell. This is a starting point towards differentiation process. Multipotential daughter cell gives rise to usually tri- or bipotential progenitor cells. Final commitment to tissue-specific cell type is orchestrated by "master switches" transcription factors: Runx2 and Osx lead the cells towards osteoblast phenotype; PPARγ2 activation gives rise to adipocytes; chondroblasts are differentiating upon Sox9 activation; MyoD activation stimulates myogenesis. Modified from Lian *et al.*, 2003[11]

Dependent on a local cellular environment, already committed MSCs may dedifferentiate during proliferation and post-mitotically assume a different phenotype[14]. Such observations have led to a growing interest in the concept of "plasticity" of stromal and other adult stem cells.

Cells with features similar to adult bone marrow MSCs can be isolated from different sources. Some examples include: adult peripheral blood[15,16], fetal cord blood[17], fetal liver[18] or tooth pulp[19]. Possibility for using those cells with high regenerative potential in development of cell and gene therapy approaches for treatment of various diseases or in a reparative medicine is enormous and a highly exciting field nowadays.

2.2.2 Osteoblast differentiation process

Population of cells from bone marrow stroma or calvariae contains cells committed to the osteoblastic phenotype, osteoprogenitor cells, which will divide and differentiate into osteoblasts forming bone *in vitro*. Limiting dilution analysis has indicated that less then 1% of the cells in the, for example, rat calvaria cells are osteoprogenitor cells[20,21]. How many kinds of inducers mediate the commitment of MSCs to osteoprogenitor cells is not known yet, but molecules of TGFβ superfamily, TGFβ and bone morphogenic proteins (BMPs) appear to play regulatory role in this process[20,21]. Transcriptional regulators, members of helix-loop-helix (HLH) family of transcription factors, have been proposed to be mediators of keeping the osteoprogenitor cell in undifferentiated state[22]. Circulating or local, osteoblast-synthesized growth factors and cytokines bind to extracellular matrix (ECM) and provide, together with matrix proteins, microenvironment for recruitment of progenitor cells and differentiation process.

Committed pre-osteoblast is an early stage in osteoblast development, located near the bone surface, characterized by expression of alkaline phosphatase, the early marker of osteoblast phenotype.

Mature, active osteoblast is a polarized cell at the bone surface, usually of cuboidal shape, which is engaged in the production and secretion of extracellular matrix. This cell type is distinguished in bone sections by its large nucleus, enlarged Golgi complex and endoplasmic reticulum. Active osteoblasts have high expression of alkaline phosphatase and synthesize and secrete, at the side that is in contact with bone, collagen type I and non-collagenous proteins of osteoid.

On the quiescent bone surface, where the process of bone formation is finished, flattened osteoblasts that are becoming lining cells can be observed.

Process of osteoblast differentiation can be subdivided in three subsequent stages: 1) proliferation, 2) extracellular matrix synthesis and maturation, and 3) mineralization. Each stage is characterized by expression of distinctive osteoblast markers. Most frequently used markers of osteoblast differentiation process are alkaline phosphatase (ALP), collagen type I (Col1), osteopontin (OPN), bone sialoprotein (BSP), osteocalcin (OCN) and PTH/PTHrP receptor (PTHR). In general, ALP, BSP and Col1 are early markers of osteoblast differentiation, while PTHR and OCN appears late, concomitantly with mineralization. OPN peaks twice, during

proliferation and then again in the later stages of differentiation. The sequence of osteoblast differentiation process is shown on Figure 8.

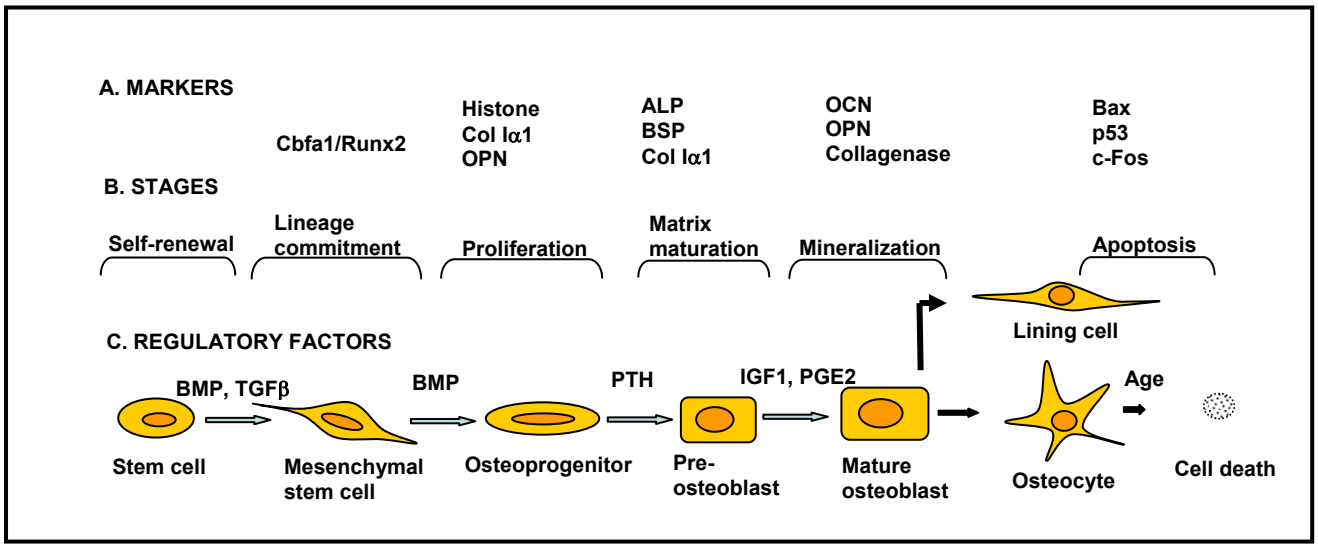

Figure 8: Osteoblast differentiation process. Modified from Lian *et al.*, 2003[11]

Regulation of osteoblast differentiation process

Factors involved in commitment, growth and differentiation of mesenchymal stem cells into osteoprogenitors and osteoblasts can be identified using several approaches: identification of genes involved in pathogenesis of human skeletal disorders; functional studies of knockout and transgenic mice that show skeletal phenotype; expression studies in bone tissue by *in situ* analysis; microarray analysis of gene expression during osteoblast differentiation process. Osteoblast differentiation process is under central (hormonal and neuronal), and local control (various growth factors and cytokines bound to ECM). Many factors have an effect on osteoblast differentiation process and the ultimate cell maturation is the result of their synchronized action. In the Table 3 major growth factors and hormones involved in osteoblast differentiation process are listed. Osteoblast-produced or circulating growth factors and cytokines are bound to the proteins of the bone ECM, where they locally influence the osteoblast differentiation process.

Growth factor / Hormone	*Human/mouse defect*	*References*
BMP2/4/7	Osteoinductive in numerous models	23
BMP3 (BMPantagonist)	Null mice : trabecular bone increased 2-fold	24
TGFβ	Constitutively active TGFβ1-Camurati-Engelmann disease	25
	TGFβ2 targeted expression: increased OB differentiation, but low bone mass	26
	TGFβ3 binding protein null mouse: ectopic ossification in skull; older mice develop osteosclerosis	27
Indian hedgehog (Ihh)	Null mouse:no bone collar; Chimeric Ihh-/- and PTHR-/- mice studies define Ihh as a signal for OB differentiation	28,29
Noggin (BMP antagonist)	Null mice: joint fusion of the appendicular skeleton	30
	Transgenic mice: osteopenia and fractures; impaired OB function; misexpression in calvarium prevents suture fusion	31
SOST (BMPantagonist)	Sclerosteosis and Van Buchem disease	32,33,34
FGF2	Major role in skeletal development	35
Wnt	Osteoporosis-pseudoglioma syndrome; high bone mass syndrome	36,37,38
Prostaglandins	Potent local regulators of bone cell function	39
GH, IGF-I	Stimulators of osteoblast proliferation and activity	40
PTH/ PTHrP	Targeted receptor inactivation: skeletal dysplasia	41
	Constitutive receptor activation : delayed bone formation	42
Leptin	Inhibitor of bone formation	43,44

Table 3: Major growth factors and hormones involved in bone formation and osteoblast differentiation process (modified from Lian *et al.*, 2003[11]).

Central control of osteoblast differentiation

Two principal hormonal regulators of bone metabolism and osteoblast differentiation are parathyroid hormone (PTH) and adipocyte-produced hormone leptin.

Bone serves as major source of calcium ions. Calcium release requires bone destruction, and the principal mediators of this process are PTH hormone and its downstream effector [1,25$(OH)_2$ vitamin D] [45]. Administration of PTH leads to release of calcium from a rapidly turning-over pool of calcium near the surface of bone; after

several hours, calcium is also released from an additional pool that turns over more slowly. Chronic administration of PTH (or increased secretion of PTH associated with primary hyperparathyroidism) leads to an increase in osteoclast cell number and activity, and ultimately results in increased bone resorption. The osteoblasts and its precursors, the marrow stromal cells, have central roles in directing the catabolic (bone resorption) effect of PTH. Oseoblasts abundantly express on their surface the PTH/PTHrP receptor. PTH administration stimulates in osteoblasts expression of RANKL and M-CSF, molecules that support osteoclastogenesis. At the same time, PTH inhibits expression of OPG in osteoblastic cells, a soluble decoy receptor for RANKL that competes withg osteoclastic receptor RANK for binding of RANKL. This, by increasing M-CSF and RANKL and inhibiting OPG expressed locally by cells of the osteoblast lineage, PTH stimulates osteoclastogenesis and the activity of mature osteoclasts (reviewed in Jueppner *et al.*, 2004[45]).

At the same time, intermittent application of PTH has anabolic effect on bone, by increasing osteoblast number and activity, and it is used in therapy of osteoporosis[9]. The mechanism whereby PHT increases bone formation is complicated and less well understood.

Leptin, adipocyte-produced hormone acts as a physiological inhibitor of bone formation. This inhibition is achieved by leptin action on subpopulation of hypothalamic neurons, which then act through sympathetic nervous system and β2 adrenergic receptors present on osteoblasts. Mice lacking leptin or leptin receptor gene have increased bone formation[43,44].

Local control of osteoblast differentiation: Bone Morphogenic Proteins

A number of growth factors and cytokines influence osteoblasts in the various stages of differentiation process. The most potent local factors, which are also used in this study, are the bone morphogenic proteins (BMPs), members of transforming growth factor β (TGFβ) superfamily.

Bone morphogenic proteins were first described as constituent of demineralized bone matrix that induced ectopic bone formation in muscular tissues of rodents[46]. At present, at least 15 BMPs have been cloned. They are all members of transforming growth factor ß (TGF- ß) superfamily of secreted signalling molecules, except of BMP-1 (metalloproteinase). BMPs are synthesised as large precursors that form

homo- or heterodimers. Proteolytic cleavage releases the biologically active C-terminal dimer with 7 highly conserved cysteines (reviewed in[47]).

BMPs play an important role in development and growth of bone (reviewed in[23]). However, evaluation of role of individual BMPs is complicated because of a few in vitro studies with the same cell system and because of use of bone-derived BMPs, which usually present a mixture of different BMPs. For several recombinant BMPs (BMP2, BMP4, BMP7) it was shown that they induce ectopic bone formation in vivo; in vitro they induce the differentiation of MSC into osteoblasts (increase ALP activity and mineralization). They are called osteogenic BMPs[47].

BMPs exert their effect through signaling via BMP receptor type I and II (serine/threonine kinase) and BMP signaling molecules, Smad 1, 5 and 8 transcription factors (receptor regulated Smads or R-Smads), which become phosphorylated by the receptor, translocated to the nucleus in a complex with common partner protein, Smad4, where they regulate transcription of target genes. (Figure 9). Inhibitory Smads (I-Smads), Smad 6 and 7, compete with R-Smads for binding for Smad4 and present a negative regulation of this signaling pathway (reviewed in Sakou, 1998[47]).

BMP regulation of osteoblast gene expression involves direct interaction of R-Smad-Smad 4 complexes with enhancer sequences of target genes (Smad binding elements or SBEs)[48], binding of Smads to other nuclear factors, the most important being cooperative action with Runx2[49], as well as up-regulation of separate transcription factors necessary for osteoblast differentiation, including Runx2 and Osterix (Osx)[48,50,51].

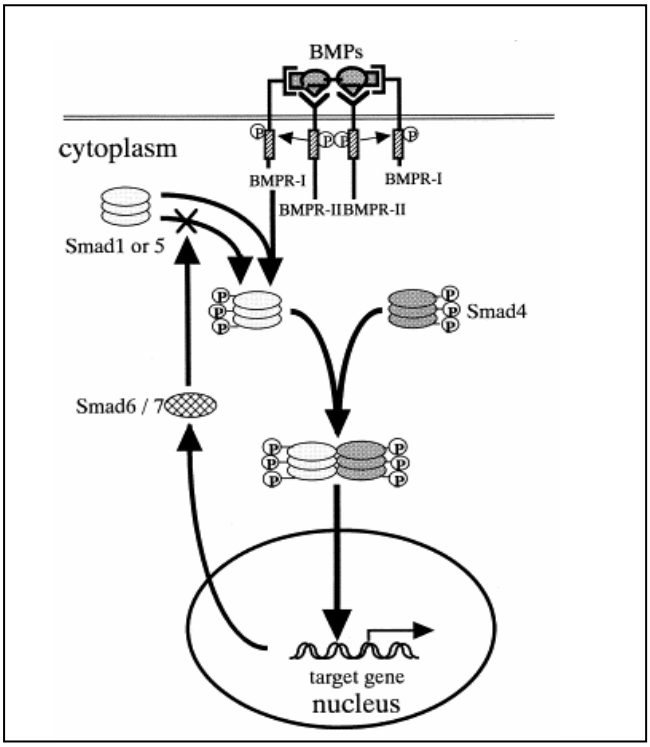

Figure 9: BMP signaling pathway. Sakou, 1998[47]

2.3 Transcriptional control of osteoblast differentiation

2.3.1 Runx2

The first described osteoblast-specific transcription factor and the "master switch" for osteoblast differentiation from MSCs is Runx2, also known as osteoblast-specific factor (Osf-2), polyomavirus enhancer binding protein 2αA (PEBP2αA) or core binding factor α (Cbfa1). Runx family of transcription factor proteins consists of three known members (Runx1-3) that share a high degree of sequence homology within their coding regions and in gene organization. The amino terminal part of these proteins comprises a region of 128 amino acids with conserved sequence homology to the Drosophila transcription factor *runt.* This so-called Runt Homology Domain (RHD) binds to DNA in a sequence specific manner. All members of Runx family play a role in various cell differentiation process. While Runx1 is essential for mature haematopoiesis, Runx3 has a function in nervous system (reviewed in Otto *et al.*, 2003[52]). The loss of Runx3 function is also often seen in gastric cancer[53].

Runx2 was shown to be essential for osteoblast differentiation in Runx2 knockout mice that have no osteoblasts and, consequently, no bone, but just a cartilage

"anlagen"[54,55]. In humans, heterozygous mutations in Runx2 cause cleidocranial dysplasia (CCD), a disorder characterized by hypoplasia or aplasia of the clavicles, short stature, supernumerary teeth, patent fontanelles, and other changes in skeletal patterning and growth[56]. Heterozygous Runx2 knockout mice have abnormalities that are characteristic of CCD, confirming that CCD derives from haplo-insufficiency of Runx2[54,55]. Runx2 is also expressed in differentiated osteoblasts and trans-activates genes involved in the deposition of bone matrix, such as osteocalcin, type I collagen, osteopontin and collagenase 3 by binding to specific enhancer regions containing the core binding sequence, PuCCPuCA[57,58,59,60]. This findings further indicated a role for Runx2 in mature osteoblasts.

Runx2 gene and protein

The human *Runx2* gene resides on chromosome 6p21, occupying over ≈ 250 kb. It consists of 8 exons and it is transcribed from two separate promoters, P1 and P2 (Figure 10A). The upstream promoter, which utilizes the first 5' exon of *Runx2,* drives the expression of osteoblast-specific forms of Runx2, named type II isforms (reviewed in Levanon *et al.*, 2004[61]). P2 promoter is located within intron 1 and drives the expression of isoforms that are mainly expressed in T-cells[62,63], but also in osteoblasts and other mesenchymal cells[64,65]. This kind of dual promoter organization is shared with other *Runx* genes*, Runx1* and *3*. Both P1 and P2 promoters in all 3 genes contain several dispersed Runx-binding sites, raising the possibility of cross-regulation between the *Runx* genes (reviewed in Levanon *et al.*, 2004[61]). Both P1- and P2-promoter-derived primary transcripts are processed into a diverse repertoire of alternatively spliced mRNA isoforms that are differentially expressed in various cell types and at different developmental stages (reviewed in Zhang *et al.*, 2000[49], Levanon *et al.*, 2004[49,61]). They give rise to different protein isoforms. The most abundant Runx2 isoforms in osteoblasts are so called "MASN/p57" or "type II", osteoblast-specific, isoform, whose expression is driven by P1 promoter[56]. Second main isoform is "MRIPVD/p56" or "type I" isoform, more widely expressed, which is the first described Runx2 protein in T cells. The expression of type I Runx2 is driven by the P2 promoter[63].

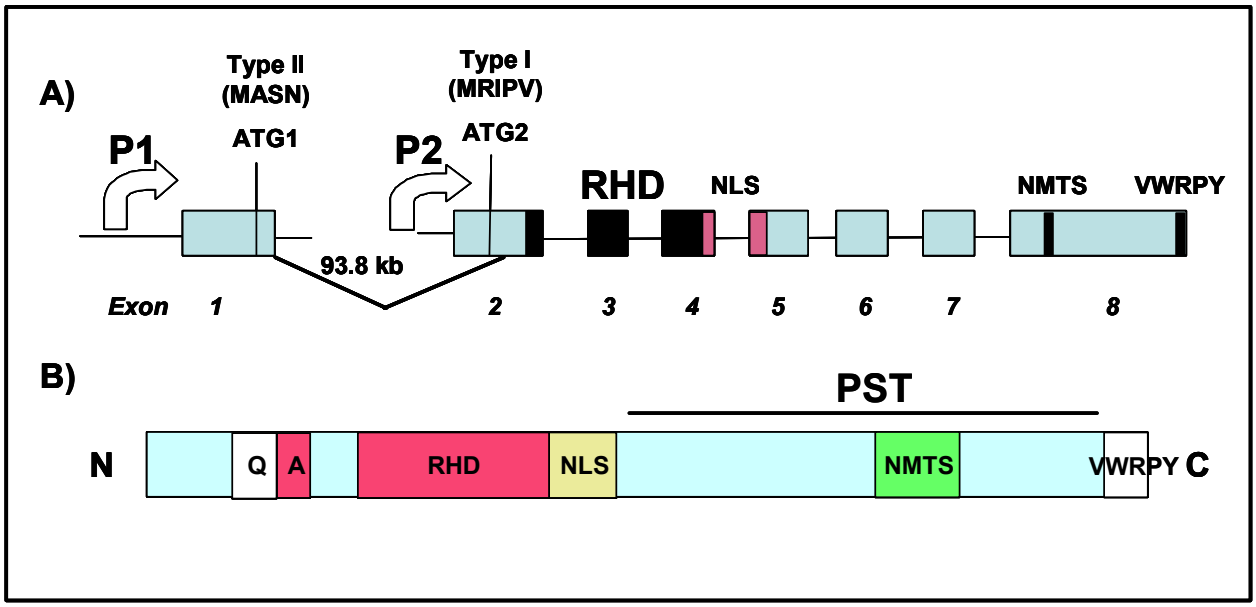

Figure 10. A) Schematic structure of *Runx2* gene. B) Schematic structure of Runx2 protein. RHD - runt homology domain; NLS – nuclear localization signal; NMTS – nuclear matrix targeting signal; PST – proline, serine and threonine rich domain

Runx2 protein structure is shown on Figure 10B. Type I and II isoforms differ only in few N-terminal amino acids. They both contain stretches of glutamine (Q) and alanine (A) that serve as transactivation domains; runt homology domain (RHD), which is a DNA binding domain and also can serve as a transactivation domain; nuclear localization signal (NLS); C-terminal PST domain, rich in proline, serine and threonine, which includes nuclear matrix targeting signal (NMTS) and transactivation sequences; C-terminal end motif VWRPY, which is conserved among all runt proteins [49,50,63,66,67].

Type I and II isoforms of Runx2 protein were presumed to have distinct roles based on the predominant expression of the type II isoform in osteoblasts, and the type I isoform in non-osseous tissues, but their separate functions have not been experimentally established. In the recent study, selective Runx2-II-deficient mice have been generated by targeted deletion of the distal promoter and exon 1, to assess the role of the "bone-specific" isoform in skeletogenesis[68]. Unexpectedly, homozygous knockout mice still formed axial, appendicular, and craniofacial bones derived from either intramembranous ossification or mesenchymal cells of the bone collar, but they failed to form the posterior cranium and other bones derived from endochondral ossification. Heterozygous Runx2-II-defficient mice had grossly normal skeleton, but were osteopenic. The commitment of mesenchymal cells ex vivo to the osteoblast lineage occurred in Runx2-II -/- mice, but osteoblastic gene expression

was impaired, with largely decreased expression of osteoblast markers, alkaline phosphatase, osteocalcin and osteopontin, and Osterix, a transcriptional regulator down-stream of Runx2. Compensatory increase in Runx2-I expression occurred in Runx2-II -/- mice. The authors concluded that Runx2 I and II isoforms have distinct function in the control of skeletogenesis: Runx2-I is sufficient for early osteoblastogenesis and intramembranous ossification, whereas Runx2-II is necessary for complete osteoblastic maturation and endochondral bone formation.

Regulation of Runx2 activity

Runx2 is a focal point where a variety of signals affecting osteoblast activity integrate. Therefore, regulation of its activity is a very important issue. Runx2 activity is regulated on transcriptional, translational level, by post-translational modification, subnuclear targeting or by interacting with partner proteins.

Transcriptional regulation of Runx2 gene

Functional analysis using transfection assays have demonstrated that both P1 and P2 region of *Runx2* gene possess promoter activity[69,70,71]. Several Runx binding sites have been identified in both proximal and distal promoters, suggesting auto-regulation and cross-regulation of different Runx genes[72]. In vitro studies by several groups evaluated the bone specific activity of Runx2 P1 distal promoter. Two distinct sites regulating transcriptional activity from this promoter have been identified: an NF1 site seems to bind NF1-A in non-osseous cells and suppress *Runx2* activity, while an AP1 site preferentially binds FosB to increase transcription in osteoblastic cells[71]. Furthermore, the transcription factors Msx2, Bapx1, Hoxa-2, PPARγ2 and Twist have been shown to regulate Runx2 expression, although no evidence for a direct interaction of these factors with the Runx2 promoters could be demonstrated so far[73,74,75,76,77].

A number of cytokines have been shown to influence expression level of Runx2. Bone morphogenic proteins (BMPs), best characterized inducers of osteoblast differentiation, and of bone formation in vivo after local application, exert their effect mostly by activating the transcription of Runx2 via Smad proteins[48,50,78]. TGFβ suppresses Runx2 expression in primary calvarial osteoblasts, and this inhibition is mediated by Smad3, TGFβ signaling Smad, which also interact physically with Runx2

and represses its transcriptional activity on Runx2-binding OSE2 promoter sequence in the promoter of Runx2[79]. However, in C2C12 myoblasts, TGFβ induces Runx2 expression[78]. The different effect on Runx2 expression may reflect the cellular context of accessory proteins in control of Runx2 expression. FGF, another growth factor important for osteoblast differentiation and proliferation, was also shown to regulate Runx2 expression[80].

Translational and post-translational regulation of Runx2

P1 and P2 promoter usage produces *Runx2* mRNA with two different 5' untranslated regions (UTR1 and UTR2). Both UTR1 and 2 are long and have complex secondary structure, which could potentially inhibit cap-dependent translation. However, both elements possess internal ribosome entry site (IRES) elements, which permit fine tuning of Runx2 expression over the wide range of cellular conditions that do not favor cap-dependent translation. For example, IRES elements of Runx2 5'UTR1 and 2 mediated increased translation under genotoxic stress induced by mitomycin C and during osteoblast maturation[81,82].

The most important post-translational activating modification of Runx2 protein is a phosphorylation in the PST domain. This phosphorylation event is crucial for Runx2 to be transcriptionally active. Phosphorylation can be stimulated by several signaling pathways, as shortly described below and shown on the Figure 11 (reviewed in Franceschi et Xiao, 2003[83]):

1) Osteoblasts must establish a type I collagen-containing extracellular matrix (ECM) before they can differentiate, express osteoblast-related genes and, ultimately, mineralize. The ECM signals to the differentiating preosteoblasts by binding to β1 subunit-containing integrins (α2β1 and, possibly, α1β1). This binding activates focal adhesion kinase (FAK) and, ultimately, MEK/ERK branch of the MAPK pathway. MAPK phosphorylates and activates Runx2 in the PST domain in the C-terminal portion of the molecule, although the specific amino acid residues that get phosphorylated have not been identified yet.

2) FGF2 stimulation of osteoblasts also results in Runx2 phosphorylation and activation, since activation of receptor tyrosine kinase through Ras and Raf also leads to MAPK pathway activation.

3) Mechanical loading plays and important role in the regulation of bone homeostasis and skeletal morphology, by increasing bone density and strength. It is shown that MAPK pathway via integrin stimulation is also one of the principle signal transduction pathways associated with mechanotransduction, therefore leading to Runx2 phosphorylation and activation.

4) The classic protein kinase A (PKA) pathway activated by parathyroid hormone/parathyroid hormone related peptide (PTH/PTHrP) also results in phosphorylation of Runx2 on PKA-specific sites distinct from those utilized by MEK/ERK pathway. Alternatively, stimulation of the MAPK pathway via protein kinase C (PKC) is a potential route for cross-signaling from the PTH/PTHrP receptor via Gq proteins. The PKA pathway also up-regulates AP-1 related factors like c-Fos and c-Jun by phosphorylation of cAMP response element binding proteins (CREBP). AP-1 factor binds to AP-1 sites in osteoblast-related genes as well as interact with Runx2[84,85].

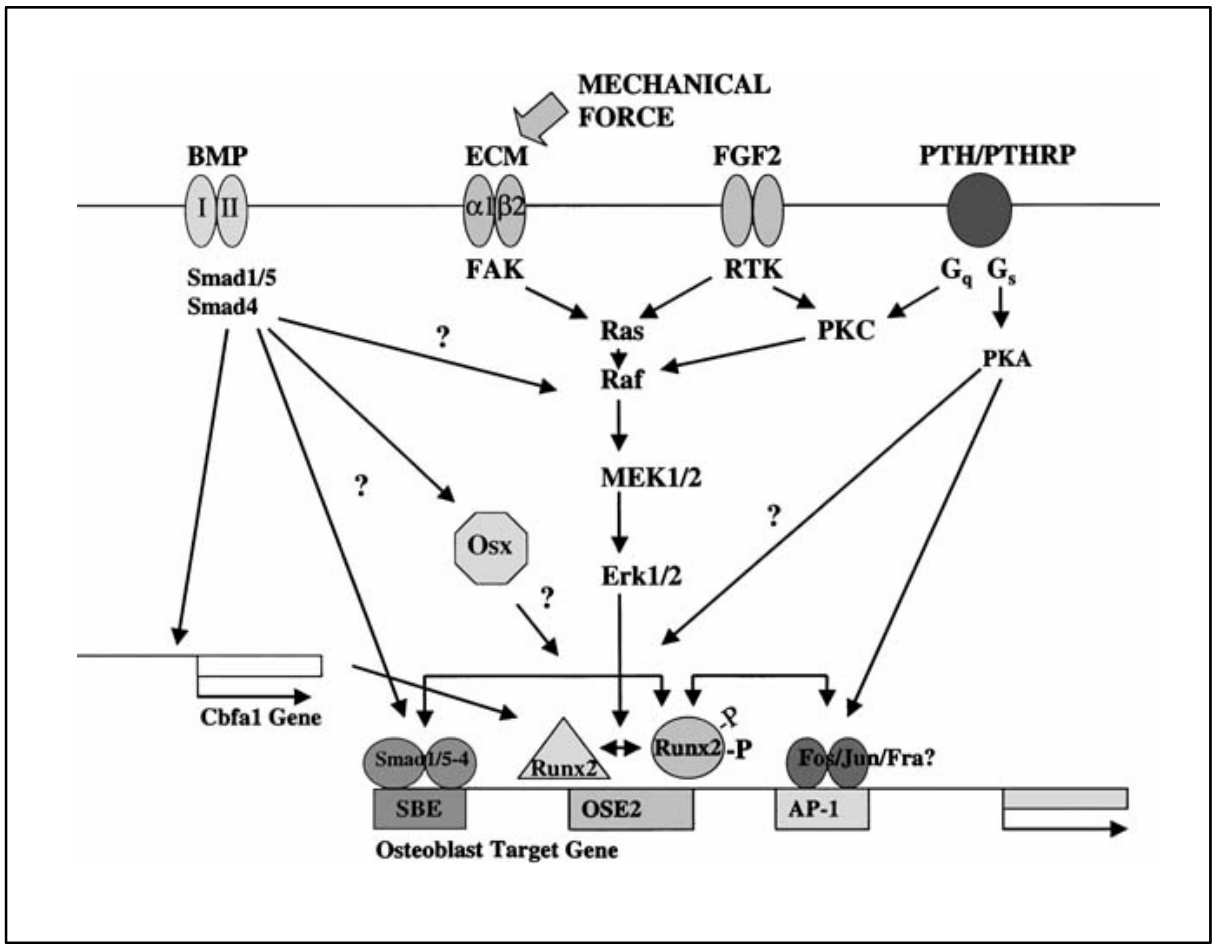

Figure 11: Overview of signal transduction pathways affecting Runx2 activity. Franceschi et Xiao, 2003[83]

Subnuclear targeting of Runx2 protein

Deletion of intranuclear targeting signal in the C-terminal exon of the Runx2 gene results in severe phenotype of complete absence of intramembranous and endochondral bone formation. Mutant protein is expressed at normal level and retains DNA binding and nuclear import properties, which underlies the importance of Runx2 interaction with proteins of nuclear matrix and its subnuclear localization, since loss of this function has the same phenotype as the complete loss of Runx2 in knockout mice[67].

Runx2 interacting proteins

Many transcription factors involved in regulation of osteoblast differentiation process exert their action by interacting with Runx2.

Non-DNA binding core-binding factor β (Cbfβ) is obligatory heterodimerizing partner of Runx1 and 3. Mice lacking Cbfβ die during embryogenesis due to defects in haematopoiesis[86]. Transgenic rescue of haematopoiesis in embryonic lethal Cbfβ-null mice by introducing Cbfβ using the Gata1 promoter allowed survival of mice, but they showed severely delayed ossification, indicating a role of Runx2-Cbfβ dimerisation in bone[87,88]. However, unlike Runx2-null mice that completely lack bone and osteoblasts, ossification is initiated in these mice, suggesting that Runx2 can act with a reduced efficiency in the absence of Cbfβ. Therefore, for a full activity of Runx2, Cbfβ is clearly required, in contrast to an initial proposal by the group of Karsenty[66].

Interaction of Runx2 with AP-1 transcriptional complex is well-established. Studies of collagenase 3 (Matrix Metalloprotease 13, MMP13) gene promoter have been particularly informative in studying this interaction. Parathyroid hormone induces collagenase-3 gene transcription in rat osteoblastic cells. The minimal parathyroid hormone-responsive region in the promoter of collagenase 3 contains two conserved enhancer sequences, a Runx2 binding site and an AP-1 binding site. These two sequences are necessary for the responsiveness to PTH: Overexpression of c-Fos, c-Jun, Runx2, and Cbfβ increased the response to parathyroid hormone of the wild type promoter, but not of promoter containing mutations of either or both the activator protein-1 and runt domain binding sites[89]. Runx2 and AP-1 showed cooperative

function in response to PTH, which suggested their direct interaction. Indeed, immunoprecipitation experiments and yeast two-hybrid studies proved interaction of c-Jun and c-Fos with Runx2, which depends on the leucine zipper domain of c-Fos or c-Jun and on the Runt domain of Runx2. Insertion of base pairs that disrupted the helical phasing between the AP-1- and RD-binding sites also inhibited collagenase-3 promoter activation, indicating that physical contact between AP-1 and Cbfa transcription complexes was disrupted[84,85].

Interaction of Runx2 with Smad transcription factors, signaling molecules of TGFβ superfamilly, occurs at several levels. Both BMP- and TGFβ- regulated Smads regulate expression of Runx2[78]. In addition, Runx2 and Smad proteins also physically interact and cooperatively activate osteoblast-specific genes, such as osteocalcin[79]. Runx2 is shown to interact with BMP-regulated Smad1 in C2C12 cells[49], or with TGFβ- regulated Smad 3 in 10T1/2 and ROS cells[79], only after the cells are treated with either BMP or TGFβ, respectively, which brings Smads into the activated, phosphorylated form.

Signal transducers and activators of phosphorylation (Stat) are family of latent transcription factors in the cytoplasm, activated by tyrosine phosphorylation as a response to various growth factors, hormones and cytokine signaling. In bone, Stat-1 transcription factor is important in mediating inhibitory effect of interferon γ and β on osteoclastogenesis[90,91]. In the bones of Stat-1 deficient mice excessive osteoclastogenesis is observed. However, the bone mass is unexpectedly increased in these mice, caused by excessive osteoblast differentiation. Latent, non-phosphorylated form of Stat-1 was shown to interact with the Runt domain of Runx2 in the cytoplasm, inhibiting its nuclear localization and activation of osteoblast genes, like osteocalcin and osteopontin. Activation and phosphorylation of Stat-1 release Runx2, allowing activation of osteoblast genes and cell differentiation. In the absence of Stat-1, Runx2 is not inhibited and osteoblast differentiation process is excessive[92].

Twist-1 and Twist-2 are vertebrate basic helix-loop-helix transcription factors, important for embryonic development. Knockout mice of either of these genes are lethal: Twist-1 is required for closure of the neural tube during mouse development[93], while mice homozygous for a Twist-2 null allele show elevated expression of proinflamatory cytokines causing perinathal death[94]. Twist-1 heterozygotes (both in mice and humans) exhibit craniosynostosis, a disease caused by premature osteoblast differentiation in the skull[95,96]. This phenotype is almost an exact opposite

of cleidocranial dysplasia, a phenotype of Runx2 heterozygot knockout mice. It is shown that double heterozygotes for Twist-1 and Runx2 deletion have none of the skull abnormalities, while Twist-2-null background saves clavicle phenotype of Runx2+/- mice. Twist-1 or-2 deficiency leads to premature osteoblast differentiation, seen by premature osteocalcin expression and mineralization staining in developing bones. Twist-1 overexpression in ROS 17/2.8 osteoblastic cells led to a decrease in expression of osteocalcin, a direct Runx2 target gene, without affecting Runx2 expression[22]. Therefore, Twist proteins are "anti-osteogenic" proteins, which bind to and inhibit Runx2 activity. This interaction is mediated by a novel domain, the Twist box, which directly interacts with the Runt domain of Runx2[22]. In embryonic development, Twist-1 and -2 are expressed in Runx2-expressing cells throughout the skeleton early during development, and osteoblast-specific gene expression occurs only when the expression of Twist-1 and -2 decreases[22].

By using C-terminus of Runx1 in a yeast two-hybrid screen, its interaction with a member of Groucho /Transducin-like enhancer of split (TLE) /R-esp repressor proteins was unraveled. The interaction involves a 5 amino acid C-terminal sequence from Runx1 (VWRPY), which is conserved in the Runx family[97]. Co-expression assays revealed that mammalian TLE proteins repress transcriptional activity of all three Runx proteins on osteocalcin promoter[97]. TLE 1 and 2 co-localize with Runx proteins in the nucleus and associate with the nuclear matrix. For Runx2, it was shown that Hes1, a mammalian counterpart of the Drosophila Hairy and Enhancer of split family member, can antagonize the binding of Runx2 to TLE proteins, and potentiate Runx2-mediated transactivation. Hes1-Runx2 physical interaction is mediated by the C-terminal domains of both proteins[98].

Runx2 protein is shown to interact with a number of transcriptional co-activators. Direct Runx2 binding and increasing the activation of Runx2 target genes was shown for retinoblastoma protein (pRb)[99], transcriptional co-activator with PDZ-binding motif (TAZ)[100], p300 histone acetyltransferase[101]. Isoform of adipogenic transcription factor CAAT/enhancer binding protein β (C/EBPβ), liver-enriched inhibitory protein (LIP), which lacks the transcriptional activation domain, is recently shown to stimulates transcriptional activity and the osteogenic action of Runx2[102].

Few co-repressors were also shown to be important for regulating Runx2 activity. Groucho /Transducin-like enhancer of split (TLE) /R-esp repressor proteins were mentioned above[97]. Histone deacetilase 4 (HDAC4), is shown to be interacting with

and inhibiting the activity of Runx2 in chondrocyte hypertrophy[103]. HDAC4-null mice display premature ossification of developing bones due to ectopic and early onset chondrocyte hypertrophy, mimicking the phenotype that results from constitutive Runx2 expression in chondrocytes. Conversely, over-expression of HDAC4 in proliferating chondrocytes *in vivo* inhibits chondrocyte hypertrophy and differentiation, mimicking a Runx2 loss-of-function[103].

2.3.2 AP-1

The AP-1 family of basic leucine zipper transcription factors comprises various combinations of Jun (c-Jun, JunB, and JunD) and Fos (c-Fos, FosB, Fra-1, and Fra-2) family proteins, which regulate gene transcription by binding as dimers to consensus response elements 5'-TGAG/CTCA-3' in the promoter regions of target genes[104]. While the Fos proteins can only heterodimerize with the members of the Jun family, the Jun proteins can both homo- and heterodimerize with Fos members to form transcriptionally active complex. AP-1 has been implicated in a large variety of biological processes including cell differentiation, proliferation, apoptosis, and oncogenic transformation[105]. Several studies have demonstrated an important regulatory role of AP-1 factors, especially the Fos-related proteins, in bone formation and osteoblast function, as well as in formation and activity of osteoclasts. These data are largely derived from the analysis of genetically modified mice, in which specific AP-1 genes have been ectopically expressed, inactivated, mutated, or replaced by each other (Table 4).

Knockout		Phenotype	Affected organs/cell types	References
c-Fos		Osteopetrosis	Bone/osteoclasts	106,107
FosB		Nurturing defect	Brain/hypothalamus	108,109
Fra-1		Embryonic lethality (E9.5)	Extra-embryonic tissue/yolk sac,	110
		KO only in embryo-osteopenia	Placenta/labyrinth layer Bone/ osteoblasts	111
Fra-2		*Not reported*		
c-Jun		Embryonic lethality (E12.5)	Liver/hepatoblasts Heart/outflow tract	112
JunB		Embryonic lethality (E8.5-10)	Extra-embryonic tissue/giant thophoblast, yolk sac, Placenta/labyrint layer	113 114
		KO only in embryo-osteopenia	Bone/ osteoblasts and osteoclasts	
JunD		Male sterility	Testis/spermatogenesis	115
Transgene	**Promoters**	**Phenotype**	**Affected organs/cell types**	**References**
c-Fos	H2kb	Osteosarcoma	Bone/osteoblasts	116
FosB	H2kb	None		116
ΔFosB	TCRb	Impaired T cell	Thymus/immature thymocytes	117
	NSE	differentiation Osteosclerosis	Bone/osteoblasts	118
Fra-1	H2kb	Osteosclerosis	Bone/osteoblasts	119
Fra-2	CMV	Occular malformation	Eye/anterior eye structures	120
c-Jun	H2kb	None		116
JunB	Ubiquitin C	None		121
	CD4	Enhanced Th2 maturation	Thymus/CD4 thymocytes	122
JunD	*Not reported*			

Table 4: AP-1 knockout and transgenic mice phenotypes. Jochum *et al.*, 2001[105]

AP-1 activity in osteoblasts can be induced by TGFβ / BMP growth factors, by parathyroid hormone or 1,2-dixidroxy vitamin D[123]. The various members of the AP-1 complex are differentially expressed during osteoblast maturation *in vitro*, with all Fos and Jun proteins initially, during the proliferative phase, being highly expressed. Subsequently, during the period of extracellular matrix production and mineralization, their level decline, and Fra-2 and JunD become the major components of AP-1 complex in fully differentiated osteoblasts (reviewed in Wagner, 2002[124]).

The pattern of c-Foc expression during development suggests its critical role in endochondral ossification, although the analysis of c-Fos-deficient mice shows that c-Fos is dispensable for the differentiation of osteoblasts, while it is necessary for osteoclasts formation[106,107]. Ectopic c-Fos expression from a ubiquitous promoter results in specific transformation of osteoblasts, leading to osteogenic sarcomas

reminiscent of human osteosarcomas, majority of which have elevated level of c-Fos protein[116,125].

Interesting phenotype was observed in Fra-1 transgenic mice: transgenic mice ubiquitously overexpressing Fra-1 (under the control of the major histocompatibility complex cless I antigen H2-K^b gene promoter) develop a specific bone phenotype, with increased bone formation and osteosclerosis of the entire skeleton [119]. This phenotype in due to a cell autonomous increase in the number of mature osteoblasts, indicating that Fra-1 increases osteoblast differentiation. The life span of transgenic mice was up to 9 months, when they showed severe splenomegaly due to extramedullary haematopoiesis, because the marrow space was almost entirely filled with lamellar bone. In addition, some transgenic mice developed liver cirrhosis and bronchoalveolar tumors, but there was no evidence for any kind of bone tumor.

Similar dramatic increase in bone formation is observed in mice overexpressing naturally occurring truncated splicing isoforms of FosB, ΔFosB and Δ2ΔFosB under the control of the neuron-specific enolase (NSE) promoter, which provided high expression in brain, bone and adipose tissue[118]. Both truncated isoforms maintain the ability of DNA binding and heterodimerization with Jun proteins, but they lack the major C-terminal transactivation domain, and Δ2ΔFosB lack in addition a potential N-terminal transactivation domain. If they are expressed under the control of non-restricted NSE promoter, mice develop in addition the dramatic decrease in adipose tissue[118]. Thus, ΔFosB affects osteoblasts and adipocyte differentiation by mechanisms that do not require its own transcriptional activity. Since it was shown that ΔFosB and Δ2ΔFosB can interact with other AP-1 family members and with Smads, Runx2 and CEBP-β, they are likely to induce osteoblast and inhibit adipocyte differentiation by interfering with the activity of other transcription factors [118,126,127].

Recently, embryonic lethality of JunB and Fra-1 knockout was rescued by a specific gene deletion only in embryonic tissues, while the expression in placenta was not affected. Placental defects were the cause for lethality in knockout animals. Both JunB and Fra-1 knockout mice develop osteopenia[111,114]. JunB Δ/Δ osteoblasts and osteoclasts show reduced proliferation and differentiation *in vivo* and *in vitro*[114]. Fra-1 Δ/Δ osteoblasts show reduced expression of some bone matrix components, such as osteocalcin, collagen 1α2 and matrix Gla protein, while other matrix protein synthesis and other markers of osteoblast differentiation (ALP, Runx2 level) appear normal.

The gene for matrix Gla protein seems to be a specific target of Fra-1, since its expression was markedly increased in the long bones of Fra-1 transgenic mice[111].

2.3.3 Osterix

Osterix (Osx) is a zinc finger-containing transcription factor, initially described as induced by BMP-2 in C2C12 myoblastic cells[51]. These cells differentiate into osteoblasts upon stimulation with BMP. In Osx- null mice, no bone formation occurs: mice develop a perfectly patterned skeleton composed entirely of cartilage, lacking osteoblasts and mineralized bone matrix. Unlike Runx2 null mice, the cartilage of Osx-null mice is normal, pointing to a specific role of Osx only in osteoblast differentiation. Osx is not expressed in Runx2-null mice, while Runx2 is normally expressed in Osx-null mice. These findings suggested that Osx acts genetically downstream of Runx2 to induce osteoblastic differentiation in bi-potential Runx2-expressing chondro-osteo progenitor cells[51]. Recent findings, however, showed Osx expression was still induced by BMP-2 in C2C12 cells expressing dominant-negative Runx2 mutant, and in calvarial cells form Runx2-knockout mice, and not induced by Runx2 overexpression in C2C12 myogenic cellls. Instead, Osx induction by BMP-2 was completely abrogated by the antisense blocking of Dlx5, indicating that Osx experession is mediated by Dlx5[128]. Further work is necessary to clarify the hierarchy and specific roles of Runx2, Osx and Dlx5.

2.3.4 Msx and Dlx homeobox transcription factors

Homeobox-containing transcription factors of the Msx (Msh homeobox homolog) and Dlx (distal-less homeobox) family are expressed in the early stages of osteoblast differentiation and are proven to be important for the skeletal development: mutations in mice and human show that they are important mainly for normal intramembranous ossification, although Dlx5/Dlx6-null mice have defects also in the axial and appendicular skeleton[129,130]. *In vitro*, Msx2 is transiently up-regulated upon BMP- 2 treatment and it has been shown to stimulate osteoblast differentiation, while inhibiting adipocyte differentiation[131]. Dlx2 and Dlx5 are also BMP2-regulated genes[132] and Dlx5 was shown to be indispensable for BMP-2 induced Runx2 up-regulation in C2C12 cells[128,133].

2.3.5 Id transcription factors

Id (inhibitor of DNA binding) proteins belong to the family of helix-loop-helix proteins lacking a basic region and function as dominant-negative regulators of bHLH proteins during growth and differentiation by dimerizing with bHLH factors and inhibiting their binding to DNA (reviewed in Ruzinova *et al.*, 2003[134]). There are four members of this family, Id1-4, which have partially overlapping expression patterns and certain levels of functional redundancy. Id1-3 genes were shown to be activated by BMP signaling pathway: Id1-3 expression is strongly up-regulated during early stage of BMP stimulation in mesenchymal stem cells and is necessary for the induction of osteoblast differentiation. However, constitutive expression of Id1-3 genes also inhibited osteoblastic differentiation[135]. This findings suggest that the Id HLH proteins may play an important role in promoting the proliferation of early osteoblast progenitor cells, and that Id expression must be down-regulated during the terminal differentiation of committed osteoblasts. The proteins that interact with Id factors during osteoblast differentiation remain to be identified.

2.4 Conclusion

In conclusion, some molecular players that take part in osteoblast differentiation process have been described so far, but their exact function and interconnection is still largely unknown, and there are many unknown components of this process. With the development of new tools in molecular biology, above all microarray analysis of gene expression profiles, it has become possible to obtain a broader, comprehensive picture of molecular events during differentiation or other events studied. Therefore, the aim of this work was:

1.) to set up analysis of osteoblast differentiation at molecular level by analyzing profiles of marker genes.

2.) to choose the optimal *in vitro* model of osteoblast differentiation, which differentiates fast and in a reproducible manner, and up-regulates the largest number of marker genes.

3.) with a differentiation system chosen, to perform microarray analysis of genes regulated during early phases of the differentiation process, and to statistically and functionally analyze regulated genes.

4.) among regulated genes, to choose interesting candidates for further analysis and to analyze more in-depth the function of selected candidate genes in the osteoblast differentiation process.

We believed that this global approach together with the careful control of each step could provide us with a general picture of molecular events during the osteoblast differentiation process, and highlight new interesting players. Better knowledge about the events during the maturation of cells that form bone is the first, and we believe, essential step towards generating the new and very much needed anabolic agents that could promote bone formation and be used in the treatment of osteoporosis.

3 Results

3.1 Coordinated activation of Notch, Wnt and TGF-β signaling pathways in BMP-2 induced osteogenesis: Notch target gene Hey1 inhibits mineralization and Runx2 transcriptional activity

Journal of Biological Chemistry, 2004 September 3rd; 279 (36): 37704-37715

Natasa Zamurovic, David Cappellen, Daisy Rohner, Mira Susa*
Novartis Institutes for BioMedical Research, Arthritis and Bone Metabolism / Gastrointestinal Disease Area, Basel, Switzerland

Running title: Hey1 is negative regulator of osteoblasts

*The corresponding author
Novartis Institutes for BioMedical Research
WKL-125.9.12
CH-4002 Basel
Switzerland
Tel. (+4161) 696 44 49
FAX: (+4161) 696 38 49
E-mail: mira.susa_spring@pharma.novartis.com

3.1.1 Summary

To examine early events in osteoblast differentiation, we analyzed the expression of about 9,400 genes in the murine MC3T3 cell line, whose robust differentiation was documented cytochemically and molecularly. The cells were stimulated for 1 and 3 days with the osteogenic stimulus containing BMP-2. Total RNA was extracted and analyzed by Affymetrix GeneChip oligonucleotide arrays. A regulated expression of 394 known genes and 295 expressed sequence tags (EST) was detected. The sensitivity and reliability of detection by microarrays was shown by confirming the expression pattern for 20 genes by radioactive quantitative RT-PCR. Functional classification of regulated genes was performed, defining the groups of regulated Growth Factors, Receptors and Transcription Factors. The most interesting finding was concomitant activation of TGF-β, Wnt and Notch signaling pathways, confirmed by strong up-regulation of their target genes by PCR. TGF-β pathway is activated by stimulated production of the growth factor itself, while exact mechanism of Wnt and Notch activation remains elusive. We showed BMP-2 stimulated expression of *Hey1*, a direct Notch target gene, in mouse MC3T3 and C2C12 cells, in human mesenchymal cells and in mouse calvaria. SiRNA-mediated inhibition of *Hey1* induction led to an increase in osteoblast matrix mineralization, suggesting that Hey1 is a negative regulator of osteoblast maturation. This negative regulation is apparently achieved via interaction with Runx2: Hey1 completely abrogated Runx2 transcriptional activity. These findings identify Notch-Hey1 pathway as a negative regulator of osteoblast differentiation / maturation, which is a completely novel aspect of osteogenesis and could point to possible new targets for bone anabolic agents.

3.1.2 Introduction

Bone is a dynamic tissue that is constantly remodeled, *i.e.* degraded and renewed. These two processes are accomplished by two main types of bone cells: bone-forming osteoblasts of mesenchymal origin, and bone-resorbing osteoclasts of hematopoietic origin[136]. A synchronized action of osteoblasts and osteoclasts enables balanced bone remodeling. If this balance is changed in a way that bone resorption exceeds bone formation, osteoporosis occurs, a disease prevalent in old age and characterized by bone loss and a high risk of fractures. Most treatments for osteoporosis available so far target osteoclasts and inhibit bone resorption. In osteoporosis, however, bone loss exceeds the degree of bone gain that can be restored by inhibitors of resorption. Therefore, there is a large need for anabolic agents that would accelerate osteoblast differentiation and promote bone formation. For that purpose, knowledge about molecular events involved in osteoblast differentiation is crucial.

Osteoblast differentiation was previously examined mostly at the cellular or single gene levels. Many external regulating factors are known, but critical molecular steps in osteoblast differentiation and bone formation are largely unknown. One key player was identified recently as the Runx2 transcription factor[137]. Another transcription factor, Osterix (Osx), which cooperates with and is genetically downstream of Runx2, has also been identified [51]. However, more molecular players in osteoblast differentiation remain to be identified.

In vivo, bone forming osteoblasts develop from mesenchymal precursors and this process can be mimicked *in vitro*. Different cellular phenotypes during osteogenesis were tentatively defined as osteoprogenitors, pre-osteoblasts, mature osteoblasts and mineralizing osteoblasts, each of them characterized by an overlapping set of marker genes[138]. Classical cytochemical markers of osteoblast differentiation are alkaline phosphatase and mineralized bone nodules. In order to examine osteoblast differentiation *in vitro*, a crucial step is the use of appropriate primary cells or cell lines, and defined culture conditions, which allow an ordered step-wise differentiation process. In order to avoid many inherent problems observed with differentiation of osteosarcoma cell lines, which are transformed and may not be representative of the physiological situation, we used a non-transformed mouse calvarial cell line, MC3T3-E1. This cell line is also known for phenotypic variation in culture[139]; therefore, we

used a cell clone obtained at a low passage number from a laboratory who kept the cells at their original maintenance conditions[140]. To ensure that the cells show expected behavior also at the molecular level, we selected from this MC3T3-E1 cell batch a further clone, which efficiently activated Runx2-dependent reporter gene, and activated Runx2 mRNA and protein. This clone of MC3T3-E1 cells exhibited very robust and fast differentiation properties. We have then used this MC3T3-E1 cell clone to examine a genome-wide pattern of gene expression during early differentiation along osteoblastic lineage. The quality and biological relevance of these analyses was confirmed by detection of a number of osteoblastic markers and genes known to be regulated during osteogenesis. Importantly, we also uncovered novel genome-wide aspects of gene regulation in osteoblasts by defining three major activated signaling pathways. We further studied the function of one of them, a transcription factor of Hairy and Enhancer of Split (HES) family, Hey1. By manipulating the expression of Hey1 in both positive and negative direction, we could define its role in osteogenesis and link its function to a main osteoblast regulator, a transcription factor of the Runt family Runx2.

3.1.3 Experimental Procedures

Cell culture. Parental MC3T3-E1 cell line was a kind gift of T. Kokkubo (Novartis, Japan)[140]. MC3T3-1b clone was generated after transfection with OSE2-luciferase reporter gene, measuring the activity of Runx2, followed by a selection for clone in which luciferase was activated by the osteogenic stimulus (100-400 ng/ml BMP-2, 50 μM ascorbic acid (AA), 10 mM β-glycerophosphate (GP)). The cells were grown in α-MEM with 10% fetal calf serum (FCS, Gibco), 1% penicillin/streptomycin (Pen/Strep) and 1% L-Glutamine (L-Glu) in T175 flasks (40 ml/flask). The stimulation was done in the same medium. For RNA isolation, alkaline phosphatase and Alizarin red S staining, cells were respectively plated on 6 cm dishes ($1.5x10^5$cells/dish in 3 ml medium), 48-well plates ($1x10^4$ cells/well in 1 ml medium) and 12-well plates ($5x10^4$ cells/well in 3 ml medium). Cells were grown to confluence for 3 days at 37°C / 5% CO_2, and then stimulated with 10 mM β-glycerophosphate (GP, Sigma), 50 μM ascorbic acid (AA, Wako) and 1 μg/ml BMP-2 (Nico Cerletti, Novartis). Control cells were stimulated with 10 mM β-glycerophosphate alone. For Alizarin Red S staining, cell cultures were fed with fresh medium and osteogenic factors twice weekly.

Alkaline phosphatase staining. Three days after stimulation, cells were washed twice with PBS, fixed with 0.5 ml/well of formalin /methanol / H_2O (1:1:1.5) for 15 min at room temperature, and washed 3 times with water. For staining, one FAST BCIP/NBT tablet from Sigma (5-bromo-4-chloro-3-indolyl phosphate / nitro blue tetrazolium, alkaline phosphatase substrate) was dissolved in 10 ml of water, and 0.5 ml of substrate solution was added to the fixed cultures for 15 min at room temperature. After staining, cultures were washed 3 times with water and air-dried.

Alizarin red S staining for mineralization. Fourteen or seventeen days after stimulation, cells were washed twice in PBS, fixed with formalin /methanol / H_2O (1:1:1.5), 0.5 ml/well, 15 minutes at room temperature, and washed 3 times with water. Saturated Alizarin Red S solution was filtered, 1.5 ml was added per well, and incubated for 15 min at room temperature. Cells were then washed 4-5 times with water and air-dried.

RNA isolation. Cells were harvested in the lysis buffer containing guanidinium-isothiocyanate. Total RNA was extracted, treated with DNAse I and purified according to the manufacturer's protocol (RNeasy mini kit, QIAGEN). Calvarias were dissected and frozen in liquid nitrogen. For total RNA isolation, frozen calvarias were crushed in Bio-Grinding device (Biospec Products) 1-2 times. Crushed bone was re-frozen in liquid nitrogen; 1ml of Trizol (Invitrogen) was added and samples where rotated for 1 h. After 1 min of centrifugation at 13,000 rpm, supernatant was collected and phenol-chloroform extraction was performed: 0.2 ml of 1-bromo-3-chloropane (Sigma) was added to each tube; tubes were strongly shaken, then incubated 2-3 minute at room temperature, followed by 15 min centrifugation on 12,000 g at 4°C. The upper colorless aqueous phase (RNA phase) was collected, RNA was precipitated with isopropanol, pellet washed with 75% ethanol, air-dried and dissolved in 40 μl of water. RNA was cleaned and DNase I treated using RNeasy Clean- Up Kit (QIAGEN) according to manufacturer's instructions.

Quantitative radioactive RT-PCR (qrRT-PCR). This method was performed as previously described by us[141]. Briefly, 10 units of RNAse inhibitor (ROCHE Molecular Diagnostics) and 100 μg of random hexanucleotides (Amersham Pharmacia Biotech) were added to 1 μg of DNAse I-treated total RNA. Samples were denatured for 5 min at 65°C and chilled on ice. Then, samples were filled to 20 μl with a nuclease-free solution containing another 10 units of RNAse inhibitor, 2.5 mM of each dNTP, 50

mM Tris-HCl pH 8.3, 60 mM KCl, 10 mM $MgCl_2$ and 1 mM DTT. 20 units of Avian Myeloblastosis Virus reverse transcriptase (Stratagene) was added (cDNA) or not (RT-) to each sample. Reverse transcription reaction was performed for 2 h at 42°C, and stopped by incubation for 5 min at 95°C. Samples were then diluted 5-fold with nuclease-free water and stored at -80°C until use.

One µl of cDNA or RT- was used as a PCR template. PCR reactions were performed in a final volume of 25 µl, containing 100 µM of each dNTP, 1 µCi of α [^{32}P]-dATP, 1 µM of each primer and 1.25 units of "Hot start" thermostable DNA polymerase and corresponding reaction buffer (FastStart Taq, ROCHE Molecular Diagnostics). For PCR analysis of *PTHR, Dlx2, RAMP1, JunB, Fra-1,* and *Wnt6*, the reaction mix contained in addition 5 % glycerol. The amplification protocol was the following: initial step of 5 min at 94°C, 12-33 cycles of denaturation at 94° C for 1 min, annealing at 57/60° C (all genes at 57° C, except *PTHR, Dlx2, RAMP1, JunB, Fra-1*, at 60° C) for 1 min, and extension at 72° C for 1 min 20 s. The amplification was terminated with a final incubation step at 72° C for 10 min. Aliquots of PCR products were mixed with loading buffer (final concentrations: 5 % glycerol, 10 mM EDTA, 0.01 % SDS, 0.025 % xylene cyanol and bromophenol blue dyes) and analyzed on 8 % native polyacrylamide gels. Gels were vacuum-dried, exposed to phosphor-storage screens and imaged by PhosphorImager (Molecular Dynamics). The signals on images were quantified by the ImageQuant software (Molecular Dynamics). For each gene analyzed, a cycle curve experiment was performed and the optimal number of PCR cycles for the quantitative analysis was chosen within the linear range of amplification. The primers (forward and reverse, given in the 5' to 3' orientation) and the number of cycles used in PCR are listed below.

Gene: Primers:

Alkaline phosphatase (*ALP*):

CCCAAAGGCTTCTTCTTGC and

GCCTGGTAGTTGTTGTGAG, 30 cycles

Msx2:

CGCCTCGGTCAAGTCGGAA and

GCCCGCTCTGCTAGTGACA, 31 cycles

Parathyroid hormone receptor (*PTHR*):

ACCCCGAGTCTAAAGAGAAC and

GCCTTTGTGGTTGAAGTCAT, 28 cycles

Osteocalcin (*OCN*):

GGGCAATAAGGTAGTGAACAG and

GCAGCACAGGTCCTAAATAGT, 28 cycles

Runx2 (α/m and ε):

ATGCTTCATTCGCCTCAC and

CTCACGTCGCTCATCTTG, 29 cycles

Osteopontin (*OPN*):

CACAAGCAGACACTTTCACTC and

GAATGCTCAAGTCTGTGTGTT, 23 cycles

Osteonectin (*SPARC*- secreted protein acidic and rich in cysteine):

CCCTGCCAGAACCATCATTG and

TTGCATGGTCCGATGTAGTC, 23 cycles

Collagen 1α I (*Col1α*):

CCCTGCCTGCTTCGTGTAAA and

CCAAAGTCCATGTGAAATTATC, 22 cycles

18S ribosomal subunit RNA (*18S rRNA*):

CCTGGATACCGCAGCTAGGA and

GCGGCGCAATACGAATGCCCC, 12 cycles

Glyceraldehyde 3-phosphate dehydrogenase (*GAPDH*):

CTGCACCACCAACTGCTTAG and

AGATCCACGACGGACACATT, 19 cycles

Smad1:

TGCTGGTGGATGGTTTCACA and

TGTCGCCTGGTGTTTTCAATA, 29 cycles

Smad6:

GCAACCCCTACCACTTCAG and

GCCTCGGTTTCAGTGTAAGA, 28 cycles

JunB:

CAGCCTTTCTATCACGACGA and

GGTGGGTTTCAGGAGTTTGT, 31 cycles

Id2:

CCGATGAGTCTGCTCTACAA and

CCGTGTTCAGGGTGGTCAG, 27 cycles

Dlx2:

AAACCACGCACCATCTACTC and

TCGCCGCTTTTCCACATCTT, 31 cycles

Fra-1:

ACCGCCCAGCAGCAGAAGT and

AGGTCGGGGATAGCCAGTG, 30 cycles

Tcf7:

ACTCTGCCTTCAATCTGCTC and

GGGTGTGGACTGCTGAAATG, 27 cycles

Low density lipoprotein receptor-related protein 5 (*LRP5*):

GCCAGTGTGTCCTCATCAAG and

ACGCTGGCAGACAAAGTAGA, 25 cycles

Transforming growth factor β1 (*TGF-β1*):

CCAAAGACATCTCACACAGTA and

TGCCGTACAACTCCAGTGAC, 27 cycles

Transforming growth factor β3 (*TGF-β3*):

CACCGCTGAATGGCTGTCT and

CATTGGGCTGAAAGGTGTGA, 26 cycles

TIEG:

TTCAGCAGCAAGGGTCACTC and

GACAGGCAAACTTCTTCTCAC, 28 cycles

Hey1:

GCCGACGAGACCGAATCAAT and

GCTGGGATGCGTAGTTGTTG, 30 cycles

Receptor activity-modifying protein 1 (*RAMP1*):

TCTGGCTGCTGCTGGCTCA and

TTTCCCCAGTCACACCATAG, 31 cycles

Osterix (*Osx*):

ATGGCGTCC TCTCTGCTTGA and

GAAGGGTGGGTAGTCATTTG, 30 cycles

Gene expression analysis by high-density oligonucleotide microarrays. The results shown in this study are derived from three independent experiments with MC3T3 cells. In each experiment, the cells were treated identically: no stimulation, day 0; GP treatment at day 1 and 3; and osteogenic stimulus treatment (GP/AA/BMP-2) at day 1

and 3. Total RNA from each sample was extracted and analyzed on oligonucleotide microarrays. Before microarray analysis, for each experiment we performed a marker gene analysis and cytochemical staining for alkaline phosphatase and mineralization, in order to ensure that cell respond appropriately to the osteogenic stimulus. Microarray hybridizations were performed in the Pharmacogenomics Area, Novartis Pharma Development. Affymetrix GeneChip® Murine Genome U74Av2 arrays were used, which consist of coated glass slides with series of oligonucleotide probes synthesized *in situ*. These arrays contain probes for approximately 9,400 genes (~5,700 functionally characterized genes and ~ 3,700 EST clusters). Biotin-labeled cRNA probes were generated from each sample to be analyzed, starting form 5 µg of DNAse I-treated total cellular RNA, prepared as described above. The cRNA probes were individually hybridized on the arrays and the signals were detected according to the manufacturer's instructions (Affymetrix, Santa Clara, CA, USA).

Hybridization data were analyzed using the MAS5.0 (Affymetrix), NPGN (Novartis Pharmacogenetics Network) and Expressionist 3.0 (GeneData, Basel, Switzerland) software. Genes were considered as significantly expressed in a given experiment, if they were classified as P (present), but not as M (marginal) or A (absent) at least at one time point. Twenty was chosen as the minimal significant hybridization signal value; all lower values were set to 20. All genes discussed and studied herein were detected with gene-specific probes, but not with probe sets that recognize gene families.

Genes were selected as regulated by osteogenic stimulus, if their expression deviated more than 2-fold from the corresponding time-matched control, at any time point, in at least two out of three experiments. The Table 5 shows that mean relative expression levels (MREL) for all three experiments was around 1, showing that most of the genes do not change their expression levels upon treatment. Standard deviation of the MREL (SD) represents a degree of variation in the expression level compared to the mean value for all the genes. Thresholds of 2-fold reflect approximately one standard deviation around the MREL for all experiments.

	Exp#1		Exp#2		Exp#3	
	Day 1 T/C	Day 3 T/C	Day 1 T/C	Day 3 T/C	Day 1 T/C	Day 3 T/C
MREL	1.15	1.31	1.20	1.28	1.19	1.21
SD	1.50	2.70	1.66	2.18	2.05	2.22

Table 5: Mean relative expression level of all genes on the microarray in 3 separate experiments. MREL- Mean relative expression level; SD-standard deviation of the MREL; T/C- Treated/Control, samples treated with osteogenic stimulus were compared with non-stimulated, time-matched control.

In addition to this statistical criterion, biological data indicated that 2-fold is a meaningful difference, since some of the known BMP-2-regulated genes (such as Dlx2 and Dlx5) were induced to a similar degree (see the Results section, Table 8).

By analyzing osteoblast marker genes for each independent experiment, we observed that the kinetics of the differentiation process is not always the same, although the cells were treated exactly the same way. For example, *PTHR* was induced to a much higher degree at day 3 in experiment #3, as compared to experiments #1 and 2, suggesting that the differentiation process was faster and/or stronger in the experiment #3 (data not shown). Higher standard deviations of MREL at day 1 in Exp. #3 (Table 5) also show that in this experiment more genes are regulated already at day 1, suggesting a faster differentiation process than in Exp. #1 and #2. Because of this expected biological variability, we considered as significantly regulated only genes showing regulation in 2 out of three experiments, a criterion that better tolerates the biological variability of the differentiation process. When calculating average expression from three experiments, the median value was used, which gives less significance to outlayer values.

C2C12 myoblastic cells were treated with GP (10 mM) and BMP-2 (400 ng/μl) or GP alone for 1 and 3 days. Total RNA was extracted (RNeasy mini kit, QIAGEN) and samples were analyzed on the Affymetrix GeneChip® Murine Genome U74Av2 arrays.

Human Mesenchymal Stem Cells (hMSCS, Poietics™, Cambrex) obtained from human bone marrow withdrawn from the posterior iliac crest of the pelvic bone of

female donor, 19 years old, were treated with 10 mM βGP, 50 μM AA and 1000 ng/ml BMP-2. Total RNA was extracted (RNeasy mini kit, QIAGEN) and the samples were analyzed on the Affymetrix GeneChip® HG-U133A.

Real-time quantitative RT-PCR analysis. cDNA was synthesized using High-Capacity cDNA Archive Kit (P/N: 4322171 by Applied Biosystems), starting from 1 μg of RNA, according to the manufacturer's protocol. For real-time quantitative RT-PCR, an ABI Prism 7900HT Sequence Detection System (Applied Biosystems) was used. Reactions were performed in 394-well format in a 10 μl total volume using 5μl of 2X Master mix (TaqMan universal PCR Master Mix, Applied Biosystem), 0.5 μl of 20X primers, probes synthesized by Applied Biosystems, Assay-On-Demand (*18S rRNA*, 4310893E; *Hey1*, Mm00468865_m1), and 2 μl of cDNA (equivalent to 20 ng of RNA). Thermal conditions were the following: 10 min at 50°C, 10 min at 94°C, followed by 40 cycles of 15 s at 94°C and 1 min at 60°C. Negative controls were included in each PCR experiment, with RT (-) instead of cDNA. Fold inductions and expression ratios between two samples were calculated from differences in threshold cycles, at which an increase in reporter fluorescence above a baseline signal could be first detected (Ct value). Results were averaged from triplicate determinations. *18S rRNA* was used as a normalization control.

siRNA transfection. MC3T3 cells were plated on 6-well plates ($0.5x10^5$ cells/ well in 2 ml of medium). After 24 h, siRNA transfection was performed in a total volume of 1 ml using Oligofectamine (Life Technologies), according to the manufacturer's instructions. siRNA concentration was 0.1 μM, and the Oligofectamine amount 4 μl/well. Transfection was stopped after 4 h by adding 0.5 ml of medium containing 30% of serum, and the osteogenic stimulus. RNA was isolated after 1, 2, 3 or 4 days. For Alizarin Red S staining, medium containing 10% FCS and the osteogenic stimulus was changed twice weekly. Staining was performed after 17 days. SiRNA sequence of sense strand Hey1 siRNA was GCTAGAAAAAGCTGAGATC, with dTdT overhangs, purified by ion exchange-high pressure liquid chromatography (Xeragon Inc.). Sense strand sequence of control siRNA was AGAAGGAGCGGAATCCTCG, with dTdT overhang (provided by François Natt, Novartis).

Transient co-transfections and the luciferase assay. Runx2 and *Hey1* cDNA were cloned into the pcDNA3.1 (+) expression vector and used in a luciferase reporter assay. Primers used for *Hey1* cDNA cloning: sense: GACCCTCCTCGGAGCCCAC,

antisense: TTAGAAAGCTCCGATCTCTGTCC; The OG2luc plasmid, containing the minimal osteocalcin promoter in front of the luciferase gene was used as a reporter construct. This luciferase expression vector (without OG2 promoter) was a kind gift of Roland Schule, Freiburg, Germany. Eight times repeated wild-type (8XOSE2 wt) or mutated (8XOSE2 mut) Runx2-binding sites have been cloned upstream of the OG2 minimal promoter (Johann Wirsching, Novartis). Cells were seeded in 96-well plates ($4x10^3$ cells/well in 200 μl of medium) and grown for 24 h. Transfection was performed using Lipofectamine Plus reagent (Life Technologies), according to the manufacturer's protocol. MTS assay for cells number normalization, and luciferase assays were performed 24 h after transfection. MTS assay: to the medium (100 μl/well), 20 μl/well of MTS solution was added (Cell titer 96 Aqueous One Solutin Reagent, Promega). Cells were incubated for 20 min at 37°C. OD was measured at 490 nm in a microplate reader. Luciferase assay: cells were washed twice with PBS, 50μl/well of 1X lysis buffer (Promega) was added and incubated for 15 min at RT. Subsequently, the cultures were shaken for 5 min at RT and frozen for 1 h at -70°C. Upon thawing, 20 μl of lysate was transferred into a white 96-well plate (Costar £3912, OPAQUE PLATE), 2x50 μl Luciferase Assay Reagent was added (Promega), and luciferase luminescence was measured (MicroLumat LB 96P, Berhold).

3.1.4 Results

3.1.4.1 Characterization of osteoblastic differentiation in MC3T3 cells

In response to osteogenic stimulus (BMP-2, ascorbic acid - AA, β-glycerophosphate - GP), MC3T3-1b clone of MC3T3-E1 cells (in the further text MC3T3) showed a strong increase in alkaline phosphatase activity at day 3 (Fig. 12A). Runx2 protein levels were also increased by day 3 (Fig. 12B). Furthermore, the cells produced bone nodules, which mineralized by day 11-14 (Fig. 12C). After a longer exposure to osteogenic stimulus, the number of nodules increased dramatically, covering more than 50 % of the dish area. Thus, the whole osteoblast differentiation / maturation process is reproduced sequentially within 2 weeks, allowing the exact study of osteoblast biology.

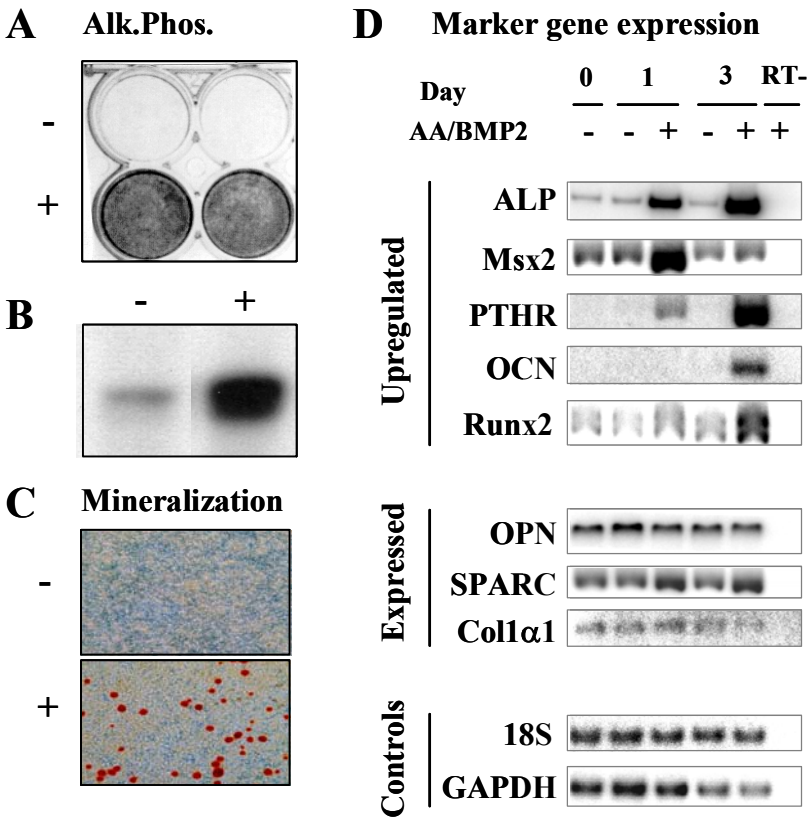

Figure 12. Characterization of osteoblastic differentiation in MC3T3 cell line.

A: Staining of MC3T3 cells for alkaline phosphatase 3 days after treatment with osteogenic stimulus. Staining is visible as dark culture wells on the shown photos. B: Western blot for Runx2 protein. Cellular lysates were prepared 3 days after treatment with osteogenic stimulus. C: Staining for mineralized bone nodules with Alizarin Red S 14 days after the start of osteogenic stimulus treatment. Staining is visible as red spots on the shown photos. D: Quantitative radioactive (qr) RT-PCR analysis of osteoblastic markers. Total RNA was extracted from non-stimulated confluent cells (day 0) and from cells treated with GP alone (-) or osteogenic stimulus (GP/AA/BMP-2, +) for 1 and 3 days. The radioactive PCR products were analyzed by polyacrylamide gel electrophoresis and visualized by PhosphorImager. *ALP* - alkaline phosphatase; *PTHR* - PTH receptor; *OCN* - osteocalcin; *OPN* - osteopontin; *SPARC* – osteonectin (secreted protein acidic and rich in cysteine); *Col1α1* - collagen 1 α 1; *18S – 18S rRNA*.

To study the differentiation process at the transcriptional level, we analyzed mRNA expression of a number of molecular markers of osteoblast differentiation. MC3T3 cells were stimulated with osteogenic stimulus for 1 and 3 days and compared with non-stimulated time-matched controls. Eight markers of osteoblast differentiation were analyzed: alkaline phosphatase (*ALP*), transcription factors *Msx2* and *Runx2*,

parathyroid hormone receptor (*PTHR*), and extracellular matrix proteins osteocalcin (*OCN*), osteopontin (*OPN*), osteonectin (*SPARC*) and collagen Iα1 (*Col Iα1*) (Fig. 12D). mRNA levels of five osteoblast markers were up-regulated in response to the osteogenic stimulus. *ALP* was strongly induced already at day 1 and further increased at day 3. *Msx2* was transiently up-regulated at day 1 and *Runx2* was induced at day 3. *PTHR* and *OCN*, late markers of osteoblast differentiation, were strongly induced at day 3. For *OPN*, *SPARC* and *Col Iα1*, high basal levels of expression were already detected in non-stimulated cells and did not change upon osteogenic treatment. As MC3T3 cells are already committed to the osteoblast lineage, high expression levels of these extracellular matrix proteins is not surprising. Similar levels of ribosomal RNA (*18S rRNA*) and glyceraldehyde-3 phosphate dehydrogenase (*GAPDH*) control mRNAs were found in all treatment conditions.

C2C12 pre-myoblastic and primary mouse calvarial cells were also considered as alternative cellular systems to MC3T3 cell line. However, they expressed smaller number of regulated markers and variability was bigger than in MC3T3 cells (data not shown). We concluded that MC3T3 cells are an appropriate system for studying changes in gene expression during osteoblastic differentiation.

3.1.4.2 Expression of osteoblast marker genes on microarrays

Having selected an appropriate *in vitro* osteoblast differentiation system, we were interested to identify genes potentially involved in this process by performing a genome-wide analysis of gene expression. MC3T3 cells were stimulated with osteogenic factors, and total RNA was extracted at days 0, 1 and 3 from three independent experiments. Gene expression was analyzed on Affymetrix GeneChip microarrays representing about 10, 000 expressed sequence tags (ESTs) and genes with known function.

In order to validate the microarray data for each independent experiment, expression of osteoblast marker genes on microarrays were compared with the qrRT-PCR data. The GeneChip contained oligonucleotide probes for seven out of eight chosen osteoblast markers and for GAPDH control gene. For these genes, both methods produced a very similar pattern of regulation. The results from a representative experiment are shown in Fig. 13.

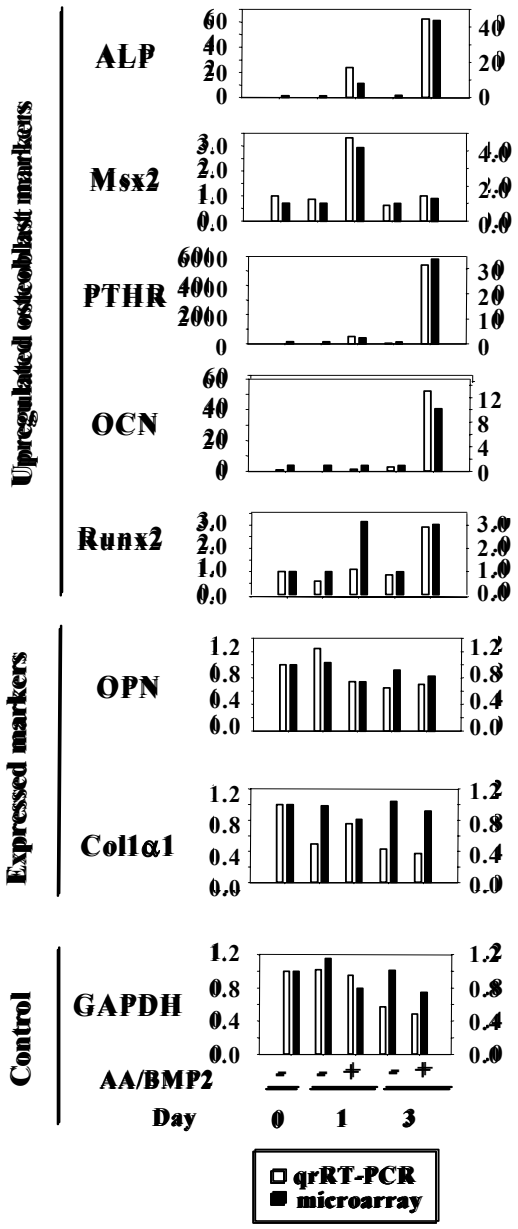

Figure 13: Comparison of marker gene expression by GeneCHIP microarray and quantitative radioactive RT-PCR.

Confluent MC3T3 cells were cultured in medium containing GP, without (-) or with (+) AA/BMP-2 for 0, 1, and 3 days. Total RNA was extracted and analyzed for expression of osteoblast markers and housekeeping genes by GeneChip microarrays and by qrRT-PCR. For both types of analyses, mRNA levels are shown as fold regulation compared to the day 0 controls. Quantification of qrRT-PCR was done by PhosphorImager; quantification of microarray hybridization was done on the GeneCHIP. White bars: qrRT-PCR data; black bars: GeneCHIP microarray data.

Reliable hybridization microarray data were obtained even for weakly expressed genes, such as those encoding transcription factors (i.e. *Msx2* and *Runx2*, Fig 2), indicating a good sensitivity of detection. We concluded that microarray detection was sensitive enough to detect expression and regulation of osteoblast markers and thus, should be a good method to detect regulation of novel genes as well.

3.1.4.3 Non-hierarchical clustering of genes regulated during osteoblast differentiation

To get an insight into the transcriptional events involved in the osteoblast differentiation, we investigated genes, whose expression levels changed upon treatment with the osteogenic stimulus. Genome-wide gene expression levels were compared between treated samples and time-matched non-stimulated controls. We detected a significant regulation (2-fold in at least 2 out of the 3 experiments) of 394 genes with known function and of 295 ESTs. In further analyses described here, we focused on the genes with known function. This subset of genes was further analyzed by a non-hierarchical clustering method, which groups genes according to their temporal regulation patterns (Fig. 14). One hundred seventy two genes were up-regulated and two hundred twenty two down-regulated. There was a very good concordance between the general gene expression patterns observed in three independent experiments and in their median (Fig. 14).

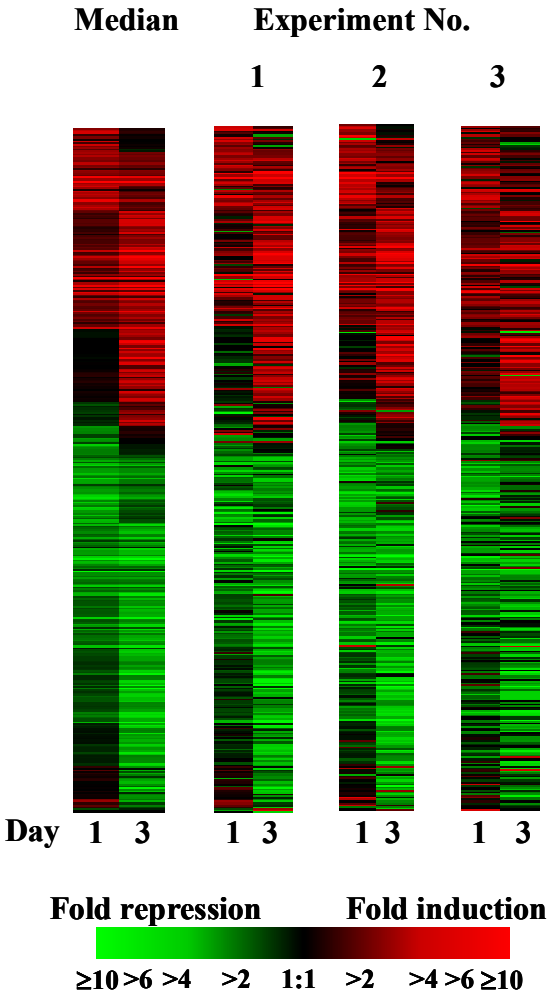

Figure 14: Clustering of transcripts regulated during osteoblast differentiation.
Confluent MC3T3 cells were cultured in medium containing GP, without (-) or with (+) AA/BMP-2 for 0, 1, and 3 days. Total RNA was extracted and genome-wide expression of osteoblast genes was analyzed by GeneChip microarrays. Microarray data were analyzed using the Expressionist software, normalized to day 0 control and expressed as fold regulation relative to time-matched, non-stimulated controls. Data for 394 regulated genes from each individual experiment and from median of three experiments are shown. Fold regulations are presented in black-red-green color code, as indicated on the bottom. Regulated transcripts were non-hierarchically clustered, based on the temporal similarity of expression profiles, using the gene layout obtained by initial clustering of median expression values. Regulation folds bigger than 10 or smaller than 0.1 were set to 10 and 0.1, respectively.

3.1.4.4 Regulated genes: growth factors

We defined several groups according to the cellular function of the up- and down-regulated genes. A large number of regulated genes encode extracellular matrix

proteins and adhesion molecules (data not shown). This is consistent with the fact that osteoblasts are adherent cells responsible for production of the bone matrix. The regulation of many genes involved in cell cycle and DNA replication is consistent with our observation that the cells, although almost confluent prior to stimulation, still continue to proliferate to a small degree up to 3 days after stimulation with the osteogenic stimulus (data not shown). This regulation is also consistent with the process of exiting cell cycle and switching to differentiation program. We focused, however, on three groups of genes, whose products could have major contributions to the differentiation process: growth factors, receptors and transcription factors.

Name	Description	PSN	Acc No	REL	
				d1	d3
TGF-β1	Transforming growth factor beta 1	101918_at	AJ009862	2.07	4.51
Gremlin2	BMP antagonist	103975_at	AB011030	3.05	2.31
TGF-β3	Transforming growth factor beta 3	102751_at	M32745	2.37	2.72
PDGF alpha	Platelet derived growth factor, alpha	94932_at	M29464	0.99	2.70
IGFBP10	Insulin-like growth factor binding protein 10	92777_at	M32490	2.70	1.61
Activin	Inhibin beta-A	100277_at	X69619	2.45	1.13
IGFBP2	Insulin-like growth factor binding protein 2	98627_at	X81580	0.49	0.83
PTHRP	Parathyroid hormone-like peptide	104262_at	M60057	0.85	0.48
IGFBP6	Insulin-like growth factor binding protein 6	103904_at	X81584	0.72	0.46
SCYA7	Small inducible cytokine A7	94761_at	X70058	0.74	0.45
TGF-β2.	Transforming growth factor beta 2	93300_at	X57413	0.95	0.43
SCYD1	Fractalkine, Neurotactin. Small inducible cytokine D1	98008_at	U92565	0.44	0.41
FGF7	Fibroblast growth factor 7	99435_at	Z22703	0.61	0.37
VEGF- D	Vascular endothelial growth factor D	92365_at	X99572	0.75	0.35
VEGF-A	Vascular endothelial growth factor A	103520_at	M95200	0.98	0.34
Angiotensinogen	Angiotensin precursor	101887_at	AF045887	0.63	0.34
PHI	Phosphohexose isomerase	100573_f_at	M14220	0.33	0.52
Ccl5	Chemokine (C-C motif) ligand 5, RANTES	98406_at	AF065947	0.42	0.25
NOV	Nephroblastoma overexpressed gene	100507_at	Y09257	0.21	0.33

Table 6: Growth factors regulated during osteoblastic differentiation of MC3T3 cells. Selected genes encoding growth factors, whose expression changed ≥ 2-fold upon stimulation with osteogenic stimulus. Black font - up-regulated transcripts; Grey font - down-regulated transcripts; PSN- Affymetrix probe set number; Acc No- sequence accession number; REL- relative expression level (median value), compared to the non-stimulated, time-matched control; d1 - day 1; d3 - day 3.

The Growth Factors group contained genes expected to be regulated in osteoblasts, but also novel genes (Table 6). Among the expected genes, we found known modulators of osteoblast proliferation: PDGFα, VEGF, FGF, IGF binding proteins (IGFBP) and PTH-rP[142,143,144,145]. The most prominent event was regulation of four members of the TGF-β superfamily: *TGF-β1, TGF-β3* and *Activin* were up-regulated,

while *TGF-β2* was down-regulated (Table 2). TGF-β family members are well-known and potent modulators of the osteoblasts and bone[146], but their regulation by osteogenic stimulus containing BMP-2 has not been reported yet. We have shown that BMP-2 within osteogenic mix is responsible for activation of *TGF-β1* (data not shown). The activation of the TGF-β signaling pathway by the osteogenic stimulus was further indicated by the regulation of several TGF-β target genes: the transcriptional repressor *TIEG*, the extracellular matrix protein tenascin C, the adhesion molecule kerato-epithelin, and the type 2 somatostatin receptor (*SSTR2*) (Table 9)[147,148,149,150]. Apart from TGF-β pathway, worth noting is a 2-3-fold up-regulation of the BMP antagonist Gremlin2, which points to a negative feed-back mechanism. These results shed a new light on the interplay between different growth factors in osteoblast differentiation.

Among down-regulated genes, we will mention *IGFBP2* and *6*, known modulators of IGF-induced osteoblast proliferation. Furthermore, angiotensinogen, a precursor of angiotensin, was progressively down-regulated at days 1 and 3. Since angiotensin II was reported to have a role in osteoblast differentiation, this could be of relevance[151]. Two additional down-regulated genes were: small inducible cytokine A7 (*SCYA7*) and *PTH-rP*, both of which can stimulate differentiation or function of bone-resorbing osteoclasts[152,153], suggesting that differentiating osteoblasts have a reduced ability to stimulate osteoclasts.

3.1.4.5 Regulated genes: receptors

Up-regulated genes in the Receptors group included those encoding for the receptors of many factors implicated in osteoblast differentiation or function, such as: PTH receptor (PTHR), LIF receptor (LIFR), leptin receptor (LEPR), prostaglandin F receptor (PTGFR), fibroblast growth factor receptor 2 (FGFR2), urokinase receptor (PLAUR), and thrombomodulin (Table 7)[145,154,155,156,157,158,159]. Some of the up-regulated receptor-encoding genes, such as the ephrin receptor EPHA2 or the somatostatin receptors SSTR4 and SSTR2, have not previously been reported to play a role in osteoblasts. The highest up-regulated receptor genes were those encoding PTH receptor (*PTHR*), an established osteoblast marker, and, surprisingly, a co-receptor for calcitonin receptor-like receptor (*RAMP1*). Interestingly, osteoprotegerin (*OPG*), a decoy receptor that inhibits the signaling of RANKL, the main cytokine in osteoclastogenesis, was up-regulated almost 4-fold. This result,

together with the down-regulation of osteoclast-stimulating *SCYA7* and *PTH-rP* described in the previous section, strongly suggests that differentiating osteoblasts have a reduced ability to stimulate bone-resorbing osteoclasts function and differentiation (Table 9).

Name	Description	PSN	Acc No	REL	
				d1	d3
RAMP1	Coreceptor in calcitonin-gene-related peptide receptor	104680_at	AJ250489	**0.95**	**8.55**
PTHR	Parathyroid hormone receptor	98482_at	X78936	**1.00**	**7.20**
OPG	Osteoprotegerin	102887_at	U94331	**1.88**	**3.84**
LIFR	Leukemia inhibitory factor receptor	104658_at	D17444	**1.11**	**3.45**
LEPR	Leptin receptor	100431_at	U42467	**1.00**	**3.25**
FGFR2	Fibroblast growth factor receptor 2	93091_s_at	M63503	**2.61**	**3.19**
SSTR2	Somatostatin receptor type 2	98350_at	AF008914	**1.96**	**2.85**
FGFR2	Fibroblast growth factor receptor 2	93090_at	M23362	**1.83**	**2.54**
PLAUR	Plasminogen activator, urokinase receptor	102663_at	X62700	**2.06**	**2.50**
Thrombomodulin	Endothelial cells receptor	104601_at	X14432	**1.35**	**2.30**
PTGFR	Prostaglandin F receptor	97769_at	D17433	**0.74**	**2.14**
SSTR4	Somatostatin receptor type 4	101717_at	U26176	**1.43**	**2.11**
EPHA2	Ephrin type A receptor 2	103980_at	U07634	**2.03**	**1.77**
sFRP-2	Secreted frizzled related protein 2	93503_at	U88567	**0.92**	**0.50**
OSMR	Oncostatin M receptor beta subunit	102255_at	AB015978	**0.86**	**0.49**
IL4R	Interleukin-4 receptor (secreted form)	102021_at	M27960	**1.09**	**0.43**
VEGFR2	Vascular endothelial growth factor receptor 2	98452_at	D88689	**0.93**	**0.43**
LRP1	Low density lipoprotein receptor related protein 1	101073_at	X67469	**0.82**	**0.38**
PDGFR α	Platelet derived growth factor receptor α	95079_at	M57683	**0.65**	**0.33**
Notch 3	Receptor for membrane-bound ligands Jagged and Delta-like	92956_at	X74760	**0.37**	**0.27**
LRP5	Low density lipoprotein receptor-related protein 5	103806_at	AF064984	**0.25**	**0.32**
Gfra1	Glial cell line derived neurotrophic factor family receptor alpha 1	93872_at	AF014117	**0.38**	**0.22**
RDC1	Chemokine orphan receptor 1	93430_at	AF000236	**0.69**	**0.17**
Notch 1	Receptor for membrane-bound ligands Jagged and Delta-like	97497_at	Z11886	**0.54**	**0.11**

Table 7: Receptors regulated during osteoblastic differentiation of MC3T3 cells. Selected genes encoding receptors, whose expression changed ≥ 2-fold upon stimulation with osteogenic stimulus. Black font - up-regulated transcripts; Grey font-down-regulated transcripts; PSN- Affymetrix probe set number; Acc No- sequence accession number; REL- relative expression level (median value), compared to the non-stimulated, time-matched control; d1 - day 1; d3 - day 3.

Notch receptors 1 and 3 were prominently down-regulated. The role of Notch signaling in osteoblast differentiation has not been much investigated; only two conflicting reports indicate that Notch signaling may influence osteoblast differentiation[160,161]. Two low density lipoprotein related proteins *LRP1* and *LRP5*, were also down-regulated. This result is intriguing, because LRP5 is an important player in bone metabolism and has been identified as a high bone mass gene[36,37,38].

3.1.4.6 Regulated genes: transcription factors

The Transcription Factors group of regulated genes is the largest (Table 8). Despite the fact that transcription factors are generally weakly expressed, we detected 33 regulated transcription factor genes, all with reliable hybridization signals. Furthermore, we confirmed regulation patterns for 10 of these genes by qrRT-PCR (Fig. 15). The regulation of a large number of transcription factors suggested that their orchestrated regulation is crucial for the osteoblast differentiation process.

Name	Description	PSN	Acc No	REL	
				d1	d3
Id2	HLH transcriptional inhibitor. BMP2 inducible	93013_at	AF077861	5.40	35.95
Id3	HLH transcriptional inhibitor. BMP2 inducible	92614_at	M60523	3.16	21.28
Tcf7 (Tcf1)	Activation of Wnt responsive genes and target of Wnt signaling.	97994_at	AI019193	1.00	9.70
Id1	HLH transcriptional inhibitor. BMP2 inducible	100050_at	M31885	4.45	6.35
Hey1	bHLH transcription factor. Notch target gene	95671_at	AJ243895	3.15	4.81
Msx2	Homeo box, msh-like 2	102956_at	X59252	4.20	1.30
Foxf2	forkhead box F2	99846_at	Y12293	1.80	4.10
SMAD6	TGF-β / BMP signalling pathway, inhibitory molecule	104220_at	AF010133	2.63	3.66
junB	BMP target gene	102363_r_at	U20735	3.45	1.49
IRF5	Interferon regulatory factor 5. HTH transcription factor	93425_at	AF028725	3.35	1.09
FoxM1	Fork head/ winged-helix	98305_at	Y11245	1.21	3.10
Dlx2	Distal-less homeobox 2	92332_at	M80540	2.86	2.74
TIEG	TGF-β inducible early growth response.	99602_at	AF064088	2.50	1.43
CLOCK	bHLH transcription factor	92257_at	AF000998	2.45	0.89
BRCA1	Zn finger protein	102976_at	U32446	2.25	2.42
Dlx1	Distal-less homeobox 1	98394_at	U51000	2.39	2.16
SMAD7	TGF-β / BMP signalling pathway, inhibitory molecule	92216_at	AF015260	2.25	1.55
Dlx5	Distal-less homeobox 5	92930_at	U67840	2.19	1.90
SMAD1	BMP signalling pathway	102984_g_at	U58992	1.51	2.08
Irx3	Iroquois related homeobox 3	99034_at	Y15001	1.19	2.08
LEF1	Lymphoid enhancer binding factor 1. Activation of Wnt responsive genes	103628_at	D16503	1.25	2.05
Oct1.	Transcription factor for small nuclear RNA and histoneH2b genes.	102894_g_at	X68363	0.51	0.54
FOG	Friend of GATA-1	97974_at	AF006492	0.79	0.49
FHL1	Four and a half LIM domains protein 1	97498_at	U41739	0.50	0.48
Ets-2	E26 avian leukemia oncogene 2, 3' domain	94246_at	J04103	0.46	0.46
ISGF3G	interferon-stimulated transcription factor 3	103634_at	U51992	0.62	0.45
EGR1/Krox 24	Early growth response 1	98579_at	M28845	0.42	1.18
Klf3	Kruppel-like factor 3 (basic)	100010_at	U36340	0.67	0.36
Six-1	Sine oculis-related homeobox 1.Myogenin activation	92722_f_at	X80339	0.51	0.32
PBX1	TALE homeobox protein subfamily.Pre B-cell leukemia transcription factor	94804_at	L27453	0.84	0.30
p51/p73L/p63/p40	p53 homolog, modulates p53 function	103810_at	AB010152	0.34	0.27
ATFx	Cyclic-AMP-dependent transcription factor	103006_at	AB012276	0.26	0.52
Id4	HLH transcriptional inhibitor	96144_at	AJ001972	0.49	0.13

Table 8: Transcription factors regulated during osteoblastic differentiation of MC3T3 cells. Selected genes encoding transcription factors, whose expression changed ≥ 2-fold upon stimulation with osteogenic stimulus. Black font - up-regulated transcripts; Grey font-down-regulated transcripts; PSN- Affymetrix probe set number; Acc No- sequence accession

number; REL- relative expression level (median value), compared to the non-stimulated, time-matched control; d1 - day 1; d3 - day 3.

Three genes encoding Smads, major components of the BMP-2 signaling pathway, were shown to be up-regulated 2-3-fold. The inhibitory Smads, *Smad6* and *7*, were transiently up-regulated at day 1 (Table 8), exposing another component of a negative feedback loop for regulation of BMP signaling. This result is in agreement with another study[162]. A BMP receptor-specific stimulatory *Smad1* was up-regulated at day 3, indicating that BMP induces components of its signaling pathway as a means of signal enhancement.

Similarly to Smads, many other regulated transcription factor genes have an already established function during osteoblast differentiation. Some genes that were previously identified as BMP-2 target genes in osteoblasts by Locklin and colleagues[162] were also found regulated in our study (Table 8). *JunB*, a component of AP-1 transcription factor complex that is involved in osteoblast differentiation[105], was strongly up-regulated at both time points studied. *Id1, 2* and *3*, encoding HLH transcriptional inhibitors shown to be direct BMP-2 target genes[163], were strongly up-regulated, while *Id4*, another member of this gene family, was down-regulated. The homeobox transcription factors of the Msx and Dlx families are important in skeletal development[164,165,166]. *Msx2*, a known BMP-2 target gene and osteoblast differentiation marker, and *Dlx2* and *Dlx5*, other known BMP-2 targets[132], were all up-regulated in our osteoblast differentiation system. Another member of the Dlx family, *Dlx1*, was also up-regulated, and this is, to our knowledge, the first report of BMP-2 regulation of this gene. These confirmatory findings further strengthen the relevance of our novel findings.

Interestingly, a Wnt pathway target gene *Tcf7* was very strongly up-regulated (about 10- fold at day 3). *LEF1* is another transcription factor mediating Wnt signaling and was also up-regulated (2-fold at day 3). This is a novel finding, and intriguing taking into account a central role of Wnt pathway in osteoblast differentiation, unraveled through LRP5, a Wnt co-receptor and a high bone mass gene[36,37,38]. However, we did not detect a consistent regulation of Wnt genes in our system, in contrast to a recent report[167]. In one from three experiments, we detected up-regulation of *Wnt6* and *Wnt10a* at day 3 (data not shown). Weak up-regulation of *Wnt6* was confirmed by qrRT-PCR (data not shown). However, in other two experiments, Wnts were not

significantly regulated. We conclude that Wnt pathway is activated, but exact mechanism of activation remains to be determined. Regulated components of Wnt pathway are shown in Table 9.

As one of the most striking novel findings, we point to a strong up-regulation of the *Hey1* transcription factor (about 3-fold at day 1 and about 5-fold at day 3, Table 4). Hey1 belongs to a family of transcription factors named Hairy and Enhancer of Split (HES), which belong to superfamily of basic helix-loop-helix (bHLH) transcription factors. Hey1 subfamily has only recently been described and it comprises three members: Hey1, Hey2 and HeyL[168]. Together with other HES family members, they are thought to be direct targets of the Notch signaling pathway[169,170]. Strong up-regulation of the Hey1 transcription factor suggested that the Notch signaling pathway is activated in MC3T3 cells during osteogenic differentiation. Regulated components of Notch signaling pathway are shown in Table 9.

3.1.4.7 Confirmation of selected gene profiles by qrRT-PCR

We selected a few representative genes from three gene groups described above and tested their expression by an independent method: qrRT-PCR (Fig. 15). Selected genes were: growth factors *TGF-β1* and *TGF-β3*, (co)receptors *LRP5* and *RAMP1*, and transcription factors *Smad1*, Smad6, *JunB*, *Id2*, *Dlx2*, *TIEG*, *Tcf7* and *Hey1*. For all the genes analyzed, the expression profiles obtained by qrRT-PCR closely corresponded to the profiles obtained by microarray analysis (Tables 6-8, Figure 15). Together with osteoblast markers and GAPDH, we analyzed and confirmed the expression levels of 20 genes, indicating again relevance of gene expression analysis in these experiments.

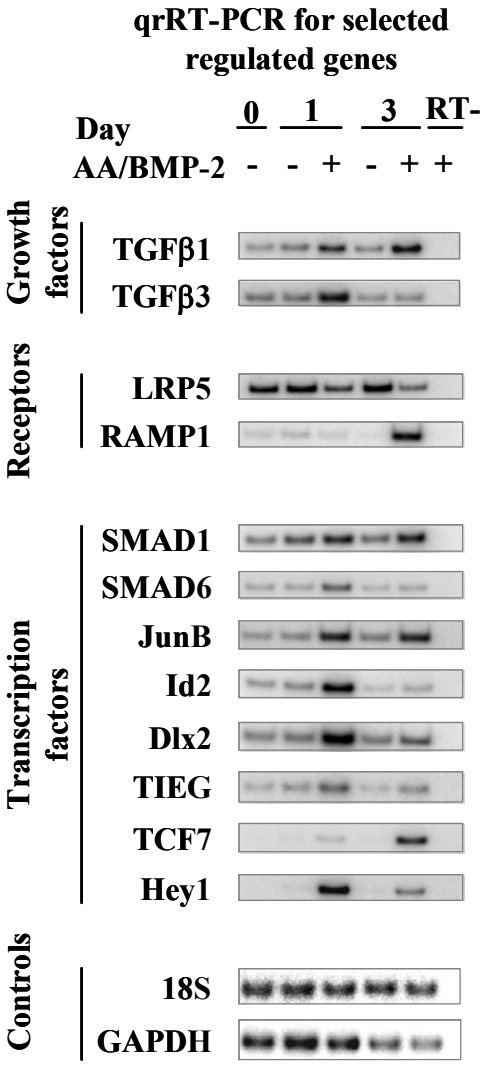

Figure 15: qrRT-PCR confirmation of selected up-regulated genes, identified by GeneCHIP microarrays. Microarray-derived expression profiles for selected genes were confirmed by qrRT-PCR. Confluent MC3T3 cells were cultured in medium containing GP, without (-) or with (+) AA/BMP-2 for 0, 1, and 3 days. Total RNA was extracted and used either for microarrays analysis or for qrRT-PCR. The radioactive PCR products were analyzed by polyacrylamide gel electrophoresis and visualized by PhosphorImager. The genes were grouped based on their function.

3.1.4.8 Hey1 expression in mouse and human osteoblastic cells and mouse calvaria

In further work we focused on expression and function of Notch target gene transcription factor *Hey1*. In order to determine which component of the osteogenis stimulus is responsible for *Hey1* up-regulation, we analyzed *Hey1* mRNA levels after treating MC3T3 cells with separate components of the osteogenic stimulus (Fig.

16A). A time course was performed during four days after addition of the stimulus. The result revealed that *Hey1* is a BMP-2 induced gene, although ascorbic acid had a small additive effect, especially noticeable at day 4 (Fig. 16A). Treatment of MC3T3 cells with TGFβ1, growth factor structurally and functionally similar to BMP family, also didn't stimulate Hey1 induction: in the microarray experiment that we have performed with cells stimulated with GP/AA/TGFβ1 or control cells stimulated with GP/AA for 1 and 3 days, level of Hey1 expression didn't change form the basal level and the signal was absent in all the samples. Next, we have analyzed *Hey1* expression in several osteoblast differentiation systems. *Hey1* is strongly induced by BMP-2 in murine C2C12 cells, which have a potential to differentiation into either myoblasts or osteoblasts (Fig. 16B). The induction was measured by qrRT-PCR at days 1 and 3 and reached about 10-fold. Human *Hey1* expression was determined by microarrays in human mesenchymal stem cells stimulated by osteogenic stimulus containing BMP-2 (Fig. 16C). The induction was persisting for up to day 15.

We analyzed *Hey1* expression in vivo in mouse calvarial bone by real-time PCR. BMP-2 was injected s.c. over calvariae and RNA was isolated after 7 and 14 days. *Hey1* mRNA levels were already high in non-treated bone tissue, comparable to the BMP-2 induced levels in MC3T3 cells (Fig. 16D and E). This is evident from similar delta Ct values for Hey1 detection, and is likely due to endogenous calvarial BMP-2. Treatment of calvariae with exogenous BMP-2 induced a trend of *Hey1* induction, visible through a reduction of Ct values at day 14. Induction of *Hey1* was strongest in MC3T3 cells treated by BMP-containing osteogenic stimulus, reaching over 1,000-fold difference in expression levels at day 4, measured by real-time PCR (Fig. 16E). We conclude that *Hey1* is induced by BMP-2 in both mouse and human cells and is expressed in mouse bone.

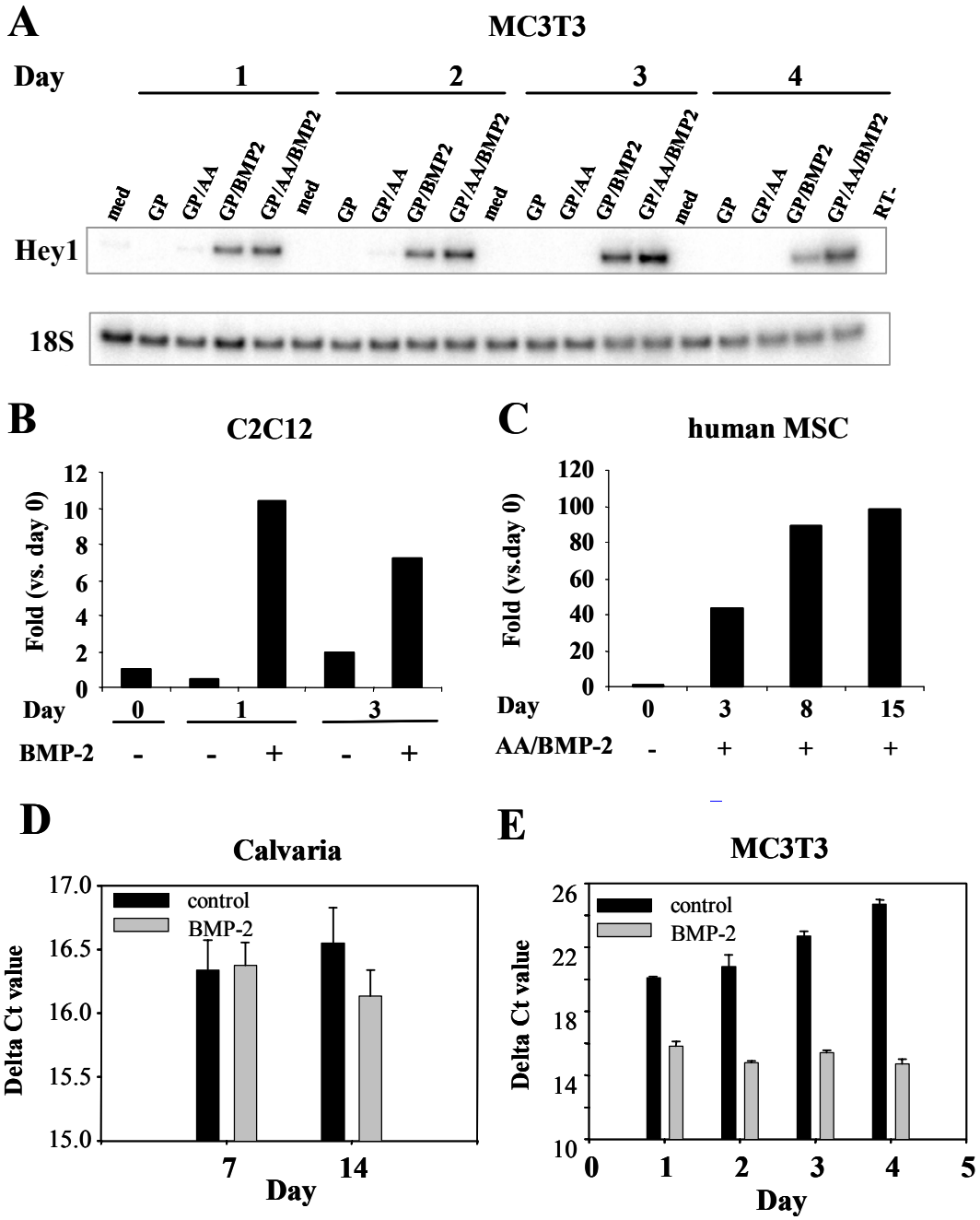

Figure 16: BMP-2 induces *Hey1* gene.

A: Induction of *Hey1* by BMP-2 in MC3T3 cells. MC3T3 cells were cultured in the absence (medium) or presence of GP, AA, and/or BMP-2 for 1, 2, 3 and 4 days, total RNA was extracted and analyzed for the expression of *Hey1* and the housekeeping 18S ribosomal RNA gene by qrRT-PCR. The radioactive PCR products were analyzed by polyacrylamide gel electrophoresis and imaged by PhosphorImager. B: Induction of *Hey1* by BMP-2 in C2C12 cells. C2C12 cells were treated with BMP-2 for 0, 1, and 3 days, total RNA was extracted and analyzed for the expression of *Hey1* by qrRT-PCR. The results shown are derived from GeneCHIP microarray analysis (Affymetrix array MG-U74Av2, probe set

number 95671_at, sequence accession number AJ243895). C: Induction of *Hey1* by BMP-2 in human mesenchymal stem cells (MSC). The results shown are derived from GeneCHIP microarray analysis (Affymetrix array HG-U133A, probe set number 218839_at, sequence accession number NM_012258). D: Quantitative real-time RT-PCR analysis of *Hey1* expression in mouse calvaria. E: Quantitative real-time RT-PCR analysis of *Hey1* expression in MC3T3 cells. Delta Ct value - difference of threshold cycle (Ct) value for *Hey1* and *18S* as normalizing control.

3.1.4.9 Down-regulation of Hey1 mRNA by siRNA stimulates mineralization

Since members of HES - Hey family work predominantly as transcriptional repressors[171], and since Hey1 inhibits myogenic differentiation[172], we tested whether the induction of Hey1 could inhibit osteogenic differentiation. For this reason we blocked BMP-2-induced *Hey1* up-regulation with a small interfering RNA (siRNA) specific for *Hey1* (Fig. 17A). *Hey1* was efficiently down-regulated at day 1 and this down-regulation persisted until day 3 (>70 % inhibition). At day 4, *Hey1* mRNA levels in siRNA-treated samples returned back to the control levels (Fig. 17A). Then we tested the effect of this transient *Hey1* down-regulation on several osteoblast early marker genes (Fig. 17B). However, all these genes (*ALP, Osx, Id2, Dlx2* and *Fra1*) were unaffected by the treatment by siRNA for *Hey1*. This result indicated that Hey1 was not involved in regulation of genes expressed early in osteoblastic lineage. Therefore, we next tested the effect of *Hey1* down-regulation on late events in osteoblastic differentiation, such as bone nodule formation and mineralization (Fig. 17C). Treatment with osteogenic stimulus induced intense mineralization in MC3T3 cultures (Fig. 17C). The mineralization capacity of MC3T3 cells treated with siRNA for *Hey1* further increased this mineralization, while control siRNA had somewhat inhibiting effect, compared with mock treated cultures (Fig. 17C). These results showed that Hey1 has an inhibitory role during matrix mineralization by osteoblasts and that even transient removal of Hey1 is sufficient to influence this process.

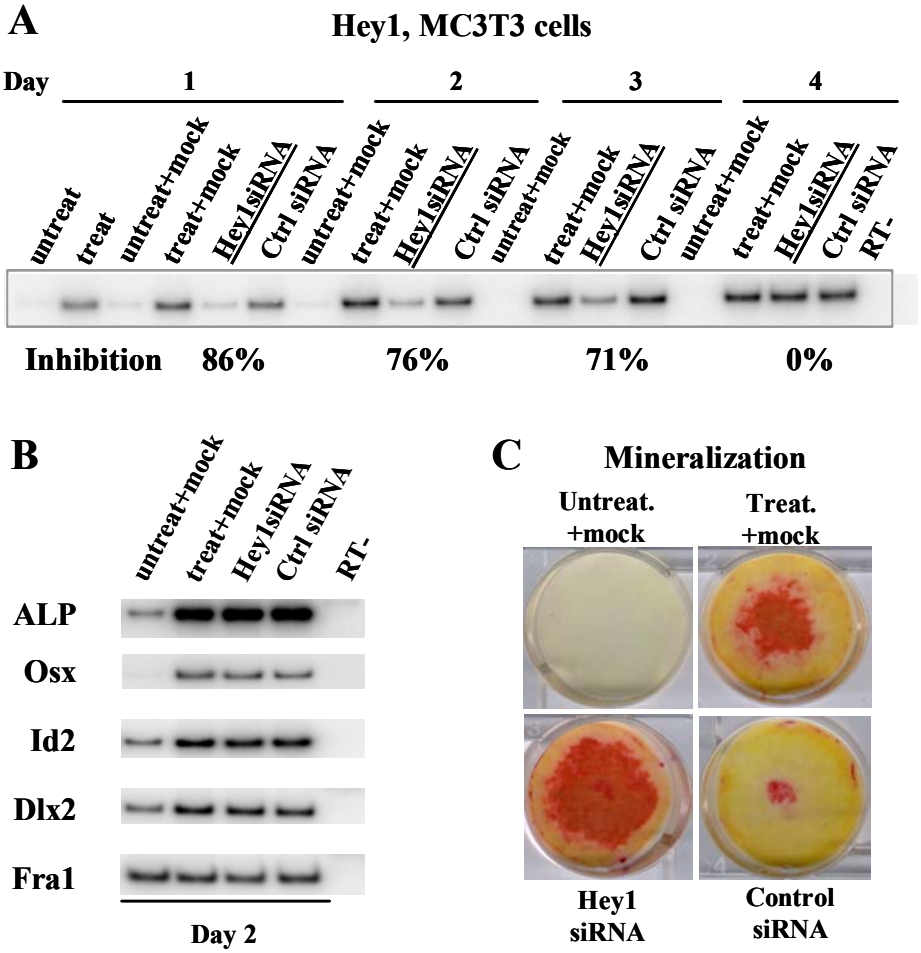

Figure 17: The effects of *Hey1*-specific siRNA on *Hey1*, early marker gene expression, and on matrix mineralization by MC3T3 cells.

A: Inhibition of osteogenic stimulus-induced *Hey1* expression by *Hey1*-specific siRNA. MC3T3 cells were: not transfected (untreat, treat), mock-transfected (untreat+mock, treat+mock); transfected with *Hey1*-pecific siRNA (Hey1siRNA); and transfected with non-silencing siRNA (control siRNA). After 4 h of siRNA transfection cells were either not treated (untreat, untreat+mock) or treated with GP/AA/BMP-2 (treat, treat+mock, Hey1siRNA, control siRNA). Total RNA was isolated after 1, 2, 3 or 4 days and *Hey1* expression was analyzed by qrRT-PCR. B: The effects of *Hey1*siRNA on expression of early osteoblast marker genes. Total RNA isolated as described in A (day 2) was used for the analysis of expression of indicated genes by qrRT-PCR. C: The effect of *Hey1*siRNA on matrix mineralization by MC3T3 cell cultures. MC3T3 cells were either mock transfected (untreat+mock, treat+mock), transfected with *Hey1*siRNA or with non-silencing siRNA (control siRNA). After 4 h of transfection cells were either not treated (untreat) or treated with GP/AA/BMP-2 (treat+mock, Hey1siRNA, control siRNA). Alizarin Red S staining was performed 17 days after transfection and is visible as red areas on the shown photos.

3.1.4.10 Hey1 inhibits Runx2 transcriptional activity

The above results prompted us to further analyze the molecular basis of enhanced osteoblast activity due to the inhibition of *Hey1* induction. Runx2 is a transcription factor that plays an essential role in osteoblast differentiation and mutations interfering with its function correlate with defects in ossification in humans and mice[56]. Many signal transduction pathways that affect osteoblast differentiation modulate Runx2 activity[83]. Therefore, we examined the effect of Hey1 on Runx2 transcriptional activity using a luciferase reporter gene driven by an artificial promoter containing 8 Runx2-binding sites (OSE2) in front of a minimal osteocalcin promoter mOG2. As shown in Fig. 18A, ectopic expression of Runx2 strongly stimulated transcription of the reporter gene controlled by the intact, wild type (Fig. 18A, lanes Cbfa1, 8xOSE2wt). As expected, Runx2 did not stimulate reporter gene activity that was controlled by the promoter without OSE2 sites, which contained only minimal osteocalcin promoter (OG2luc). Similarly, no activation by Runx2 was detected with the promoter containing mutated OSE2 sites (8xOSE2mut). Co-expression of Hey1 with Runx2, however, almost completely abrogated Runx2-driven transcription (Fig. 18A, lanes Cbfa1+Hey1). Control co-transfections showed that empty vector pcDNA3.1 had a small effect on reporter genes and that pcDNA3.1 did not affect Runx2-induced reported gene activity. Fig. 18B shows increased expression levels of *Runx2* and *Hey1* in co-transfection experiments. These results suggested that Hey1 inhibits bone matrix mineralization by osteoblasts by controlling Runx2 activity.

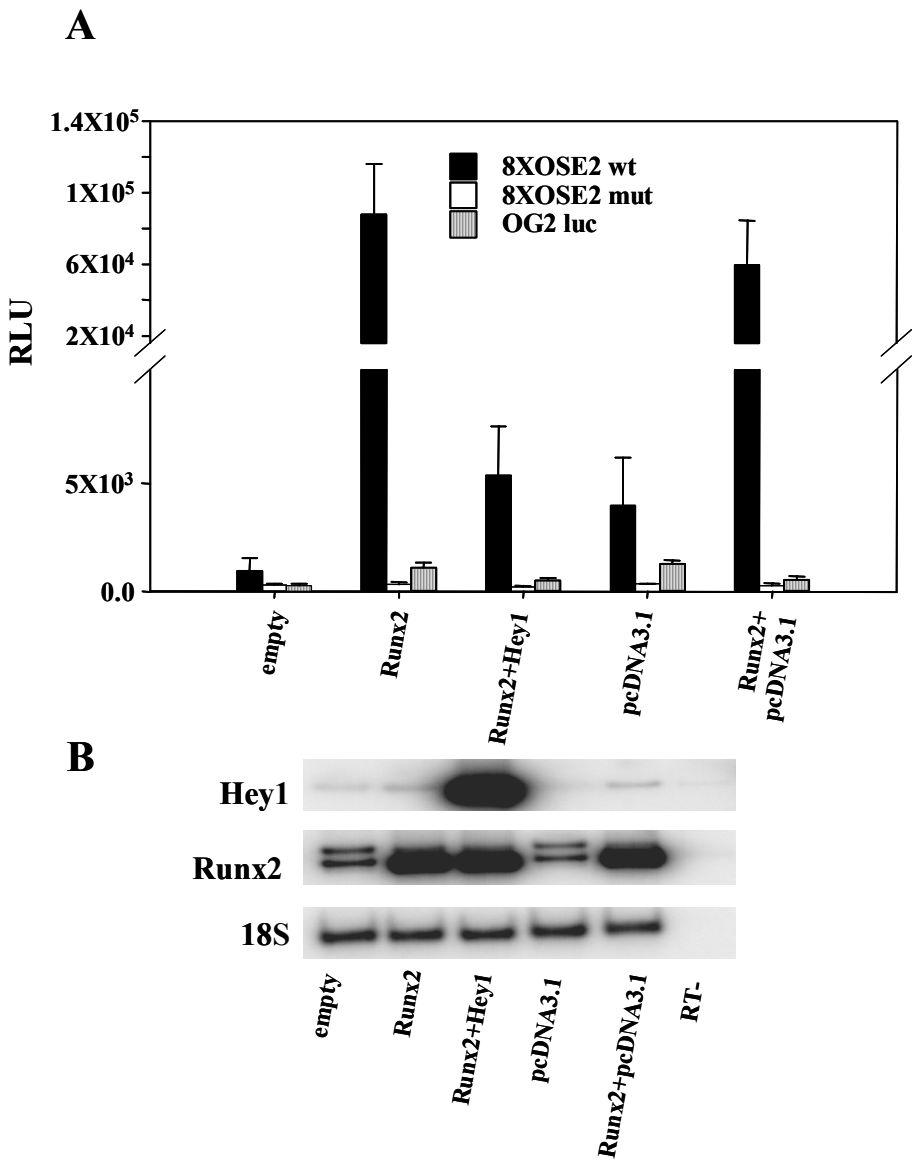

Figure 18: Hey1 inhibits Runx2 transcriptional activity.

A: Activity of OSE2-luciferase in MC3T3 cells after co-transfection of Runx2, Hey1 and OSE2-luciferase vectors. *Runx2* and *Hey1* cDNAs in pcDNA3.1 (+) expression vector, were transiently co-transfected with OSE2-luciferase reporter gene, containing minimal osteocalcin gene promoter (OG2) and 8 wild-type (8XOSE2 wt) or mutated (8XOSE2 mut) Runx2-binding sites. Transfection was done for 4 h and luciferase activity was measured after 24 h. B: Overexpression of transfected *Runx2* and *Hey1*, shown by qrRT-PCR. Transfection was done as in A and after 24 h total RNA was extracted and qrRT-PCR performed.

3.1.5 Discussion

3.1.5.1 Microarray analyses of genome-wide gene expression in osteoblasts

There is a strong interest in discovering new players in the osteoblast differentiation process, which is still far from being completely understood. One approach to unravel molecular player on osteoblast differentiation process is to analyze genome-wide gene expression profiles during differentiation, and the results of several such studies have recently been reported[162,173,174,175,176]. These studies, using different model systems of osteoblast differentiation and different differentiation agents, all highlighted some new genes involved in differentiation process, proving the usage of microarray experiments useful.

In this study, we have identified 394 genes with known function and 295 ESTs to be regulated during osteoblast differentiation. The features of this study are: a) extensive cellular and molecular characterization of the osteoblast differentiation process for each individual experiment analyzed by microarray; b) normalization to time-matched controls to eliminate gene expression changes spontaneously occurring during cell culture; c) stringent selection criteria; d) extensive qrRT-PCR validation of regulated genes, and e) annotation and classification of regulated genes according to their cellular functions. As the most interesting and novel finding we report the concomitant regulation of genes encoding components of the TGF-β, Wnt and Notch signaling pathways. Thus, although we used similar technology as studies described above, the precision of our cellular system and extensive control of experimental and analysis conditions enabled us to unravel several new sets of genes, which are regulated during osteogenesis and to come to a more compete picture of osteogenesis.

Name	Description	PSN	Acc No	REL	
				d1	d3
TGF-β signaling pathway					
TGF-β1	Transforming growth factor beta 1	101918_at	AJ009862	2.07	4.51
TGF-β3	Transforming growth factor beta 3	102751_at	M32745	2.37	2.72
Activin	inhibin beta-A	100277_at	X69619	2.45	1.13
TGF-β2	Transforming growth factor beta 2	93300_at	X57413	0.95	0.43
TIEG	TGF-β inducible early growth response. Transcription factor	99602_at	AF064088	2.50	1.43
Tenascin C	Extracellular matrix glycoprotein	101993_at	X56304	2.534541	6.299492
Kerato-epithelin	Extracellular adxesion molecule	92877_at	L19932	2.827532	2.048872
SSTR2	Somatostatin receptor type 2. GPCR	98350_at	AF008914	1.96	2.85
Wnt signaling pathway					
LRP5	Low density lipoprotein receptor-related protein 5	103806_at	AF064984	0.25	0.32
Tcf7 (Tcf1)	Activation of Wnt responsive genes and target of Wnt signalling.	97994_at	AI019193	1.00	9.70
LEF1	Lymphoid enhancer binding factor 1. Activation of Wnt responsive genes	103628_at	D16503	1.25	2.05
Notch signaling pathway					
Notch1	Receptor for membrane-bound ligands Jagged and Delta-like	97497_at	Z11886	0.54	0.11
Notch3	Receptor for membrane-bound ligands Jagged and Delta-like	92956_at	X74760	0.37	0.27
NOV	Nephroblastoma overexpressed gene	100507_at	Y09257	0.21	0.33
Hey1	bHLH transcription factor.Notch target gene	95671_at	AJ243895	3.15	4.81
Regulation of osteoclastogenesis					
OPG	Osteoprotegerin	102887_at	U94331	1.88	3.84
PTHRP	Parathyroid hormone-like peptide	104262_at	M60057	0.85	0.48
SCYA7	Small inducible cytokine A7	94761_at	X70058	0.74	0.45

Table 9: Expression profiles of regulated genes of TGFβ, Wnt and Notch signaling pathways, and genes involved in osteoclastogenesis control. Genes from TGF-β, Wnt and Notch signaling pathways, as well as genes involved in regulation of osteoclastogenesis, whose expression changed ≥ 2-fold upon stimulation with osteogenic stimulus. Black font - up-regulated transcripts; Grey font - down-regulated transcripts; PSN- Affymetrix probe set

number; Acc No- sequence accession number; REL- relative expression level (median value), compared to the non-stimulated, time-matched control; d1 - day 1; d3 - day 3.

3.1.5.2 TGF-β pathway

We showed that activation of TGF-β pathway by osteogenic stimulus and more precisely by BMP-2 is achieved by increasing the autocrine production of ligands TGF-β1 and 3 and of related ligand Activin, followed by the up-regulation of corresponding target genes (*TIEG*, tenasacin, kerato-epthelin, *SSTR2*). Biological evidence for a role for TGF-β in osteoblast regulation is ample[146], but it's mechanisms of action are complex and poorly understood. Differences in the ultimate effect appear to depend on TGFβ concentration, duration of exposure and cell differentiation status[177]. TGFβ inhibits apoptosis in osteoblasts[178], and it enhances osteoclasts differentiation[179]. It has been shown that pre-treatment of osteoblastic cells with BMP-2 changes the binding of TGFβ to its receptors by increasing binding to the type I receptor[180]. Depending on the status of the cells being tested, this binding shift enhances TGFβ-induced collagen synthesis or alkaline phosphatase activity[180]. Therefore, our result that BMP-2 induced TGFβ pathway suggests a way to broaden and diversify the direct action of BMP-2 signaling on osteoblast.

3.1.5.3 Wnt pathway

Next interesting finding was the activation of Wnt pathway by osteogenic stimulus, documented by up-regulation of two target genes, transcription factors *Tcf7* and *LEF1*. During the course of our work, Wnt pathway came into a focus in bone biology through the finding that LRP5, a co-receptor for Wnt, is a high bone mass gene and is mutated in osteoporosis-pseudoglioma syndrome[36,37,38]. Interestingly, we showed that *LRP5* was down-regulated by the osteogenic stimulus. Recently it was shown that BMP-2-induced activation of alkaline phosphatase, an early marker of osteoblast differentiation, depends on Wnt/LRP5 signaling, and that BMP-2 induces *Wnt1* and *Wnt3a* expression, resulting in autocrine Wnt pathway activation[167]. We have also observed transcriptional up-regulation of some Wnt family members, however, they were not identical to those reported (*Wnt6, Wnt10a*) and this activation was not reproduced in two from three experiments. Therefore, we concluded that this up-regulation may not be significant and that mechanisms of Wnt pathway activation by BMP-2 need further evaluation.

3.1.5.4 Notch pathway and Hey1

Another novel finding was a strong up-regulation of *Hey1*, a direct Notch target gene. Notch signaling is an evolutionarily conserved mechanism used by metazoans to control cell fates through local cell interactions[181]. Initially, Notch pathway was linked to bone biology by observations that mutations in the genes encoding a Notch ligand Delta homologue (Dll-3) and a Notch signaling molecule presenilin-1 both cause axial skeletal phenotypes[182,183]. Recently it was shown that generation of haematopoietic stem cells in bone marrow is supported by activation of Notch pathway by a ligand Jagged1, produced by osteoblasts, pointing to a Notch-mediated functional interaction between bone and bone marrow[184]. So far there were two studies investigating Notch signaling in osteoblasts, both of which used exogenous overexpression of the constitutively active Notch1 intracellular domain, and which produced conflicting results[160,161]. We argue that Notch pathway is activated by osteogenic stimulus and BMP-2, based on a strong up-regulation of Hey1 transcription factor. However, we did not detect mRNA for the Notch ligands Delta and Jagged in MC3T3 cells (data not shown), indicating that they are weakly expressed or absent. As Notch activation is achieved via proteolytic cleavage[185], a high protease expression / activity could be responsible for its activation. Another possibility for enhancing of Notch activation is association with gene NOV (nephroblastoma overexpressed gene), a growth factor from the CCN (constituted of connective tissue growth factor CTGF, cysteine-rich 61 *Cyr*61, NOV, and other related genes) gene family[186]. Namely, recently it was shown that NOV associates with Notch1 in C2C12 cells and thereby activates Notch, leading to induction of promoters of immediate target Notch genes *HES1* and *5*[187]. This activation led to an inhibition of myoblastic differentiation, an effect similar to the effect of BMP-2. Interestingly, we found that *NOV* expression is high in MC3T3 cells and it is strongly down-regulated as cells undergoing differentiation, in parallel with *Notch 1* and *3*. A graphical summary of gene activation on TGFβ, Wnt and Notch pathways is shown in Fig.19.

What is the consequence of Notch pathway activation in various cell types? Expression of constitutively active Notch inhibits differentiation of neural and myogenic cells and promotes generation of hematopoietic stem cells[187,188,189]. Very recent studies have shown that BMP and Notch signaling do collaborate during differentiation of myogenic and endothelial cells, and that Hey1 is a crucial player in

this collaboration[190,191]. Our data in osteoblast cells show that even transient inhibition of *Hey1* expression leads to enhanced matrix mineralization by osteoblast, a sign of their maturation. Therefore, in osteoblastic lineage as well Notch pathway seems to have a role of preserving pluripotent cell phenotype. Down-regulation of *Notch1*, *Notch3* and *NOV* later during osteogenesis suggests that cells are down-regulating this pathway in order to advance their differentiation. Thus, Notch pathway seems to play a transient role only at the beginning of the differentiation.

Finally, what is the mechanism of action of Hey1? One of the central players in the osteoblast differentiation process is the Runx2 transcription factor, which coordinates multiple signals involved in osteoblast differentiation[83]. So far, two transcription factors were shown to form inhibitory complexes with Runx2, and to inhibit osteoblast differentiation: Stat1[92], and Twist[22]. Our result showing that Hey1 can almost completely abrogate Runx2 transcriptional activity indicates that Hey1 is a novel inhibitory partner of Runx2.

In summary, in this study we identified a number of genes which were regulated in osteoblastic differentiation and which were either known for their involvement in this process or were novel. The analysis of activated genes showed that BMP-2-containing osteogenic stimulus, in addition to the expected activation BMP-2 pathway, concomitantly induces three other signaling pathways: those of TGFβ, Wnt and Notch (Fig. 19). Furthermore, we highlighted a negative role of a Notch target gene Hey1 in the osteogenic differentiation. Thus, these data enabled novel insights in the osteoblast biology.

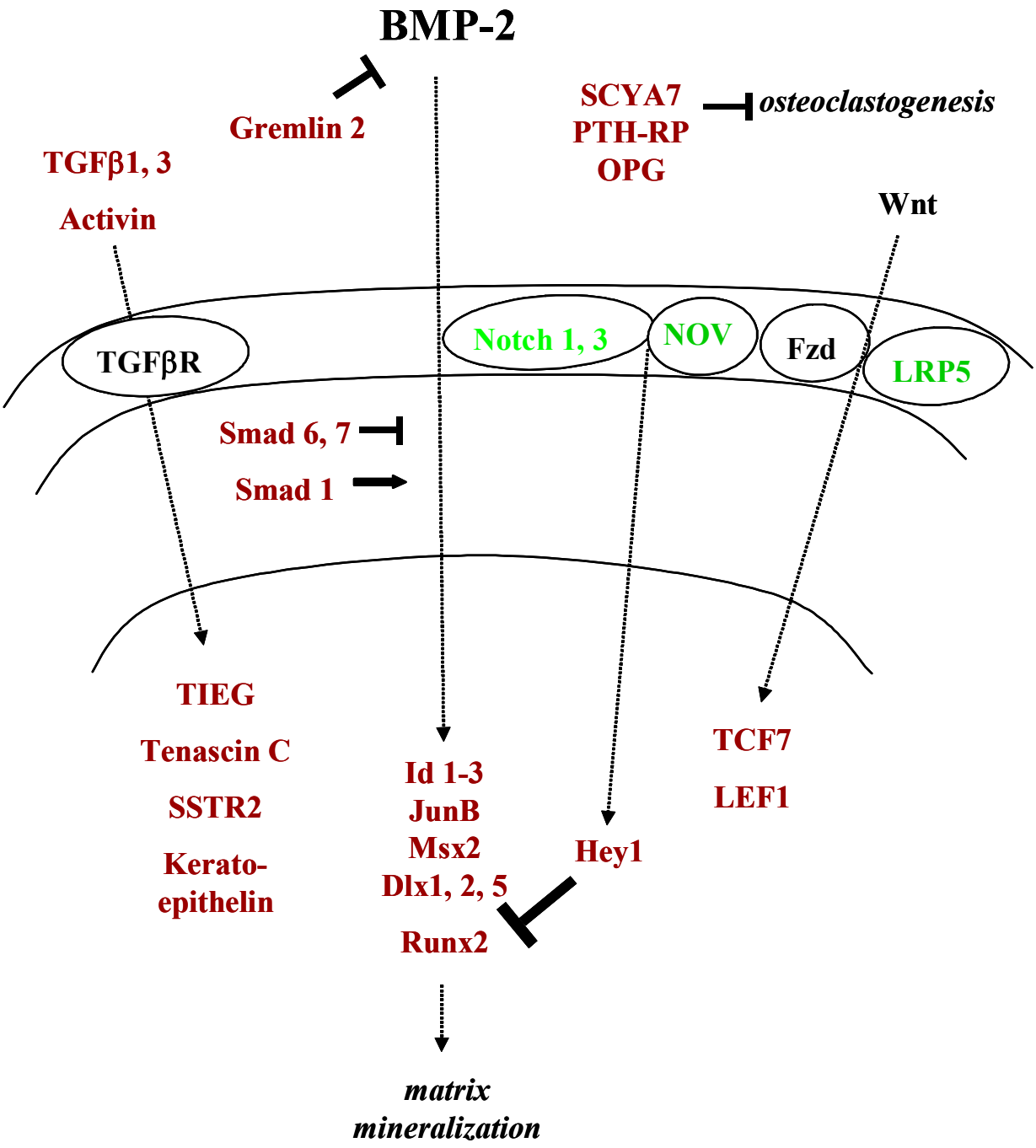

Figure 19: Schematic model of coordinated activation of Notch, Wnt and TGF-β signaling pathways in BMP-2 induced osteogenesis.

Red: up-regulated; green: down-regulated; black: expressed.

3.1.6 Footnotes

Supplementary Material

A total data set from microarray analyses is submitted to the NCBI gene expression and hybridization array data repository (GEO). GEO submission numbers: GSE1131; GSM 18546-GSM18560.

Abbreviations

AA – ascorbic acid; ALP – alkaline phosphatase; bHLH – basal helix-loop-helix; BMP-2 - bone morphogenic protein 2; EST – expressed sequence tag; GAPDH - glyceraldehyde-3-phosphate dehydrogenase; GP – beta glycerol phosphate; HES - Hairy and Enhancer of Split; Hey1 - Hairy and Enhancer of Split-related with YRPW motive 1; HLH – helix-loop-helix; hMSC – human mesenchymal stem cells; LEF1 - lymphoid enhancer binding factor 1; LRP5 – low-density lipoprotein receptor related protein 5; OSE2 – osteoblast specific element 2; PBS – phosphate buffered saline; PTH – parathyroid hormone; qrRT-PCR – quantitative radioactive reverse transcription-polymerase chain reaction; RAMP1 - receptor (calcitonin) activity modifying protein 1; Runx2 – runt-related transcription factor 2; siRNA - small interfering RNA; Smad - MAD, mothers against decapentaplegic homolog; Tcf7 - transcription factor 7, T-cell specific; TGF-β - transforming growth factor beta; Wnt – wingless-type MMTV integration site family;

Acknowledgements

The authors would like to thank Sandrine Bongiovanni, in the group of Georges Imbert, and Nicole Hartmann, in the group of Frank Staedtler, European Genome Factory, Novartis Pharma AG, who performed microarray hybridization experiments; Jo Rahuel, for his help in analyzing microarray data; Christine Halleux and Gabriela Guiglia, who performed human MCS experiment; Juerg Gasser and Andrea Rebmann, who treated mice with BMP-2 and isolated calvariae; Francois Natt, for providing us control siRNA; Johann Wirsching and Hans-Joerg Keller, for providing OSE2luc reporter gene and Cbfa1 expression plasmid, and for the advise in cloning experiments; and Reinhard Moschitz, a trainee in our laboratory, for his help with real-time PCR experiments.

3.2 Supplementary data

3.2.1 Osteoblast differentiation systems comparison by analysis of phenotypic and molecular markers

3.2.1.1 Introduction

Differentiation of mesenchymal precursors into bone-forming mature osteoblasts is a process that can be mimicked *in vitro*. There are various *in vitro* models of osteoblast cells differentiation. Since these different models represent in part distinct phases of osteoblastic differentiation and since their differentiation efficacy can greatly differ depending on experimental conditions, an appropriate model has to be carefully selected.

BMP stimulation is commonly used for studying differentiation of multipotential mesenchymal cells into osteochondrogenic lineage cells. For these analyses, multipotent mesenchymal cell line C3H10T1/2, a fibroblastic cell line isolated from an early mouse embryo, is very frequently used. Also, various cell lines deriving form bone marrow stromal cells, like ST2 or PA6 mouse cell lines, or primary cultures of bone marrow stromal cells, are commonly used in this type of studies (reviewed in Yamaguchi *et al.*, 2000[192]).

BMP also stimulates differentiation of committed osteoblast precursor cells. For these analyses, ROB-C26, committed osteoprogenitor rat cell line can be used. These cells retain the potential to differentiate into myotubes and adipocytes[193]. Few osteoblastic cell lines have been isolated from osteosarcomas, such as rat ROS17/2.8 cell line[194]. Osteosarcoma cells are usually good responders to growth factor and hormone short-term stimulation, but their transformed phenotype creates changes in gene expression and they can rarely and inefficiently differentiate into mature cells, capable of producing mineralized bone matrix. MC3T3-E1 is a clonal osteoblastic cell line isolated form calvariae of newborn mouse[140], which can mimick pre-osteoblastic proliferation, as well as early and late differentiation. It is highly BMP-responsive and can complete differentiation process and form mineralized nodules in the long-term cultures. Primary osteoblastic cells isolated from calvariae of newborn mice or rats can also generate mineralized bone nodules in culture in the presence of BMP. However, these cells, in contrast to synchronized, homogenous population of cell line

in culture, represent the mixture of cells in various stages of differentiation process. Major part of such cultures is comprised by differentiating osteoblasts, while only a small part is contributed by the precursor cells.

BMP stimulation is also used in osteogenic transdifferentiation of myogenic cells. Injection of BMPs into muscular sites demonstrated that BMPs enduced ectopic cartillage and bone formation[46,195]. Classical system for studying the regulatory mechanism of osteogenic transdifferentiation of myogenic cells by BMPs is C2C12 mouse myoblastic cell line, which was established from muscular tissue satelite cells. C2C12 cells in a low serum conditions differentiate into myocytes. BMP-2 stimulation induces differentiation to the osteoblast lineage[196].

In our study we have compared three BMP-2-driven mouse osteoblast differentiation systems: MC3T3 cell line, C2C12 cell line and primary mouse calvarial osteoblasts. Since we wanted to examine early transcriptional events during differentiation, we needed a system that would differentiate fast and up-regulate a maximal number of marker genes in a reproducible fashion. The profiles of marker genes could be used then as a quality control of each individual experiment. Since MC3T3-E1 cell line is also known for phenotypic variation in culture[139], we used a cell clone obtained at a low passage number from a laboratory who kept the cells at their original maintenance conditions[140]. To ensure that the cells show expected behavior also at the molecular level, we selected from this MC3T3-E1 cell batch a further clone, which efficiently activated Runx2-dependent reporter gene, and induced Runx2 mRNA and protein. A clone of C2C12 cells was also selected, that efficiently activated Runx2-dependent reporter gene in response to BMP-2 stimulation.

3.2.1.2 Experimental procedures

Cell culture. MC3T3 cells were grown and the stimulation was performed as described in 2.1.3.

C2C12-15a clone was generated after transfection with OSE2-luciferase reporter gene, measuring the activity of Runx2, followed by a selection for clone in which luciferase was activated by the osteogenic stimulus (100-400 ng/ml BMP-2) (Christine Halleux and Lilian Hartmann, Novartis Institutes for BioMedical Research, Basel, Switzerland) . The cells were grown in DMEM High Glucose with 15% fetal calf serum (FCS, Gibco), 1% penicillin/streptomycin (Pen/Strep), 2% L-Glutamine (L-Glu) and 1% Hepes in T175 flasks (40 ml/flask). The stimulation was done in the

same medium. For RNA isolation and alkaline phosphatase staining, C2C12 cells were respectively plated on 6 cm dishes ($1.8x10^5$cells/dish in 5 ml medium) and 48-well plates ($6.5x10^3$ cells/well in 1 ml medium. Cells were grown to confluence for 3 days at 37°C / 5% CO_2, and then stimulated with 400 ng/ml BMP-2 (Nico Cerletti, Novartis) for 1 or 3 days. Control cells were grown in medium alone.

Primary mouse calvarial osteoblasts were obtained from calvarias of 6 days old mice (performed by Daisy Rohner, Novartis Institutes for BioMedical Research, Basel, Switzerland). Ten mice were killed by decapitation. Heads were put directly in 70% ethanol, then washed once in cold Tyrode solution (4°C). All work was done under sterile conditions in laminar hood. Skin from the top of the head was removed, calvarias separated, cleaned and put in cold Tyrode solution. Then, series of digestion with collagenase enzyme were performed: Calvarias were put in Erlenmeyer with magnetic stirrer inside, 5 ml of 0.2% collagenase in PBS + 4mM EDTA was added and incubated 10 min at 37°C/5% CO2. Supernatant was discarded and calvarias washed with PBS. The same procedure was repeated once more. After second PBS washing, 10 ml of 0.2% collagenase in PBS was added and mixed slowly for 10 minutes at 37°C on a magnetic stirrer. Supernatant was stored in 50 ml Falcon tube. Calvarias were washed twice with 10ml of medium (RPMI 1640 (Gibco) with 10%FCS, 1% penicillin/streptomycin, 1% L-glutamate and 1% Hepes buffer), and added to the 50 ml Falcon tube. It was centrifuged 8 minutes at 1000 g, pellet washed with 20 ml medium and centrifuged 8 minutes at 1000 g again. Pellet was resuspended in 2 ml of medium and cells were counted in Trypan blue. 1.25X104 cells/cm2 (9X105 cells in T75 flask) were seeded and incubated at 37αC/ 5% co2. Medium was changed after 4 hours. Cells were 95% confluent after 4 days, when they were seeded for stimulation. For RNA isolation, alkaline phosphatase and Alizarin red S staining, cells were respectively plated on 6 cm dishes ($2.5x10^5$cells/dish in 5 ml medium), 48-well plates ($1x10^4$ cells/well in 1 ml medium) and 12-well plates ($5x10^4$ cells/well in 3 ml medium). Cells were grown to confluence for 3 days at 37°C / 5% CO_2, and then stimulated with 10 mM β-glycerophosphate (GP, Sigma), 50 µM ascorbic acid (AA, Wako) and 400 ng/ml BMP-2 (Nico Cerletti, Novartis), or 5 ng/ml TGFβ1 (R&D systems) for 1 and 3 days. Control cells were stimulated with 10 mM β-glycerophosphate alone, or with 10 mM β-glycerophosphate+ 50 µM ascorbic acid. For Alizarin Red S staining, cell cultures were fed with fresh medium and osteogenic factors twice weekly.

Alkaline phosphatase staining, Alizarin red S staining for mineralization, RNA isolation, and quantitative radioactive RT-PCR (qrRT-PCR) were performed as described in 2.1.3. Alkaline phosphatase staining and Alizarin red S staining were performed by Daisy Rohner, Novartis Institutes for BioMedical Research, Basel, Switzerland. Optimisation for qrRT-PCR for each individual gene analyzed was performed first. Optimal PCR conditions (annealing temperature and additives addition) were set up in a cold PCR reaction under standard conditions containing containing 100 µM of each dNTP, 1 µM of each primer and 1.25 units of "Hot start" thermostable DNA polymerase and corresponding reaction buffer (FastStart Taq, ROCHE Molecular Diagnostics), in a final volume of 25 µl. The amplification protocol was the following: initial step of 5 min at 94°C, 35 cycles of denaturation at 94° C for 1 min, annealing at 57/60° C for 1 min, and extension at 72° C for 1 min 20 s. The amplification was terminated with a final incubation step at 72° C for 10 min. Cycle curve experiment was done in a final volume of 50 µl, containing 1 µCi of α [^{32}P]-dATP, 100 µM of each dNTP, 1 µM of each primer and 1.25 units of "Hot start" thermostable DNA polymerase and corresponding reaction buffer (FastStart Taq, ROCHE Molecular Diagnostics). In addition some reaction mix contained 5% glycerol. The amplification protocol was the following: initial step of 5 min at 94°C, 35 cycles of denaturation at 94° C for 1 min, annealing at 57/60° C for 1 min, and extension at 72° C for 1 min 20 s. The amplification was terminated with a final incubation step at 72° C for 10 min. Annealing temperature was as optimized in a cold PCR reaction, 57 or 60 °C (see 2.1.3). Starting for cycle 18-20, 5 µl aliquots were taken every two cycles, and analyzed on polyacrilamide gel as described 2.1.3. Cycle curve for each gene was drawn by plotting quantified signal in a function of cycle number. Cycle number for quantitative analysis was taken from a middle of a linear range of a reaction.

3.2.1.3 Results

Phenotypic characterization of different osteoblast differentiation systems

C2C12 and MC3T3 cell lines and primary mouse calvarial osteoblasts (PMCO) were stimulated with different osteogenic stimuli. MC3T3 and PMCO were stimulated with a mixture of β-glycerophosphate, the phosphate source for the mineralization

process; ascorbic acid (AA), a cofactor in collagen synthesis and trimer formation, and BMP-2, growth factor that strongly stimulates differentiation process. Since C2C12 cells are not able to mineralize the matrix, they were stimulated with BMP-2 only, which induces their differentiation to the osteoblast lineage[196]. All differentiation systems were analyzed by Alkaline Phosphatase (ALP) staining, as an early differentiation marker, and by Alizarin Red S staining for mineralization, a late outcome of osteoblast differentiation. The results are shown in Fig. 20.

After stimulation with BMP-2, C2C12 cultures showed an increased ALP staining at both days 2 and 3. However, those cells were not able to finish differentiation process and could not form mineralized bone nodules (Figure 20).

After BMP-2 stimulation MC3T3 cells showed strong ALP staining at day 3. Already at day 11, red dots that represent mineralized bone nodules are visible in the MC3T3 cultures (Figure 20). This is an early time point, since it has been reported in the literature that these cells may need up to 30 days to mineralize [197].

PMCO have a noticeable basal level of ALP staining, which shows the presence of differentiated osteoblasts even before BMP-2 stimulation. Staining was significantly increased after stimulation with ascorbic acid, and even more with ascorbic acid and BMP-2 together. TGFβ1 did not significantly increase ALP staining. Ascorbic acid alone induced formation of mineralized bone nodules, and this effect was greatly enhanced by BMP-2 (Figure 20).

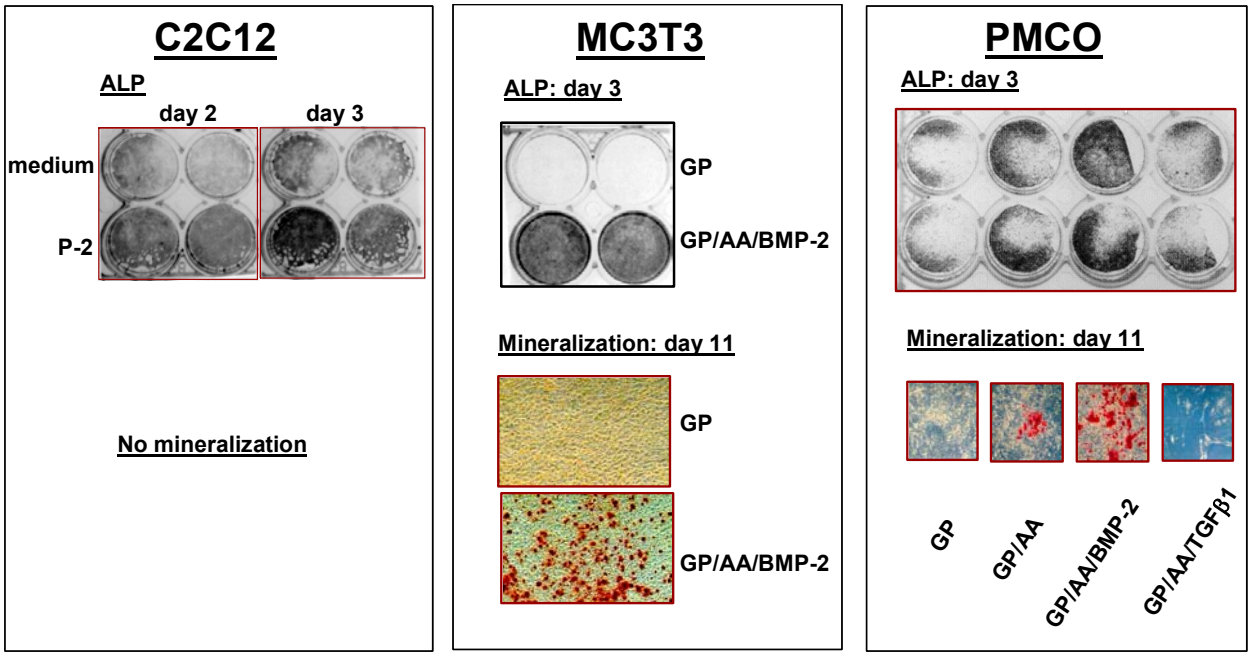

Figure 20: Phenotypic comparison of C2C12, MC3T3 cells and primary mouse calvarial osteoblasts (PMCO). Experimental work performed by D. Rohner.

Optimization of radioactive quantitative RT-PCR analysis for osteoblast marker genes

The flowchart of a typical optimization procedure is shown on the Figure 21: Extracted total RNA was checked for its quality on the 1 % agarose gel. After reverse transcription reaction, cold PCR amplification was performed (Fig. 21, *ALP* gene, with two different sets of primers, and *Msx2* gene), and eventual optimization of amplification conditions was performed if necessary. Negative control is always included (-), in which no reverse transcriptase was added, for verifying that there is no contamination with genomic DNA. Once amplification conditions were optimized, the cycle curve experiment was performed in a radioactive PCR reaction, with an aim to determine linear range of the reaction. The aliquots were taken every two cycles and analyzed on polyacrylamide gel. The signals from the bands of expected molecular weight were quantified and plotted against the number of cycles (Fig. 21) PCR reaction first proceeds in a linear amplification range, during which the amount of product is doubled in each amplification cycle. Radioactive quantitative PCR is done with a cycle number at the lower end of the linear range. This phase is followed by a saturation phase, when the reaction reaches the plateau. The number of cycles when reaction will reach the plateau depends on the starting amount of the PCR

template, e.g. on the gene expression level. Therefore, it is necessary to do the optimization of each individual gene in a particular sample.

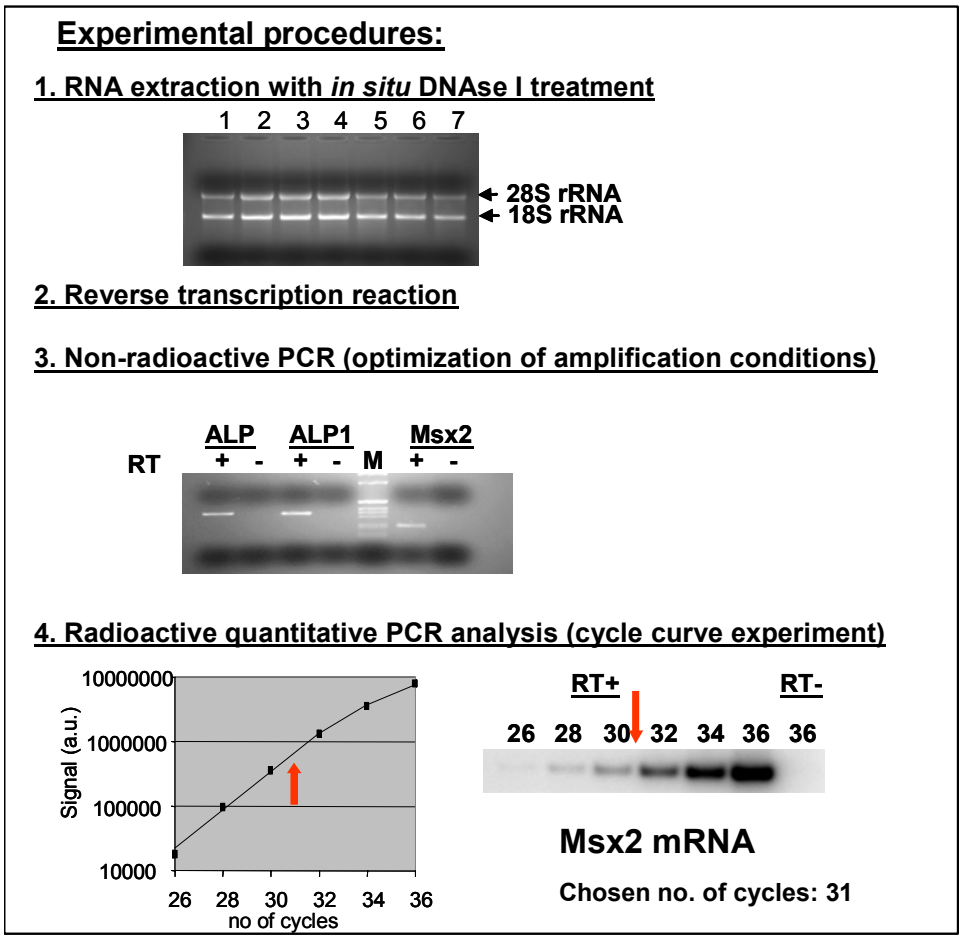

Figure 21: Flowchart of the optimization procedure for rqRT-PCR reaction.

Comparison of marker genes profiles

Comparative analysis for 5 most frequently used markers of osteoblast differentiation was performed: alkaline phosphatase (ALP), transcription factors Msx2 and Runx2, osteocalcin (OCN) and parathyroide hormone receptor (PTHR) (Fig. 22).

C2C12 cells up-regulate *ALP* gene expression in response to BMP-2 stimulation. *Runx2* was also up-regulated at day 1. However, we didn't detect any expression of *Msx2* or *PTHR* gene, and *OCN* was very weakly expressed and not regulated up to day 3 (Figure 22).

MC3T3 cells showed regulation of all the genes analyzed. *ALP* was strongly induced already at day 1 and further increased at day 3. *Msx2* was transiently up-regulated at day 1 and *Runx2* was induced at day 3. *PTHR* and *OCN*, late markers of osteoblast differentiation, were strongly induced already at day 3 (Figure 22).

PMCO stimulated with BMP-2 showed strong *ALP* induction and weak up--regulation of *Runx2*. *Msx2* was strongly expressed in all the samples, while *OCN* was not detected up to day 3. *PTHR* expression was not analyzed in this system (Figure 22).

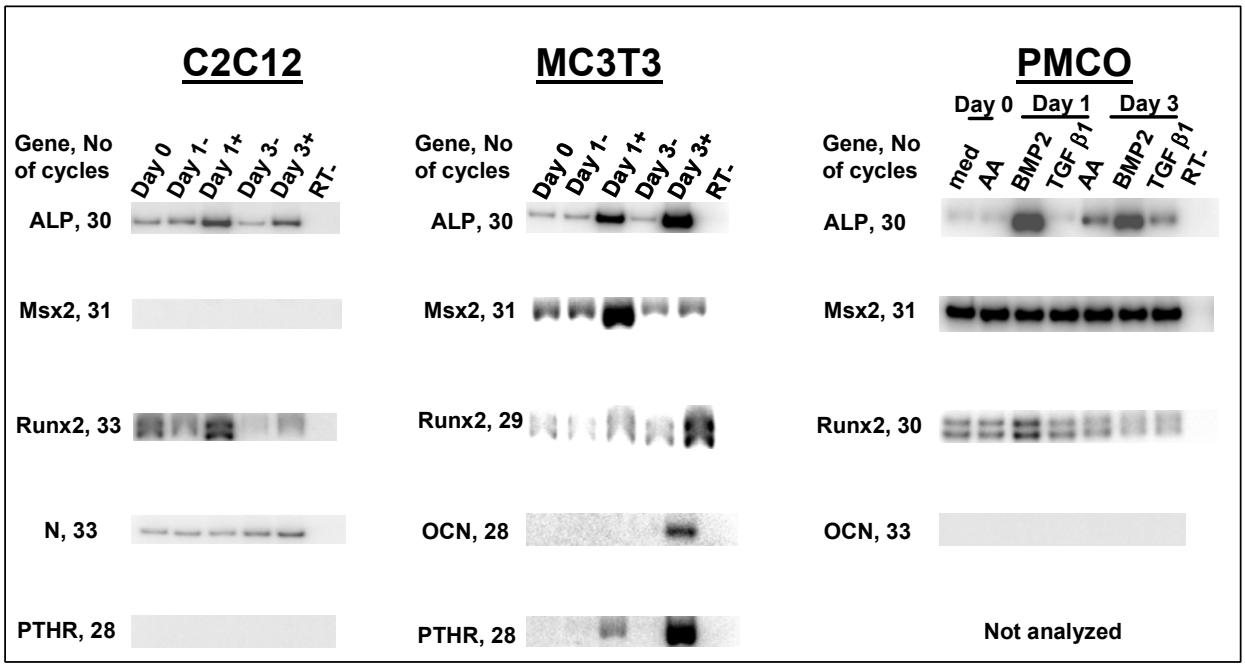

Figure 22: Comparative analysis of osteoblast marker genes profiles in C2C12, MC3T3 cells and primary mouse calvarial osteoblasts.

3.2.1.4 Discussion

Phenotypic and molecular characterization of 3 different systems of osteoblast differentiation convinced us that MC3T3 cells are the fastest, most reproducible differentiation system, which up-regulates most expected marker genes. C2C12 cells were not able to finish differentiation process, and regulated only an early marker of osteoblast commitment, alkaline phosphatase. Primary calvarial osteoblasts on a phenotypic level showed strong and fast mineralization staining at day 11. However, in marker genes analysis we did not detect important marker of late osteoblastogenesis, osteocalcin, while *Msx2*, early marker important for a proliferative phase was constitutively highly expressed. Primary calvarial osteoblasts are a mixture of cells in different phases of differentiation process, and the signal that is obtained for a particular gene expression present an average of the situation that in the individual cells can be very variable. The kinetics of differentiation process using primary osteoblasts can be very variable too, as we have shown in repeated experiment (data not shown). Therefore, these cells are not an optimal system for reproducible gene expression analyses. In conclusion, MC3T3 cells were shown to be the best system for our experiments purposes, and we continued working with this cell line.

3.2.2 Other regulated functional gene groups

3.2.2.1 Introduction

DNA microarray technique-history

The DNA microarray is the latest in a line of techniques to exploit a potent feature of the DNA duplex - the sequence complementation of the two strands (reviewed in Southern *et al.*, 1999[198]). It is remarkable that a molecule of such great structural complexity can reassemble with perfect fidelity from the separated strands. Early studies of duplex melting and reformation, which were carried out with DNA solution, provided valuable basic information: the dependence of melting temperature (Tm) on G+C content and on salt concentration; and the dependence of rate of re-association on sequence complexity.

The introduction of solid supports greatly increased the range of applications of the hybridization method. The starting point was the observation that single-stranded DNA binds strongly to nitrocellulose membrane and permits hybridization to complementary RNA. This simple method proved to be important in the generation of fundamentally important data: measuring the number of copies of repeated genes, such as those for the ribosomal RNAs and tRNAs, or measuring changes in number of copies during amplification processes. When cloning was introduced, it provided a way of finding the clones containing the specific sequences. It was the direct antecedent of the “blotting” methods, the first of which combined filter hybridization with gel separation of DNA restriction digests, and enabled the detection of specific sequence (“Southern” blotting method, Southern, 1975[199]). More relevant to microarrays are the methods of “dot-blotting”, where cloned DNA is blotted to the membrane in dots, without previous restriction digestion and electrophoresis. Hybridization with the labeled probe enables detection of specific sequences.

Subsequent automation and miniaturization of the dot-blot showed how hybridization could be used on a large scale. The main distinction between dot blots and DNA microarrays is in the use of an impermeable, rigid substrate, such as glass, which has a number of practical advantages over porous membrane.

At the present time, the main large-scale application of microarrays is comparative expression analysis. Another application, the analysis of DNA variation on a genome-wide scale, is becoming an increasingly viable prospect. Both applications have become important tool is basic research and their clinical application is increasing.

There are two main types of microarrays, which differ in a type of probe immobilized on a rigid surface. **cDNA microarrays** have long DNA targets, usually in a form of 3' expressed sequence tags (ESTs) spotted onto glass slides. **Oligonucleotide microarrays** have shorter, 20-100 nucleotide long probes spotted or synthesized *in situ* on the glass surface. Various procedures of spotting or synthesizing the probes, hybridization procedures, signal detection and data interpretation and analysis comprise each a topic of its own.

High density synthetic oligonucleotide arrays

Nowadays, one of the most widely used microarray type are high density synthetic oligonucleothide arrays, produced by Affymetrix (reviewed in Lipshutz *et al.*, 1999[200]). They have focused on light-directed synthesis for the construction of high-density DNA probe arrays using two techniques: photolithography and solid-phase DNA synthesis. A glass support is derivatized with a covalently bound linker containing a photochemically removable protecting group. Light is directed through a mask to de-protect and activate selected sites, and protected nucleotides are coupled to the activated sites. The process is repeated, thereby activating a different set of sites and coupling of different bases. This process allows for arbitrary DNA probes to be designed at each site (Figure 23). Photolithography enables the construction of arrays with an extremely high information content (Figure 24, A).

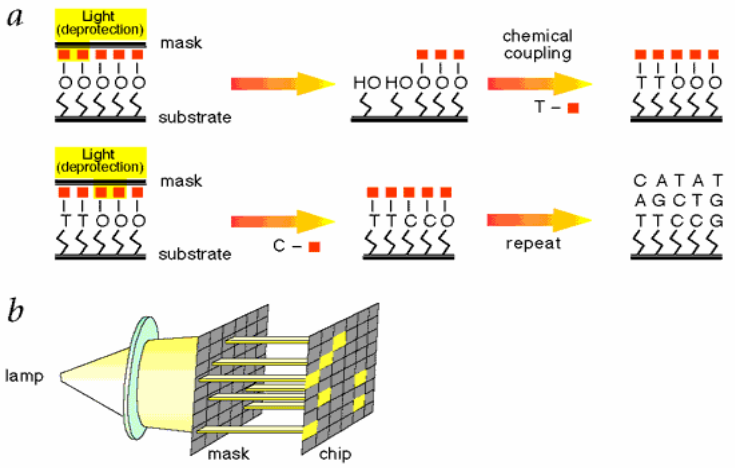

Figure 23. A) Light directed oligonucleotide synthesis. B) Schematic representation of the lamp, mask and array.

Oligonucleotide arrays for expression monitoring are designed and synthesized based on sequence information alone, without the need for physical intermediates such as clones, PCR products, cDNAs and alike. A key to their use is the targeted design of sets of probes to specifically monitor the expression level of as many genes as possible. The sets of independent 25-mer oligomers are selected to serve as sensitive, unique, sequence-specific detectors. Multiple probes (10-20) are designed for every gene, cDNA or EST and each perfect match (PM) probe is paired with a mismatch (MM) control probe that differs only in one base in a central position (Figure 13B). The hybridization signal for every gene is calculated as PM minus MM signal, and then averaged across a set of probes. This approach reduces greatly the contribution of a background and cross-hybridization and increases the quantitative accuracy and reproducibility of the measurement.

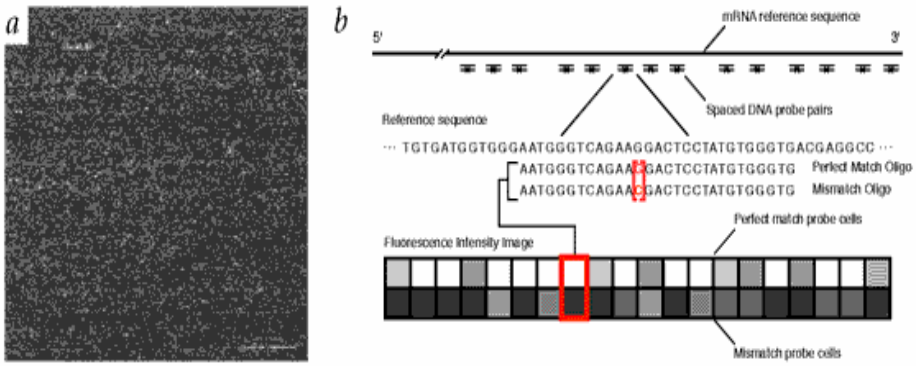

Figure 24. A) A single 1.28X1.28 cm array containing probe sets for approx. 40 000 human genes and ESTs. B) Expression probe and array design

High-density DNA probe arrays are powerful tools for a broad set of application including gene expression monitoring, sequence analysis, and genotyping.

Standards for microarray data

Microarray experiments provide the scientists with a large amount of data, that then have to be carefully analyzed and presented. First task is always a careful experiment design, with a clear question addressed. Next, issues to be tackled are: data normalization to enable comparison of expression levels, and data mining to select genes for further analysis. These are not trivial tasks and bear a potential risk for mistakes (reviewed in Quackenbush, 2002[201]).

In order to enable exchange of published microarray data, a standardized data presentation has been proposed (minimum information about a microarray

experiment (MIAME) standards). These standards should facilitate the establishment of databases and public repositories and enable the development of data analysis tools[202]. Today most journals ask for the submission of the microarray data to public databases according to MIAME standards prior to manuscript publication.
Annotation for microarray probe sets is currently incomplete. Affymetrix and other microarray producers are making an effort to improve the sequence annotation, provide links to various public databases, information about predicted protein domains and motifs, ortologous sequences and links to relevant pathways[203]. This information is necessary for a meaningful data analysis.

In our work we have used Affymetrix GeneChip® Murine Genome U74Av2 arrays to analyze gene expression during differentiation process in MC3T3 osteoblastic cells. MG_U74Av2 microarray contains probes for about 10, 000 expressed sequence tags (ESTs) and genes with known function. Some of the data obtained are presented in Chapter 1. Here we present data that were not included in Chapter 1.

3.2.2.2 Experimental procedures

Sample preparation, microarray hybridization, and data analysis are described in 2. 1. 3.

3.2.2.3 Results

To get an insight into the transcriptional events involved in the osteoblast differentiation, we investigated genes, whose expression levels changed upon treatment with the osteogenic stimulus. Genome-wide gene expression levels were compared between treated samples and time-matched non-stimulated controls. We detected a significant regulation (2-fold in at least 2 out of the 3 experiments) of 394 genes with known function and of 295 ESTs. In further analyses described here, we focused on the genes with known function. The functional analysis of 394 regulated genes led us to define ten large groups of regulated genes: 1) Matrix Proteins and Adhesion (25); 2) Growth Factors (19); 3) Receptors (24); 4) Cytoskeleton (5); 5) Signaling (11); 6) Kinases (11); 7) Transcription Factors (33); 8) Cell cycle and apoptosis (15); 9) DNA replication (11); and 10) Others (228) (Tables 5-9, 10-16). In Tables, within each of these groups, the genes were sorted from high to low degree of regulation, including both days 1 and 3. Growth Factors, Receptors and

Transcription Factors were discussed in details in the Chapter 1, and here other functional groups will be presented.

Genes encoding adhesion molecules and proteins of extracellular matrix are the largest group of genes regulated (Table 10). This shows that osteoblasts, even in this early state of the differentiation process, actively synthesize and secrete extracellular matrix proteins, and adhesion molecules that would provide a connection with the matrix, essential for the differentiation process. Some of them are strongly up-regulated very early, such as collagen-binding proteins (fibromodulin, keratho-epithelin, which will be bound to already actively synthesized collagen Iα1, a main component of the bone matrix). Late markers of osteoblast differentiation, bone sialoprotein, osteocalcin and osteomodulin, are all strongly up-regulated at day 3. Of interest is also up-regulation of TGFβ binding protein 2, that binds TGFβ to the extracellular matrix (ECM) and targets its action towards osteoblasts. Genes coding another types of collagen, which do not take part in the bone ECM, are strongly down-regulated, as well as the genes for collagenase enzymes. Extremely high level of *Col Iα1* gene expression, with only 22 cycles done in rqRT-PCR reaction for its detection (2.1.3) shows that collagen type I is a major product of MC3T3 cells. Summary of gene regulation for genes encoding extracellular matrix proteins and adhesion proteins are shown in Table 10.

Regulated genes involved in forming cytoskeleton structures are shown in table 11. Two up-regulated genes, kinesin family motor proteins 4 and C2 are involved in central spindle formation during anafase[204], which is in line with active proliferation of MC3T3 cells.

In Table 12 regulated genes involved in transmitting the signal of various signal transduction pathways are shown.

Group of regulated genes encoding Kinases (Table 13) includes few kinases involved in mitosis regulation, which again confirms the fact that MC3T3 osteoblasts are still proliferating in this early phases of differentiation. Up-regulation of two kinases of Src subfamily, Yes1 and Lyn, is probably a negative feed-back mechanism, since Src/Yes tyrosine kinases are known to inhibit osteoblast differentiation[205], through recruiting Yes-associated protein, YAP, that interacts with prolin-rich motif in C-terminus of Runx2 and represses its activity[206].

A number of regulated genes are involved in the cell cycle and in DNA replication process (Tables 14, 15), indicating a proliferative activity of the differentiating cells.

From the genes that were not classified into any of the functional groups presented, we found interesting regulation of several components of plasminogen system (Table 16). Plasminogen activators are involved in tissue remodeling, and recently it was shown that mice lacking plasminogen activators have increased bone formation[207]. Another interesting observation was strong up-regulation of cyclo-oxygenase 2 (Cox2), inducible form of main enzyme for prostaglandin biosynthesis. HGM-CoA reductase, a rate-limiting enzyme in cholesterol biosynthesis, representing the first step in prostaglandins synthesis, is also strongly up-regulated. Prostaglandins are potent regulators of osteoblast differentiation, and they act in an autocrine or paracrine fashion[156].

Name	Description	Acc No	REL	
			day 1	day 3
Fibromodulin	Small collagen binding proteoglycan	X94998	7.52	10.00
TGFBI. Kerato-epithelin	Extracellular adxesion molecule,binds to Col 1,2 i 4	L19932	2.83	2.05
Tenascin C	Extracellular matrix glycoprotein	X56304	2.54	6.30
Latent TGF beta binding protein 2.	Structural extracellular matrix protein for targeting TGF-beta action.	AF004874	2.02	1.04
Bone sialoprotein	Integrin binding sialoprotein	L20232	1.60	3.65
Osteocalcin	Bone gamma carboxyglutamate protein 1	L24431	1.00	7.95
Osteomodulin	Proteoglican, bone matrix protein	AB007848	1.00	6.35
MMP13	Collagenase-3	X66473	1.66	0.37
Lysyl oxidase-2	Extracellular copper enzyme that initiates the crosslinking of collagens and elastin	U79144	1.02	0.44
NID. Nidogen 1 (entactin)	Basement membrane protein	L17324	0.93	0.48
CHST2.	Carbohydrate (chondroitin 6/keratan) sulfotransferase 2	AB011451	0.92	0.37
Periplakin	Component of the cornified envelope of keratinocytes	AF013715	0.89	2.36
Fibulin 2	Extracellular matrix protein, binds to fibronectin	X75285	0.79	0.32
Decorin	Small collagen binding proteoglycan	X53929	0.79	4.02
MMP3	Matrix metaloproteinase 3	AB021228	0.74	0.29
VCAM-1	Vascular cell adhesion molecule 1	M84487	0.71	0.45
Fibrillin 1.	Major constituent of the 10-12 nm extracellular microfibrils	L29454	0.70	0.32
VCAM-1	Vascular cell adhesion molecule-1	U12884	0.67	0.27
Procollagen, type IV, alpha 2	Matrix protein precursor	X04647	0.65	0.46
AOC3. Amine oxidase, copper containing 3	Vascular adhesion protein 1	AF078705	0.48	0.20
Procollagen, type IV, alpha 1	Matrix protein precursor	M15832	0.48	0.20
JUP. Junction plakoglobin	Common junctional plaque protein	M90365	0.45	0.54
Osteoglycin	Small leucine-rich proteoglycan. Induces bone formation	D31951	0.41	0.46
NID2 Nidogen 2 (osteonidogen, entactin-2)	Basement membrane protein	AB017202	0.33	0.18
P4HA1	Posttranslational formation of 4-hydroxyproline in collagens	U16162	0.33	0.38

Table 10. Matrix and Adhesion genes regulated during osteoblastic differentiation of MC3T3 cells. Selected genes encoding extracellular matrix proteins and adhesion proteins, whose expression changed ≥ 2-fold upon stimulation with osteogenic stimulus. Black font - up-regulated transcripts; Grey font - down-regulated transcripts; PSN- Affymetrix probe set number; Acc No- sequence accession number; REL- relative expression level (median value from three independent experiments), compared to the non-stimulated, time-matched control.

Name	Description	Acc No	REL	
			day 1	day 3
KIF4	Kinesin family motor protein 4	D12646	1.09	2.33
KIFC1	Kinesin family motor protein C1	D49544	1.01	3.44
ARHGAP5	Rho GTPase activating protein 5	U67160	0.91	0.43
LSP1. Lymphocyte-specific protein 1	Cytoskeleton-associated protein	D49691	0.47	0.80
VIL2. Vilin	Connections of major cytoskeletal structures to the plasma membrane	X60671	0.39	0.50

Table 11. Cytoskeleton genes regulated during osteoblastic differentiation of MC3T3 cells. Selected genes encoding cytoskeleton proteins, whose expression changed ≥ 2-fold upon stimulation with osteogenic stimulus. Black font - up-regulated transcripts; Grey font - down-regulated transcripts; PSN- Affymetrix probe set number; Acc No- sequence accession number; REL- relative expression level (median value from three independent experiments), compared to the non-stimulated, time-matched control.

Name	Description	Acc No	REL	
			day 1	day 3
IFI204. Interferon activated gene 204,	Probably mediates growth inhibitory efect of interferon	M31419	2.50	2.57
NEDD9 (cas l).	Docking protein. Plays a central role for tyrosine-kinase-based signaling related to cell adhesion	AF009366	1.26	0.37
SOCS-2. Suppressor of cytokine signalling-2	Jak/STAT signalling inhibitor	U88327	0.91	0.48
TPD52L1. Tumor protein D52-like 1	Calcium-mediated signal transduction and cell proliferation	AF004428	0.77	0.48
ACK2	Non-receptor protein tyrosine kinase. Associated with integrin signaling. Cdc42-regulated	AF037260	0.59	0.37
CAPN6. Calpain 6.	Ca2+-dependent intracellular nonlysosomal protease believed to participate in signal transduction	Y12582	0.59	0.43
GOA-alpha	Guanine nucleotide-binding protein Go, alpha subunit	M36777	0.56	0.42
WISP-2	Wnt-1-induced signaling protein. Connective tissue growth factors family	AF100778	0.55	0.27
GBP2	Guanylate binding protein 2, interferon-inducible	AJ007970	0.36	0.28
NOV. Nephroblastoma overexpressed gene	Insulin-like growth factor bindin protein family	Y09257	0.21	0.33
CRABP2. Cellular retinoic acid binding protein II.	Regulates the access of retinoic acid to the nuclear retinoic acid receptors.	M35523	0.14	0.10

Table 12. Signaling factors genes regulated during osteoblastic differentiation of MC3T3 cells. Selected genes encoding signaling factors, whose expression changed ≥ 2-fold upon stimulation with osteogenic stimulus. Black font - up-regulated transcripts; Grey font - down-regulated transcripts; PSN- Affymetrix probe set number; Acc No- sequence accession number; REL- relative expression level (median value from three independent experiments), compared to the non-stimulated, time-matched control.

Name	Description	Acc No	REL	
			day 1	day 3
Yes1	Tyr protein kinase, Src subfamily	X67677	1.91	2.60
STK18	Ser/Thr kinase 18. Polo-family of mitotic regulators	L29480	1.47	2.01
PLK Polo-like kinase homolog	Ser/Thr kinase, required for mitosis	U01063	1.27	2.71
Esk/TTK kinase	Ser/Thr/Tyr (dual-specificity) kinase, in rapidly proliferating cell lines	M86377	1.16	3.16
Mst1	Stress-responsive protein kinase	U28726	1.15	4.21
LYN	Tyr protein kinase, Src subfamily	M57696	1.15	2.41
STK6	Ser/Thr kinase 6 -mitotic centosomal protein kinase	U80932	1.11	2.48
BUB1	Mitotic checkpoint serine/threonine-protein kinase	AF002823	1.08	2.71
Serine/threonine kinase 5	Possible role in cell growth	D21099	1.03	4.77
EEF2K	Eukaryotic elongation factor-2 kinase	U93848	1.00	2.28
DMPK. Dystrophia myotonica kinase	Important role in Ca2+ homeostasis and signal transduction system	Z38015	0.42	0.35

Table 13. **Kinases regulated during osteoblastic differentiation of MC3T3 cells**. Selected genes encoding kinases, whose expression changed ≥ 2-fold upon stimulation with osteogenic stimulus. Black font - up-regulated transcripts; Grey font - down-regulated transcripts; PSN- Affymetrix probe set number; Acc No- sequence accession number; REL- relative expression level (median value from three independent experiments), compared to the non-stimulated, time-matched control.

Name	Description	Acc No	REL	
			day 1	day 3
MyD118	Negative growth control	X54149	3.94	1.65
CDCREL-1 homolog	Cell division control	AF033350	2.22	1.49
Caspase 7	Apoptosis-related cysteine protease	U67321	1.84	2.88
GTSE-1	G2 and S phase expressed protein	AJ222580	1.66	3.11
GAS6	Growth-arrest	X59846	1.36	0.44
CDC25C	Protein tyrosine phosphatase. Progression of cell cycle	U15562	1.27	3.85
Ect2	Regulation of citokinesis	L11316	1.06	2.05
Survivin -BIRC5	Inhibitor of caspase 3 and 7	AB013819	1.01	2.57
Cyclin A2	Cell cycle control	X75483	0.99	2.15
CDC25C	Dosage-dependent inducer in mitotic control	L16926	0.87	2.07
Sha1	S-M checkpoint control	AF062378	0.79	2.30
BNIP3L	Nuclear gene encoding mitochondrial protein. Induces apoptosis	AF067395	0.48	0.54
GAS2	Growth arrest specific 2	M21828	0.45	1.15
BID	Induces ice-like proteases and apoptosis	U75506	0.41	0.40
Proliferin	Secreted protein. Stimulate cell proliferation	K03235	0.38	0.29

Table 14. **Cell cycle and apoptosis genes regulated during osteoblastic differentiation of MC3T3 cells**. Selected genes encoding cell cycle and apoptosis related proteins, whose expression changed ≥ 2-fold upon stimulation with osteogenic stimulus. Black font - up-regulated transcripts; Grey font - down-regulated transcripts; PSN- Affymetrix probe set number; Acc No- sequence accession number; REL- relative expression level (median value from three independent experiments), compared to the non-stimulated, time-matched control.

Name	Description	Acc No	REL	
			day 1	day 3
POLD2	DNA polymerase delta 2, regulatory subunit	Z72486	6.90	10.00
Ribonucleotide reductase M2 subunit	Provides precursors for DNA synthesis	M14223	2.23	1.85
CHAFA	Chromatin assembly factor-I p150 subunit	AJ132771	2.03	2.76
CDC46	Initiation of DNA replication	D26090	1.96	2.89
CDC6-related protein	Initiation of DNA replication	AJ223087	1.84	2.53
MCMD4	Initiation of DNA replication	D26089	1.66	2.23
IMPDH1	Rate limiting enzyme in de novo synthesis of guanine nucleotide	U00978	1.61	2.10
P1	Mcm3 (S. cerevisiae) homolog. Initiation of DNA replication	X62154	1.61	2.14
HMG2	Nonhistone structural protein of chromatine	X67668	1.31	2.28
NASP	Transporting newly synthesised histones to the nucleus. Testis and sperm-specific.	AF034610	1.29	3.17
POLE2	DNA polymerase epsilon small subunit	AF036898	1.00	2.00

Table 15. DNA replication genes regulated during osteoblastic differentiation of MC3T3 cells. Selected genes encoding proteins involved in DNA replication process, whose expression changed ≥ 2-fold upon stimulation with osteogenic stimulus. Black font - up-regulated transcripts; Grey font - down-regulated transcripts; PSN- Affymetrix probe set number; Acc No- sequence accession number; REL- relative expression level (median value from three independent experiments), compared to the non-stimulated, time-matched control; d1 - day 1; d3 - day 3.

Name	Description	Acc No	REL	
			day 1	day 3
COX2. Cyclooxigenase2	Prostaglandin-endoperoxide synthase 2. Mitogens and cytokines inducible form	M88242	6.87	2.74
Plasminogen				
PAI-1	Plasminogen activator inhibitor	M33960	2.95	1.25
tPA	Plasminogen activator, tissue	J03520	0.73	2.11
Nexin-I	Inhibitor of urokinase-type plasminogen activator (uPA)	X70296	0.87	0.39
Cholesterol				
HMG-CoA reductase	Control of cholesterol biosynthesis, rate-limiting enzym in steroide synthesis	M62766	2.14	11.65
LAL . Lysosomal acid lipase	Intracellular control of cholesterol and trygliceride catabolism	Z31689	2.09	0.50

Table 16. Other selected genes regulated during osteoblastic differentiation of MC3T3 cells. Selected genes encoding some interesting proteins, whose expression changed ≥ 2-fold upon stimulation with osteogenic stimulus. Black font - up-regulated transcripts; Grey font - down-regulated transcripts; PSN- Affymetrix probe set number; Acc No- sequence accession number; REL- relative expression level (median value from three independent experiments), compared to the non-stimulated, time-matched control; d1 - day 1; d3 - day 3.

3.2.2.4 Discussion

We have shown that a microarray analysis of osteoblast differentiation is a useful tool both to identify new genes involved in a differentiation process and to gain a global overview of events involved. Differentiating osteoblastic cells in the early stage of differentiation process are still weakly proliferating cells, since a number of regulated genes are involved in the cell cycle and in DNA replication. They are actively synthesizing proteins of extracellular matrix, such as collagen I, osteopontin, osteocalcin, osteonectin and bone syaloprotein. They are also very autonomous, synthesizing growth factors and cytokines such as TGFβ family members, PDGFα, or IGF binding proteins, that are necessary for further stimulation of the differentiation. Several negative feed-back control mechanisms are activated, like increased synthesis of BMP antagonist Gremlin 2 or activation of Notch pathway, showing that kinetics of differentiation is of crucial importance and that there is a tight control of every differentiation step.

3.2.3 Hey1 siRNA: optimization of siRNA transfection conditions and best Hey siRNA sequence selection

3.2.3.1 Introduction

Small interfering RNA (siRNA) are the effector molecules of the RNA interference (RNAi) pathway, which was discovered in 1998 when Fire and colleagues injected double-stranded RNA (dsRNA) into the nematode *Caenorhabditis elegans*. DsRNA initiated a potent, sequence-specific degradation of cytoplasmic mRNA containing the same sequence as the dsRNA trigger[208]. The discovery of RNAi mechanism of action in nematodes revealed that post-transcriptional gene silencing in plants, quelling, post-transcriptional silencing in fungi and RNAi action in nemadotes, were related processes that were all triggered by dsRNA. RNAi-dependent gene silencing was found to occur also in protozoa and almost all higher eukaryotes tested, and it was rapidly developed as a tool to study gene function.

Initially this approach could not have been used in mammalian cells, because long stretches of dsRNA induced the antiviral interferon response, which usually leads to cell death[209]. However, the usage of short, 21-24 nucleotide long siRNA, instead of long dsRNA of around 200 nucleotides effectively reduced gene expression without triggering the interferon response[210], which enabled a range of opportunities for applications in basic and applied research.

Study of the mechanism of RNAi showed that the cellular machinery for this process is highly conserved among species. DsRNA that is produced endogenously or introduced into the cell through a dsRNA virus or by experimental manipulation is cleaved by the RNase-III-type enzyme named **Dicer**[211] into 21- to 28- nucleotide siRNA duplexes that contain 2-nucleotide 3' overhangs on both ends with 5' phosphate and 3' hydroxyl termini. Other components of the RNAi machinery specifically recognize the siRNA duplex and incorporate a single siRNA strand into a protein complex[212] named the RNA-induced silencing complex (**RISC**). Unwinding of the double-stranded RNA and RISC complex activation is an ATP-dependent process during which RISC complex binds to the target mRNA based on the complementarity between the target and siRNA. RISC cleaves mRNA containing perfectly complementary sequences, 10 nucleotides from the 5' end of the incorporated siRNA strand. Mechanism of RNAi is schematically presented on Figure 25 and reviewed in Hannon, 2002[213] and Dorsett *et al.*, 2004[214].

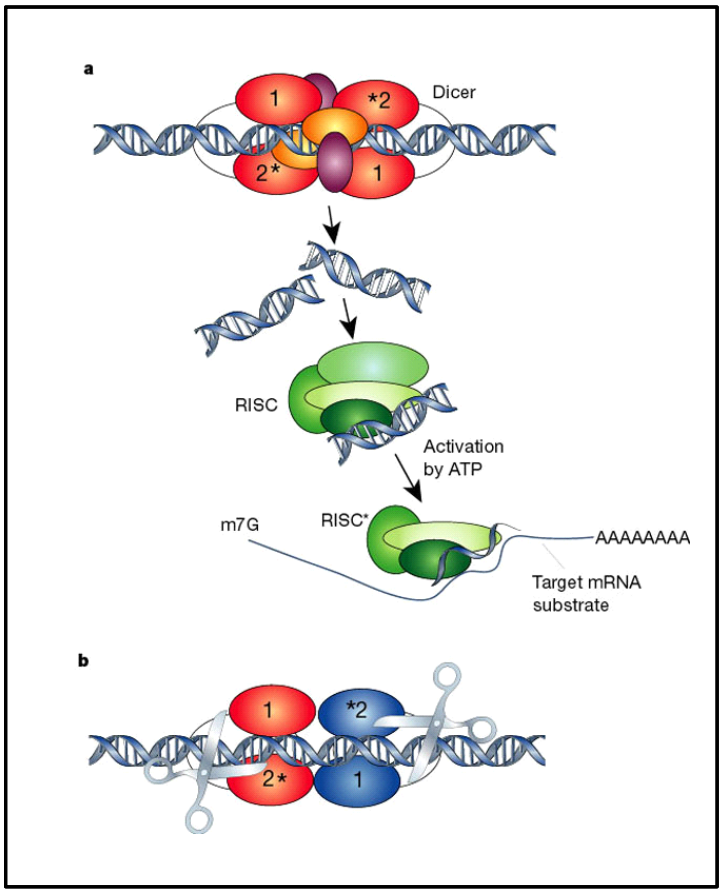

Figure 25: RNAi mechanism. Taken from Hannon, 2002[213]

siRNAs are a powerful tool for gene silencing experiments. However, some experimental problems persist: it was shown that application of RNAi in mammalian cells can affect gene expression non-specifically, stimulating the expression of subsets of genes involved in interferon response, although the cellular growth arrest was not induced[215,216]. Non-specific effect of siRNA depends on siRNA concentration, cell type, delivery reagents and mode of siRNA expression. By bringing siRNA concentration to a minimum and carefully optimizing delivery reagents this problem can be overcame. Besides their non-specific effects, siRNA are prone to inducing off-target effects by targeting sequences closely related to the target of interest. In extreme cases, as little as 11- to 14- nucleotide complementarity between 5' end of either siRNA strand to an mRNA can cause a reproducible reduction in transcript levels[217]. Therefore, a particular attention has to be paid to selection of appropriate siRNA sequence to achieve efficiency and specificity: off-target complementarity has to be checked, and probability of sense-strand binding to RISC complex minimized (Figure 26). In addition, multiple siRNA have to be tested to identify a potent, efficacious sequence.

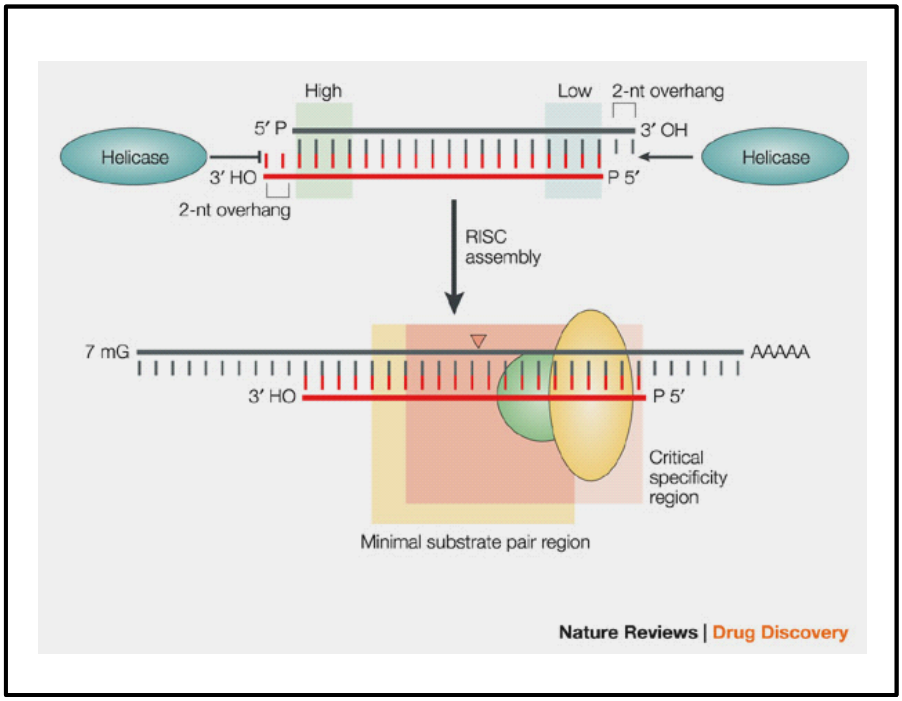

Figure 26: Features of efficient and specific siRNAs[214]. The thermodynamic stability of the first few base pairs of either siRNA strand can affect the ratio of RISCs containing the antisense (red line) or sense strands of siRNAs. The relatively low thermodynamic stability (blue shaded box) in the 5' end of the antisense strand (blue shaded box) compared with the high thermodynamic stability (green shaded box) in the 5' end of the sense strand (green shaded box) leads to a bias for the incorporation of the antisense strand into RISC.
The 5' half of siRNAs has a more important role in target recognition than the 3' half. The orange arrowhead indicates the site of mRNA cleavage. The minimal substrate for a siRNA observed so far is comprised of central 13 nucleotides (yellow rectangle). Critical region for specific target recognition is shown as pink rectangle.

If siRNA is introduced into the cells by transfection, its effect is transient and depends on the rate of cell division. Therefore, vectors have been introduced that allow the production of a small hairpin RNA (shRNA), which will be processed into the siRNA in the cell. These vectors can stably integrate into the genome and mediate the long-term knockdown of endogenous transcripts in cell culture and *in vivo*. In addition, adenoviral, retroviral and lentiviral vectors have been developed, which use a similar mechanism to produce siRNA within the cell. (reviewed in Dorsett *et al.*, 2004[214]).
RNA interference is becoming a promising tool for several applications: investigation of a single gene function *in vitro* and *in vivo*, in functional genomics for genome-wide screening of gene function, and for use as therapeutic agents.
In our work we used Hey1-specific siRNA to inhibit Hey1 induction upon stimulation of MC3T3 cells with osteogenic stimulus, and to investigate the consequences of this

inhibition. For this purpose, we first performed optimization experiments for transfection conditions and the selection of an effective siRNA sequence.

3.2.3.2 Experimental procedures

siRNA design. Control siRNA against *Shc* gene, which encodes Src homology 2 domain-containing transforming protein 1, was a kind gift from Romina Marone, Laboratory of Dr. Nency Hynes, Friedrich Michener Institute for Biomedical Research, Basel, Switzerland. The Shc siRNA sense strand sequence was CTA CTT GGT TCG GTA CAT GGG.

Hey1 siRNA 1 and 2 were designed by myself, according to the instructions from the siRNA user's guide, Tomas Tuschl lab, Rockefeller University, NY, USA (http://www.rockefeller.edu/labheads/tuschl/sirna.html), and synthesized by Xeragon Inc. (Huntsville, USA). Hey1 siRNA1 sense strand sequence was r(GCU AGA AAA AGC UGA GAU C)d(TT). Hey1 siRNA2 sense strand sequence was r(GUU GCC CGU UAU CUG AGC A)d(TT). Hey siRNA2 sense strand was 3' labeled with fluorescein. Both siRNA were provided as sense-antisense duplexes, purified by ion exchange HPLC. Before using, lyophilized duplexes were dissolved in 1 ml of the hybridization buffer (100 mM potassium acetate, 30 mM HEPES-KOH, 2 mM magnesium acetate, pH 7.4) to obtain a 20 μM solution. Tubes were heated to 90°C for 1 min, incubated at 37°C for 60 minutes and stored at -20°C. This procedure disrupts higher aggregates, which may have formed during the lyophilization process. Hey1 535, 404, and 1876 siRNA and Hey1 1876 siRNA mismatch control (mm) were provided by François Natt, Novartis. Hey1 siRNA 535 sense strand sequence: r(AGT GAG GTG AAG GGA GAA A)d(TT); Hey1 siRNA 404 sense strand sequence: r(GTT GGC AGC AAG CAA GAC A)d(TT); Hey1 siRNA 1876 sense strand sequence: r(AGA CGG AGA GGC ATC ATC G)d(TT); Hey1 siRNA 1876mm sense strand sequence: r(AGA AGG AGC GGA ATC CTC G)d(TT). Four mismatch nucleotides are shown in red. All siRNA were provided as already annealed sense-antisense duplexes, in 20μM in hybridization buffer 100mM potassium acetate, 30 mM HEPES-KOH, 2 mM magnesium acetate, pH 7.4), ready to use.

siRNA transfection. The optimized transfection procedure using Oligofectamine (Gibco BRL) transfection reagent was the following: MC3T3 cells were plated on 6-well plates ($0.5x10^5$ cells/ well in 2 ml of medium). After 24 h, siRNA transfection was

performed in a total volume of 1 ml using Oligofectamine (Life Technologies), according to the manufacturer's instructions. siRNA concentration was 0.1 μM, and the Oligofectamine amount 4 μl/well. Transfection was stopped after 4 h by adding 0.5 ml of medium containing 30% of serum, and the osteogenic stimulus (optional). RNA and protein were extracted after 2 or 3 days. For testing of different transfection reagents: JetPEI (Polytransfection), Metafectene (Biontex), Trans-Messenger (Qiagen) and TransIT-TKO (Mirus), the transfection was done in MC3T3 cells according to manufacturer's instruction and will be discussed briefly in Results section.

RNA isolation and quantitative radioactive RT-PCR (qrRT-PCR) were performed as described in 2.1.3. For Hey1 and 18S rRNA, primers used are described in 2.1.3. qrRT-PCR conditions for analysis of Shc gene expression were optimized. Primers used were the following, given in a 5'-3' orientation: forward GGA ATG CCA ATC ACT CTC ACT, reverse AGC AAG CCC TTC AGG ACA C. Number of PCR cycles used in qrRT-PCR was 29.

Protein isolation. All the steps are done on ice. Medium was removed and the cells were washed 2 times with cold (4°C) PBS w/o Ca/Mg. Two hundred fifty μl of NP-40 Lysis buffer (final concentration 25 mM Tris pH 7.4, 10% glycerol, 1% NP-40 (IGEPAL), 50mM NaF) + protease inhibitors (final concentration 1mM Na3VO4, 10μg/ml Aprotinin, 10μg/ml Leupeptin, 10μg/ml Pepstatin, 1mM PMSF) was added to each 6-well plate well. Cells were scraped, the lysate transferred to Eppendorf tubes and lysed further for 20 min at 4°C, with occasional vortexing. Lysate was centrifuged for 5 min at 14 000 rpm and 4°C. Supernatant was collected, protein concentration measured with Bio-Rad Protein Assay (Badford, Micromethod), according to manufacturer's instruction. One hundred μl aliquots of supernatant were prepared for gel electrophoresis analyses by mixing with 20 μl 6X SDS sample buffer (7 ml Tris-HCl 0.5M, pH 6.8, 3 ml glycerol, water free (Fluka), 1 g SDS (BioRad), 0.93 g DTT (Sigma), 1.2 mg bromphenol blue (BioRad), H_2O up to 10 ml), incubated 4 min at 95°C, cooled down to room temperature, briefly centrifuged and kept at -20°C. The rest of supernatant was quickly frozen on dry ice and stored at -80°C.

Western blot analysis: Twenty μl of protein sample was loaded on 15 % polyacrylamide SDS gel (1.5 mm thick) and run for 2 h at 20 mA in Running buffer (25mM Tris, 192 mM glycine, 0.4 % SDS). Transfer on the PVDF membrane

(Immobilon P) was done in the Bio-Rad Mini Trans-Blot Unit, overnight at 30 V in the cold room (4°C), in a freshly prepared Transfer buffer (50 mM Tris, 384 mM glycine, 20% methanol, 10^{-4}% SDS). Protein transfer was checked by staining with Ponceau red, the membrane was destained with water and washed for 5 min in PBS. Blocking was done in 3 % gelatin in PBS, 0.1 % Tween for 1 h, then membrane was washed shortly in PBS,0.1 % Tween and incubated with the first antibody. Anti-Shc antibody (Transduction Laboratory, Lexington, USA) was diluted 1 : 2000 in 1% gelatin/PBS/0.1% Tween. The membrane was incubated in the antibody solution for 2 h with shaking, washed 3 times for 5 min in PBS, 0.1 % Tween and incubated for 30 min with secondary antibody (peroxidase - conjugated goat IgG fraction to rabbit immunoglobulins (ICN Pharmaceuticals, Inc., Aurora, Ohio, USA, Cat. No. 55682)) diluted 1:10 000 in 1% gelatin/PBS/0.1% Tween. The membrane was washed three times for 5 min in PBS, 0.3% Tween, 3 times for 5 min in PBS,0.1% Tween, and 2 times for 5 min in PBS. Detection of the signal was done with ECL Western Blotting Detection Reagents (Amersham Biosciences, Cat. No. RPN2135), according to the manufacturer's instructions.

3.2.3.3 Results

Optimization of efficiency of transfection

In order to optimize siRNA transfection conditions in MC3T3 cells, we have used siRNA for *Shc* gene, which was previously shown to be effective in T47D breast carcinoma cells (David Cappellen, personal communication). Shc protein, as an adaptor protein in tyrosine kinase receptors signaling transduction, is ubiquitously expressed and it was likely expressed in our cell line. Western blot analysis have shown the strong expression of Shc protein in MC3T3 cells (Figure 16, lines 1, 3, 5, 7-controls). In order to optimize conditions for siRNA transfection, first we have tested the recommended Oligofectamine transfection reagents (http://www.rockefeller.edu/labheads/tuschl/sirna.html), starting with two different cell numbers and isolating proteins 2 and 3 days after transfection. Set-up of the experiment and the results are shown on the Figure 27. Shc siRNA was effective in inhibiting the Shc protein level in MC3T3 cells. This inhibition was as twice as strong when a lower cell number was used: around 60% inhibition was obtained with seeding $1X10^5$ cells / 3.4 cm^2 well, while 80% inhibition with $0.5X10^5$ cells / 3.4 cm^2 well. The level of inhibition was the same at day 2 and 3. We proceeded further optimization experiments with the lower cell number, $0.5X10^5$ cells/well.

number	name	siRNA test conc (μM)	Stock conc (μM)	Cell number seeded	Time after transfection
1	Vehicle			$1X10^5$	2 days
2	siRNA	0.1	40	"	"
3	Vehicle			$0.5X10^5$	"
4	siRNA	0.1	40	"	"
5	Vehicle			$1X10^5$	3 days
6	siRNA		40	"	"
7	Vehicle			$0.5X10^5$	"
8	siRNA		40	"	"

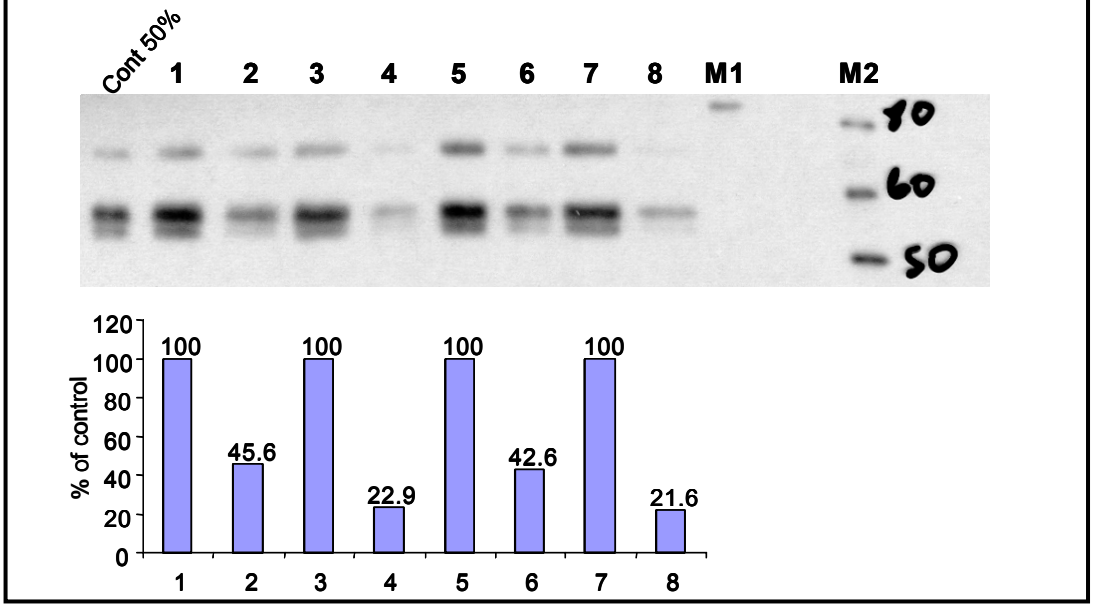

Figure 27: Optimization of transfection efficiency of Shc siRNA in MC3T3 cell line. **M1**: 10 μl Gibco BioBench ladder; **M2**: 5 μl 10 X diluted Magic Marker, Invitrogen; **Cont. 50%**: quantification control (10 μg of sample 1)

Testing of different transfection reagents

In order to try to achieve even higher inhibition level, we have tested different transfection reagents and compared them with Oligofectamine in a Shc siRNA transfection experiment. Five different transfection reagents have been used: JetPEI (Polytransfection), Metafectene (Biontex), Trans-messenger (Qiagen), TransIT-TKO (Mirus) and Oligofectamine (Life Technologies). Set-up of the experiment is shown in Figure 28A. For each transfection method an appropriate vehicle control was used and the amount of transfected Shc siRNA was as recommended by the manufacturer.

JetPEI showed a strong toxic effect on MC3T3 cells (Figure 28B), thus the protein was not analyzed from these samples. For other samples, proteins were isolated 3 days after transfection and levels of Shc protein compared. As it can be seen on

Figure 28C, Metafectene and Trans-messenger transfection gave lower level of inhibition than Oligofectamine (65 and 43 %, respectively, compared to 80 % inhibition following Oligofectamine transfection). TransIT-TKO transfection gave similar level of inhibition as Oligofectamine (79%). A possible advantage of TransIT-TKO transfection reagents is application of complete, serum-containing medium instead of serum-free medium required for Oligofectamine transfection. Also, three times lower concentration of siRNA used in TransIT-TKO transfection could possibly reduce unspecific effects and save material. However, testing of two different batches of TransIT-TKO showed that one of them was completely inactive. This variability level would require testing of each new batch separately and,. therefore, we decided to continue using a simpler protocol with Oligofectamine transfection reagent.

Analysis of Shc mRNA level 3 days after siRNA transfection (Figure 28D) showed 60 % inhibition compared to vehicle control. At the same time point, the inhibition on the protein level was more extensive (80%). This could be explained by the transient effect of siRNA: after 3 days, mRNA level is probably starting to recover, while the protein level is still low.

In conclusion, Oligofectamine-mediated transfection of Shc siRNA into MC3T3 cells resulted in a strong, but transient inhibition at both mRNA and protein levels. We continued to use this reagent in optimization experiments for Hey1 siRNA transfection.

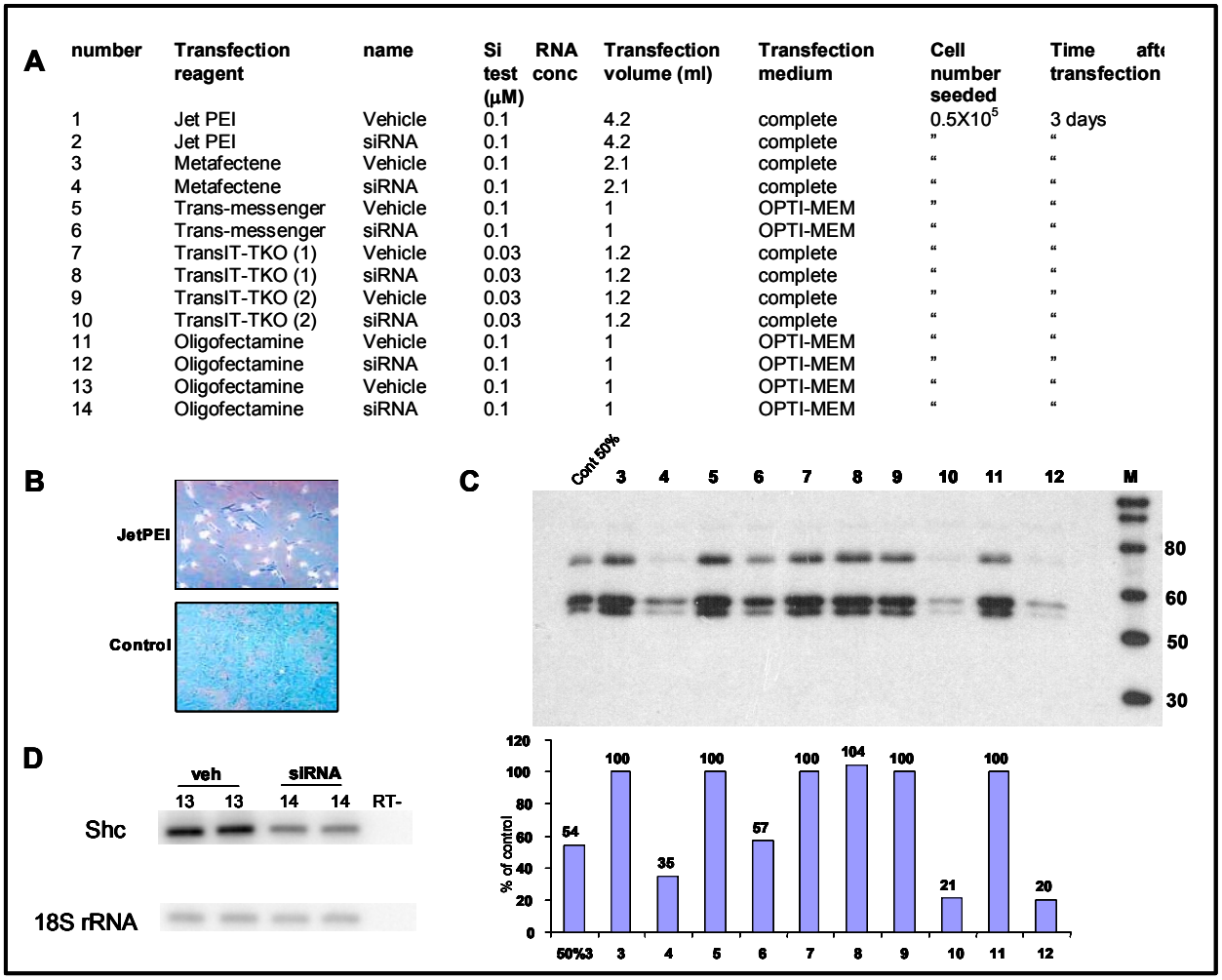

Figure 28: Testing of different transfection reagents. A - Experiment set-up. **B** - Jet PEI transfection reagent was highly toxic for MC3T3 cells, compared to control non-transfected cells. **C** - Shc protein level after siRNA transfection mediated by different transfection reagents. Samples 1 and 2 were not used for protein isolation, as JetPEI reagent was toxic. M-5 μl 10X diluted Magic Mark Invitrogen; Cont. 50% : quantification control (10 μg sample 3). **D** – Shc mRNA level 3 days after Oligofectamine mock transfection or siRNA transfection. Samples 13 and 14 were used for total RNA isolation.

Testing of different Hey1 siRNA sequences

In order to find the most efficient siRNA sequence for knock-down the Hey1 expression in MC3T3 cells after stimulation with osteogenic stimulus, 5 different siRNA sequences have been tested (Figure 29). We have designed siRNA1 and siRNA2-FL (fluorescently labeled) and ordered them from an external company, Xeragon. Three other sequences: siRNA 535, 404 and 1867, together with mismatch

control for siRNA 1867, were designed and synthesized in-house, by Novartis Functional Genomic group.

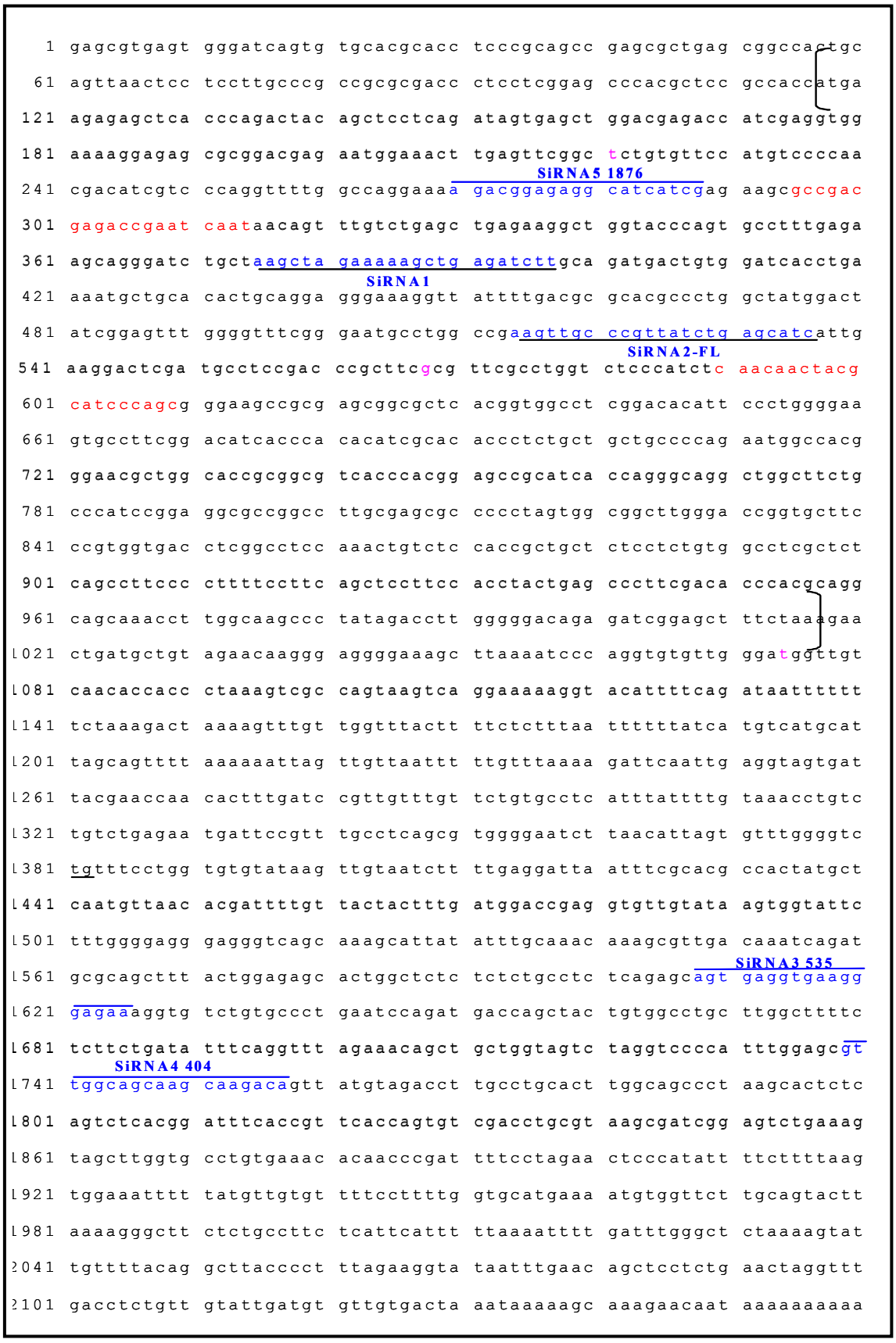

Figure 29: Positions of siRNA and PCR primer sequences on mouse Hey1 mRNA (Acc. No. AJ243895). Coding region is labelled with brackets. Known polymorphisms are shown in pink. Primers used in qrRT-PCR are shown in red. Tested siRNA sequences are shown in blue.

The results of inhibition of Hey1 mRNA induction upon transfection of different siRNA sequences are shown in Figure 30. Hey1 siRNA1 was the most effective, reducing an induced Hey1 mRNA level by 70%. Hey1 siRNA2-FL was moderately effective, with inhibition of 50%. siRNAs 535, 404 and 1867 were ineffective, the Hey1siRNA 535 even inducing the mRNA level for 65%. Similar effect is seen with 1867 mismatch control, which induced mRNA level for 85%. This results indicate that mock transfection or transfection of an inactive siRNA are not inert, but can produce unexpected effects. Therefore, the best practice is to have both of these controls included in the experiment. In our further work we used Hey1 siRNA1 for inhibiting the induction of Hey1 mRNA, while Hey1 siRNA1867mm was used as a control.

Hey1 siRNAs-FL was intended to be used for determination of transfection efficacy by fluorescent microscopy, but we have shown that the fluorescent signal intensity was not strong enough to determine the number of transfected cells (data not shown). However, we have previously shown that fluorescently-labeled antisense oligonucleotides enter MC3T3 cells after Oligofectamine-mediated transfection with almost 100 % efficiency (Daisy Rohner, data not shown). Therefore, we expect that the efficacy of transfection with siRNA was similarly high.

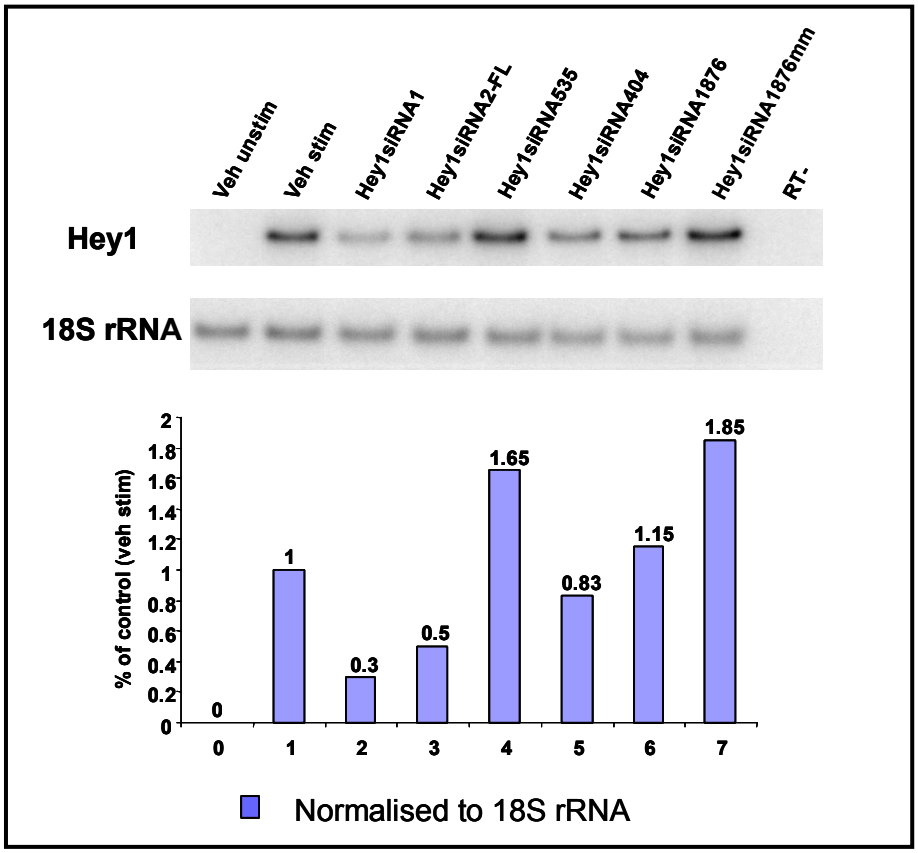

Figure 30: Effects of different siRNA sequences on the Hey1 mRNA level.

3.2.3.4 Discussion

Optimization experiments that we have performed to obtain a maximal inhibitory effect of Hey1 siRNA in MC3T3 cells showed that this process is dependant on several factors, such as seeding cell number, the transfection reagent (even though those are all reagents recommended for siRNA transfections by manufacturers), as well as on selection of appropriate siRNA sequence. These results show that optimization of conditions for siRNA transfection is a necessary step, which should be done carefully with each new siRNA sequence and cell line. Our results showed that, from 5 tested siRNA sequences, only one was sufficiently effective to be used further experiments. The work from other laboratories showed that different siRNAs vary in their efficacy and that multiple sequences have to be tested to obtain an efficient silencer (reviewed in Dorsett *et al.*, 2004[214]).

3.2.4 Hey1 antibody testing

3.2.4.1 Introduction

The Hey family of transcription factors has only recently been described[168] and, therefore, few tools are available for studying their function. Antibody for the detection

of Hey1 protein is not commercially available. We therefore set out to produce Hey1 polyclonal anti-peptide antibody.

3.2.4.2 Experimental procedures

Hey1 peptide production, rabbit immunization and serum production. 3 different peptide sequence were ordered and obtained from Neosystem (Strasbourg, France). The peptides were subsequently used for immunization of rabbits.

1.) E-18-C-NH2. Immunograde purified. Sequence: Glu-Leu-Asp-Glu-Thr-Ile-Glu-Val-Glu-Lys-Glu-Ser-Ala-Asp-Glu-Asn-Gly-Cys-NH2. This peptide was previously reported to be used in the production of Hey1 antibody [169] which was subsequently used in immunohistochemisty experiments.

2.) C-17-F. Immunograde purified. Sequence: Cys-Asn-Leu-Gly-Lys-Pro-Tyr-Arg—Pro-Trp-Gly-Thr-Glu-Ile-Gly-Ala-Phe (C terminus of mouse Hey1 protein).

3.) M-17-C-NH2. Immunograde purified. Sequence: Met-Lys-Arg-Ala-His-Pro-Asp-Tyr-Ser-Ser-Ser-Asp-Ser-Glu-Leu-Asp-Cys-NH2 (N terminus of mouse Hey1 protein).

E-18-C-NH2 peptide was conjugated with ovalbumine carrier protein and multiple immunization of two rabbits was performed at Neosystem, Strasbourg, France. Pre-immunization serum sample, serum samples after each immunization step and serum after the final bleeding of rabbits were obtained and stored at -20°C.

C-17-F and M-17-C-NH2 were conjugated to KLH carrier protein and used in a classical immunization protocol (two rabbits per peptide) by Barbara Winkler at the Antibody production Center, Novartis Pharma AG, Basel, Switzerland. Pre-immunization serum sample, serum samples after each immunization step and serum after the final bleeding of rabbits were obtained and stored at -20°C.

Cell culture. MC3T3 clone 1b cells were grown in α-MEM with 10% fetal calf serum (FCS, Gibco), 1% penicillin/streptomycin (Pen/Strep) and 1% L-Glutamine (L-Glu) in T175 flasks (40 ml/flask). The stimulation was done in the same medium. For nuclear protein isolation, cells were plated on 6 cm dishes ($3x10^5$cells/dish in 5 ml medium, grown to confluence for 3 days at 37°C / 5% CO_2, and then stimulated with 10 mM β-glycerophosphate (GP, Sigma), 50 µM ascorbic acid (AA, Wako) and 1 µg/ml BMP-2 (Nico Cerletti, Novartis). Control cells were not stimulated. Stimulation lasted for 2 days, after which nuclear proteins were extracted.

Nuclear protein extraction. Cells were washed twice with cold PBS (2ml/dish) that contained a mix of protease inhibitors: aprotinin (10 µg/ml, Sigma A1153), leupeptin

(10 µg/ml, Sigma L2884), PMSF (1mM, Sigma P7626), pepstatin (10 µg/ml, Sigma P4265), Na_3VO_4 (1mM, Sigma S6508). 1 ml / dish of cold buffer A (10mM Hepes, pH 7.9; 10mM KCL; 0.1 mM EDTA; 0.1mM EGTA; 1mM DTT; 0.5mM PMSF; 1mM Na_3VO_4; 10 µg/ml aprotinin; 10 µg/ml leupeptin; 10 µg/ml pepstatin) was added. Cells were kept 15 minutes on ice, with mild shaking every 3-4 minutes. Cells were then scraped and transferred to 1.5 ml tubes. In each tube 62 µl buffer B (10% NP-40 in H2O (IGEPAL CA-630, Sigma I3021)) was added (final conc. 0.62% NP-40). Tubes were vortexed for 10 seconds and centrifuged for 10 seconds at 14 000 rpm at room temperature. Supernatant that contained cytosol proteins was discarded. The pellet was dissolved in 60 µl cold buffer C (20 mM Hepes, pH 7.9; 400 mM KCL; 1 mM EDTA; 1 mM EGTA; 1 mM DTT; 1 mM PMSF; 1 mM Na_3VO_4; 10 µg/ml aprotinin; 10 µg/ml leupeptin; 10 µg/ml pepstatin) using a pipette, briefly vortexed, shaken for 15 minutes at 4°C and centrifuged for 5 minutes at 14 000 rpm at 4°C. Supernatant with nuclear proteins was transferred to a fresh tube. Samples that were treated the same way were pooled together (6 times 6 cm dish).

Protein concentration was measured with the Bio-Rad Protein Assay (Bradford, Micromethod), according to manufacturer's instruction. 50 µl of protein sample was quickly frozen on dry ice and stored at -80°C. The rest of the sample was prepared for gel electrophoresis analyses by mixing with 6X SDS sample buffer (7 ml Tris-HCl 0.5M, pH 6.8, 3 ml glycerol, water free (Fluka), 1 g SDS (BioRad), 0.93 g DTT (Sigma), 1.2 mg bromphenol blue (BioRad), H_2O up to 10 ml), incubated 4 min at 95°C, cooled down to room temperature, briefly centrifuged and kept at -20°C.

Western blot analysis: The procedure was described in detail in 1.2.3.2. Different dilutions of serum (1:500; 1:1000; 1:2000; 1:4000) and of secondary antibody (peroxidase - conjugated goat IgG fraction to rabbit immunoglobulins (ICN Pharmaceuticals, Inc., Aurora, Ohio, USA, Cat. No. 55682)) (1:10 000; 1:20 000) in 1% gelatin/PBS/0.1% Tween were tested.

3.2.4.3 Results

Testing of different serums for endogenously induced Hey1 detection

Since Hey1 mRNA is almost absent from non-stimulated MC3T3 cells (see Figure 5, for example) and strongly induced in GP/AA/BMP-2 stimulated cells, we wanted to confirm that this induction is visible on a protein level as well. For that purpose, three different Hey1 peptides were synthesized and used for immunization of rabbits, in

order to obtain sera with anti-Hey1 polyclonal antibodies. Nuclear protein extracts from non-stimulated and GP/AA/BMP-2-stimulated cells were prepared. Scheme of initial serum testing is shown in the Table 17. Western blot analysis was performed according to the standard procedure used in our lab (see Experimental procedure). For each condition tested, membrane stripe containing proteins from unstimulated (-) and GP/AA/BMP-2 stimulated (+) cells was prepared. All sera were tested in three different dilutions, and incubated with the membrane stripes for 2 hours. Secondary antibody was diluted 1 : 10 000, and incubated with the membrane stripes for 30 minutes.

sample number	immunization peptide	rabbit	serum dilution	bleeding	company
1	E-18-C-NH2-OVA	K25 253	1 : 500	terminal	Neosystem
2	E-18-C-NH2-OVA	K25 253	1 : 1 000	terminal	Neosystem
3	E-18-C-NH2-OVA	K25 253	1 : 2 000	terminal	Neosystem
4	E-18-C-NH2-OVA	K25 283	1 : 500	terminal	Neosystem
5	E-18-C-NH2-OVA	K25 283	1 : 1 000	terminal	Neosystem
6	E-18-C-NH2-OVA	K25 283	1 : 2 000	terminal	Neosystem
7	C-17-F-KLH	232 403	1 : 500	second	Novartis
8	C-17-F-KLH	232 403	1 : 1 000	second	Novartis
9	C-17-F-KLH	232 403	1 : 2 000	second	Novartis
10	M-17-C-NH2-KLH	232 409	1 : 500	second	Novartis
11	M-17-C-NH2-KLH	232 409	1 : 1 000	second	Novartis
12	M-17-C-NH2-KLH	232 409	1 : 2 000	second	Novartis
13	C-17-F-KLH	232 359	1 : 1 000	second	Novartis
14	C-17-F-KLH	232 359	1 : 2 000	second	Novartis
15	C-17-F-KLH	232 359	1 : 4 000	second	Novartis
16	M-17-C-NH2-KLH	232 352	1 : 1 000	second	Novartis
17	M-17-C-NH2-KLH	232 352	1 : 2 000	second	Novartis
18	M-17-C-NH2-KLH	232 352	1 : 4 000	second	Novartis

Table 17: Scheme for initial serum testing.

The results of the initial serum testing is shown in Figure 31. The expected molecular weight of Hey1 protein is 30 KDa. In that range, we could detect a faint band under some conditions (lines 5, 6, 7, 8, 15), but no up-regulation in stimulated samples under any of the conditions tested was visible. No further optimizations (different serum dilutions, different dilutions of secondary antibody, different amount of proteins loaded) yielded a clean Western blot with up-regulation of a band of the expected size in stimulated samples (data not shown). We concluded that the amount of endogenous Hey1 protein in our samples is too low to be detected under the conditions tested.

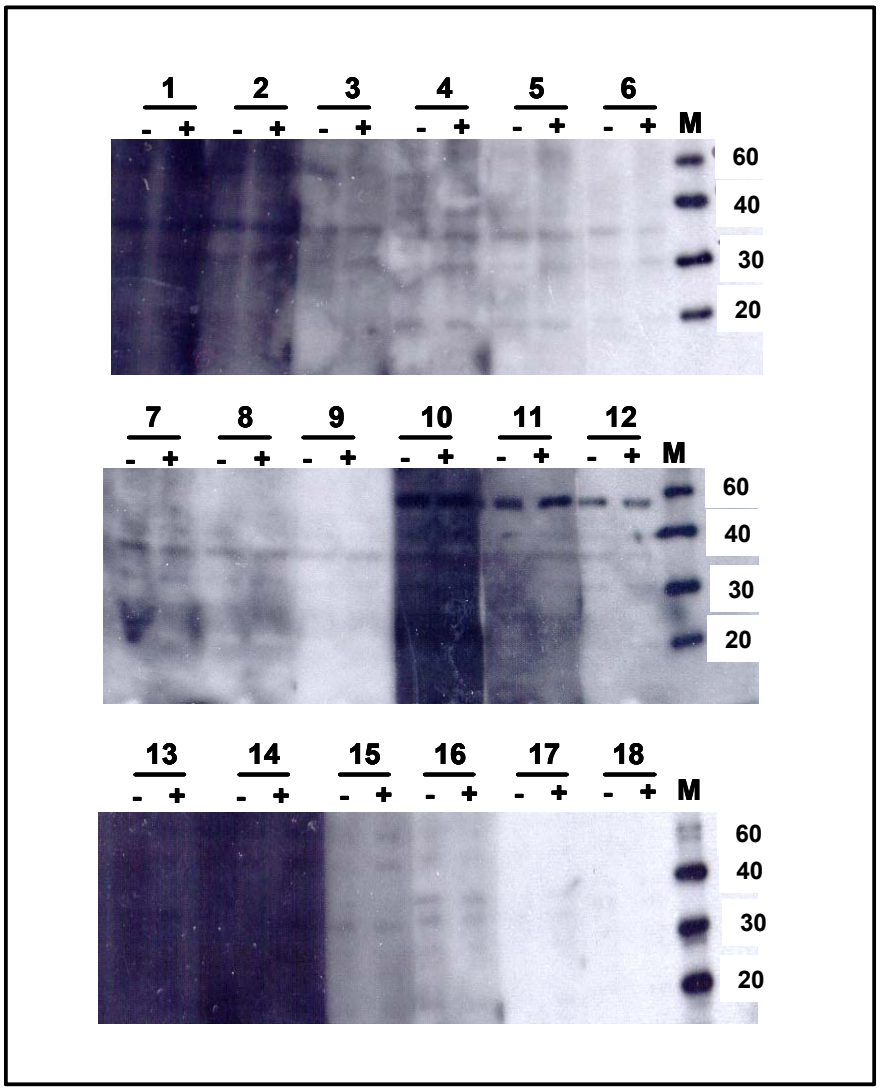

Figure 31. Testing of different serums for detection of Hey1 protein. M: 5 μl 10 X diluted Magic Marker, Invitrogen.

3.2.4.4 Discussion

Production of polyclonal Hey1 antibody for detection of endogenous protein has proven to be difficult. By using 6 different sera obtained from rabbits after immunization with three different Hey1 peptides, we could not detect unequivocally a band of the expected size. Moreover, the strong up-regulation of Hey1 protein in GP/AA/BMP-2 stimulated cells which we detected on the mRNA level could not be seen. This has convinced us that the Western blot conditions we used did not permit us to detect endogenous Hey1 protein. Polyclonal Hey1 antibody production for Western blot usage has presented difficulties in other labs as well (Dr. Manfred Gessler, personal communication). In our future work, we will try to optimize Western

blot conditions with proteins isolated from cells overexpressing Hey1 protein, which would contain much larger amounts of expressed protein.

3.2.5 Mouse Hey1 cloning

3.2.5.1 Introduction

Hey subfamily of transcription factors has recently been described[168] and, therefore, few tools are available for studying their function. In order to study the effect of Hey1 over-expression in MC3T3 cells, we set out to amplify Hey cDNA from Hey1-expressing RNA sample and to clone it into the expression plasmid. An antibody against Hey1 protein is also not commercially available, and out attempts to produce Hey1 polyclonal anti-peptide antibody did not succeed (separate chapter). Therefore, we decided to make expression constructs for both wild-type Hey1, and for tagged-Hey1, which contained a FLAG sequence on C-terminal. Flag tag will enable the detection of protein by Western blotting.

3.2.5.2 Experimental procedures

Primer design for Hey1 cloning. Two forward and two reverse primers were initially designed for amplification of mouse Hey1 (mHey1) cDNA. Both forward primers (F1, F2) contained EcoRI restriction site on the 5'end, while both reverse primers (R1, R2) contained NotI restriction site on 5' end, in order to facilitate cloning into the expression vector pcDNA3.1(+) (Invitrogen). R1 reverse primer was designed to omit the stop codon, and to enable transcription of FLAG tag at the 3' end. (Figure 32). Later, R3 primer was designed to introduce the stop codon into F1/R1 fragment. Positions of the used primers are shown in Figure 32.

Mouse Hey1, Accession Number NM_010423

F1: EcoRI: agaattcgcgtgagtgggatcagtgt

F2: EcoRI: agaattcgaccctcctcggagcccac

R1 (flag): NotI: agcggccgcagaaagctccgatctctgtcc

R2: NotI: agcggccgcccttgttctacagcatcag

R3: ttagaaagctccgatctctgtcc

Figure 32: Positions of primers used for amplification of mHey1 cDNA. R3 primer has the same sequence as R1 primer, except that instead of NotI restriction site it contains tt sequence at the 5' end, which creates a stop codon at the end of the amplified fragment (see picture). Brockets are showing the coding region of mHey1 mRNA.

PCR amplification of mHey1 cDNA. cDNA obtained from MC3T3 cells stimulated with GP, AA and BMP-2 for 3 days was used as a sample for Hey1 cDNA amplification. This sample was previously shown to highly express Hey1 gene. RNA isolation and reverse transcription reaction are described in 2.1.3.

Two µl of cDNA or RT- control was used as a PCR template. PCR reactions were performed in a final volume of 25 µl, containing 100 µM of each dNTP, 2 µM of each primer and 1.25 units of "Hot start" thermostable DNA polymerase and corresponding reaction buffer (FastStart Taq, ROCHE Molecular Diagnostics). The amplification protocol was the following: initial step of 5 min at 94°C, 35 or 25 cycles (35 cycles with cDNA template, while 25 cycles with plasmid template) of denaturation at 94° C for 1 min, annealing at for 1 min, and extension at 72° C for 1 min 20 s. The amplification was terminated with a final incubation step at 72° C for 10 min. Annealing temperature options in different reactions were: 55°C; 57°C; 60°C; 5 cycles at 55°C followed by 30 cycles at 64°C; temperature gradient from 50°C-58.4°C or from 55.5°C-66.8°C (see Results). Reactions were performed in 0.2 ml "thin-wall" Eppendorf tubes, in a Diade 220 (MJ research) PCR machine. Aliquots of PCR products were mixed with loading buffer (final concentrations: 5 % glycerol, 10 mM EDTA, 0.01 % SDS, 0.025 % xylene cyanol and bromophenol blue dyes) and analyzed on 1% agarose gels.

DNA extraction from agarose gel. The bands were cut out from the agarose gels under the UV light with a clean, sharp scalpel. The size of the gel around the band was minimized by removing surrounding agarose as much as possible. For DNA purification, the QIAquick Gel Extraction Kit (Qiagen) was used according to manufacturer's protocol.

Restriction digestion. Restriction digestion with EcoRI (10U/µl, Roche) and/or NotI (10U/µl, Roche) was done according to the manufacturer's protocol, 1 h at 37°C, followed by a 15 min enzyme inactivation at 65°C.

Plasmid dephosphorylation. Dephosphorylation of EcoRI digested pcDNA 3.1(+) plasmid (Invitrogen) was done with Shrimp Alkaline Phosphatase (Amersham), according to manufacturer's protocol. Reaction was performed for 2 h at 37°C, followed by a 15 min enzyme inactivation at 65°C.

Ligation. Ligation of PCR product with the linear form of pGEM-T Easy vector (Promega) or ligation of restriction digestion products was done by Rapid DNA

Ligation Kit (Roche), 5 min at room temperature, according to manufacturer's protocol.

Transformation of bacteria. XL1 blue Chemically Competent *E. coli* (Stratagene, Cat. No. 200249) were used for transformation. The ligation reaction has been briefly centrifuged and placed on ice. Aliquots of bacteria (100 µl) were thawed on ice. Five µl of ligation reaction were added to 100 µl of competent cells and the tube was mixed by gentle tapping. The vial was incubated on ice for 10 min. Subsequently, the bacteria were heat-shocked for exactly 45 s at 42° C. The vial was placed on ice for 2 min and 400 µl of pre-warmed LB-medium was added to the vial. The vial was shaken at 37° C for 30 min at 225 rpm in an Eppendorf shaker.

Plating of bacteria. The whole volume of the transformed cells was spread on LB agar plates containing 100 µg/ml ampicillin. The plates were incubated overnight at 37° C. Colonies from different plates were picked and checked for the presence of the insert.

PCR testing of colonies. To check the plasmids for the presence of the insert, the following primers were used: Forward T7: 5' TTA ATA CGA CTC ACT ATA GGG 3'; Reverse SP6: 5' ATT TAG GTG ACA CTA TAG AA 3' Several colonies were picked with colony picker, and were placed into tubes containing 10 µl of water. The colony picker was then put into prepared PCR mix. 100 µl of LB medium was added into 10 µl of water, which was inoculated with bacteria and these pre-cultures were incubated at 37° C with shaking (250 rpm, Eppendorf shaker). During this incubation the PCR reaction were performed (around 2 h).

<u>PCR reaction mix</u>

- 2,5 µl buffer (500 mM Tris/HCl, KCl, $(NH_4)_2SO_4$, 20 mM $MgCl_2$, pH 8.3, Roche)
- 2,5 µl dNTPs mix (1mM each)
- 0,25 µl Fast Start Taq polymerase(5 U/µl)
- 1 µl primer T7 (10 µM)
- 1 µl primer SP6 (10 µM)
- 0.25 µl Fast Start Taq polymerase (5U/µl, Roche)
- Water up to 25 µl

The amplification protocol was the following: initial step of 5 min at 94°C, 25 cycles of denaturation at 94° C for 1 min, annealing at 57°C for 1 min, and extension at 72° C for 1 min 20 s. The amplification was terminated with a final incubation step at 72° C

for 10 min. PCR products were analyzed on 1% agarose gels. Positive colonies were used for plasmid preparation.

Plasmid preparation: For preparation of small amounts of plasmids, NucleoSpin Plasmid (Macherey-Nagel) kit was used. For preparation of larger plasmid amounts, EndoFree Plasmid Maxi Kit (Qiagen) was used. Preparations were done according to the manufacturer's instructions.

Sequencing. Sequencing of the constructs was done by Bioanalytik Solvias AG (Basel, Switzerland).

3.2.5.3 Results

mHey1 cDNA amplification

All combinations of forward and reverse primers and four different annealing profiles were tested for the amplification of mHey1 full-length cDNA (Figure 33A). R1 and R2 reverse primers were providing the amplification of cDNA without or with stop codon, respectively (Figure 32). As it can be seen on the picture (Figure 33A), a good amplification was obtained with F1/R1 combination at 55°C and with F2/R2 combination at 60°C. To further optimize amplification conditions, PCR reaction was repeated with F1/R1 primers on 6 different annealing temperatures ranging in equal intervals from 50°C-58.4°C (annealing gradient). Same was done with F2/R2 combination of primers and annealing temperatures ranging from 55.5°C to 66.8°C (Figure 33B). The best annealing temperatures were shown to be 55°C for F1/R1 primer combination, and 60°c for F2/R2 primer combination. However, a longer run of agarose gel electrophoresis (Figure 33C) revealed that F1/R1 primers amplified two different fragments of similar size. Two F1/R1 fragments and F2/R2 fragment were cut out from a gel, cleaned, and ligated with a linear form of pGEM T-Easy plasmid (Promega). This plasmid is very frequently used as a shuttle vector for initial ligations. Its linear form has one single-stranded T on each 5' end, while most polymerases used in PCR amplifications add one A at the 3' end of each strand. This feature is used for easy cloning into pGEM T-Easy plasmid. Ligation products were used to transform chemically competent *E. Coli* XL1 blue strain, and transformants were grown on the ampicillin-containing agar plates overnight at 37°C. Significant number of separate colonies was obtained. Colony PCR was used to check for the presence of insert. Five different colonies were analyzed for the presence of the F1/R1 insert, and they were all positive, containing inserts of two different sizes

(Figure 33D). From 5 colonies analyzed for the presence of F2/R2 insert, 3 were positive (Figure 33D). All positive colonies were expanded in ampicillin-containing LB medium, the plasmids were isolated and sent for the sequencing, which was performed by using 4 different primers; T7, SP6, Hey1-F, and Hey1-R. Hey1-F and Hey1-R primers are the same as used in rqRT-PCR. Sequencing result showed that clones 1 and 5 do not contain the correct insert, but instead a fragment of mouse E1A binding protein 300 mRNA. Clones 2, 3 and 4 contained the correct insert, however, the sequence in clones 2 and 3 contained 2 mismatches probably created in PCR amplifications with Fast Start Taq polymerase, which does not have 3'-5' exonuclease proofreading activity. Clone 4 contained the correct insert with no mismatches. Clones 6, 9 and 10 all contained the right F2/R2 fragment, but with 2 mismatches.

In conclusion, we have obtained one clone containing pGEM T-Easy plasmid with a full length mHey1 sequence, however, without the stop codon (Figure 33 E).

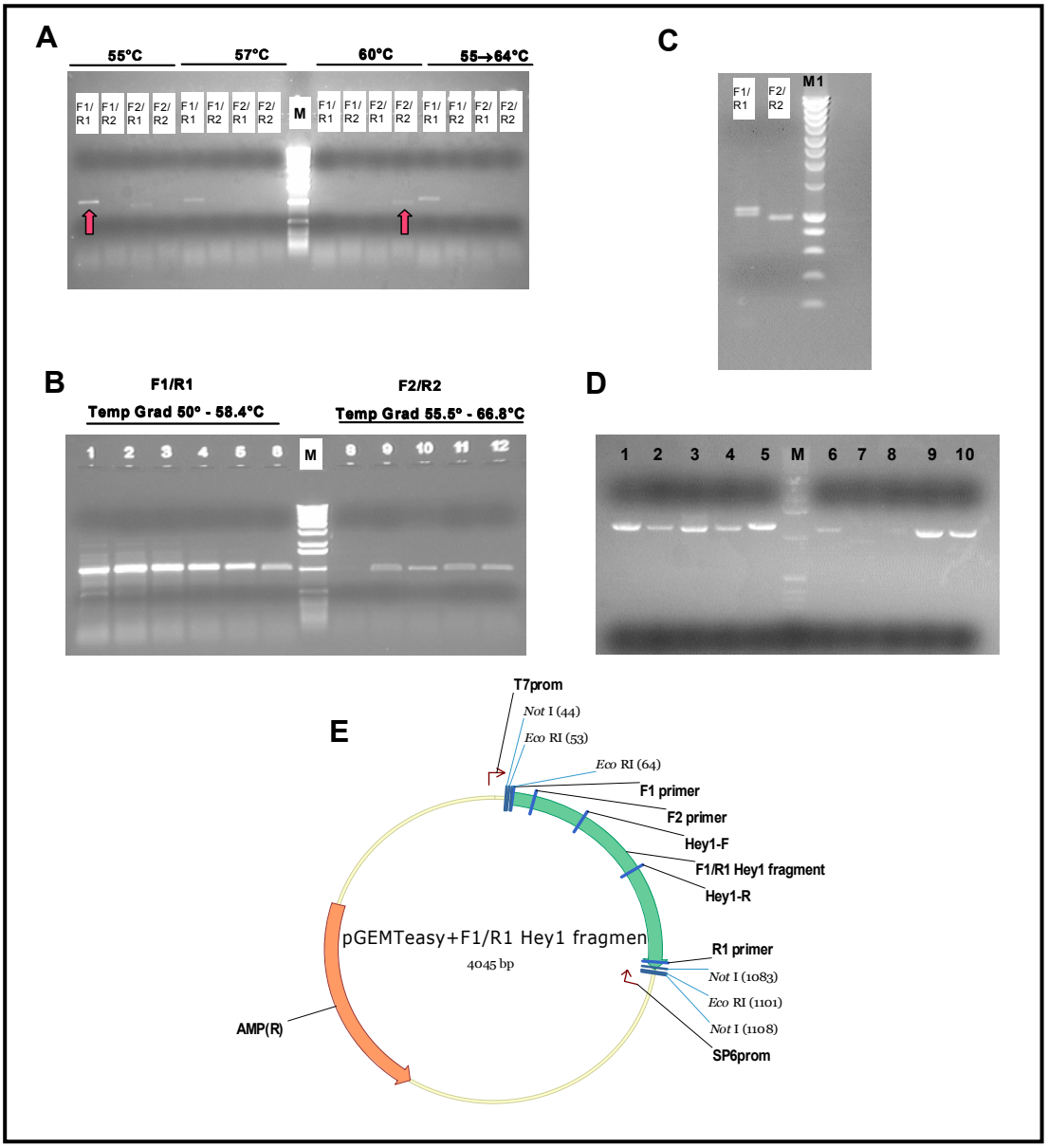

Figure 33. Amplification of the full-length mHEY1 cDNA and its cloning into pGEM T-Easy vector. A). Testing of different primers combinations and different annealing temperatures. B). Annealing temperature optimisation for selected primer pairs. C). F1/R1 primers amplified 2 fragments of a similar lenght, while F2/R2 primers amplified a single fragment. D). Colony PCR.

Cloning of Hey1 into the Expression vectors

In the next step, we decided to use construct with the correct sequence of Hey1, in order to amplify wild type mHey1 cDNA sequence. For that purpose we introduced a stop codon in a PCR reaction. pGEM T-Easy +F1/R1 fragment was used as a template, from which a DNA fragment was amplified with F2 and R3 forward and reverse primers. We have obtained a PCR product that contained full length mHey1

cDNA sequence and a stop codon, introduced by R3 primer (Figure 34). PCR product was first cloned into pGEM T-Easy vector, and then both fragments were re-cloned into pcDNA3.1 (+) expression vector (Figure 34). The correct sequence and orientation of wile type mHey1 insert in pcDNA3.1(+) vector were confirmed by two-strand sequencing.

In conclusion, we obtained two expression plasmids, one containing mouse Hey1 cDNA and one with mouse Hey1 labeled on the 3' end with a Flag tag.

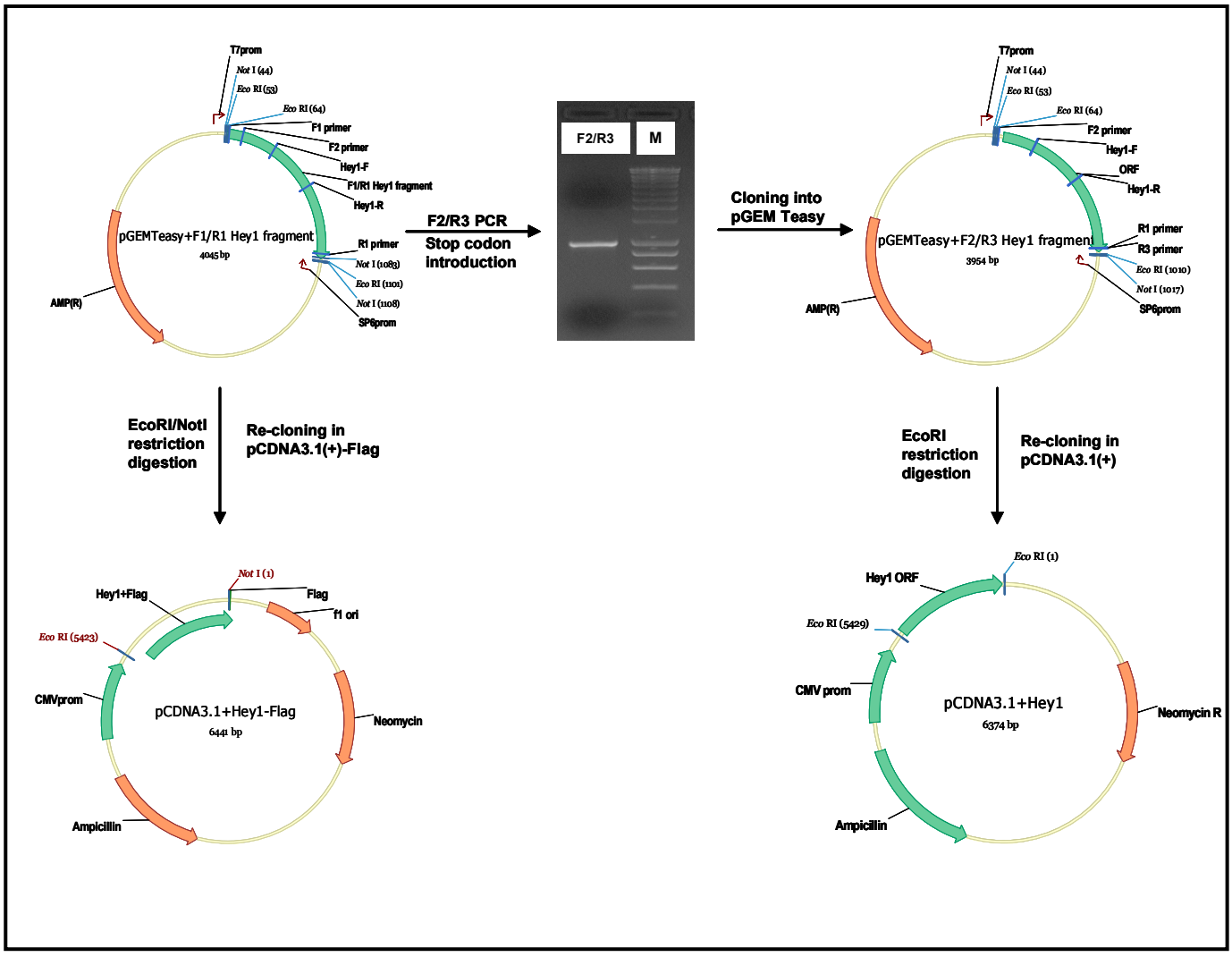

Figure 34. Introducing the stop codon and re-cloning of inserts into pCDNA3.1(+) expression vector.

3.2.5.4 Discussion

mHey1 cDNA contains sequence stretches with high GC content, and therefore its amplification by PCR was not straightforward and required several optimization steps, testing of different primers combinations and different annealing temperatures. Testing of two different proof-reading enzymes, which could repair errors during

polymerization, did not give good results (data not shown). Therefore, we have used Fast Start Taq polymerase, enzyme with very high processivity, but lacking proofreading activity. Since the amplifying fragment was not too long (≈1000 bp), we managed to obtain a fragment that did not have any amplification errors. However, in amplification of longer fragments that require absolute fidelity, this would not be an enzyme of choice and more proof-reading enzymes would have to be tested.
We have obtained two expression plasmids, one containing mouse Hey1 cDNA, and another containing FLAG-tagged mouse Hey1 cDNA. These constructs were used in subsequent co-transfection experiments.

3.3 Effect of Notch inhibition on BMP-2 induced HES1 and Hey1 activation

3.3.1 Introduction

Recent data have confirmed that Hey1 is the direct target gene of the Notch signaling pathway in many different systems (reviewed in Iso *et al.*, 2003[171]), and that cross-talk between Notch and BMP signaling pathways can lead to Hey1 activation (discussed in detail in Final Discussion). Functional Notch signaling is shown to be necessary for BMP-2-dependent Hey1 induction in myogenic cells[190] and endothelial cells[191]. In order to confirm that Notch signaling is necessary for BMP-2-mediated Hey1 induction in osteoblastic cells, we performed experiments to block Notch signaling with inhibitors of γ-secretase, the enzyme which prevents cleavage and release of the Notch intracellular domain upon ligand binding[218]. To confirm the potency of γ-secretase inhibition on direct Notch signaling, we also activated Notch by calcium depletion. The extracellular and transmembrane subunits of the Notch receptor interact non-covalently, and this interaction can be disrupted with divalent calcium chelators such as EDTA[219]. Rand *et al.*, 2000 have shown that a 15 minute treatment of NIH 3T3 cells with 0.5 to 10 mM EDTA, resulted in the rapid detaching of the extracellular part of Notch from the cell surface, the transient appearance of a polypeptide of expected size of the Notch intracellular domain (NICD), and the transient activation of a Notch-sensitive reporter gene driven by the HES1 promoter[219].
As a readout of Notch pathway activation, we measured endogenous mRNA levels of two direct Notch target genes, HES1 and Hey1. We have compared the profiles of the HES1 and Hey1 genes upon direct activation of the Notch pathway by calcium

depletion with the gene profiles upon BMP-2 stimulation in MC3T3 cells, as well as the effect of γ-secretase inhibitor on these gene profiles. Gamma-secretase inhibitor L-685,458 was used. This is a highly specific and potent inhibitor of γ secretase activity which inhibits cleavage of Amyloid β precursor protein[220] and Notch receptor[221]. This inhibitor was used previously to study the BMP-2-Notch signaling interaction[190], when it was shown that Notch signaling is required for BMP-2 induction of Hey1 in myoblastic cells.

3.3.2 Experimental procedures

Cell culture. MC3T3 cells were plated on 6-well plates ($1.5x10^5$ cells/ well in 3 ml of medium), and grown to confluence for 3 days at 37°C / 5% CO_2, after which the stimulation was performed, either with EDTA treatment or GP/AA/BMP-2 stimulation.

EDTA treatment. Confluent MC3T3 cells were treated either with phosphate-buffered saline (PBS), 0.5 or 5 mM EDTA in PBS for 15 minutes at room temperature. Cells were then rinsed with medium once and incubated for an additional 1, 2 ,4, 6, 20 or 30 h in medium at 37°C / 5 % CO2 prior to RNA isolation.

GP/ AA / BMP-2 treatment: Confluent MC3T3 cells were stimulated with 10 mM β-glycerophosphate (GP, Sigma), 50 μM ascorbic acid (AA, Wako) and 1 μg/ml BMP-2 (Nico Cerletti, Novartis). Control cells were stimulated with medium alone. RNA isolation was performed 1, 6 or 24 hours after stimulation.

Gamma-secretase inhibitor treatment: L-685,458 was purchased form Sigma (Cat. No. L1790-1MG). The substance was diluted in filter-sterilized DMSO to 10 mM stock solution, single-use aliquoted and kept at -20°C. Inhibitor was added to the cells at a concentration of 1 or 5 μM, 12 hours prior to stimulation, to ensure that cleaved NICD, already generated by low level endogenous Notch signaling, was degraded prior to stimulation. Fresh inhibitor compound was added together with the stimulus and after the stimulation (EDTA treatment), or only together with the stimulus (GP/AA/BMP-2 treatment).

RNA isolation and Real-time quantitative RT-PCR analysis. Analysis were performed as described in 2.3.1. Applied Biosystems, Assay-On-Demand for mouse *HES1* gene was Mm00468601_m1. Fold induction was always calculated in comparison to the time matched control sample (PBS-treated cells, EDTA treatment; Medium-treated cells, GP / AA / BMP-2 treatment). *18S rRNA* was used as a normalization control.

3.3.3 Results

Calcium depletion by EDTA induces HES1 and Hey1 genes

Depletion of calcium by EDTA treatment induces transient activation of the Notch pathway[219]. Therefore, we used this approach to activate Notch in MC3T3 cells. After treatment of MC3T3 cells with two different EDTA concentration (0.5 and 5 mM) we isolated RNA after 1, 2, 4, 6, 20 and 30 hours, and measured the HES1 and Hey1 endogenous mRNA levels. Calcium depletion proved to be an effective method for activation of Notch target genes. Interestingly, the kinetics of HES1 and Hey1 induction were very different (Figure 35).

The HES1 gene was induced very strongly, around 20-fold, compared with the time-matched, PBS-treated control cells, 1 h after the stimulation (Figure 35A). This induction was of a transient nature: already after two hours the HES1 mRNA level came back to its basal level. There was no difference in stimulation level between the two different EDTA concentrations used, corroborating the previously published observation that stimulation with 0.5 mM EDTA is sufficient to achieve maximal Notch activation[219].

After 1 h, the Hey1 gene was induced, to a lower degree than HES1 (around 4-fold compared with the time-matched, PBS-treated control cells). Induction of the Hey1 gene lasted longer than induction of HES1: with some fluctuation it remained 3-fold above basal level up to 6 h after stimulation. At later time points, 20 hours and 30 hours after simulation, Hey1 level returned to its basal level (Figure 35B).

The basal level of Hey1 gene expression was much lower that the level of HES1 expression (Ct values of 35 versus 27, respectively) . Basal level of expression did not change significantly with time for either of the genes.

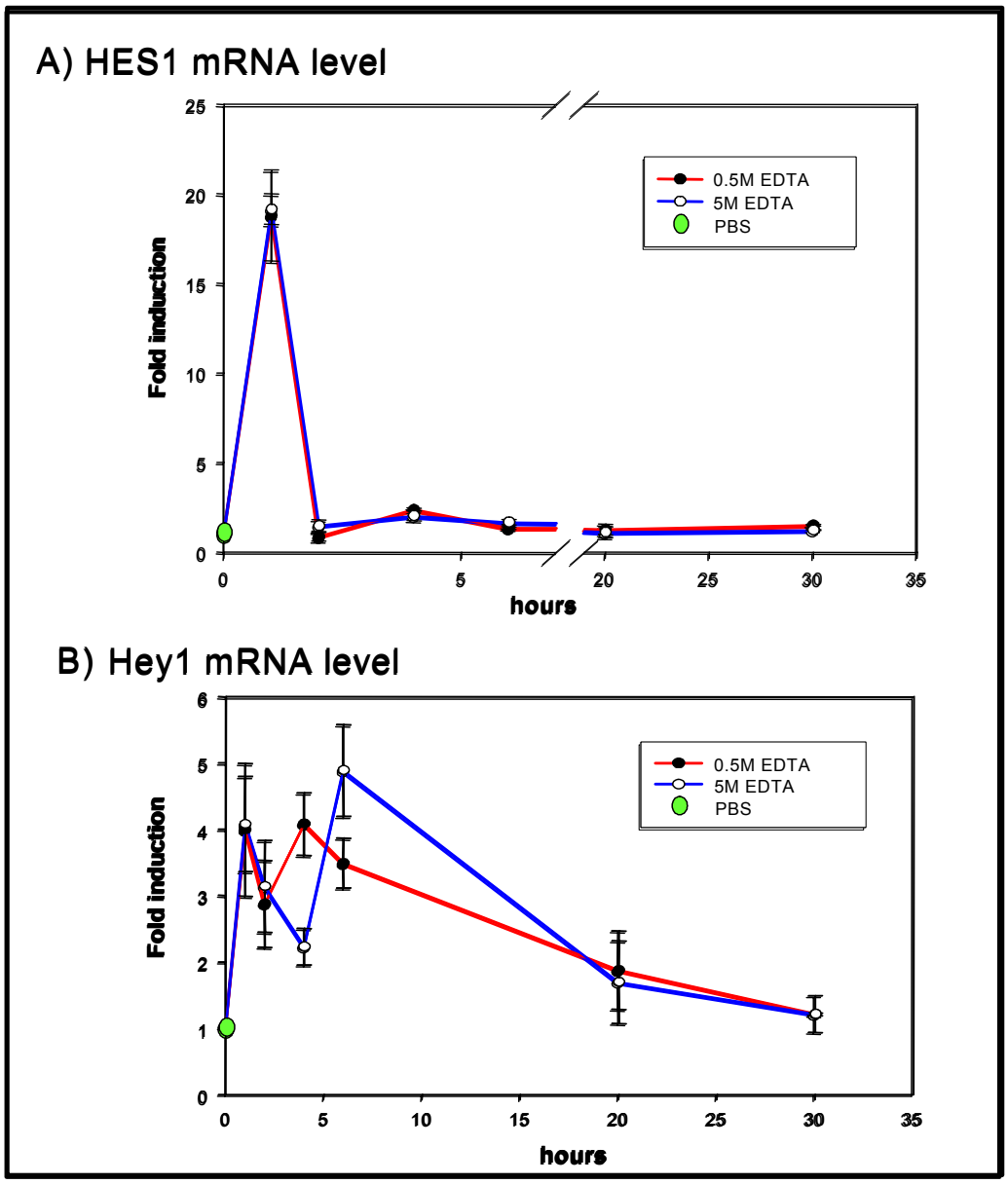

Figure 35. Time-course of HES1 and Hey1 gene expression upon EDTA treatment.

EDTA induction of HES1 and Hey1 genes is abolished by γ secretase inhibitor treatment

In the next experiment, cells were treated with 0.5 mM EDTA for 1 h with or without addition of two different concentrations (1 and 5 μM) of L-685,458 γ-secretase inhibitor, and the level of HES1 and Hey1 mRNA was monitored. Induction of both genes was already completely abolished with a lower concentration of the inhibitor, proving that the γ-secretase inhibitor treatment is an effective way of inhibiting the Notch signaling pathway (Figure 36).

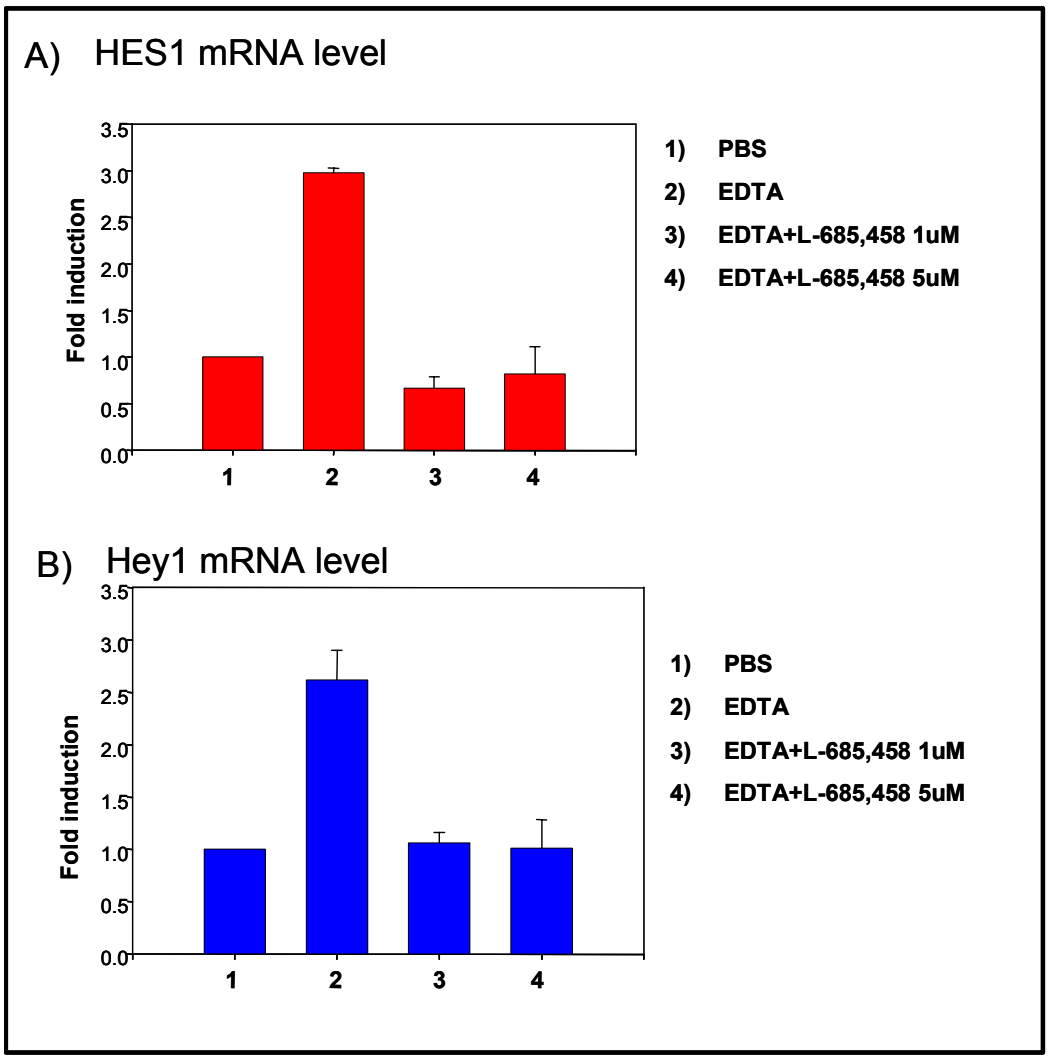

Figure 36. Treatment with L-685,458 γ-secretase inhibitor completely abolished HES1 and Hey1 induction by EDTA.

Different profiles of HES1 and Hey1 genes upon BMP-2 treatment; different effects of γ-secretase inhibitor

Profiles of HES1 and Hey1 genes upon GP/AA/BMP-2 treatment looked completely different: One hour after the stimulation, HES1 induction was very weak, below 2-fold, in comparison to the time-matched control. After 6 hours, a much bigger induction (around 4.5-fold) could be seen, and HES1 mRNA came back almost to the level of time-matched control 24 hours after induction (Figure 37A). Hey1 induction could be seen already after 1 h (around 3-fold, Figure 37B), and the induction was growing with time, reaching 25-fold after 6 h and 130-fold after 24 h.

The effect of the γ-secretase inhibitor was also very different on the two gene profiles: L-685,458 completely abrogated HES1 induction (Figure 37A), but it had only a minimal, not statistically significant ($p < 0.05$), effect on Hey1 induction at any time point (Figure 37B).

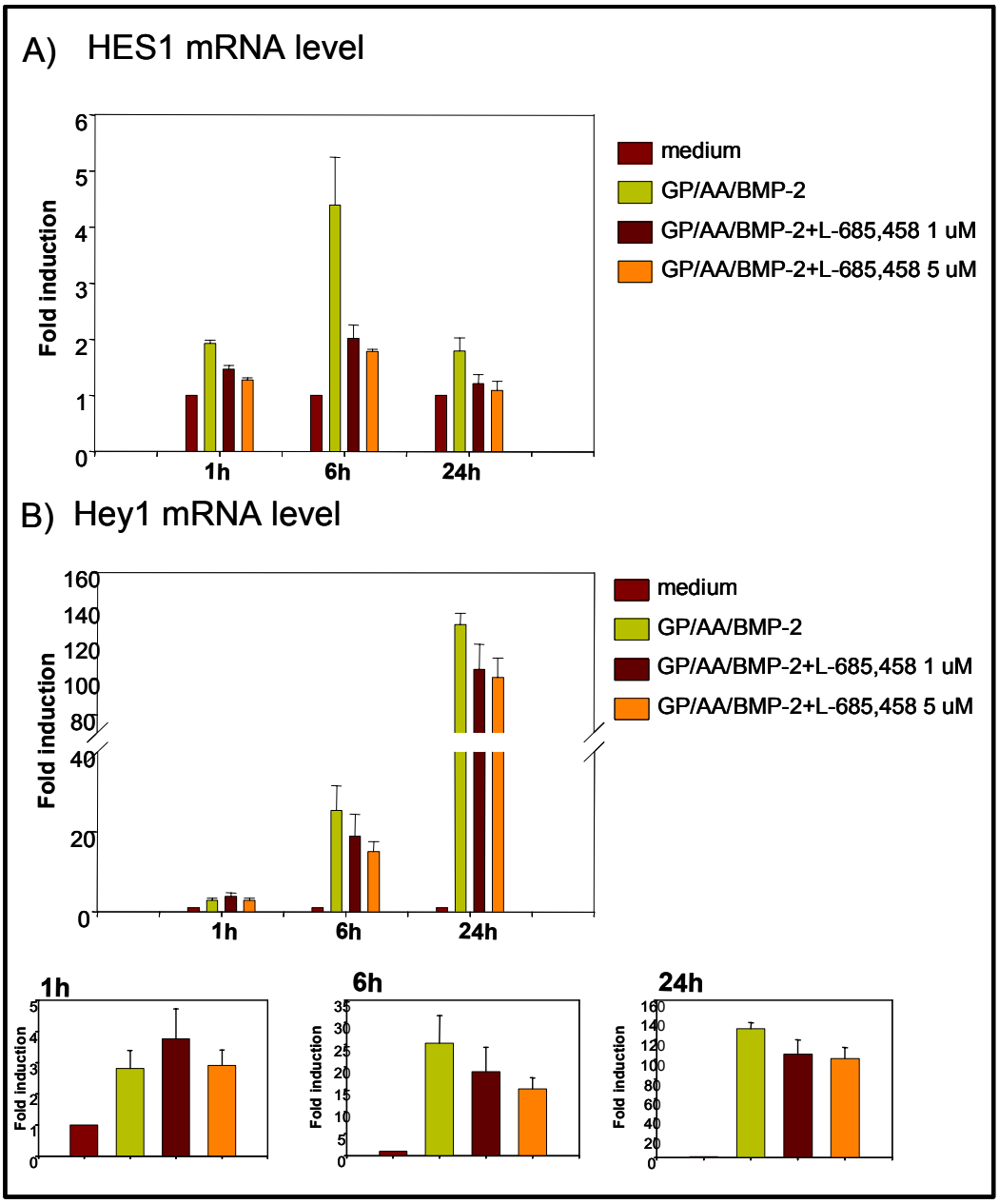

Figure 37. Profiles of HES1 (A) and Hey1 (B) mRNA level upon GP/AA/BMP-2 treatment and treatment with γ-secretase inhibitor.

3.3.4 Discussion

Calcium depletion by EDTA treatment has proven to be a successful means of activating the Notch pathway, since we saw a clear induction of two direct Notch target genes. Different profiles of HES1 and Hey1 upon Notch activation could be explained by interaction of the NICD-CSL complex with different co-activators in activation of HES1 and Hey1 promoters. The precise mode of regulation of these two promoters is still largely unknown.

Gamma-secretase inhibitor treatment was also shown to be an effective way of inhibiting Notch signaling: the treatment with the inhibitor completely abolished EDTA-induced HES1 and Hey1 genes.

BMP-2 induced HES1 and Hey1 activation profiles and the effect of the γ-secretase inhibitor on those two genes profiles were very different. HES1 showed a delayed and transient induction by BMP-2, and this induction could be completely reverted by addition of the inhibitor. This finding proves that Notch pathway does get activated upon BMP-2 stimulation of MC3T3 osteoblastic cells, since its activation led to the transient induction of HES1, and its inhibition by γ-secretase inhibitor abolished completely this induction.

The Hey1 induction profile looked very different. Hey1 induction is quick, visible already 1 h after BMP-2 stimulation, suggesting that Hey1 might be partly stimulated as a direct target of BMP2-Smad signaling in MC3T3 cells. GC-rich palindromic sites which are potential Smad-binding sites are described in the promoter of Hey1 gene [191], and could possibly mediate this induction. The observed stimulation increases with a time, reaching 130-fold activation after 24 h. This observation might suggest that there is more than one path of Hey1 gene activation. One pathway could be a direct activation by Smads, and the other, delayed mechanism, would start upon activation of Notch or some other pathway. The two paths could be synergistic. Another study showed that Hey1 induction by BMP-2 in C2C12 myoblastic cell line is only partly inhibited upon protein synthesis inhibition, which would also suggest the existence of multiple activation mechanisms[222].

Gamma-secretase inhibitor treatment had only minimal inhibitory effect on the strong Hey1 induction by BMP-2. This result suggests that BMP-2 induced Hey1 activation does not depend greatly on activation of the Notch pathway. Since Hey1 is a proven direct target and effector of the Notch signaling pathway[171], and so far no other signaling pathway is shown to be able to activate its transcription, this finding came as a surprise. It should be noted that these are only preliminary data from the first experiments performed to address this question. In a previous study investigating BMP and Notch pathway cross-talk, a synergistic effect of BMP and Notch signaling pathways on the Hey1 promoter was shown[191]. The study showed that this synergistic effect on the Hey1 promoter is mediated via multiple RBP-Jk binding sites and GC-rich binding sites, which are potential Smad-binding sites, located in proximity to each other, within the first 1,000 base pairs of the Hey1 promoter.

Interaction between NICD and SMAD further potentiates Hey1 promoter activation. In that study, BMP stimulation or Smad proteins overexpression alone lead only to marginal activation of Hey1. Our finding would suggest that in osteoblastic cells Hey1 activation is possible even in the absence (or with very low concentration) of NICD. Possibly, Smad interaction with some other, osteoblast-specific cofactors, and their subsequent binding to the Smad binding sites in the proximal Hey1 promoter, or to some other sites in a distal promoter that is not sequenced yet, could lead to this cell-specific behavior of Hey1 gene. Further work is necessary to confirm these preliminary results.

4 Final Discussion

4.1 Role of Hey1 transcription factor and Notch pathway activation in osteoblast differentiation

One of the most interesting and novel findings of our work was the strong BMP-2 induced up-regulation of the Hey1 transcription factor, a member of the recently described basic helix-loop-helix family which are shown to be a direct target of the Notch signaling pathway. Connecting the Notch pathway components to osteoblast biology is exciting, since until now this pathway was studied very little in the bone field, and it could open new possibilities for promoting bone formation.

4.1.1 Notch signaling pathway

Notch signaling is an evolutionarily conserved mechanism that is used by metazoans to control cell fates through local cell-cell interactions. Components of the Notch pathway, such as *Notch, bigbrain, Delta, mastermind, neuralized* and *enhancer of split complex*, were isolated originally as neurogenic genes in *Drosophila*, since embryos lacking these genes contained an increased number of neuroblasts at the expense of epidermal precursors. It has subsequently been demonstrated that the Notch pathway, besides its role in neurogenesis, controls the development of many other organs derived from all three germ lines, in all metazoans ranging from sea urchins to humans (reviewed in[181,223]). Mutations in Notch loci result in diverse phenotypes, ranging from the notching of wings in Drosophila[224] to the malignant transformation of human T cells[225]. In vertebrates, mutations of the components of the Notch pathway lead to abnormalities in many tissues, including vessels, thymus, craniofacial region, limb, rib, somite, central nervous system, heart, kidney, as well as haematopoietic cells (reviewed in Iso *et al.*, 2003[171]).

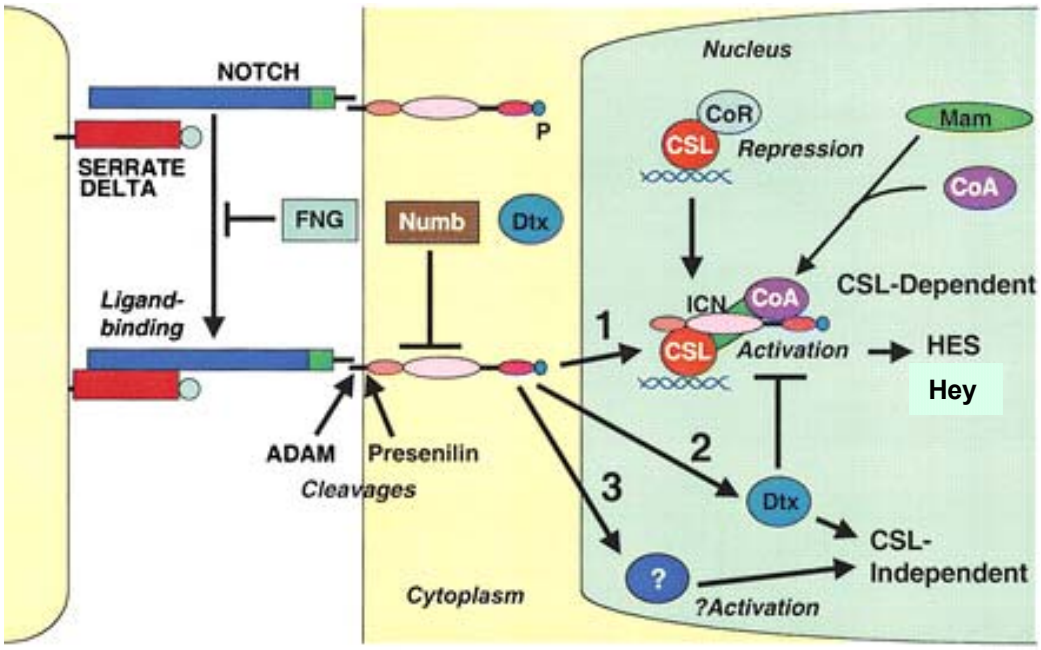

Figure 38. Components for the Notch signaling pathway. Modified from Allman *et al.*, 2002[226].

Notch receptors are large single-pass transmembrane proteins. During trafficking to the cell surface, Notch proteins are cleaved within the trans-Golgi network by a furin-like protease, giving rise to mature heterodimeric receptors comprised of non-covalently associated extracellular and transmembrane subunits. Multiple lines of investigations have converged on a model of intracellular signaling by Notch, in which the Notch intracellular domain (NICD) is cleaved and translocated to the nucleus in a ligand-dependent fashion (Figure 38). Binding of Notch receptors to ligands of the Serrate and Delta families results in two successive cleavages of Notch: first in the extracellular domain by the ADAM-type protease, and then in the transmembrane domain by presenilin-dependent γ secretase complex. The cleavage events release NICD and permit its translocation to the nucleus. The ability of Serrate-like ligands to activate Notch can be antagonized by Fringe (FNG) glycosylases, which modify Notch extracellular domains. In the nucleus, NICD binds to transcription factor CSL (CBF1/RBP-Jk in mammals, Suppressor of Hairless in *Drosophila*, and LAG-1 in *C. elegans*), displacing corepressors (CoR), and recruiting coactivators (CoA), including mastermind (MAM), and activates gene expression from the CSL binding site (GTGGGAA) (pathway 1 on Figure 38). The NICD-CSL complex up-regulates expression of primary target genes of Notch signaling, such as HES in mammals, *Enhancer of Split* in *Drosophila*, and a new, recently described mammalian

transcription factor family named Hey. These target genes are all bHLH transcriptional repressors and act as Notch effectors by negatively regulating expression of downstream target genes. Poorly characterized CSL-independent pathways also exist, which may proceed through deltex (Dtx) (pathway 2 on Figure 38) or unknown factors (pathway 3 on Figure 38). Several proteins are described to interact with NICD and positively or negatively regulate Notch signaling, such as Numb or Deltex (Dtx)[171,181,223,226].

Component	*Drosophila*	Mammals
Receptors	Notch	Notch1-6
Ligands	Delta	Delta-like 1-4
	Serrate	Jagged 1,2
Downstream transcription effectors	Su(H)	CBF1/RBP-Jk/CSL
Modulators	Fringe	Lunatic, Radical, Manic Fringe
	Numb	Numb, Numb-like
	Deltex	Deltex 1-3
	Mastermind	Mastermind-like 1-3
Target genes	Hairy/En(spl)	Hes 1, 5, 7
		Hey 1, 2, L
Processing molecules	Presenilin	Presenilin 1,2
	Metallo-protease	Metallo-protease
	Furin-like protease	Furin-like protease

Table 18. Conservation of Notch signaling. Su(H) - Suppressor of Hairless; Hairy/En(spl) – hairy-like enhancer of split; CBF1-C promoter-binding factor 1; RBP-Jk- recombination signal-binding protein 1 for J-kappa. Iso *et al.*, 2003; Allman *et al.*, 2002[171,226].

Components of the Notch signaling pathway are highly conserved in all metazoans. Comparison of Drosophila and mammal elements of Notch signaling is shown in Table 18. Increasing number of Notch components in mammals is adding complexities to Notch signaling. Link among specific isoforms of ligands, receptor, and effectors might create a cell-type specific sub-pathway of Notch signaling, and contribute to generation of different cell fates. This hypothesis is supported partly by the tissue-specific distribution of different isoforms of Notch components. Distinct functions of each isoform in animals are clearly demonstrated at least for Notch receptors and ligands, by the gene disruption studies for three receptors (Notch 1, 2 and 4) and four ligands (Delta-like 1, 3, Jagged 1, 2). Mice with mutations of one of these genes show different phenotypic changes, indicating distinct roles of the isoforms (reviewed in Iso *et al.*, 2003[171]). Much less work has been done on clarifying

the function of Notch signaling effectors, bHLH transcriptional inhibitors of the HES and Hey family, which by means of their number, different expression patterns and ability to homo- and hetero-dimerise give also possibility for differential regulation of Notch signaling.

4.1.2 HES and Hey transcription factors: effectors of Notch signaling

The HES/E(spl) (Enhancer of Split) family proteins are basic helix-loop-helix (bHLH) type transcriptional repressors. To date, seven HES members have been isolated in mammals (reviewed in Iso *et al.*, 2003[171]). HES proteins act as Notch effectors by negatively regulating expression of downstream target genes such as tissue-specific transcription factors. For instance, HES1 and HES5 were shown to be up-regulated by NICD and necessary to prevent neuronal differentiation of neural precursor cells form mouse embryos, by negative regulation of proneural genes[227].

Recently, a new bHLH family has been isolated and named Hey/Hesr/HRT/CHF/gridlock/HERP (hereafter Hey). Different nomenclature used in the literature is shown in Table 19. Their high sequence similarity with the HES family has raised the possibility that the Hey gene family might be new targets of Notch. In line with this, over-expression of NICD can stimulate expression of all studied Hey members in reporter gene assays following transient transfection[228,229]. Definitive proof that Hey genes are up-regulated by Notch was obtained by co-culturing Notch receptor-bearing target cells with Notch ligand-expressing stimulator cells, a situation that is more physiological than the massive NICD over-expression. Hey1[169] and Hey2[170] mRNA was up-regulated in naturally Notch-expressing cells after co-culturing them with ligand –expressing cells, even in the presence of cycloheximide-induced suppression of protein synthesis, establishing those genes as direct targets of Notch signaling.

Abbreviations			Full name	References
Hey1	Hey2	HeyL	Hairy/E(spl)-related with YRPW	168,230
HERP2	HERP1	HERP3	HES-related repressor protein	169,170,171
Hesr1	Hesr2	Hesr3	Hairy/E(spl)-related	231
HRT1	HRT2	HRT3	Hairy-related transcription factor	229
CHF2	CHF1		Cardiovascular helix-loop-helix factor	232
	Gridlock			233

Table 19. Hey family nomenclature. Columns contain synonyms for the same gene.

Structural similarities and differences among HES and Hey families

HES and Hey families of transcription factors share many common structural features (Figure 39). They contain bHLH domain, and another domain, termed the Orange (or helix 3-helix 4) in the corresponding regions carboxy-terminal to bHLH region. The amino acid sequences of these domains are highly conserved within each family, but less so among two different families. The most remarkable difference that distinguishes HES from Hey proteins is a proline residue (P) in the basic region (Figure 39) that is conserved in all HES members from *Drosophila* to human. Hey family has a glycine (G) at the corresponding position (Figure 39) that is also strictly conserved in all family members. All HES members share the C-terminal tetrapeptide WRPW motif, whereas the Hey family has YRPW or its variants. Hey family has an additional conserved region carboxyl-terminal to the tetrapeptide motif, TE(V/I)GAF, which is absent in HES.

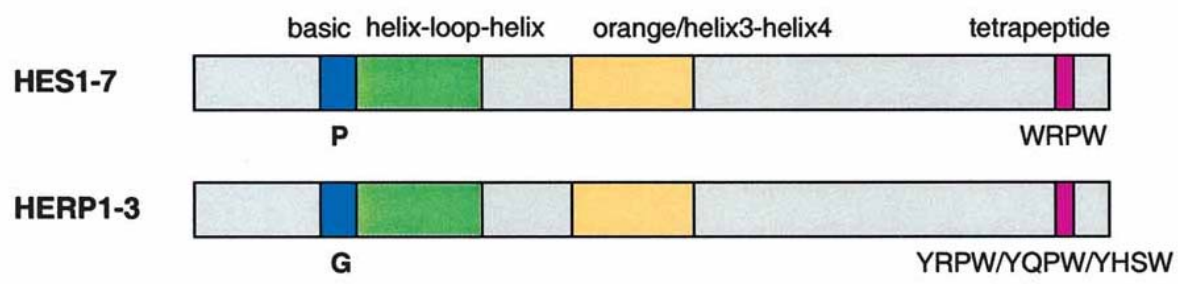

Figure 39. Schematic diagram of HES and Hey proteins structure. Iso *et al.*, 2003[171].

Repression mechanisms of the HES and Hey families

HES and Hey proteins form a distinct subgroup in the class C of bHLH proteins. They can bind to both a class C (CACGNG) and N box (CACNAG) consensus sites, and to some degree to a class B consensus site (CANCTG), and they function as transcriptional repressors (reviewed in Iso *et al.*, 2003[171]). Although HES and Hey families have similar domains, they appear to use different repression mechanisms.

Three mechanisms of transcriptional repression used by the HES family have been proposed. First mechanism is DNA-binding-dependent transcriptional repression, also known as active repression[234]. HES proteins form a homodimer and bind class C or N box consensus DNA sites. They recruit co-repressor Groucho or its mammalian homologue TLE (transducin-like enhancer of split) via the C-terminal WRPW motif. This motif is both necessary and sufficient to confer repression, when expressed as a fusion protein with a heterologous DNA binding domain of Gal4 (reviewed in Iso *et al.*, 2003[171]). In Drosophila, it was shown that Groucho can recruit the histone deacetylase (HDAC) Rpd3, an ortologue of mammalian HDAC[235]. The histone deacetylase then may repress transcription by altering local chromatin structure. Whether mammalian TLE employs the same mechanism remains to be determined.

The second mechanism is a passive repression involving protein sequestration. For instance, HES1 can form a non-functional heterodimer with other bHLH factors such as E47, a common heterodimer partner of tissue-specific bHLH factors such as MyoD and Mash1, thereby disrupting the formation of functional heterodimers such as MyoD-E47 and Mash1-E47[236].

The third mechanism is mediated by the Orange/helix3-helix4 domain[237]. The authors have shown that the Orange domain of HES1 is essential to repress transcription of its own promoter, as well as the $p21^{WAF}$ promoter in PC12 cells. The repression is functional in the absence of WRPW motif, however, it requires the presence of DNA-binding bHLH motif. Orange domain cannot repress transcription when fused to heterologous, Gal4 DNA binding motif.

A study using Hey2 deletion mutants fused with the Gal4-DNA binding domain unexpectedly revealed that the repression activity of Hey family resides primarily in the bHLH domain rather than C-terminal tetrapeptide (YQPW) motif[238]. The bHLH domain of Hey2 is both necessary and sufficient for recruitment of a co-repressor complex including N-CoR, mSin3A, and HDAC. Thus, despite similarities of their domains, HES and Hey appear to employ different repression mechanisms involving

heterologous sets of corepressor proteins-Groucho/TLE for HES and N-CoR/mSin3A/HDAC for Hey.

Passive repression mechanisms have also been proposed for members of Hey family. It was shown[172] that Hey1 (CHF2) inhibits MyoD-dependent transcription of the myogenin promoter as well as muscle conversion, by forming a complex with MyoD and disturbing the binding of MyoD-E47 heterodimer to the E-box binding site. This repression activity of Hey1 (CHF2) mapped to a hydrophobic carboxyl-terminal region containing the Orange domain and did not require either the bHLH domain or YRPW motif.

In conclusion, despite very high structural similarity between HES and Hey family members, they are using distinct repression mechanisms in repressing the expression of target genes.

HES and Hey proteins also associate with each other in solution and form stable HES-Hey heterodimer upon DNA binding. HES-Hey heterodimers have both a greater DNA binding activity and a stronger repression activity then do the respective homodimers[238]. In tissues where HES and Hey proteins are co-expressed, HES-Hey heterodimer may be a predominant repression complex that binds DNA with greater affinity and is able to recruit a more diverse set of co-repressor.

In vivo role of HES and Hey proteins

Except for few cases *in vivo* target genes for HES and Hey family have not been firmly established. Disruption of HES1 in mice is shown to up-regulate expression of neural differentiation factor Mash1 and other neural HLH factors, confirming the role of HES1 as a natural transcriptional inhibitor of these genes[239]. Identification of target genes for HES and Hey homodimers, as well as HES-Hey heterodimers is among the most important issues to be addressed in future.

Hey family is involved in multiple aspects of vascular development including smooth muscle differentiation, angiogenic processes, arterial-venous cell fate determination, and vascular morphogenesis (reviewed in Iso *et al.*, 2003, Sun *et al.*, 2001[171,172]). Hey2 role is of particular importance for vascular system development. Hey2 KO mice have severe heart defects, ventricular septal defect and cardiomiopathy[240], while in zebrafish, the gridlock mutation (grl^{m145}), homolog of Hey2, shows an abnormal assembly of the aorta[233]. Hey1 knockout mice has no apparent phenotypic defect; however, double Hey1/Hey2 knockout mice show a major defect in embryonic

vascular development, that leads to embryonic death at day 9.5[241]. Since expression of members of HES family has not been observed in the vascular system, these data together suggest that Hey family members are main Notch effectors in vascular development.

Members of HES and Hey family also play a crucial role in somitogenesis, and gliogenesis, while inhibiting neurogenesis (reviewed in Iso *et al.*, 2003[171]). Recent data also suggest that the members of the HES and Hey family play a role in differentiation of various lineages derived from mesenchymal stem cells, myoblasts, adipocytes, and, lately, osteoblasts.

4.1.3 Role of Notch signaling pathway and Hey1 transcription factor in osteogenesis

Initially, Notch pathway was linked to bone biology by observations that mutations in the genes encoding a Notch ligand Delta homologue (Dll-3) and a Notch signaling molecule presenilin-1 both cause axial skeletal phenotypes[182,183]. Recently it was shown that generation of haematopoietic stem cells in bone marrow is supported by activation of Notch pathway by a ligand Jagged1, produced by osteoblasts, pointing to a Notch-mediated functional interaction between bone and bone marrow[184]. Different labs demonstrated expression of Notch 1 and 2 and the Notch ligands Delta 1 and Jagged 1 in osteoblasts[242,243]. Several studies investigating effects of Notch signaling in different models of osteoblast differentiation process, all of which used exogenous overexpression of the constitutively active Notch1 intracellular domain[160,161,244]. Two studies reported inhibition of osteoblast differentiation by constitutive expression of Notch intracellular domain[161,244], while one reported stimulation of differentiation process[160]. However, this stimulation occurred very late, after expression of NICD became undetectable, and was preceded by inhibition of differentiation markers, e.g. osteocalcin mRNA level. Given the tight regulation that maintains native NICD at an extremely low concentration, the physiological relevance of these controversial findings was unclear. The question on the role, if any, of endogenous Notch signaling in osteoblast differentiation process remained open.

Recently we reported strong induction of Hey1 gene in osteoblasts in BMP-2 stimulated differentiation[245]. Hey1 mRNA was strongly and quickly, one day after the

stimulation, up-regulated upon BMP-2 stimulation in MC3T3 osteoblastic cells, C2C12 myogenic cells, and mesenchymal stem cells. High Hey1 endogenous expression was detected in mouse calvarias. In MC3T3 cells, Hey1 was induced 1 day after stimulation, and mRNA level stayed high as long as the measurements were made, up to day 4. Hey1 expression was selectively regulated by BMP-2, not being induced by other modulators of differentiation process, ascorbic acid[245], or TGFβ1[246] (and our unpublished observation). These findings prompted us to investigate the mechanism and the role of Hey1 induction. By blocking Hey1 induction in MC3T3 osteoblasts using Hey1 specific siRNA, we have shown that inhibition of Hey1 induction leads to increased bone nodule formation. This finding highlighted Hey1 gene as a negative regulator of osteoblast differentiation process.

Recent studies confirmed that Hey1 is induced by BMP-2 in C2C12 cells[222]. By studying short time points after stimulation, they showed that Hey1 belongs to late early genes induced by BMP-2, being up-regulated only after 24 h. BMP-2 stimulation in the presence of cyclohexamide showed that Hey1 induction is partly, but not completely dependent on de novo protein synthesis, indicating that there might be more than one mechanism of Hey1 induction.

What is the mechanism of Hey1 induction? Recent data have confirmed that Hey1 is the direct target gene of Notch signaling pathway in many different systems (reviewed in Iso *et al.*, 2003[171]) and we argue that Notch signaling is necessary for Hey1 induction by BMP-2. Experiments with blocking Notch signaling, for example by inhibitors of γ-secretase, which prevent cleavage and release of Notch intracellular domain upon ligand binding[218], or by dominant negative NICD transfection, could confirm this hypothesis, and this is the subject of our current studies. An open question is how is Notch pathway activated by BMP-2 stimulation? Very recent data show the cross-talk between Notch and BMP signaling pathways that leads to Hey1 activation. Functional Notch signaling is shown to be necessary for BMP-2-dependent Hey1 induction in myogenic[190] and endothelial cells[191]. These studies showed that synergistic effect on the Hey1 promoter is mediated via RBP-Jk binding sites and GC-rich binding sites, which are potential SMAD-binding sites. Interaction between NICD and SMAD further potentiates Hey1 promoter activation. This interaction is further enhanced by transcriptional coactivator p/CAF, which was shown to interact both with NICD and SMAD proteins[191]. Upon BMP-2 stimulation, endogenous Notch signal that exists between neighboring cells expressing Notch

receptor and a Notch ligand is strong enough to participate in activation of Hey1 by BMP-2. However, the ultimate effect of Notch and BMP-2 signal in myogenic and endothelial cells is different: in myogenic cells they synergistically inhibit myogenic differentiation; while in endothelial cells they antagonize each other's effect on cell migration. In myogenic cells Hey1 binds to and inhibits MyoD, master factor of myogenic differentiation[172]. In endothelial cells, BMP-2 up-regulates Id1 to promote migration and Hey1 antagonizes this migration by targeting Id1 for degradation[191]. In myogenic cells, the level of Id1 was stable despite an increase in Hey1 expression, indicating a high specificity of Hey1 action in different cell types. Therefore, the potentiation of Notch signaling by interaction of NICD with activated SMAD proteins could be the explanation of Hey1 induction in osteoblastic cells.

Our preliminary experiments (Chapter 2.3) with blocking Notch receptor activation by using the γ-secretase inhibitor suggest that, unlike in other cellular systems studied, activated Notch receptor does not play a major role in BMP-2-induced Hey1 activation in MC3T3 osteoblastic cells. Further experiments are required to confirm this finding. If only a minimal amount of NICD would be enough to participate in Hey1 induction, Notch signalling may still participate in Hey1 activation. We can not exclude the possibility that Notch signal was not completely blocked by γ-secretase inhibitor. This finding opens the possibility that in osteoblastic cells other mechanisms beside the Notch receptor activation play a major role in upregulation of Hey1, a Notch effector gene, and ultimately produce the phenotype identical to Notch receptor activation.

As the effect of Hey1 is cell-type specific, as seen in myogenic[172] and endothelial cells[191], the question is: what is the mechanism by which Hey1 inhibits differentiation process specifically in osteoblasts?

Hey family members are bHLH transcriptional repressors, which inhibit transcription by either binding to DNA and recruiting co-repressors[238], or by forming inactive complexes with other transcription factors. As Hey1 is reported to inhibit myogenic differentiation by binding to and inactivating master regulator of myogenesis, MyoD [172], we investigated a possible influence of Hey1 on the master regulator of osteogenesis Runx2, which coordinates multiple signals involved in osteoblast differentiation [83]. In a co-transfection assay, Hey1 co-expression almost completely abolished Runx2 transcriptional activity, indicating that at least one of the

mechanisms of Hey1 repression of differentiation is to block Runx2-induced transcription.

So far, few transcription factors were shown to form inhibitory complexes with Runx2, and to inhibit osteoblast differentiation: Stat1[92], and Twist[22]. Latent, non-phosphorylated form of Stat-1 interacts with Runx2 in the cytoplasm, thereby inhibiting its nuclear localization and activation of transcription. Interaction between those two transcription factors is made by their respective DNA-binding domains: DNA binding domain (DBD) and linker domain of STAT1 and *runt* domain of Runx2. In the Stat1-/- mice, loss of inhibition of Runx2 activity results in the increased bone mass in the adult knockout mice. However, bone formation during developmental period is not affected, suggesting that Stat1 is selectively involved in the Runx2 regulation in bone remodeling at the postnatal stage[92]. On the other hand, bHLH transcription factors Twist 1 and 2 are shown to transiently inhibit Runx2 function during skeletogenesis. This interaction is mediated by a novel domain, the Twist box, which interacts with Runx2 Runt domain. In embryonic development, Twist-1 and -2 are expressed in Runx2 expressing cells throughout the skeleton early during development, and osteoblast-specific gene expression occurs only when their expression decreases[22].

Our result showing that Hey1 can almost completely abrogate Runx2 transcriptional activity indicates that Hey1 is a novel inhibitory partner of Runx2. It would be interesting to show which stage of skeletal modeling or remodeling process is affected by Hey1. de Jong *et al.*, 2004 have shown that during skeletal development Hey1 expression partly, but significantly overlaps with the expression of Runx2. However, Hey1 knockout mice had no apparent phenotypic defect, including no big skeletal abnormalities[241]. It is tempting to speculate that Hey1 inhibition does not have major importance in the skeletogenesis and that it could be more important in the bone remodeling process during adult life. Thus, it would be very interesting to investigate bone phenotype in detail in aging Hey1 knockout mice.

Could we speculate if Hey1 inhibition of Runx2 transcriptional activity will have ultimate positive or negative effect on the bone formation rate? On a first glance, Stat1 example suggests that in the absence of Runx2 inhibition by Hey1, bone formation would be increased. Nevertheless, faster osteoblast differentiation does not always mean more bone. It is known that *in vivo* TGFβ administration results in increased osteoprogenitor proliferation and new bone formation[247,248]. In vitro,

however, TGFβ inhibits osteoblast differentiation markers, including alkaline phosphatase activity, osteocalcin expression, and bone nodule formation[249], while it has stimulatory effect on osteoprogenitor proliferation[247,248] and migration[250]. In the knockout mice of Smad3 transcription factor, an intracellular effector of TGFβ pathway, decreased rate of bone formation is observed, with increased osteocyte number and apoptosis. In a Smad 3 knockout mice, TGFβ inhibition of osteoblast differentiation is lost, osteoblast lifespan is shortened, ultimately resulting in osteopenia[251]. Transgenic Runx2 mice are also reported to develop osteopenia due to decreased number of finally differentiated osteoblasts[252], or increased osteoclast-stimulating properties of differentiating osteoblasts[253]. In vitro, however, overexpression of Runx2 leads to increased expression of osteoblast markers[254]. Hey1 inhibition of Runx2 could be the mechanism of slowing-down the differentiation process, keeping the cells longer in active, matrix-producing state. Notch signaling pathway activation is shown to inhibit haematopoietic stem cells differentiation and increase their growth, keeping the pool of precursor cells[184]. Therefore, only in vivo analyses could show if the activation of Notch pathway in osteoblasts leads to increased or decreased bone mass. It would be also interesting to examine later time points in the differentiation process, to see if Hey1 induction is transient and whether it ultimately releases Runx2 from its inhibition.

Another interesting topic to investigate is a mode of interaction between Hey and Runx2. It would be interesting to determine the regions responsible for the interaction. DNA binding *runt* domain of Runx2 is shown to be responsible for its interaction with Stat1 and Twist, but only deletion mutants analysis can give answer whether the same region interact with Hey1.

4.1.4 Role of Notch signaling pathway and Hey1 transcription factor in mesenchymal cells differentiation

There is a substantial amount of *in vitro* data showing that Notch signaling inhibits myogenic cells differentiation and that Hey1 transcription factor is likely the principal mediator of this effect. Co-culture of C2C12 myoblast cells with Notch ligand-expressing cells blocks muscle differentiation by inhibiting expression of muscle differentiation markers such as myogenin, myosin light chain 1, 2 and 3, α-myoglobin, troponin T and MyoD[255,256,257,258]). Notch-ligand stimulation induces strong

and continuous Hey1 mRNA expression in C2C12 cells[169], whereas HES1 mRNA expression is only weakly and transiently induced in these cells[169,255]. These findings suggested that Hey1 plays a more important role than HES1 in inhibiting myogenic differentiation. To support this idea, Sun *et al.*, 2001 showed that Hey1 mRNA is expressed at high levels in undifferentiated C2C12 myoblasts, while its level declines as differentiation process proceeds. Overexpression of Hey1 inhibited MyoD-induced myogenic conversion of 10T1/2 cells, by associating with MyoD and inhibiting DNA binding activity of MyoD-E47 heterodimers[172].

Co-culture of 3T3-L1 pre-adipocytes with cells expressing Notch ligand or constitutive expression of HES1 transcription factor blocked differentiation process by suppressing the induction of adipocyte markers C/EBPα and peroxisome proliferator-activated receptor γ (PPARγ2)[259]. This block could be overcome by retroviral expression of either of these transcription factors, suggesting that HES1 does not affect the activity of either of these factors directly, but probably some upstream, yet non-identified factor. Surprisingly, the authors have noticed that siRNA-mediated reduction of HES1 mRNA also inhibited differentiation. HES1 down-regulates transcription of DLK/Pref-1, a secreted protein known to inhibit differentiation of 3T3-L1 cells by unknown mechanism [260]. Therefore, the authors have proposed the mechanism of dual action of HES1 in adipocyte differentiation: it is required in early stages, to down regulate the expression of inhibitors. However, later, HES1 level must decline to allow upregulation of PPARγ and C/EBPα and to differentiation process to continue.

These data, together with our finding that Hey1 induction inhibits osteoblastogenesis, suggest that Notch pathway activation could be a general inhibitory mechanism of mesenchymal cells differentiation. The principal mediators of Notch activation would be either Hey1, in myogenesis and osteoblastogenesis, or HES1 in adipogenesis. The means of differentiation process inhibition are also cell-type specific. What could be the physiological meaning of this, *in vitro* observed, inhibition?

Recent finding offers an exciting possibility as an answer. Conboy *et al.*, 2002 have studied the regeneration process of the skeletal muscle in response to injury. The primary cellular constituents of mature muscle, responsible for the regenerative potential, are the satellite cells. These are quiescent mononuclear cells, defined by their location adjacent to mature myofibers, but beneath the basal lamina that surrounds them. When activated by stimuli, such as muscle injury or exercise,

satellite cells begin to proliferate and to commit to a myoblast cell fate, defined by the expression of certain myogenic regulatory factors (MRFs) and lineage markers, such as MyoD or desmin, and by the fusion to nascent myotubes[261]. Such cells must have a tremendous proliferative potential and must have some capacity for asymmetric cell division to allow for self-renewal of satellite cells to maintain the precursor pool. To investigate further this issue, the authors have developed an *ex vivo* myofiber explant system, which allows culturing isolated myofibers and mimics an injury of skeletal muscle *in vivo* with respect to progenitor satellite cells activation and proliferation. They have studied the role of Notch-1 and its inhibitor Numb in the activation of satellite cells. Numb is an inhibitor of Notch signaling that interacts with the intracellular portion of Notch and antagonizes its activity by preventing nuclear translocation (Figure 38). Using immunoblotting and immunohistochemical analysis, they show that Notch-1 becomes activated in proliferating satellite cells in vitro and in vivo in a muscle after injury. Numb was present initially, its level decreased over the first 24 h, and then increased again with time ex vivo. Immunostaining for Numb in activated satellite cells showed asymmetrical localization in actively dividing cells, suggesting an asymmetric cell division and divergent cell fate of daughter cells. By a series of experiments with overexpressing Notch-1 or Numb or attenuating their function by siRNA in muscle progenitor cells, authors further proved that enhanced Notch signaling promoted the proliferation of myogenic precursor cells expressing the premyoblast marker Pax3. Attenuation of Notch signaling by increase in Numb expression led to the commitment of progenitor cells to the myoblast cell fate and the expression of myogenic regulatory factors, desmin, and Pax7, markers of differentiation process. These data proved that, upon injury, Notch signaling is activated in satellite cells and that it enhances their proliferation. The expansion of muscle progenitor cells is also accompanied by the upregulation of Numb, which, by localizing asymmetrically in dividing myogenic progenitor cells, gives rise to a heterogeneous population of cells with respect to the levels of Notch-1 signaling activity: cells with high Notch activity, witch continue to proliferate, and cells with high level of Numb, Notch inhibitor, which start the differentiation process.

In a following exciting paper, Conboy *et al.*, 2003 showed that diminished regenerative potential of aged muscle is due to insufficient up-regulation of the Notch ligand Delta on the site of injury, and thus, diminished activation of Notch in satellite cells of aged regenerating muscle. Inhibition of Notch led to an impaired regeneration

of young muscle, while forced activation of Notch restored regenerative potential to old muscle. Thus, Notch signaling is a key determinant of muscle regenerative potential that declines with age.

In a light of knowledge that Notch signaling *in vitro* function as an inhibitor of differentiation process of other mesenchymal cells types, specifically osteoblasts, could we speculate that it would be possible that Notch signal could be a general mechanism for controlling the balance between differentiating cells and maintaining the precursor pool? The processes analog to muscle regeneration in bone are: a) bone remodeling, a physiological process that repeats periodically throughout our life (described in detail in Introduction), and b) fracture healing. How are osteoprogenitor cells stimulated to differentiate? It is not easy to study this process, because, unlike muscle progenitor cells, osteoprogenitor cells are difficult to distinguish morphologically or by their position. The *in vivo* stimulus for start of proliferation and differentiation process is not well characterized either because of extremely complicated control of bone remodeling process, that is regulated by number of systemic hormones and local factors. However, the plausible candidates are obviously growth factors from BMP family. *In vitro*, osteogenic members of BMP family are most potent inducers of osteoblast differentiation[23]. Postnatally, substantial amount have been found only in bone matrix, from where they have been initially isolated, identified by their ability to induce ectopic bone formation when injected into rat muscle[46]. However, there is little evidence of the physiological roles of endogenous BMPs in bone formation, since mice deficient in BMPs and the receptors so far reported were normal or exhibited abnormalities in skeletal patterning or morphogenesis unless they died during embryonic development[262]. Recent abstracts indicated, by using conditional knockout mice for one of the osteogenic BMP, BMP4, or double deficient mice for BMP2 and BMP6 (BMP-2+/-, BMP6-/-), that these members of BMP family have important role in bone formation and remodeling, since those mice develop osteopenia due to impaired osteoblast function[263,264,265]. BMP stimulation of osteprogenitor cells at the same time could induce enhancement of Notch signaling to Hey1, based on our results and data from endothelial and myogenic cells. The induction of Hey1 could be a negative feedback mechanism that keeps the cells in the proliferative, progenitor state for longer periods of time. If that is true, mechanism analogous to expression of Notch inhibitor, Numb, could exist in osteoblast cells to allow a pool of the cells to exit the proliferative phase and finish

the differentiation process. We did not detect the Numb mRNA expression in MC3T3 osteoblastic cells by microarray analysis (our unpublished observation), a result that would need confirmation by another method. However, we did detect strong downregulation of Notch-1 and Notch-3 receptors, and NOV, gene involved in enhancing Notch signal[245], which could happen in the osteoblasts in vivo in the later stages of differentiation, during their migration towards bone surface and synthesis of bone matrix. This hypothesis opens the exciting possibility that, analogous to haematopoietic stem cells[184] and myogenic cells[261,266] Notch pathway would be the mechanism for maintenance or enlargement of the progenitor state of osteogenic cells. Whether the asymmetry of this process, observed in the myogenic cells, could exist in the osteogenic cells as well, or whether it is a general mechanism that would keep the cells longer in the proliferative state, giving as an ultimate result more osteoblasts, are the possibilities worthy of investigation .

Finally, could the Notch pathway in osteoblasts be a plausible drug target? If the hypothesis that Notch pathway activation increases the number of progenitor osteoblastic cells is true, it opens an exciting possibility for improving the state of osteoporotic patients or enhance the fracture healing process by stimulating Notch pathway and increasing the pool of progenitor cells. This hypothesis becomes even more interesting in the light of a possibility to simultaneously increase the regenerative potential of the muscles in elderly patients. It should be pointed that the involvement of Notch pathway in many processes in the organism would make its systemic stimulation risky, with unknown consequences. Notch signaling is reported to be activated in several cases of human cancer (reviewed in Nam *et al.*, 2002[267]). *Ex vivo* growing of patient's osteoprogenitor cells for using them in fracture healing therapy would be another possibility. Osteoprogenitor cells could be obtained from mesenchymal stem cells from peripheral blood, directed to osteoblastic phenotype by BMP stimulation and kept in proliferative state by stimulation of Notch pathway. The unique characteristic of Notch pathway to keep the organism "younger" by being involved in self-renewal of increasing number of stem cells will certainly remain an interesting field of basic and clinical research in the future.

5 Abbreviations

AA – ascorbic acid

ALP – alkaline phosphatase

bHLH – basal helix-loop-helix

BMP-2 - bone morphogenic protein 2

EDTA - ethylenediaminetetraacetic acid

EST – expressed sequence tag

GAPDH - glyceraldehyde-3-phosphate dehydrogenase

GP – beta glycerol phosphate

HES - Hairy and Enhancer of Split

Hey1 - Hairy and Enhancer of Split-related with YRPW motive 1

HLH – helix-loop-helix

hMSC – human mesenchymal stem cells

LEF1 - lymphoid enhancer binding factor 1

LRP5 – low-density lipoprotein receptor related protein 5

M-CSF - macrophage colony-stimulating factor

MSC – mesencymal stem cells

OSE2 – osteoblast specific element 2

PBS – phosphate buffered saline

PTH – parathyroid hormone

qrRT-PCR – quantitative radioactive reverse transcription-polymerase chain reaction

RAMP1 - receptor (calcitonin) activity modifying protein 1

RANK - receptor for activation of nuclear factor kappa B (NF-κB)

RANKL - receptor for activation of nuclear factor kappa B (NF-κB) (RANK) ligand

Runx2 – runt-related transcription factor 2

siRNA - small interfering RNA

Smad - MAD, mothers against decapentaplegic homolog

Tcf7 - transcription factor 7, T-cell specific

TGF-β - transforming growth factor beta

Wnt – wingless-type MMTV integration site family

6 References

1 Ehrlich, P. J.; Lanyon, L. E. Mechanical Strain and Bone Cell Function: a Review. *Osteoporos. Int.* **2002,** *13,* 688-700.

2 Udagawa, N.; Takahashi, N.; Akatsu, T.; Tanaka, H.; Sasaki, T.; Nishihara, T.; Koga, T.; Martin, T. J.; Suda, T. Origin of Osteoclasts: Mature Monocytes and Macrophages Are Capable of Differentiating into Osteoclasts Under a Suitable Microenvironment Prepared by Bone Marrow-Derived Stromal Cells. *Proc. Natl. Acad. Sci. U. S. A* **1990,** *87,* 7260-7264.

3 Lacey, D. L.; Timms, E.; Tan, H. L.; Kelley, M. J.; Dunstan, C. R.; Burgess, T.; Elliott, R.; Colombero, A.; Elliott, G.; Scully, S.; Hsu, H.; Sullivan, J.; Hawkins, N.; Davy, E.; Capparelli, C.; Eli, A.; Qian, Y. X.; Kaufman, S.; Sarosi, I.; Shalhoub, V.; Senaldi, G.; Guo, J.; Delaney, J.; Boyle, W. J. Osteoprotegerin Ligand Is a Cytokine That Regulates Osteoclast Differentiation and Activation. *Cell* **1998,** *93,* 165-176.

4 Teitelbaum, S. L. Bone Resorption by Osteoclasts. *Science* **2000,** *289,* 1504-1508.

5 Rodan, G. A.; Martin, T. J. Therapeutic Approaches to Bone Diseases. *Science* **2000,** *289,* 1508-1514.

6 Cooper, C. Epidemiology of Osteoporosis. In *Primer on the Metabolic Bone Diseases and Disorders of Mineral Metabolism*; Favus, M. J., Ed.; American Society for Bone and Mineral Research: Washington,D.C., 2003; Chapter 49.

7 Wasnich, R. D. Epidemiology of Osteoporosis in the United States of America. *Osteoporos. Int.* **1997,** *7 Suppl 3,* S68-S72.

8 Missbach, M.; Jeschke, M.; Feyen, J.; Muller, K.; Glatt, M.; Green, J.; Susa, M. A Novel Inhibitor of the Tyrosine Kinase Src Suppresses Phosphorylation of Its Major Cellular Substrates and Reduces Bone Resorption in Vitro and in Rodent Models in Vivo. *Bone* **1999,** *24,* 437-449.

9 Neer, R. M.; Arnaud, C. D.; Zanchetta, J. R.; Prince, R.; Gaich, G. A.; Reginster, J. Y.; Hodsman, A. B.; Eriksen, E. F.; Ish-Shalom, S.; Genant, H. K.; Wang, O.; Mitlak, B. H. Effect of Parathyroid Hormone (1-34) on Fractures and Bone Mineral Density in Postmenopausal Women With Osteoporosis. *N. Engl. J. Med.* **2001,** *344,* 1434-1441.

10 Greenspan, S. L. PTH:Clinical aspects. 2004. Advances in Skeletal Anabolic Agents for the Treatment of Osteoporosis, May 24-25 2004, Bethesda, MD, USA.
Ref Type: Conference Proceeding

11 Lian, J. B.; Stein, G. S.; Aubin, J. E. Bone Formation: Maturation and Functional Activities of Osteoblast Lineage Cells. In *Primers on the Metabolic Bone Diseases and Disorders of Mineral Metabolism*; Favus, M. J., Ed.; American Society for Bone and Mineral Research: Waschington, D.C., 2003; Chapter 3.

12 Jeon, M. J.; Kim, J. A.; Kwon, S. H.; Kim, S. W.; Park, K. S.; Park, S. W.; Kim, S. Y.; Shin, C. S. Activation of Peroxisome Proliferator-Activated Receptor-Gamma Inhibits the Runx2-Mediated Transcription of Osteocalcin in Osteoblasts. *J. Biol. Chem.* **2003,** *278,* 23270-23277.

13 Lecka-Czernik, B.; Gubrij, I.; Moerman, E. J.; Kajkenova, O.; Lipschitz, D. A.; Manolagas, S. C.; Jilka, R. L. Inhibition of Osf2/Cbfa1 Expression and Terminal Osteoblast Differentiation by PPARgamma2. *J. Cell Biochem.* **1999,** *74,* 357-371.

14 Park, S. R.; Oreffo, R. O.; Triffitt, J. T. Interconversion Potential of Cloned Human Marrow Adipocytes in Vitro. *Bone* **1999,** *24,* 549-554.

15 Huss, R.; Lange, C.; Weissinger, E. M.; Kolb, H. J.; Thalmeier, K. Evidence of Peripheral Blood-Derived, Plastic-Adherent CD34(-/Low) Hematopoietic Stem Cell Clones With Mesenchymal Stem Cell Characteristics. *Stem Cells* **2000,** *18,* 252-260.

16 Kuznetsov, S. A.; Mankani, M. H.; Gronthos, S.; Satomura, K.; Bianco, P.; Robey, P. G. Circulating Skeletal Stem Cells. *J. Cell Biol.* **2001,** *153,* 1133-1140.

17 Erices, A. A.; Allers, C. I.; Conget, P. A.; Rojas, C. V.; Minguell, J. J. Human Cord Blood-Derived Mesenchymal Stem Cells Home and Survive in the Marrow of Immunodeficient Mice After Systemic Infusion. *Cell Transplant.* **2003,** *12,* 555-561.

18 Campagnoli, C.; Roberts, I. A.; Kumar, S.; Bennett, P. R.; Bellantuono, I.; Fisk, N. M. Identification of Mesenchymal Stem/Progenitor Cells in Human First-Trimester Fetal Blood, Liver, and Bone Marrow. *Blood* **2001,** *98,* 2396-2402.

19 Shi, S.; Gronthos, S. Perivascular Niche of Postnatal Mesenchymal Stem Cells in Human Bone Marrow and Dental Pulp. *J. Bone Miner. Res.* **2003,** *18,* 696-704.

20 Aubin, J. E.; Liu, F.; Malaval, L.; Gupta, A. K. Osteoblast and Chondroblast Differentiation. *Bone* **1995,** *17,* 77S-83S.

21 Malaval, L.; Liu, F.; Roche, P.; Aubin, J. E. Kinetics of Osteoprogenitor Proliferation and Osteoblast Differentiation in Vitro. *J. Cell Biochem.* **1999,** *74,* 616-627.

22 Bialek, P.; Kern, B.; Yang, X.; Schrock, M.; Sosic, D.; Hong, N.; Wu, H.; Yu, K.; Ornitz, D. M.; Olson, E. N.; Justice, M. J.; Karsenty, G. A Twist Code Determines the Onset of Osteoblast Differentiation. *Dev. Cell* **2004,** *6,* 423-435.

23 Canalis, E.; Economides, A. N.; Gazzerro, E. Bone Morphogenetic Proteins, Their Antagonists, and the Skeleton. *Endocr. Rev.* **2003,** *24,* 218-235.

24 Daluiski, A.; Engstrand, T.; Bahamonde, M. E.; Gamer, L. W.; Agius, E.; Stevenson, S. L.; Cox, K.; Rosen, V.; Lyons, K. M. Bone Morphogenetic Protein-3 Is a Negative Regulator of Bone Density. *Nat. Genet.* **2001,** *27,* 84-88.

25 Kinoshita, A.; Saito, T.; Tomita, H.; Makita, Y.; Yoshida, K.; Ghadami, M.; Yamada, K.; Kondo, S.; Ikegawa, S.; Nishimura, G.; Fukushima, Y.; Nakagomi, T.; Saito, H.; Sugimoto, T.; Kamegaya, M.; Hisa, K.; Murray, J. C.; Taniguchi, N.; Niikawa, N.; Yoshiura, K. Domain-Specific Mutations in TGFB1 Result in Camurati-Engelmann Disease. *Nat. Genet.* **2000,** *26,* 19-20.

26 Erlebacher, A.; Derynck, R. Increased Expression of TGF-Beta 2 in Osteoblasts Results in an Osteoporosis-Like Phenotype. *J. Cell Biol.* **1996,** *132,* 195-210.

27 Dabovic, B.; Chen, Y.; Colarossi, C.; Obata, H.; Zambuto, L.; Perle, M. A.; Rifkin, D. B. Bone Abnormalities in Latent TGF-[Beta] Binding Protein (Ltbp)-3-Null Mice Indicate a Role for Ltbp-3 in Modulating TGF-[Beta] Bioavailability. *J. Cell Biol.* **2002,** *156,* 227-232.

28 Chung, U. I.; Schipani, E.; McMahon, A. P.; Kronenberg, H. M. Indian Hedgehog Couples Chondrogenesis to Osteogenesis in Endochondral Bone Development. *J. Clin. Invest* **2001,** *107,* 295-304.

29 St Jacques, B.; Hammerschmidt, M.; McMahon, A. P. Indian Hedgehog Signaling Regulates Proliferation and Differentiation of Chondrocytes and Is Essential for Bone Formation. *Genes Dev.* **1999,** *13,* 2072-2086.

30 Brunet, L. J.; McMahon, J. A.; McMahon, A. P.; Harland, R. M. Noggin, Cartilage Morphogenesis, and Joint Formation in the Mammalian Skeleton. *Science* **1998,** *280,* 1455-1457.

31 Devlin, R. D.; Du, Z.; Pereira, R. C.; Kimble, R. B.; Economides, A. N.; Jorgetti, V.; Canalis, E. Skeletal Overexpression of Noggin Results in Osteopenia and Reduced Bone Formation. *Endocrinology* **2003,** *144,* 1972-1978.

32 Balemans, W.; Ebeling, M.; Patel, N.; Van Hul, E.; Olson, P.; Dioszegi, M.; Lacza, C.; Wuyts, W.; Van Den, E. J.; Willems, P.; Paes-Alves, A. F.; Hill, S.; Bueno, M.; Ramos, F. J.; Tacconi, P.; Dikkers, F. G.; Stratakis, C.; Lindpaintner, K.; Vickery, B.; Foernzler, D.; Van Hul, W. Increased Bone Density in Sclerosteosis Is Due to the Deficiency of a Novel Secreted Protein (SOST). *Hum. Mol. Genet.* **2001,** *10,* 537-543.

33 Brunkow, M. E.; Gardner, J. C.; Van Ness, J.; Paeper, B. W.; Kovacevich, B. R.; Proll, S.; Skonier, J. E.; Zhao, L.; Sabo, P. J.; Fu, Y.; Alisch, R. S.; Gillett, L.; Colbert, T.; Tacconi, P.; Galas, D.; Hamersma, H.; Beighton, P.; Mulligan, J. Bone Dysplasia Sclerosteosis Results From Loss of the SOST Gene Product, a Novel Cystine Knot-Containing Protein. *Am. J. Hum. Genet.* **2001,** *68,* 577-589.

34 Balemans, W.; Patel, N.; Ebeling, M.; Van Hul, E.; Wuyts, W.; Lacza, C.; Dioszegi, M.; Dikkers, F. G.; Hildering, P.; Willems, P. J.; Verheij, J. B.; Lindpaintner, K.; Vickery, B.; Foernzler, D.; Van Hul, W. Identification of a 52 Kb Deletion Downstream of the SOST Gene in Patients With Van Buchem Disease. *J. Med. Genet.* **2002,** *39,* 91-97.

35 Marie, P. J. Fibroblast Growth Factor Signaling Controlling Osteoblast Differentiation. *Gene* **2003,** *316,* 23-32.

36 Gong, Y.; Slee, R. B.; Fukai, N.; Rawadi, G.; Roman-Roman, S.; Reginato, A. M.; Wang, H.; Cundy, T.; Glorieux, F. H.; Lev, D.; Zacharin, M.; Oexle, K.; Marcelino, J.; Suwairi, W.; Heeger, S.; Sabatakos, G.; Apte, S.; Adkins, W. N.; Allgrove, J.; Arslan-Kirchner, M.; Batch, J. A.; Beighton, P.; Black, G. C.; Boles, R. G.; Boon, L. M.; Borrone, C.; Brunner, H. G.; Carle, G. F.; Dallapiccola, B.; De Paepe, A.; Floege, B.; Halfhide, M. L.; Hall, B.; Hennekam, R. C.; Hirose, T.; Jans, A.; Juppner, H.; Kim, C. A.; Keppler-Noreuil, K.; Kohlschuetter, A.; LaCombe, D.; Lambert, M.; Lemyre, E.; Letteboer, T.; Peltonen, L.; Ramesar, R. S.; Romanengo, M.; Somer, H.; Steichen-Gersdorf, E.; Steinmann, B.; Sullivan, B.; Superti-Furga, A.; Swoboda, W.; van den Boogaard, M. J.; Van Hul, W.; Vikkula, M.; Votruba, M.; Zabel, B.; Garcia, T.; Baron, R.; Olsen, B. R.; Warman, M. L. LDL Receptor-Related Protein 5 (LRP5) Affects Bone Accrual and Eye Development. *Cell* **2001,** *107,* 513-523.

37 Little, R. D.; Carulli, J. P.; Del Mastro, R. G.; Dupuis, J.; Osborne, M.; Folz, C.; Manning, S. P.; Swain, P. M.; Zhao, S. C.; Eustace, B.; Lappe, M. M.; Spitzer, L.; Zweier, S.; Braunschweiger, K.; Benchekroun, Y.; Hu, X.; Adair, R.; Chee, L.; FitzGerald, M. G.; Tulig, C.; Caruso, A.; Tzellas, N.; Bawa, A.; Franklin, B.; McGuire, S.; Nogues, X.; Gong, G.; Allen, K. M.; Anisowicz, A.; Morales, A. J.; Lomedico, P. T.; Recker, S. M.; Van Eerdewegh, P.; Recker, R. R.; Johnson, M. L. A Mutation in the

LDL Receptor-Related Protein 5 Gene Results in the Autosomal Dominant High-Bone-Mass Trait. *Am. J. Hum. Genet.* **2002,** *70,* 11-19.

38 Kato, M.; Patel, M. S.; Levasseur, R.; Lobov, I.; Chang, B. H.; Glass, D. A.; Hartmann, C.; Li, L.; Hwang, T. H.; Brayton, C. F.; Lang, R. A.; Karsenty, G.; Chan, L. Cbfa1-Independent Decrease in Osteoblast Proliferation, Osteopenia, and Persistent Embryonic Eye Vascularization in Mice Deficient in Lrp5, a Wnt Coreceptor. *J. Cell Biol.* **2002,** *157,* 303-314.

39 Raisz, L. G. Potential Impact of Selective Cyclooxygenase-2 Inhibitors on Bone Metabolism in Health and Disease. *Am. J. Med.* **2001,** *110 Suppl 3A,* 43S-45S.

40 Olney, R. C. Regulation of Bone Mass by Growth Hormone. *Med. Pediatr. Oncol.* **2003,** *41,* 228-234.

41 Karaplis, A. C.; Luz, A.; Glowacki, J.; Bronson, R. T.; Tybulewicz, V. L.; Kronenberg, H. M.; Mulligan, R. C. Lethal Skeletal Dysplasia From Targeted Disruption of the Parathyroid Hormone-Related Peptide Gene. *Genes Dev.* **1994,** *8,* 277-289.

42 Schipani, E.; Lanske, B.; Hunzelman, J.; Luz, A.; Kovacs, C. S.; Lee, K.; Pirro, A.; Kronenberg, H. M.; Juppner, H. Targeted Expression of Constitutively Active Receptors for Parathyroid Hormone and Parathyroid Hormone-Related Peptide Delays Endochondral Bone Formation and Rescues Mice That Lack Parathyroid Hormone-Related Peptide. *Proc. Natl. Acad. Sci. U. S. A* **1997,** *94,* 13689-13694.

43 Takeda, S.; Elefteriou, F.; Levasseur, R.; Liu, X.; Zhao, L.; Parker, K. L.; Armstrong, D.; Ducy, P.; Karsenty, G. Leptin Regulates Bone Formation Via the Sympathetic Nervous System. *Cell* **2002,** *111,* 305-317.

44 Ducy, P.; Amling, M.; Takeda, S.; Priemel, M.; Schilling, A. F.; Beil, F. T.; Shen, J.; Vinson, C.; Rueger, J. M.; Karsenty, G. Leptin Inhibits Bone Formation Through a Hypothalamic Relay: a Central Control of Bone Mass. *Cell* **2000,** *100,* 197-207.

45 Jueppner, H.; Kronenberg, H. M. Parathyroid Hormone. In *Primer on the Metabolic Bone Diseases and Disorders of Mineral Metabolism*; Favus, M. J., Ed.; American Society for Bone and Mineral Research: Washington,D.C., 2004.

46 Urist, M. R. Bone: Formation by Autoinduction. 1965. *Clin. Orthop.* **2002,** 4-10.

47 Sakou, T. Bone Morphogenetic Proteins: From Basic Studies to Clinical Approaches. *Bone* **1998,** *22,* 591-603.

48 Watanabe, M.; Whitman, M. The Role of Transcription Factors Involved in TGFbeta Superfamily Signaling During Development. *Cell Mol. Biol. (Noisy. -le-grand)* **1999,** *45,* 537-543.

49 Zhang, Y. W.; Yasui, N.; Ito, K.; Huang, G.; Fujii, M.; Hanai, J.; Nogami, H.; Ochi, T.; Miyazono, K.; Ito, Y. A RUNX2/PEBP2alpha A/CBFA1 Mutation Displaying Impaired Transactivation and Smad Interaction in Cleidocranial Dysplasia. *Proc. Natl. Acad. Sci. U. S. A* **2000,** *97,* 10549-10554.

50 Ducy, P.; Zhang, R.; Geoffroy, V.; Ridall, A. L.; Karsenty, G. Osf2/Cbfa1: a Transcriptional Activator of Osteoblast Differentiation. *Cell* **1997,** *89,* 747-754.

51 Nakashima, K.; Zhou, X.; Kunkel, G.; Zhang, Z.; Deng, J. M.; Behringer, R. R.; de Crombrugghe, B. The Novel Zinc Finger-Containing Transcription Factor Osterix Is Required for Osteoblast Differentiation and Bone Formation. *Cell* **2002,** *108,* 17-29.

52 Otto, F.; Lubbert, M.; Stock, M. Upstream and Downstream Targets of RUNX Proteins. *J. Cell Biochem.* **2003,** *89,* 9-18.

53 Li, Q. L.; Ito, K.; Sakakura, C.; Fukamachi, H.; Inoue, K.; Chi, X. Z.; Lee, K. Y.; Nomura, S.; Lee, C. W.; Han, S. B.; Kim, H. M.; Kim, W. J.; Yamamoto, H.; Yamashita, N.; Yano, T.; Ikeda, T.; Itohara, S.; Inazawa, J.; Abe, T.; Hagiwara, A.; Yamagishi, H.; Ooe, A.; Kaneda, A.; Sugimura, T.; Ushijima, T.; Bae, S. C.; Ito, Y. Causal Relationship Between the Loss of RUNX3 Expression and Gastric Cancer. *Cell* **2002,** *109,* 113-124.

54 Komori, T.; Yagi, H.; Nomura, S.; Yamaguchi, A.; Sasaki, K.; Deguchi, K.; Shimizu, Y.; Bronson, R. T.; Gao, Y. H.; Inada, M.; Sato, M.; Okamoto, R.; Kitamura, Y.; Yoshiki, S.; Kishimoto, T. Targeted Disruption of Cbfa1 Results in a Complete Lack of Bone Formation Owing to Maturational Arrest of Osteoblasts. *Cell* **1997,** *89,* 755-764.

55 Otto, F.; Thornell, A. P.; Crompton, T.; Denzel, A.; Gilmour, K. C.; Rosewell, I. R.; Stamp, G. W.; Beddington, R. S.; Mundlos, S.; Olsen, B. R.; Selby, P. B.; Owen, M. J. Cbfa1, a Candidate Gene for Cleidocranial Dysplasia Syndrome, Is Essential for Osteoblast Differentiation and Bone Development. *Cell* **1997,** *89,* 765-771.

56 Mundlos, S.; Otto, F.; Mundlos, C.; Mulliken, J. B.; Aylsworth, A. S.; Albright, S.; Lindhout, D.; Cole, W. G.; Henn, W.; Knoll, J. H.; Owen, M. J.; Mertelsmann, R.; Zabel, B. U.; Olsen, B. R. Mutations Involving the Transcription Factor CBFA1 Cause Cleidocranial Dysplasia. *Cell* **1997,** *89,* 773-779.

57 Ducy, P.; Starbuck, M.; Priemel, M.; Shen, J.; Pinero, G.; Geoffroy, V.; Amling, M.; Karsenty, G. A Cbfa1-Dependent Genetic Pathway Controls Bone Formation Beyond Embryonic Development. *Genes Dev.* **1999,** *13,* 1025-1036.

58 Sato, M.; Morii, E.; Komori, T.; Kawahata, H.; Sugimoto, M.; Terai, K.; Shimizu, H.; Yasui, T.; Ogihara, H.; Yasui, N.; Ochi, T.; Kitamura, Y.; Ito, Y.; Nomura, S. Transcriptional Regulation of Osteopontin Gene in Vivo by PEBP2alphaA/CBFA1 and ETS1 in the Skeletal Tissues. *Oncogene* **1998,** *17,* 1517-1525.

59 Kern, B.; Shen, J.; Starbuck, M.; Karsenty, G. Cbfa1 Contributes to the Osteoblast-Specific Expression of Type I Collagen Genes. *J. Biol. Chem.* **2001,** *276,* 7101-7107.

60 Selvamurugan, N.; Chou, W. Y.; Pearman, A. T.; Pulumati, M. R.; Partridge, N. C. Parathyroid Hormone Regulates the Rat Collagenase-3 Promoter in Osteoblastic Cells Through the Cooperative Interaction of the Activator Protein-1 Site and the Runt Domain Binding Sequence. *J. Biol. Chem.* **1998,** *273,* 10647-10657.

61 Levanon, D.; Groner, Y. Structure and Regulated Expression of Mammalian RUNX Genes. *Oncogene* **2004,** *23,* 4211-4219.

62 Ogawa, E.; Inuzuka, M.; Maruyama, M.; Satake, M.; Naito-Fujimoto, M.; Ito, Y.; Shigesada, K. Molecular Cloning and Characterization of PEBP2 Beta, the Heterodimeric Partner of a Novel Drosophila Runt-Related DNA Binding Protein PEBP2 Alpha. *Virology* **1993,** *194,* 314-331.

63 Ogawa, E.; Maruyama, M.; Kagoshima, H.; Inuzuka, M.; Lu, J.; Satake, M.; Shigesada, K.; Ito, Y. PEBP2/PEA2 Represents a Family of Transcription Factors Homologous to the Products of the Drosophila Runt Gene and the Human AML1 Gene. *Proc. Natl. Acad. Sci. U. S. A* **1993,** *90,* 6859-6863.

64 Xiao, Z. S.; Thomas, R.; Hinson, T. K.; Quarles, L. D. Genomic Structure and Isoform Expression of the Mouse, Rat and Human Cbfa1/Osf2 Transcription Factor. *Gene* **1998,** *214,* 187-197.

65 Harada, H.; Tagashira, S.; Fujiwara, M.; Ogawa, S.; Katsumata, T.; Yamaguchi, A.; Komori, T.; Nakatsuka, M. Cbfa1 Isoforms Exert Functional Differences in Osteoblast Differentiation. *J. Biol. Chem.* **1999,** *274,* 6972-6978.

66 Thirunavukkarasu, K.; Mahajan, M.; McLarren, K. W.; Stifani, S.; Karsenty, G. Two Domains Unique to Osteoblast-Specific Transcription Factor Osf2/Cbfa1 Contribute to Its Transactivation Function and Its Inability to Heterodimerize With Cbfbeta. *Mol. Cell Biol.* **1998,** *18,* 4197-4208.

67 Choi, J. Y.; Pratap, J.; Javed, A.; Zaidi, S. K.; Xing, L.; Balint, E.; Dalamangas, S.; Boyce, B.; van Wijnen, A. J.; Lian, J. B.; Stein, J. L.; Jones, S. N.; Stein, G. S. Subnuclear Targeting of Runx/Cbfa/AML Factors Is Essential for Tissue-Specific Differentiation During Embryonic Development. *Proc. Natl. Acad. Sci. U. S. A* **2001,** *98,* 8650-8655.

68 Xiao, Z. S.; Hjelmeland, A. B.; Quarles, L. D. Selective Deficiency of the "Bone-Related" Runx2-II Unexpectedly Preserves Osteoblast-Mediated Skeletogenesis. *J. Biol. Chem.* **2004,** *279,* 20307-20313.

69 Fujiwara, M.; Tagashira, S.; Harada, H.; Ogawa, S.; Katsumata, T.; Nakatsuka, M.; Komori, T.; Takada, H. Isolation and Characterization of the Distal Promoter Region of Mouse Cbfa1. *Biochim. Biophys. Acta* **1999,** *1446,* 265-272.

70 Xiao, Z. S.; Liu, S. G.; Hinson, T. K.; Quarles, L. D. Characterization of the Upstream Mouse Cbfa1/Runx2 Promoter. *J. Cell Biochem.* **2001,** *82,* 647-659.

71 Zambotti, A.; Makhluf, H.; Shen, J.; Ducy, P. Characterization of an Osteoblast-Specific Enhancer Element in the CBFA1 Gene. *J. Biol. Chem.* **2002,** *277,* 41497-41506.

72 Drissi, H.; Luc, Q.; Shakoori, R.; Chuva De Sousa, L. S.; Choi, J. Y.; Terry, A.; Hu, M.; Jones, S.; Neil, J. C.; Lian, J. B.; Stein, J. L.; van Wijnen, A. J.; Stein, G. S. Transcriptional Autoregulation of the Bone Related CBFA1/RUNX2 Gene. *J. Cell Physiol* **2000,** *184,* 341-350.

73 Kanzler, B.; Kuschert, S. J.; Liu, Y. H.; Mallo, M. Hoxa-2 Restricts the Chondrogenic Domain and Inhibits Bone Formation During Development of the Branchial Area. *Development* **1998,** *125,* 2587-2597.

74 Lecka-Czernik, B.; Gubrij, I.; Moerman, E. J.; Kajkenova, O.; Lipschitz, D. A.; Manolagas, S. C.; Jilka, R. L. Inhibition of Osf2/Cbfa1 Expression and Terminal Osteoblast Differentiation by PPARgamma2. *J. Cell Biochem.* **1999,** *74,* 357-371.

75 Satokata, I.; Ma, L.; Ohshima, H.; Bei, M.; Woo, I.; Nishizawa, K.; Maeda, T.; Takano, Y.; Uchiyama, M.; Heaney, S.; Peters, H.; Tang, Z.; Maxson, R.; Maas, R. Msx2 Deficiency in Mice Causes Pleiotropic Defects in Bone Growth and Ectodermal Organ Formation. *Nat. Genet.* **2000,** *24,* 391-395.

76 Tribioli, C.; Lufkin, T. The Murine Bapx1 Homeobox Gene Plays a Critical Role in Embryonic Development of the Axial Skeleton and Spleen. *Development* **1999,** *126,* 5699-5711.

77 Yousfi, M.; Lasmoles, F.; Marie, P. J. TWIST Inactivation Reduces CBFA1/RUNX2 Expression and DNA Binding to the Osteocalcin Promoter in Osteoblasts. *Biochem. Biophys. Res. Commun.* **2002,** *297,* 641-644.

78 Lee, K. S.; Kim, H. J.; Li, Q. L.; Chi, X. Z.; Ueta, C.; Komori, T.; Wozney, J. M.; Kim, E. G.; Choi, J. Y.; Ryoo, H. M.; Bae, S. C. Runx2 Is a Common Target of Transforming Growth Factor Beta1 and Bone Morphogenetic Protein 2, and Cooperation Between Runx2 and Smad5 Induces Osteoblast-Specific Gene Expression in the Pluripotent Mesenchymal Precursor Cell Line C2C12. *Mol. Cell Biol.* **2000,** *20,* 8783-8792.

79 Alliston, T.; Choy, L.; Ducy, P.; Karsenty, G.; Derynck, R. TGF-Beta-Induced Repression of CBFA1 by Smad3 Decreases Cbfa1 and Osteocalcin Expression and Inhibits Osteoblast Differentiation. *EMBO J.* **2001,** *20,* 2254-2272.

80 Zhou, Y. X.; Xu, X.; Chen, L.; Li, C.; Brodie, S. G.; Deng, C. X. A Pro250Arg Substitution in Mouse Fgfr1 Causes Increased Expression of Cbfa1 and Premature Fusion of Calvarial Sutures. *Hum. Mol. Genet.* **2000,** *9,* 2001-2008.

81 Xiao, Z. S.; Simpson, L. G.; Quarles, L. D. IRES-Dependent Translational Control of Cbfa1/Runx2 Expression. *J. Cell Biochem.* **2003,** *88,* 493-505.

82 Sudhakar, S.; Li, Y.; Katz, M. S.; Elango, N. Translational Regulation Is a Control Point in RUNX2/Cbfa1 Gene Expression. *Biochem. Biophys. Res. Commun.* **2001,** *289,* 616-622.

83 Franceschi, R. T.; Xiao, G. Regulation of the Osteoblast-Specific Transcription Factor, Runx2: Responsiveness to Multiple Signal Transduction Pathways. *J. Cell Biochem.* **2003,** *88,* 446-454.

84 Hess, J.; Porte, D.; Munz, C.; Angel, P. AP-1 and Cbfa/Runt Physically Interact and Regulate Parathyroid Hormone-Dependent MMP13 Expression in Osteoblasts Through a New Osteoblast-Specific Element 2/AP-1 Composite Element. *J. Biol. Chem.* **2001,** *276,* 20029-20038.

85 D'Alonzo, R. C.; Selvamurugan, N.; Karsenty, G.; Partridge, N. C. Physical Interaction of the Activator Protein-1 Factors C-Fos and C-Jun With Cbfa1 for Collagenase-3 Promoter Activation. *J. Biol. Chem.* **2002,** *277,* 816-822.

86 Sasaki, K.; Yagi, H.; Bronson, R. T.; Tominaga, K.; Matsunashi, T.; Deguchi, K.; Tani, Y.; Kishimoto, T.; Komori, T. Absence of Fetal Liver Hematopoiesis in Mice Deficient in Transcriptional Coactivator Core Binding Factor Beta. *Proc. Natl. Acad. Sci. U. S. A* **1996,** *93,* 12359-12363.

87 Kundu, M.; Javed, A.; Jeon, J. P.; Horner, A.; Shum, L.; Eckhaus, M.; Muenke, M.; Lian, J. B.; Yang, Y.; Nuckolls, G. H.; Stein, G. S.; Liu, P. P. Cbfbeta Interacts With Runx2 and Has a Critical Role in Bone Development. *Nat. Genet.* **2002,** *32,* 639-644.

88 Yoshida, C. A.; Furuichi, T.; Fujita, T.; Fukuyama, R.; Kanatani, N.; Kobayashi, S.; Satake, M.; Takada, K.; Komori, T. Core-Binding Factor Beta Interacts With Runx2 and Is Required for Skeletal Development. *Nat. Genet.* **2002,** *32,* 633-638.

89 Selvamurugan, N.; Chou, W. Y.; Pearman, A. T.; Pulumati, M. R.; Partridge, N. C. Parathyroid Hormone Regulates the Rat Collagenase-3 Promoter in Osteoblastic Cells Through the Cooperative Interaction of the Activator Protein-1 Site and the Runt Domain Binding Sequence. *J. Biol. Chem.* **1998,** *273,* 10647-10657.

90 Takayanagi, H.; Ogasawara, K.; Hida, S.; Chiba, T.; Murata, S.; Sato, K.; Takaoka, A.; Yokochi, T.; Oda, H.; Tanaka, K.; Nakamura, K.; Taniguchi, T. T-Cell-Mediated Regulation of Osteoclastogenesis by Signalling Cross-Talk Between RANKL and IFN-Gamma. *Nature* **2000,** *408,* 600-605.

91 Takayanagi, H.; Kim, S.; Matsuo, K.; Suzuki, H.; Suzuki, T.; Sato, K.; Yokochi, T.; Oda, H.; Nakamura, K.; Ida, N.; Wagner, E. F.; Taniguchi, T. RANKL Maintains Bone Homeostasis Through C-Fos-Dependent Induction of Interferon-Beta. *Nature* **2002,** *416,* 744-749.

92 Kim, S.; Koga, T.; Isobe, M.; Kern, B. E.; Yokochi, T.; Chin, Y. E.; Karsenty, G.; Taniguchi, T.; Takayanagi, H. Stat1 Functions As a Cytoplasmic Attenuator of Runx2 in the Transcriptional Program of Osteoblast Differentiation. *Genes Dev.* **2003,** *17,* 1979-1991.

93 Chen, Z. F.; Behringer, R. R. Twist Is Required in Head Mesenchyme for Cranial Neural Tube Morphogenesis. *Genes Dev.* **1995,** *9,* 686-699.

94 Sosic, D.; Richardson, J. A.; Yu, K.; Ornitz, D. M.; Olson, E. N. Twist Regulates Cytokine Gene Expression Through a Negative Feedback Loop That Represses NF-KappaB Activity. *Cell* **2003,** *112,* 169-180.

95 el, G., V; Le Merrer, M.; Perrin-Schmitt, F.; Lajeunie, E.; Benit, P.; Renier, D.; Bourgeois, P.; Bolcato-Bellemin, A. L.; Munnich, A.; Bonaventure, J. Mutations of the TWIST Gene in the Saethre-Chotzen Syndrome. *Nat. Genet.* **1997,** *15,* 42-46.

96 Howard, T. D.; Paznekas, W. A.; Green, E. D.; Chiang, L. C.; Ma, N.; Ortiz de Luna, R. I.; Garcia, D. C.; Gonzalez-Ramos, M.; Kline, A. D.; Jabs, E. W. Mutations in TWIST, a Basic Helix-Loop-Helix Transcription Factor, in Saethre-Chotzen Syndrome. *Nat. Genet.* **1997,** *15,* 36-41.

97 Javed, A.; Guo, B.; Hiebert, S.; Choi, J. Y.; Green, J.; Zhao, S. C.; Osborne, M. A.; Stifani, S.; Stein, J. L.; Lian, J. B.; van Wijnen, A. J.; Stein, G. S. Groucho/TLE/R-Esp Proteins Associate With the Nuclear Matrix and Repress RUNX (CBF(Alpha)/AML/PEBP2(Alpha)) Dependent Activation of Tissue-Specific Gene Transcription. *J. Cell Sci.* **2000,** *113 (Pt 12),* 2221-2231.

98 McLarren, K. W.; Lo, R.; Grbavec, D.; Thirunavukkarasu, K.; Karsenty, G.; Stifani, S. The Mammalian Basic Helix Loop Helix Protein HES-1 Binds to and Modulates the Transactivating Function of the Runt-Related Factor Cbfa1. *J. Biol. Chem.* **2000,** *275,* 530-538.

99 Thomas, D. M.; Carty, S. A.; Piscopo, D. M.; Lee, J. S.; Wang, W. F.; Forrester, W. C.; Hinds, P. W. The Retinoblastoma Protein Acts As a Transcriptional Coactivator Required for Osteogenic Differentiation. *Mol. Cell* **2001,** *8,* 303-316.

100 Cui, C. B.; Cooper, L. F.; Yang, X.; Karsenty, G.; Aukhil, I. Transcriptional Coactivation of Bone-Specific Transcription Factor Cbfa1 by TAZ. *Mol. Cell Biol.* **2003,** *23,* 1004-1013.

101 Sierra, J.; Villagra, A.; Paredes, R.; Cruzat, F.; Gutierrez, S.; Javed, A.; Arriagada, G.; Olate, J.; Imschenetzky, M.; van Wijnen, A. J.; Lian, J. B.; Stein, G. S.; Stein, J. L.; Montecino, M. Regulation of the Bone-Specific Osteocalcin Gene by P300 Requires Runx2/Cbfa1 and the Vitamin D3 Receptor but Not P300 Intrinsic Histone Acetyltransferase Activity. *Mol. Cell Biol.* **2003,** *23,* 3339-3351.

102 Hata, K.; Nishimura, R.; Ueda, M.; Ikeda, F.; Matsubara, T.; Ichida, F.; Hisada, K.; Nokubi, T.; Yamaguchi, A.; Yoneda, T. A CCAAT/Enhancer Binding Protein Beta Isoform, Liver-Enriched Inhibitory Protein, Regulates Commitment of Osteoblasts and Adipocytes. *Mol. Cell Biol.* **2005,** *25,* 1971-1979.

103 Vega, R. B.; Matsuda, K.; Oh, J.; Barbosa, A. C.; Yang, X.; Meadows, E.; McAnally, J.; Pomajzl, C.; Shelton, J. M.; Richardson, J. A.; Karsenty, G.; Olson, E. N. Histone Deacetylase 4 Controls Chondrocyte Hypertrophy During Skeletogenesis. *Cell* **2004,** *119,* 555-566.

104 Karin, M.; Liu, Z.; Zandi, E. AP-1 Function and Regulation. *Curr. Opin. Cell Biol.* **1997,** *9,* 240-246.

105 Jochum, W.; Passegue, E.; Wagner, E. F. AP-1 in Mouse Development and Tumorigenesis. *Oncogene* **2001,** *20,* 2401-2412.

106 Johnson, R. S.; Spiegelman, B. M.; Papaioannou, V. Pleiotropic Effects of a Null Mutation in the C-Fos Proto-Oncogene. *Cell* **1992,** *71,* 577-586.

107 Wang, Z. Q.; Ovitt, C.; Grigoriadis, A. E.; Mohle-Steinlein, U.; Ruther, U.; Wagner, E. F. Bone and Haematopoietic Defects in Mice Lacking C-Fos. *Nature* **1992,** *360,* 741-745.

108 Gruda, M. C.; van Amsterdam, J.; Rizzo, C. A.; Durham, S. K.; Lira, S.; Bravo, R. Expression of FosB During Mouse Development: Normal Development of FosB Knockout Mice. *Oncogene* **1996,** *12,* 2177-2185.

109 Brown, J. R.; Ye, H.; Bronson, R. T.; Dikkes, P.; Greenberg, M. E. A Defect in Nurturing in Mice Lacking the Immediate Early Gene FosB. *Cell* **1996,** *86,* 297-309.

110 Schreiber, M.; Wang, Z. Q.; Jochum, W.; Fetka, I.; Elliott, C.; Wagner, E. F. Placental Vascularisation Requires the AP-1 Component Fra1. *Development* **2000,** *127,* 4937-4948.

111 Eferl, R.; Hoebertz, A.; Schilling, A. F.; Rath, M.; Karreth, F.; Kenner, L.; Amling, M.; Wagner, E. F. The Fos-Related Antigen Fra-1 Is an Activator of Bone Matrix Formation. *EMBO J.* **2004,** *23,* 2789-2799.

112 Eferl, R.; Sibilia, M.; Hilberg, F.; Fuchsbichler, A.; Kufferath, I.; Guertl, B.; Zenz, R.; Wagner, E. F.; Zatloukal, K. Functions of C-Jun in Liver and Heart Development. *J. Cell Biol.* **1999,** *145,* 1049-1061.

113 Schorpp-Kistner, M.; Wang, Z. Q.; Angel, P.; Wagner, E. F. JunB Is Essential for Mammalian Placentation. *EMBO J.* **1999,** *18,* 934-948.

114 Kenner, L.; Hoebertz, A.; Beil, T.; Keon, N.; Karreth, F.; Eferl, R.; Scheuch, H.; Szremska, A.; Amling, M.; Schorpp-Kistner, M.; Angel, P.; Wagner, E. F. Mice Lacking JunB Are Osteopenic Due to Cell-Autonomous Osteoblast and Osteoclast Defects. *J. Cell Biol.* **2004,** *164,* 613-623.

115 Thepot, D.; Weitzman, J. B.; Barra, J.; Segretain, D.; Stinnakre, M. G.; Babinet, C.; Yaniv, M. Targeted Disruption of the Murine JunD Gene Results in Multiple Defects in Male Reproductive Function. *Development* **2000,** *127,* 143-153.

116 Grigoriadis, A. E.; Schellander, K.; Wang, Z. Q.; Wagner, E. F. Osteoblasts Are Target Cells for Transformation in C-Fos Transgenic Mice. *J. Cell Biol.* **1993,** *122,* 685-701.

117 Carrozza, M. L.; Jacobs, H.; Acton, D.; Verma, I.; Berns, A. Overexpression of the FosB2 Gene in Thymocytes Causes Aberrant Development of T Cells and Thymic Epithelial Cells. *Oncogene* **1997,** *14,* 1083-1091.

118 Sabatakos, G.; Sims, N. A.; Chen, J.; Aoki, K.; Kelz, M. B.; Amling, M.; Bouali, Y.; Mukhopadhyay, K.; Ford, K.; Nestler, E. J.; Baron, R. Overexpression of DeltaFosB Transcription Factor(s) Increases Bone Formation and Inhibits Adipogenesis. *Nat. Med.* **2000,** *6,* 985-990.

119 Jochum, W.; David, J. P.; Elliott, C.; Wutz, A.; Plenk, H., Jr.; Matsuo, K.; Wagner, E. F. Increased Bone Formation and Osteosclerosis in Mice Overexpressing the Transcription Factor Fra-1. *Nat. Med.* **2000,** *6,* 980-984.

120 McHenry, J. Z.; Leon, A.; Matthaei, K. I.; Cohen, D. R. Overexpression of Fra-2 in Transgenic Mice Perturbs Normal Eye Development. *Oncogene* **1998,** *17,* 1131-1140.

121 Schorpp, M.; Jager, R.; Schellander, K.; Schenkel, J.; Wagner, E. F.; Weiher, H.; Angel, P. The Human Ubiquitin C Promoter Directs High Ubiquitous Expression of Transgenes in Mice. *Nucleic Acids Res.* **1996,** *24,* 1787-1788.

122 Li, B.; Tournier, C.; Davis, R. J.; Flavell, R. A. Regulation of IL-4 Expression by the Transcription Factor JunB During T Helper Cell Differentiation. *EMBO J.* **1999,** *18,* 420-432.

123 Karsenty, G.; Wagner, E. F. Reaching a Genetic and Molecular Understanding of Skeletal Development. *Dev. Cell* **2002,** *2,* 389-406.

124 Wagner, E. F. Functions of AP1 (Fos/Jun) in Bone Development. *Ann. Rheum. Dis.* **2002,** *61 Suppl 2,* ii40-ii42.

125 Wu, J. X.; Carpenter, P. M.; Gresens, C.; Keh, R.; Niman, H.; Morris, J. W.; Mercola, D. The Proto-Oncogene C-Fos Is Over-Expressed in the Majority of Human Osteosarcomas. *Oncogene* **1990,** *5,* 989-1000.

126 Sims, N. A.; Sabatakos, G.; Chen, J. S.; Kelz, M. B.; Nestler, E. J.; Baron, R. Regulating DeltaFosB Expression in Adult Tet-Off-DeltaFosB Transgenic Mice Alters Bone Formation and Bone Mass. *Bone* **2002,** *30,* 32-39.

127 Kveiborg, M.; Sabatakos, G.; Chiusaroli, R.; Wu, M.; Philbrick, W. M.; Horne, W. C.; Baron, R. DeltaFosB Induces Osteosclerosis and Decreases Adipogenesis by Two Independent Cell-Autonomous Mechanisms. *Mol. Cell Biol.* **2004,** *24,* 2820-2830.

128 Lee, M. H.; Kwon, T. G.; Park, H. S.; Wozney, J. M.; Ryoo, H. M. BMP-2-Induced Osterix Expression Is Mediated by Dlx5 but Is Independent of Runx2. *Biochem. Biophys. Res. Commun.* **2003,** *309,* 689-694.

129 Bendall, A. J.; Abate-Shen, C. Roles for Msx and Dlx Homeoproteins in Vertebrate Development. *Gene* **2000,** *247,* 17-31.

130 Robledo, R. F.; Rajan, L.; Li, X.; Lufkin, T. The Dlx5 and Dlx6 Homeobox Genes Are Essential for Craniofacial, Axial, and Appendicular Skeletal Development. *Genes Dev.* **2002,** *16,* 1089-1101.

131 Ichida, F.; Nishimura, R.; Hata, K.; Matsubara, T.; Ikeda, F.; Hisada, K.; Yatani, H.; Cao, X.; Komori, T.; Yamaguchi, A.; Yoneda, T. Reciprocal Roles of Msx2 in Regulation of Osteoblast and Adipocyte Differentiation. *J. Biol. Chem.* **2004**.

132 Harris, S. E.; Guo, D.; Harris, M. A.; Krishnaswamy, A.; Lichtler, A. Transcriptional Regulation of BMP-2 Activated Genes in Osteoblasts Using Gene Expression Microarray Analysis: Role of Dlx2 and Dlx5 Transcription Factors. *Front Biosci.* **2003,** *8,* s1249-s1265.

133 Lee, M. H.; Kim, Y. J.; Kim, H. J.; Park, H. D.; Kang, A. R.; Kyung, H. M.; Sung, J. H.; Wozney, J. M.; Kim, H. J.; Ryoo, H. M. BMP-2-Induced Runx2 Expression Is Mediated by Dlx5, and TGF-Beta 1 Opposes the BMP-2-Induced Osteoblast Differentiation by Suppression of Dlx5 Expression. *J. Biol. Chem.* **2003,** *278,* 34387-34394.

134 Ruzinova, M. B.; Benezra, R. Id Proteins in Development, Cell Cycle and Cancer. *Trends Cell Biol.* **2003,** *13,* 410-418.

135 Peng, Y.; Kang, Q.; Luo, Q.; Jiang, W.; Si, W.; Liu, B. A.; Luu, H. H.; Park, J. K.; Li, X.; Luo, J.; Montag, A. G.; Haydon, R. C.; He, T. C. Id Helix-Loop-Helix Proteins Mediate BMP-Induced Osteoblast Differentiation of Mesenchymal Stem Cells. *J. Biol. Chem.* **2004**.

136 Baron, R. In *Primer on the Metabolic Bone Diseases and Disorders of Mineral Metabolism*; American Society for Bone and Mineral Research, Washington D.C.: 2003.

137 Karsenty, G. Role of Cbfa1 in Osteoblast Differentiation and Function. *Semin. Cell Dev. Biol.* **2000,** *11,* 343-346.

138 Aubin, J. E.; Liu, F.; Malaval, L.; Gupta, A. K. Osteoblast and Chondroblast Differentiation. *Bone* **1995,** *17,* 77S-83S.

139 Leis, H. J.; Hulla, W.; Gruber, R.; Huber, E.; Zach, D.; Gleispach, H.; Windischhofer, W. Phenotypic Heterogeneity of Osteoblast-Like MC3T3-E1 Cells: Changes of Bradykinin-Induced Prostaglandin E2 Production During Osteoblast Maturation. *J. Bone Miner. Res.* **1997,** *12,* 541-551.

140 Sudo, H.; Kodama, H. A.; Amagai, Y.; Yamamoto, S.; Kasai, S. In Vitro Differentiation and Calcification in a New Clonal Osteogenic Cell Line Derived From Newborn Mouse Calvaria. *J. Cell Biol.* **1983,** *96,* 191-198.

141 Cappellen, D.; Luong-Nguyen, N. H.; Bongiovanni, S.; Grenet, O.; Wanke, C.; Susa, M. Transcriptional Program of Mouse Osteoclast Differentiation Governed by the Macrophage Colony-Stimulating Factor and the Ligand for the Receptor Activator of NFkappa B. *J. Biol. Chem.* **2002,** *277,* 21971-21982.

142 Canalis, E.; Rydziel, S. In *Principles of Bone Biology*; Bilezikian, J. P., Raisz, L. G., Rodan, G. A., Eds.; Academic press Inc: 1996; Chapter 44.

143 Conover, C. In *Principles of Bone Biology*; Bilezikian, J. P., Raisz, L. G., Rodan, G. A., Eds.; Academic press Inc: 1996; Chapter 43.

144 Hurley, M.; Florkiewicz, R. In *Principles of Bone Biology*; Bilezikian, J. P., Raisz, L. G., Rodan, G. A., Eds.; Academic press Inc: 1996; Chapter 45.

145 Swarthout, J. T.; D'Alonzo, R. C.; Selvamurugan, N.; Partridge, N. C. Parathyroid Hormone-Dependent Signaling Pathways Regulating Genes in Bone Cells. *Gene* **2002,** *282,* 1-17.

146 Kim, S. J.; Ballock, R. T. In *Cellular and Molecular Biology of Bone*; Koda, M., Ed.; Academic press: 1993.

147 Hefferan, T. E.; Subramaniam, M.; Khosla, S.; Riggs, B. L.; Spelsberg, T. C. Cytokine-Specific Induction of the TGF-Beta Inducible Early Gene (TIEG): Regulation by Specific Members of the TGF-Beta Family. *J. Cell Biochem.* **2000,** *78,* 380-390.

148 Kim, J. E.; Kim, E. H.; Han, E. H.; Park, R. W.; Park, I. H.; Jun, S. H.; Kim, J. C.; Young, M. F.; Kim, I. S. A TGF-Beta-Inducible Cell Adhesion Molecule, Betaig-H3, Is Downregulated in Melorheostosis and Involved in Osteogenesis. *J. Cell Biochem.* **2000,** *77,* 169-178.

149 Mackie, E. J.; Abraham, L. A.; Taylor, S. L.; Tucker, R. P.; Murphy, L. I. Regulation of Tenascin-C Expression in Bone Cells by Transforming Growth Factor-Beta. *Bone* **1998,** *22,* 301-307.

150 Puente, E.; Saint-Laurent, N.; Torrisani, J.; Furet, C.; Schally, A. V.; Vaysse, N.; Buscail, L.; Susini, C. Transcriptional Activation of Mouse Sst2 Somatostatin Receptor Promoter by Transforming Growth Factor-Beta. Involvement of Smad4. *J. Biol. Chem.* **2001,** *276,* 13461-13468.

151 Hagiwara, H.; Hiruma, Y.; Inoue, A.; Yamaguchi, A.; Hirose, S. Deceleration by Angiotensin II of the Differentiation and Bone Formation of Rat Calvarial Osteoblastic Cells. *J. Endocrinol.* **1998,** *156,* 543-550.

152 Choi, Y.; Woo, K. M.; Ko, S. H.; Lee, Y. J.; Park, S. J.; Kim, H. M.; Kwon, B. S. Osteoclastogenesis Is Enhanced by Activated B Cells but Suppressed by Activated CD8(+) T Cells. *Eur. J. Immunol.* **2001,** *31,* 2179-2188.

153 Guise, T. A.; Yin, J. J.; Taylor, S. D.; Kumagai, Y.; Dallas, M.; Boyce, B. F.; Yoneda, T.; Mundy, G. R. Evidence for a Causal Role of Parathyroid Hormone-Related Protein in the Pathogenesis of Human Breast Cancer-Mediated Osteolysis. *J. Clin. Invest* **1996,** *98,* 1544-1549.

154 Malaval, L.; Aubin, J. E. Biphasic Effects of Leukemia Inhibitory Factor on Osteoblastic Differentiation. *J. Cell Biochem. Suppl* **2001,** *Suppl 36,* 63-70.

155 Gordeladze, J. O.; Reseland, J. E.; Drevon, C. A. Pharmacological Interference With Transcriptional Control of Osteoblasts: a Possible Role for Leptin and Fatty Acids in Maintaining Bone Strength and Body Lean Mass. *Curr. Pharm. Des* **2001,** *7,* 275-290.

156 Pilbeam, C.; Harrison, J.; Raisz, L. In *Principles of Bone Biology*; Bilezikian, J. P., Raisz, L. G., Rodan, G. A., Eds.; Academic press Inc: 1996; Chapter 51.

157 Wilkie, A. O. Craniosynostosis: Genes and Mechanisms. *Hum. Mol. Genet.* **1997,** *6,* 1647-1656.

158 Allan, E. H.; Martin, T. J. The Plasminogen Activator Inhibitor System in Bone Cell Function. *Clin. Orthop.* **1995,** *313,* 54-63.

159 Maillard, C.; Berruyer, M.; Serre, C. M.; Amiral, J.; Dechavanne, M.; Delmas, P. D. Thrombomodulin Is Synthesized by Osteoblasts, Stimulated by 1,25-(OH)2D3 and Activates Protein C at Their Cell Membrane. *Endocrinology* **1993,** *133,* 668-674.

160 Tezuka, K.; Yasuda, M.; Watanabe, N.; Morimura, N.; Kuroda, K.; Miyatani, S.; Hozumi, N. Stimulation of Osteoblastic Cell Differentiation by Notch. *J. Bone Miner. Res.* **2002,** *17,* 231-239.

161 Sciaudone, M.; Gazzerro, E.; Priest, L.; Delany, A. M.; Canalis, E. Notch 1 Impairs Osteoblastic Cell Differentiation. *Endocrinology* **2003,** *144,* 5631-5639.

162 Locklin, R. M.; Riggs, B. L.; Hicok, K. C.; Horton, H. F.; Byrne, M. C.; Khosla, S. Assessment of Gene Regulation by Bone Morphogenetic Protein 2 in Human Marrow Stromal Cells Using Gene Array Technology. *J. Bone Miner. Res.* **2001,** *16,* 2192-2204.

163 Lopez-Rovira, T.; Chalaux, E.; Massague, J.; Rosa, J. L.; Ventura, F. Direct Binding of Smad1 and Smad4 to Two Distinct Motifs Mediates Bone Morphogenetic Protein-Specific Transcriptional Activation of Id1 Gene. *J. Biol. Chem.* **2002,** *277,* 3176-3185.

164 Wilkie, A. O.; Tang, Z.; Elanko, N.; Walsh, S.; Twigg, S. R.; Hurst, J. A.; Wall, S. A.; Chrzanowska, K. H.; Maxson, R. E., Jr. Functional Haploinsufficiency of the Human Homeobox Gene MSX2 Causes Defects in Skull Ossification. *Nat. Genet.* **2000,** *24,* 387-390.

165 Jumlongras, D.; Bei, M.; Stimson, J. M.; Wang, W. F.; DePalma, S. R.; Seidman, C. E.; Felbor, U.; Maas, R.; Seidman, J. G.; Olsen, B. R. A Nonsense Mutation in MSX1 Causes Witkop Syndrome. *Am. J. Hum. Genet.* **2001,** *69,* 67-74.

166 Kraus, P.; Lufkin, T. Mammalian Dlx Homeobox Gene Control of Craniofacial and Inner Ear Morphogenesis. *J. Cell Biochem.* **1999,** *Suppl 32-33,* 133-140.

167 Rawadi, G.; Vayssiere, B.; Dunn, F.; Baron, R.; Roman-Roman, S. BMP-2 Controls Alkaline Phosphatase Expression and Osteoblast Mineralization by a Wnt Autocrine Loop. *J. Bone Miner. Res.* **2003,** *18,* 1842-1853.

168 Leimeister, C.; Externbrink, A.; Klamt, B.; Gessler, M. Hey Genes: a Novel Subfamily of Hairy- and Enhancer of Split Related Genes Specifically Expressed During Mouse Embryogenesis. *Mech. Dev.* **1999,** *85,* 173-177.

169 Iso, T.; Sartorelli, V.; Chung, G.; Shichinohe, T.; Kedes, L.; Hamamori, Y. HERP, a New Primary Target of Notch Regulated by Ligand Binding. *Mol. Cell Biol.* **2001,** *21,* 6071-6079.

170 Iso, T.; Chung, G.; Hamamori, Y.; Kedes, L. HERP1 Is a Cell Type-Specific Primary Target of Notch. *J. Biol. Chem.* **2002,** *277,* 6598-6607.

171 Iso, T.; Kedes, L.; Hamamori, Y. HES and HERP Families: Multiple Effectors of the Notch Signaling Pathway. *J. Cell Physiol* **2003,** *194,* 237-255.

172 Sun, J.; Kamei, C. N.; Layne, M. D.; Jain, M. K.; Liao, J. K.; Lee, M. E.; Chin, M. T. Regulation of Myogenic Terminal Differentiation by the Hairy-Related Transcription Factor CHF2. *J. Biol. Chem.* **2001,** *276,* 18591-18596.

173 Balint, E.; Lapointe, D.; Drissi, H.; van der, M. C.; Young, D. W.; van Wijnen, A. J.; Stein, J. L.; Stein, G. S.; Lian, J. B. Phenotype Discovery by Gene Expression Profiling: Mapping of Biological Processes Linked to BMP-2-Mediated Osteoblast Differentiation. *J. Cell Biochem.* **2003,** *89,* 401-426.

174 Beck, G. R., Jr.; Zerler, B.; Moran, E. Gene Array Analysis of Osteoblast Differentiation. *Cell Growth Differ.* **2001,** *12,* 61-83.

175 Doi, M.; Nagano, A.; Nakamura, Y. Genome-Wide Screening by CDNA Microarray of Genes Associated With Matrix Mineralization by Human Mesenchymal Stem Cells in Vitro. *Biochem. Biophys. Res. Commun.* **2002,** *290,* 381-390.

176 Korchynskyi, O.; Dechering, K. J.; Sijbers, A. M.; Olijve, W.; ten Dijke, P. Gene Array Analysis of Bone Morphogenetic Protein Type I Receptor-Induced Osteoblast Differentiation. *J. Bone Miner. Res.* **2003,** *18,* 1177-1185.

177 Centrella, M.; Horowitz, M. C.; Wozney, J. M.; McCarthy, T. L. Transforming Growth Factor-Beta Gene Family Members and Bone. *Endocr. Rev.* **1994,** *15,* 27-39.

178 Chua, C. C.; Chua, B. H.; Chen, Z.; Landy, C.; Hamdy, R. C. TGF-Beta1 Inhibits Multiple Caspases Induced by TNF-Alpha in Murine Osteoblastic MC3T3-E1 Cells. *Biochim. Biophys. Acta* **2002,** *1593,* 1-8.

179 Chambers, T. J. Regulation of the Differentiation and Function of Osteoclasts. *J. Pathol.* **2000,** *192,* 4-13.

180 Centrella, M.; Casinghino, S.; Kim, J.; Pham, T.; Rosen, V.; Wozney, J.; McCarthy, T. L. Independent Changes in Type I and Type II Receptors for Transforming Growth Factor Beta Induced by Bone Morphogenetic Protein 2 Parallel Expression of the Osteoblast Phenotype. *Mol. Cell Biol.* **1995,** *15,* 3273-3281.

181 Artavanis-Tsakonas, S.; Rand, M. D.; Lake, R. J. Notch Signaling: Cell Fate Control and Signal Integration in Development. *Science* **1999,** *284,* 770-776.

182 Bulman, M. P.; Kusumi, K.; Frayling, T. M.; McKeown, C.; Garrett, C.; Lander, E. S.; Krumlauf, R.; Hattersley, A. T.; Ellard, S.; Turnpenny, P. D. Mutations in the Human Delta Homologue, DLL3, Cause Axial Skeletal Defects in Spondylocostal Dysostosis. *Nat. Genet.* **2000,** *24,* 438-441.

183 Shen, J.; Bronson, R. T.; Chen, D. F.; Xia, W.; Selkoe, D. J.; Tonegawa, S. Skeletal and CNS Defects in Presenilin-1-Deficient Mice. *Cell* **1997,** *89,* 629-639.

184 Calvi, L. M.; Adams, G. B.; Weibrecht, K. W.; Weber, J. M.; Olson, D. P.; Knight, M. C.; Martin, R. P.; Schipani, E.; Divieti, P.; Bringhurst, F. R.; Milner, L. A.; Kronenberg, H. M.; Scadden, D. T. Osteoblastic Cells Regulate the Haematopoietic Stem Cell Niche. *Nature* **2003,** *425,* 841-846.

185 Mumm, J. S.; Kopan, R. Notch Signaling: From the Outside in. *Dev. Biol.* **2000,** *228,* 151-165.

186 Perbal, B. CCN Proteins: Multifunctional Signalling Regulators. *Lancet* **2004,** *363,* 62-64.

187 Sakamoto, K.; Yamaguchi, S.; Ando, R.; Miyawaki, A.; Kabasawa, Y.; Takagi, M.; Li, C. L.; Perbal, B.; Katsube, K. The Nephroblastoma Overexpressed Gene (NOV/Ccn3) Protein Associates With Notch1 Extracellular Domain and Inhibits Myoblast Differentiation Via Notch Signaling Pathway. *J. Biol. Chem.* **2002,** *277,* 29399-29405.

188 Morrison, S. J.; Perez, S. E.; Qiao, Z.; Verdi, J. M.; Hicks, C.; Weinmaster, G.; Anderson, D. J. Transient Notch Activation Initiates an Irreversible Switch From Neurogenesis to Gliogenesis by Neural Crest Stem Cells. *Cell* **2000,** *101,* 499-510.

189 Nofziger, D.; Miyamoto, A.; Lyons, K. M.; Weinmaster, G. Notch Signaling Imposes Two Distinct Blocks in the Differentiation of C2C12 Myoblasts. *Development* **1999,** *126,* 1689-1702.

190 Dahlqvist, C.; Blokzijl, A.; Chapman, G.; Falk, A.; Dannaeus, K.; Ibanez, C. F.; Lendahl, U. Functional Notch Signaling Is Required for BMP4-Induced Inhibition of Myogenic Differentiation. *Development* **2003,** *130,* 6089-6099.

191 Itoh, F.; Itoh, S.; Goumans, M. J.; Valdimarsdottir, G.; Iso, T.; Dotto, G. P.; Hamamori, Y.; Kedes, L.; Kato, M.; Dijke, P. P. Synergy and Antagonism Between Notch and BMP Receptor Signaling Pathways in Endothelial Cells. *EMBO J.* **2004,** *23,* 541-551.

192 Yamaguchi, A.; Komori, T.; Suda, T. Regulation of Osteoblast Differentiation Mediated by Bone Morphogenetic Proteins, Hedgehogs, and Cbfa1. *Endocr. Rev.* **2000,** *21,* 393-411.

193 Yamaguchi, A.; Kahn, A. J. Clonal Osteogenic Cell Lines Express Myogenic and Adipocytic Developmental Potential. *Calcif. Tissue Int.* **1991,** *49,* 221-225.

194 Maliakal, J. C.; Asahina, I.; Hauschka, P. V.; Sampath, T. K. Osteogenic Protein-1 (BMP-7) Inhibits Cell Proliferation and Stimulates the Expression of Markers Characteristic of Osteoblast Phenotype in Rat Osteosarcoma (17/2.8) Cells. *Growth Factors* **1994,** *11,* 227-234.

195 Wozney, J. M.; Rosen, V.; Celeste, A. J.; Mitsock, L. M.; Whitters, M. J.; Kriz, R. W.; Hewick, R. M.; Wang, E. A. Novel Regulators of Bone Formation: Molecular Clones and Activities. *Science* **1988,** *242,* 1528-1534.

196 Katagiri, T.; Yamaguchi, A.; Komaki, M.; Abe, E.; Takahashi, N.; Ikeda, T.; Rosen, V.; Wozney, J. M.; Fujisawa-Sehara, A.; Suda, T. Bone Morphogenetic Protein-2 Converts the Differentiation Pathway of C2C12 Myoblasts into the Osteoblast Lineage. *J. Cell Biol.* **1994,** *127,* 1755-1766.

197 Choi, J. Y.; Lee, B. H.; Song, K. B.; Park, R. W.; Kim, I. S.; Sohn, K. Y.; Jo, J. S.; Ryoo, H. M. Expression Patterns of Bone-Related Proteins During Osteoblastic Differentiation in MC3T3-E1 Cells. *J. Cell Biochem.* **1996,** *61,* 609-618.

198 Southern, E.; Mir, K.; Shchepinov, M. Molecular Interactions on Microarrays. *Nat. Genet.* **1999,** *21,* 5-9.

199 Southern, E. M. Detection of Specific Sequences Among DNA Fragments Separated by Gel Electrophoresis. *J. Mol. Biol.* **1975,** *98,* 503-517.

200 Lipshutz, R. J.; Fodor, S. P.; Gingeras, T. R.; Lockhart, D. J. High Density Synthetic Oligonucleotide Arrays. *Nat. Genet.* **1999,** *21,* 20-24.

201 Quackenbush, J. Microarray Data Normalization and Transformation. *Nat. Genet.* **2002,** *32 Suppl,* 496-501.

202 Brazma, A.; Hingamp, P.; Quackenbush, J.; Sherlock, G.; Spellman, P.; Stoeckert, C.; Aach, J.; Ansorge, W.; Ball, C. A.; Causton, H. C.; Gaasterland, T.; Glenisson, P.; Holstege, F. C.; Kim, I. F.; Markowitz, V.; Matese, J. C.; Parkinson, H.; Robinson, A.; Sarkans, U.; Schulze-Kremer, S.; Stewart, J.; Taylor, R.; Vilo, J.; Vingron, M. Minimum Information About a Microarray Experiment (MIAME)-Toward Standards for Microarray Data. *Nat. Genet.* **2001,** *29,* 365-371.

203 Liu, G.; Loraine, A. E.; Shigeta, R.; Cline, M.; Cheng, J.; Valmeekam, V.; Sun, S.; Kulp, D.; Siani-Rose, M. A. NetAffx: Affymetrix Probesets and Annotations. *Nucleic Acids Res.* **2003,** *31,* 82-86.

204 Gruneberg, U.; Neef, R.; Honda, R.; Nigg, E. A.; Barr, F. A. Relocation of Aurora B From Centromeres to the Central Spindle at the Metaphase to Anaphase Transition Requires MKlp2. *J. Cell Biol.* **2004,** *166,* 167-172.

205 Marzia, M.; Sims, N. A.; Voit, S.; Migliaccio, S.; Taranta, A.; Bernardini, S.; Faraggiana, T.; Yoneda, T.; Mundy, G. R.; Boyce, B. F.; Baron, R.; Teti, A. Decreased C-Src Expression Enhances Osteoblast Differentiation and Bone Formation. *J. Cell Biol.* **2000,** *151,* 311-320.

206 Zaidi, S. K.; Sullivan, A. J.; Medina, R.; Ito, Y.; van Wijnen, A. J.; Stein, J. L.; Lian, J. B.; Stein, G. S. Tyrosine Phosphorylation Controls Runx2-Mediated Subnuclear Targeting of YAP to Repress Transcription. *EMBO J.* **2004,** *23,* 790-799.

207 Daci, E.; Everts, V.; Torrekens, S.; Van Herck, E.; Tigchelaar-Gutterr, W.; Bouillon, R.; Carmeliet, G. Increased Bone Formation in Mice Lacking Plasminogen Activators. *J. Bone Miner. Res.* **2003,** *18,* 1167-1176.

208 Fire, A.; Xu, S.; Montgomery, M. K.; Kostas, S. A.; Driver, S. E.; Mello, C. C. Potent and Specific Genetic Interference by Double-Stranded RNA in Caenorhabditis Elegans. *Nature* **1998,** *391,* 806-811.

209 Stark, G. R.; Kerr, I. M.; Williams, B. R.; Silverman, R. H.; Schreiber, R. D. How Cells Respond to Interferons. *Annu. Rev. Biochem.* **1998,** *67,* 227-264.

210 Elbashir, S. M.; Harborth, J.; Lendeckel, W.; Yalcin, A.; Weber, K.; Tuschl, T. Duplexes of 21-Nucleotide RNAs Mediate RNA Interference in Cultured Mammalian Cells. *Nature* **2001,** *411,* 494-498.

211 Bernstein, E.; Caudy, A. A.; Hammond, S. M.; Hannon, G. J. Role for a Bidentate Ribonuclease in the Initiation Step of RNA Interference. *Nature* **2001,** *409,* 363-366.

212 Martinez, J.; Patkaniowska, A.; Urlaub, H.; Luhrmann, R.; Tuschl, T. Single-Stranded Antisense SiRNAs Guide Target RNA Cleavage in RNAi. *Cell* **2002,** *110,* 563-574.

213 Hannon, G. J. RNA Interference. *Nature* **2002,** *418,* 244-251.

214 Dorsett, Y.; Tuschl, T. SiRNAs: Applications in Functional Genomics and Potential As Therapeutics. *Nat. Rev. Drug Discov.* **2004,** *3,* 318-329.

215 Sledz, C. A.; Holko, M.; de Veer, M. J.; Silverman, R. H.; Williams, B. R. Activation of the Interferon System by Short-Interfering RNAs. *Nat. Cell Biol.* **2003,** *5,* 834-839.

216 Bridge, A. J.; Pebernard, S.; Ducraux, A.; Nicoulaz, A. L.; Iggo, R. Induction of an Interferon Response by RNAi Vectors in Mammalian Cells. *Nat. Genet.* **2003,** *34,* 263-264.

217 Jackson, A. L.; Bartz, S. R.; Schelter, J.; Kobayashi, S. V.; Burchard, J.; Mao, M.; Li, B.; Cavet, G.; Linsley, P. S. Expression Profiling Reveals Off-Target Gene Regulation by RNAi. *Nat. Biotechnol.* **2003,** *21,* 635-637.

218 Kimberly, W. T.; Wolfe, M. S. Identity and Function of Gamma-Secretase. *J. Neurosci. Res.* **2003,** *74,* 353-360.

219 Rand, M. D.; Grimm, L. M.; Artavanis-Tsakonas, S.; Patriub, V.; Blacklow, S. C.; Sklar, J.; Aster, J. C. Calcium Depletion Dissociates and Activates Heterodimeric Notch Receptors. *Mol. Cell Biol.* **2000,** *20,* 1825-1835.

220 Shearman, M. S.; Beher, D.; Clarke, E. E.; Lewis, H. D.; Harrison, T.; Hunt, P.; Nadin, A.; Smith, A. L.; Stevenson, G.; Castro, J. L. L-685,458, an Aspartyl Protease Transition State Mimic, Is a Potent Inhibitor of Amyloid Beta-Protein Precursor Gamma-Secretase Activity. *Biochemistry* **2000,** *39,* 8698-8704.

221 Doerfler, P.; Shearman, M. S.; Perlmutter, R. M. Presenilin-Dependent Gamma-Secretase Activity Modulates Thymocyte Development. *Proc. Natl. Acad. Sci. U. S. A* **2001,** *98,* 9312-9317.

222 de Jong, D. S.; Vaes, B. L.; Dechering, K. J.; Feijen, A.; Hendriks, J. M.; Wehrens, R.; Mummery, C. L.; van Zoelen, E. J.; Olijve, W.; Steegenga, W. T. Identification of Novel Regulators Associated With Early-Phase Osteoblast Differentiation. *J. Bone Miner. Res.* **2004,** *19,* 947-958.

223 Greenwald, I. LIN-12/Notch Signaling: Lessons From Worms and Flies. *Genes Dev.* **1998,** *12,* 1751-1762.

224 Mohr, O. L. Character changes caused by mutation of an entire region of a chromosome in Drosophila. Genetics 4, 275-282. 1919.
Ref Type: Magazine Article

225 Ellisen, L. W.; Bird, J.; West, D. C.; Soreng, A. L.; Reynolds, T. C.; Smith, S. D.; Sklar, J. TAN-1, the Human Homolog of the Drosophila Notch Gene, Is Broken by Chromosomal Translocations in T Lymphoblastic Neoplasms. *Cell* **1991,** *66,* 649-661.

226 Allman, D.; Punt, J. A.; Izon, D. J.; Aster, J. C.; Pear, W. S. An Invitation to T and More: Notch Signaling in Lymphopoiesis. *Cell* **2002,** *109 Suppl,* S1-11.

227 Ohtsuka, T.; Ishibashi, M.; Gradwohl, G.; Nakanishi, S.; Guillemot, F.; Kageyama, R. Hes1 and Hes5 As Notch Effectors in Mammalian Neuronal Differentiation. *EMBO J.* **1999,** *18,* 2196-2207.

228 Maier, M. M.; Gessler, M. Comparative Analysis of the Human and Mouse Hey1 Promoter: Hey Genes Are New Notch Target Genes. *Biochem. Biophys. Res. Commun.* **2000,** *275,* 652-660.

229 Nakagawa, O.; McFadden, D. G.; Nakagawa, M.; Yanagisawa, H.; Hu, T.; Srivastava, D.; Olson, E. N. Members of the HRT Family of Basic Helix-Loop-Helix Proteins Act As Transcriptional Repressors Downstream of Notch Signaling. *Proc. Natl. Acad. Sci. U. S. A* **2000,** *97,* 13655-13660.

230 Steidl, C.; Leimeister, C.; Klamt, B.; Maier, M.; Nanda, I.; Dixon, M.; Clarke, R.; Schmid, M.; Gessler, M. Characterization of the Human and Mouse HEY1, HEY2, and HEYL Genes: Cloning, Mapping, and Mutation Screening of a New BHLH Gene Family. *Genomics* **2000,** *66,* 195-203.

231 Kokubo, H.; Lun, Y.; Johnson, R. L. Identification and Expression of a Novel Family of BHLH CDNAs Related to Drosophila Hairy and Enhancer of Split. *Biochem. Biophys. Res. Commun.* **1999,** *260,* 459-465.

232 Chin, M. T.; Maemura, K.; Fukumoto, S.; Jain, M. K.; Layne, M. D.; Watanabe, M.; Hsieh, C. M.; Lee, M. E. Cardiovascular Basic Helix Loop Helix Factor 1, a Novel Transcriptional Repressor Expressed Preferentially in the Developing and Adult Cardiovascular System. *J. Biol. Chem.* **2000,** *275,* 6381-6387.

233 Zhong, T. P.; Rosenberg, M.; Mohideen, M. A.; Weinstein, B.; Fishman, M. C. Gridlock, an HLH Gene Required for Assembly of the Aorta in Zebrafish. *Science* **2000,** *287,* 1820-1824.

234 Kageyama, R.; Ohtsuka, T.; Tomita, K. The BHLH Gene Hes1 Regulates Differentiation of Multiple Cell Types. *Mol. Cells* **2000,** *10,* 1-7.

235 Chen, G.; Fernandez, J.; Mische, S.; Courey, A. J. A Functional Interaction Between the Histone Deacetylase Rpd3 and the Corepressor Groucho in Drosophila Development. *Genes Dev.* **1999,** *13,* 2218-2230.

236 Sasai, Y.; Kageyama, R.; Tagawa, Y.; Shigemoto, R.; Nakanishi, S. Two Mammalian Helix-Loop-Helix Factors Structurally Related to Drosophila Hairy and Enhancer of Split. *Genes Dev.* **1992,** *6,* 2620-2634.

237 Castella, P.; Sawai, S.; Nakao, K.; Wagner, J. A.; Caudy, M. HES-1 Repression of Differentiation and Proliferation in PC12 Cells: Role for the Helix 3-Helix 4 Domain in Transcription Repression. *Mol. Cell Biol.* **2000,** *20,* 6170-6183.

238 Iso, T.; Sartorelli, V.; Poizat, C.; Iezzi, S.; Wu, H. Y.; Chung, G.; Kedes, L.; Hamamori, Y. HERP, a Novel Heterodimer Partner of HES/E(Spl) in Notch Signaling. *Mol. Cell Biol.* **2001,** *21,* 6080-6089.

239 Ishibashi, M.; Ang, S. L.; Shiota, K.; Nakanishi, S.; Kageyama, R.; Guillemot, F. Targeted Disruption of Mammalian Hairy and Enhancer of Split Homolog-1 (HES-1) Leads to Up-Regulation of Neural Helix-Loop-Helix Factors, Premature Neurogenesis, and Severe Neural Tube Defects. *Genes Dev.* **1995,** *9,* 3136-3148.

240 Sakata, Y.; Kamei, C. N.; Nakagami, H.; Bronson, R.; Liao, J. K.; Chin, M. T. Ventricular Septal Defect and Cardiomyopathy in Mice Lacking the Transcription Factor CHF1/Hey2. *Proc. Natl. Acad. Sci. U. S. A* **2002,** *99,* 16197-16202.

241 Fischer, A.; Schumacher, N.; Maier, M.; Sendtner, M.; Gessler, M. The Notch Target Genes Hey1 and Hey2 Are Required for Embryonic Vascular Development. *Genes Dev.* **2004,** *18,* 901-911.

242 Pereira, R. M.; Delany, A. M.; Durant, D.; Canalis, E. Cortisol Regulates the Expression of Notch in Osteoblasts. *J. Cell Biochem.* **2002,** *85,* 252-258.

243 Schnabel, M.; Fichtel, I.; Gotzen, L.; Schlegel, J. Differential Expression of Notch Genes in Human Osteoblastic Cells. *Int. J. Mol. Med.* **2002,** *9,* 229-232.

244 Shindo, K.; Kawashima, N.; Sakamoto, K.; Yamaguchi, A.; Umezawa, A.; Takagi, M.; Katsube, K.; Suda, H. Osteogenic Differentiation of the Mesenchymal Progenitor Cells, Kusa Is Suppressed by Notch Signaling. *Exp. Cell Res.* **2003,** *290,* 370-380.

245 Zamurovic, N.; Cappellen, D.; Rohner, D.; Susa, M. Coordinated Activation of Notch, Wnt and TGF-Beta Signaling Pathways in BMP-2 Induced Osteogenesis: Notch Target Gene Hey1 Inhibits Mineralization and Runx2 Transcriptional Activity. *J. Biol. Chem.* **2004**.

246 de Jong, D. S.; Steegenga, W. T.; Hendriks, J. M.; van Zoelen, E. J.; Olijve, W.; Dechering, K. J. Regulation of Notch Signaling Genes During BMP2-Induced Differentiation of Osteoblast Precursor Cells. *Biochem. Biophys. Res. Commun.* **2004,** *320,* 100-107.

247 Rosen, D.; Miller, S. C.; DeLeon, E.; Thompson, A. Y.; Bentz, H.; Mathews, M.; Adams, S. Systemic Administration of Recombinant Transforming Growth Factor Beta 2 (RTGF-Beta 2) Stimulates Parameters of Cancellous Bone Formation in Juvenile and Adult Rats. *Bone* **1994,** *15,* 355-359.

248 Joyce, M. E.; Roberts, A. B.; Sporn, M. B.; Bolander, M. E. Transforming Growth Factor-Beta and the Initiation of Chondrogenesis and Osteogenesis in the Rat Femur. *J. Cell Biol.* **1990,** *110,* 2195-2207.

249 Harris, S. E.; Bonewald, L. F.; Harris, M. A.; Sabatini, M.; Dallas, S.; Feng, J. Q.; Ghosh-Choudhury, N.; Wozney, J.; Mundy, G. R. Effects of Transforming Growth Factor Beta on Bone Nodule Formation and Expression of Bone Morphogenetic Protein 2, Osteocalcin, Osteopontin, Alkaline Phosphatase, and Type I Collagen MRNA in Long-Term Cultures of Fetal Rat Calvarial Osteoblasts. *J. Bone Miner. Res.* **1994,** *9,* 855-863.

250 Pfeilschifter, J.; Wolf, O.; Naumann, A.; Minne, H. W.; Mundy, G. R.; Ziegler, R. Chemotactic Response of Osteoblastlike Cells to Transforming Growth Factor Beta. *J. Bone Miner. Res.* **1990,** *5,* 825-830.

251 Borton, A. J.; Frederick, J. P.; Datto, M. B.; Wang, X. F.; Weinstein, R. S. The Loss of Smad3 Results in a Lower Rate of Bone Formation and Osteopenia Through Dysregulation of Osteoblast Differentiation and Apoptosis. *J. Bone Miner. Res.* **2001,** *16,* 1754-1764.

252 Liu, W.; Toyosawa, S.; Furuichi, T.; Kanatani, N.; Yoshida, C.; Liu, Y.; Himeno, M.; Narai, S.; Yamaguchi, A.; Komori, T. Overexpression of Cbfa1 in Osteoblasts Inhibits Osteoblast Maturation and Causes Osteopenia With Multiple Fractures. *J. Cell Biol.* **2001,** *155,* 157-166.

253 Geoffroy, V.; Kneissel, M.; Fournier, B.; Boyde, A.; Matthias, P. High Bone Resorption in Adult Aging Transgenic Mice Overexpressing Cbfa1/Runx2 in Cells of the Osteoblastic Lineage. *Mol. Cell Biol.* **2002,** *22,* 6222-6233.

254 Byers, B. A.; Pavlath, G. K.; Murphy, T. J.; Karsenty, G.; Garcia, A. J. Cell-Type-Dependent Up-Regulation of in Vitro Mineralization After Overexpression of the Osteoblast-Specific Transcription Factor Runx2/Cbfal. *J. Bone Miner. Res.* **2002,** *17,* 1931-1944.

255 Kuroda, K.; Tani, S.; Tamura, K.; Minoguchi, S.; Kurooka, H.; Honjo, T. Delta-Induced Notch Signaling Mediated by RBP-J Inhibits MyoD Expression and Myogenesis. *J. Biol. Chem.* **1999,** *274,* 7238-7244.

256 Lindsell, C. E.; Shawber, C. J.; Boulter, J.; Weinmaster, G. Jagged: a Mammalian Ligand That Activates Notch1. *Cell* **1995,** *80,* 909-917.

257 Jarriault, S.; Le Bail, O.; Hirsinger, E.; Pourquie, O.; Logeat, F.; Strong, C. F.; Brou, C.; Seidah, N. G.; Isra l A Delta-1 Activation of Notch-1 Signaling Results in HES-1 Transactivation. *Mol. Cell Biol.* **1998,** *18,* 7423-7431.

258 Luo, B.; Aster, J. C.; Hasserjian, R. P.; Kuo, F.; Sklar, J. Isolation and Functional Analysis of a CDNA for Human Jagged2, a Gene Encoding a Ligand for the Notch1 Receptor. *Mol. Cell Biol.* **1997,** *17,* 6057-6067.

259 Ross, D. A.; Rao, P. K.; Kadesch, T. Dual Roles for the Notch Target Gene Hes-1 in the Differentiation of 3T3-L1 Preadipocytes. *Mol. Cell Biol.* **2004,** *24,* 3505-3513.

260 Smas, C. M.; Sul, H. S. Pref-1, a Protein Containing EGF-Like Repeats, Inhibits Adipocyte Differentiation. *Cell* **1993,** *73,* 725-734.

261 Conboy, I. M.; Rando, T. A. The Regulation of Notch Signaling Controls Satellite Cell Activation and Cell Fate Determination in Postnatal Myogenesis. *Dev. Cell* **2002,** *3,* 397-409.

262 Chen, D.; Zhao, M.; Harris, S. E.; Mi, Z. Signal Transduction and Biological Functions of Bone Morphogenetic Proteins. *Front Biosci.* **2004,** *9,* 349-358.

263 Guo, D.; Harris, S.; Yang, W.; Harris, M.; Zhang, J.; Feng, J.; Anderson, C.; Kream, B.; Lichtler, A.; Hogan, B.; Kulessa, H. Absence of both BMP2 and BMP4 during skeletal development results in severe defects in osteoblasts but not in chondrocytes. 26th ASBMR Annual Meeting, 1st-5th October 2005, Seattle,USA presentation number: 1049. 2004.

264 Kugimiya, F.; Kamekura, S.; Chikuda, K.; Nakamura, H.; Kawaguchi, U.; Chung, U. Physiological Role of Combination of BMP2 and BMP6 in Bone Formation. 26th ASBMR Annual Meeting, 1st-5th October 2005, Seattle,USA presentation number: 1038. 2004.

265 Tsuji, K.; Bandyopadhyay, A.; Cox, K.; Harfe, B.; Tabin, C. J.; Rosen, V. BMP4 is necessary for bone formation: conditional BMP4 knock-out using the 3.6kb and 2.3kb collagen 1a1 promoter-Cre and BMP4 floxed mice. 26th ASBMR Annual Meeting, 1st-5th October 2005, Seattle,USA presentation number: 1037. 2004.

266 Conboy, I. M.; Conboy, M. J.; Smythe, G. M.; Rando, T. A. Notch-Mediated Restoration of Regenerative Potential to Aged Muscle. *Science* **2003,** *302,* 1575-1577.

267 Nam, Y.; Aster, J. C.; Blacklow, S. C. Notch Signaling As a Therapeutic Target. *Curr. Opin. Chem. Biol.* **2002,** *6,* 501-509.

7 Curriculum vitae

Nataša Zamurović

Personal details:

Born: 17/10/1974, Belgrade, Serbia and Montenegro
Address: Klingentalstrasse 79, 4057 Basel, Switzerland
E-mail: natasa.zamurovic@novartis.com
Phone/Fax: +41 61 696 74 45/ +41 61 696 38 49

Education:

December 2004-April 2005: Post-doctoral position in the Bone Metabolism Group, Novartis Pharma, Basel, Switzerland

2001-November 2004: PhD studies jointly hosted by Novartis Pharma and the University of Basel, Switzerland
Title: "*Transcriptional program of osteoblast differentiation: Coordinated activation of Notch, Wnt, and TGF-β signalling pathways in MC3T3 cell line*".
PhD thesis committee: Dr. Mira Susa, PD Dr. Patrick Matthias, Prof. Michael N. Hall.

1998-2000: Postgraduate Studies, Faculty of Biology, University of Belgrade, Yugoslavia
Major: Molecular Biology and Biochemistry
Average grade: 100%
MSc thesis: "*Molecular genetics of hereditary motor and sensory neuropathies: Analysis of mutations in chromosomal region 17p11.2"*

1993-1998: Graduate Studies, Faculty of Biology, University of Belgrade, Yugoslavia
Major: Molecular Biology and Physiology
Awarded the title of the Student of the Year by the University of Belgrade after achieving 100% average for all exams during the course of the studies
Diploma thesis: "*Comparison of the number of CAG repeats of the AR gene in patients with schizophrenia and in the control Yugoslav population*"

Research Experience:

2000-present: Work placement and PhD studies in the Bone Metabolism Group, Novartis Pharma, Basel, Switzerland

- Maintenance and functional analysis of different cellular osteoblast differentiation systems.
- Quantitative RT-PCR analysis methods development for a set of osteoblast differentiation markers.
- Affymetrix GeneCHIP analysis of osteoblast differentiation process using different cell systems.
- Statistical and functional microarray data analysis using different analysis software, extensive literature search and different public databases.
- Microarray data confirmation for large number of genes using various quantitative RT-PCR methods (radioactive and real-time RT-PCR).
- Functional analysis of selected target genes in different cellular systems using siRNA knock down approach; cloning in expression plasmids; overexpression analysis using the luciferase reporter system.
- Functional analysis of BMP, TGF-β and Notch pathway activation and inhibition in osteoblasts.
- Design and characterization of transgenic and knockout mouse models (genotyping, expression analysis in different tissues and primary cells culture).

1999-2000: Elaboration of MSc thesis. Center for Advancement and Application of PCR, University of Belgrade, Yugoslavia.

- *Developed PCR and Southern blotting based diagnostic tests for duplication/deletion in 17p11.2 chromosomal region.*
- *Performed diagnostic tests on large number of patients diagnosed as candidates for the mutations*
- *Performed statistical analysis on a large sample of Yugoslav patients.*

1998: Elaboration of Diploma thesis. Center for Advancement and Application of PCR, University of Belgrade, Yugoslavia.

- Developed PCR based method for analysis the number of CAG repeats in the polymorphic region of AR gene.
- Performed diagnostic tests on several patients diagnosed as candidates for the mutations in this region
- Analyzed and statistically compared number of CAG repeats of AR gene in patients with schizophrenia and in a control Yugoslav population.

Computer skills:

- Microarray data analysis using software Expressionist 3.0 and GeneSpring 6.0.
- *Extensive knowledge of bioinformatic analysis of nucleotide and protein sequences, as well as primer and siRNA oligonucleotide design using biological software tools. Regular usage of public databases such as NCBI, GenBank, EMBL, SWISS-PROT.*
- Experienced user of MS Word, MS Excel, MS Power Point, MS Photo Editor, Acrobat Illustrator.

Sense of organisation and responsibilities:

- Participated in advanced molecular biology diagnostic procedures for several neurological and neuro-muscular diseases.
- Team work.
- Supervision (diploma students, trainees, technicians).

Professional organization and societies:

1998-2000: Member of European Consortium for Charcot-Marie-Tooth Disease and Related Peripheral Disorders

Courses:

May 31st – June 7th 2003: EMBO practical course “Microarray technology: Genome-Proteome-Function”

Awards:

Young Investigator Award at the ASBMR meeting “Advances in Skeletal Anabolic Agents for the treatment of Osteoporosis”, May 24-25 2004, Bethesda, Maryland, USA.
Oral presentation “Hey1, a direct Notch target gene, is up-regulated by BMP-2 and reduces osteoblast mineralization and cbfa1/Runx2 transcriptional activity”.

Publications:

1. **Zamurovic N**, Cappellen D, Rohner D, Susa M. “Coordinated activation of Notch, Wnt and TGF-β signalling pathways in BMP-2 induced osteogenesis: Notch target gene Hey1 inhibits mineralization and Runx2 transcriptional activity”. **J Biol Chem.** 2004 September 3rd; 279 (36): 37704-37715

2. Susa M, Luong-Nguyen NH, Cappellen D, **Zamurovic N**, Gamse R. “Human primary osteoclasts: in vitro generation and applications as pharmacological and clinical assay”. **Journal of Translational medicine** 2004 2:6

3. Keckarevic M, Savic D, Culjkovic B**, Zamurovic N**, Major T, Keckarevic D, Todorovic S, Romac S. “Duchenne's and Becker's muscular dystrophy: analysis of phenotype-genotype correlation in 28 patients”. **Serbian Archive of Medicine** 2002 May-Jun; 130(5-6):154-8.

4. **Zamurovic N**, Milic V, Dackovic J, Zamurovic D, Culjkovic B, Apostolski S, Romac S. “Analysis of mutations in 17p11.2 region in patients with Charcot-Marie-Tooth type I disease and patients with Tomaculose Neuropathy”. **Serbian Archive of Medicine** 2002 Mar-Apr;130(3-4):59-63

5. Dackovic J, Rakocevic-Stojanovic V, Pavlovic S, **Zamurovic N**, Dragasevic N, Romac S, Apostolski S. “Hereditary neuropathy with liability to pressure palsies associated with central nervous system lesions”. **European Journal of Neurology** 2001; vol 8:1-4

6. Culjkovic B, Stojkovic O, Savic D, **Zamurovic N**, Nesic M, Major T, Keckarevic D, Zamurovic B, Vukosavic S, Romac S. “Comparison of the number of triplets in SCA1, MJD/SCA3, HD, SBMA, DRPLA, MD, FRAXA and FRDA genes in schizophrenic patients and a healthy population”. **American Journal of Medical Genetics** (Neuropsychiatric Genetics) 2000; 96: 884-887

7. **Zamurovic N**, Culjkovic B, Stojkovic O, Romac S. “Comparison of the number of CAG repeats of the AR gene in patients with schizophrenia and in the control Yugoslav population”. **Serbian Archive of Medicine** 2000 Mar-Apr; 128(3-4):71-74

8. Zamurovic D, **Zamurovic N** “Hereditary neuropathies”. in: **Problems in Pediatry**, Zavod za udzbenike i nastavna sredstva, Belgrade, 2000; 21:142-146

9. Rakocevic-Stojanovic V, Pavlovic S, Dackovic J, Trikic R, Lavrnic D, **Zamurovic N**, Romac S, Apostolski S. “Hereditary neuropathy with tendency toward pressure palsies associated with central nervous system demyelination”. **European Journal of Neurology** 2000; vol 17(3): 45-49

10. Pavlovic S, Dackovic J, Trikic R, **Zamurovic N**, Rakocevic-Stojanovic V, Stevic Z, Romac S, Apostolski S. “Clinical and electrophysiological features of hereditary neuropathy with liability to pressure palsies in 14 members of one family”. **Clinical Neurophysiology** 2000; 541-549

11. Romac S, Culjkovic B, Vukosavic S, Stojkovic O, Savic D, Keckarevic D, **Zamurovic N**, Major T, Keckarevic M, Topisirovic I. “Dynamic mutations as a cause of hereditary neurological and psychiatric diseases”. **Yugoslav Medical Biochemistry** 2000; 10:1-7

Complementary Information:

Knowledge of foreign languages: English-fluent, French-fluent, German-basic

Leisure activities: Singing, dancing, skiing

Referees:

Dr. Mira Susa Spring, Novartis Pharma AG,
WKL-125.9.12, Klybeckstrasse 141, CH-4057 Basel, Switzerland.
Phone: +41 61 6964449 (direct)
Fax: +41 61 6963849 (direct)
e-mail: mira.susa_spring@pharma.novartis.com

PD Dr. Patrick Matthias, Friedrich Miescher Institute for Biomedical Research
WRO-1066.2.10, P.O. Box 2543, CH-4002 Basel, Switzerland
Tel: + 41 61 6976661 (direct)
Fax: + 41 61 6973976 (direct)
e-mail: patrick.matthias@fmi.ch

Prof. Stanka Romac, Head of the Department of Molecular Biology, Faculty of Biology, University of Belgrade
Studentski Trg 16, p.o.box 52
11000 Belgrade
Serbia and Montenegro
Phone/Fax: + 381 11 639 100
e-mail: stanka@bf.bio.bg.ac.yu